Interactions of adherent-invasive *Escherichia coli* with human colonic epithelium

Bethan Fay Evans, MSc, BSc (Hons)

Thesis submitted in fulfilment of the requirements of the University of East Anglia for the degree of Doctor of Philosophy

Metabolic Health Research Centre

Norwich Medical School

University of East Anglia, Norwich, UK

2025

Acknowledgements

Firstly, I would like to thank my primary supervisor, Dr Stephanie Schüller, for her continued support and guidance throughout this PhD project, for which this thesis would not have been possible. To my secondary supervisor Dr Linda Troeberg, thank you for your helpful suggestions, ideas and support when I needed it most.

Thank you in advance to my *viva voce* examiners, Dr Donal Wall and Dr Gary Rowley, for taking the time to read my thesis and discuss it with me.

To everyone at the BCRE, thank you for making me feel welcome since my first day. In particular Dixie, who had to put up with my endless questions, terrible singing and silly comments both in the office and the lab. To anyone in the BCRE PhD student cohort who ever joined me for a coffee break, had a chat over lunch, a pint (or many) at the pub, or watched a football game with me – thank you for keeping me sane. Thank you to Jasmine, for introducing me to Albi and Suka – the Norfolk stays, beach walks and dog cuddles will forever be welcomed.

To my friend, Abi, thank you for always listening to me, giving me advice, and being my biggest supporter throughout this PhD – you have always had more confidence in me than I've had in myself.

Last but by no means least, I am incredibly grateful to my loving and supportive family. To my Mum and sisters who have no idea what I do yet are always proud of me for pursuing a PhD – it's finally finished!

Abstract

Adherent-invasive *Escherichia coli* (AIEC) is associated with Crohn's Disease (CD), a type of inflammatory bowel disease (IBD) affecting over 120,000 people in the UK. AIEC have been shown to adhere to and invade epithelial cell lines and replicate within macrophages but their interaction with fully differentiated human intestinal epithelia remains largely unexplored. Here, the pathogenesis of AIEC prototype strain LF82 was investigated using differentiated human colon carcinoma cell lines and patient-derived colonic organoids.

While LF82 adherence and biofilm formation was significantly increased compared to non-pathogenic *E. coli* MG1655, invasion and intracellular replication were comparable in both strains. Notably, LF82 binding was mediated by type I fimbriae but occurred independently of the established AIEC receptor CEACAM-6. Despite low invasion and intracellular replication, infection with LF82 resulted in cytotoxicity which was dependent on bacterial contact but not invasion or type VI secretion of effector proteins. Similar to CD, LF82-infected colonic epithelia exhibited reduced barrier function and increased release of TNF-α, IL-6 and IL-8.

Extension of these studies to other AIEC isolates demonstrated highly divergent infection strategies. Overall, these results suggest that AIEC LF82 pathogenesis in the human colon is strain-specific and mediated by the formation of biofilms, contact-dependent cytotoxicity, epithelial permeability, and pro-inflammatory cytokine secretion.

Table of Contents

List of Figures

List of Tables

List of Abbreviations

A/E	attaching and effacing
AIEC	adherent-invasive *Escherichia coli*
AMP	antimicrobial peptide
APC	antigen-presenting cell
ASC	adult stem cell
ATCC	American Type Culture Collection
BSA	bovine serum albumin
C	Celsius
CCK	cholecystokinin
CD	Crohn's Disease
CEABAC10	carcinoembryonic antigen bacterial artificial chromosome 10
CEACAM	carcinoembryonic antigen-related cell adhesion molecule
CEACAM-1	carcinoembryonic antigen-related cell-adhesion molecule 1
CEACAM-5	carcinoembryonic antigen-related cell-adhesion molecule 5
CEACAM-6	carcinoembryonic antigen-related cell-adhesion molecule 6
CEACAM-7	carcinoembryonic antigen-related cell-adhesion molecule 7
CFU	colony forming units
CHI3L1	Chitinase 3-Like-1
CO_2	carbon dioxide
CRD	carbohydrate recognition domain
DAPI	4',6-diamidino-2-phenylindole
DC	dendritic cell
dH2O	deionised water
DMEM	Dulbecco's Modified Eagle's Medium
DMEM/F-12	Dulbecco's Modified Eagle's Medium/Nutrient F-12 Ham
DMSO	dimethyl sulfoxide
DSS	dextran sodium sulfate
EAEC	enteroaggregative *E. coli*
ECACC	European Collection of Authenticated Cell Cultures
ECM	extracellular matrix

eDNA	extracellular DNA
EDTA	ethylenediaminetetraacetic acid
EGF	epithelial growth factor
EHEC	enterohaemorrhagic *E. coli*
EIMs	extraintestinal manifestations
ELISA	enzyme-linked immunosorbent assay
EPEC	enteropathogenic *E. coli*
EPS	exopolysaccharide
ER	endoplasmic reticulum
ESC	embryonic stem cells
ETEC	enterotoxigenic *E. coli*
FACS	fluorescence-activated cell sorting
FAE	follicle-associated epithelium
FBS	foetal bovine serum
FITC	fluorescein isothiocyanate
FMT	faecal microbiota transplantation
GFP	green fluorescent protein
GI	gastrointestinal tract
GIP	glucose-dependent insulinotropic polypeptide
GLP-1	glucagon-like peptide-1
GuMi	Gut Microbiome physiomimetic platform
GWAS	genome-wide association studies
HIF1α	hypoxia-inducible factor-1α
HuMiX	Human-Microbe crosstalk model
IBCs	intracellular bacterial communities
IBD	inflammatory bowel disease
ICAM-1	intercellular adhesion molecule-1
IEC	intestinal epithelial cell
IFN	interferon
IFS	immunofluorescent staining
IL	interleukin
IL-1β	interleukin-1beta

IL-6	interleukin-6
IL-8	interleukin-8
IL-25	interleukin-25
ILC	innate lymphoid cells
iPSC	induced pluripotent stem cells
IRGM	immunity-related GTPase M
ISC	intestinal stem cell
JAM	junctional adhesion molecule
LB	lysogeny broth
LPF	long polar fimbriae
MAP	*Mycobacterium avium* subsp. *paratuberculosis*
M cells	microfold cells
MDP	muramyl dipeptide
MOI	multiplicity of infection
mRNA	messenger ribonucleic acid
MUC2	mucin-2
NF-κB	nuclear factor-κB
NI	non-infected
NK	natural killer
NLR	nod-like receptor
NODs	nucleotide oligomerization domain receptors
OD	optical density
OMP	outer membrane protein
OMVs	outer membrane vesicles
ONC	overnight culture
P/S	penicillin/streptomycin
PAI	pathogenicity islands
PAMP	pathogen-associated molecular pattern
PBS	phosphate-buffered saline
PHE	Public Health England
PI	propidium iodide
PMN	polymorphonuclear leukocyte

PP	Peyer's patches
PRR	pathogen recognition receptor
PRR	pattern recognition receptor
PSC	pluripotent stem cell
PYY	peptide YY
qRT-PCR	quantitative reverse transcription polymerase chain reaction
ROS	reactive oxygen species
SCFA	short-chain fatty acid
SDS	sodium dodecyl sulfate
siRNA	small interfering ribonucleic acid
SNP	single-nucleotide polymorphism
STEC	Shiga toxin-producing *E. coli*
T3SS	Type III Secretion System
T6SS	Type VI Secretion System
TEER	trans-epithelial electrical resistance
T_H	T helper
TJ	tight junction
TLR	toll-like receptor
TNBS	trinitrobenzene sulfonic acid
TNF	tumour necrosis factor
TNF-α	tumour necrosis factor alpha
UC	ulcerative colitis
UPEC	uropathogenic *E. coli*
VCC	*Vibrio cholerae* cytolysin
VDC	vertical diffusion chamber
ZO	zonula occludens
ZO-1	zonula occludens protein-1

Chapter 1. Introduction

1.1 Crohn's Disease

1.1.1 Pathology, epidemiology and current treatments

Crohn's Disease (CD) and ulcerative colitis (UC) are subtypes of inflammatory bowel disease (IBD), characterised by chronic, uncontrolled and relapsing inflammation of the gastrointestinal tract (GI). CD and UC differ in pathophysiology, symptoms and complications. UC affects only the colon and presents with continuous lesions and superficial inflammation that can lead to erosions, ulcers and bloody diarrhoea. CD can affect any segment of the GI, presenting with chronic, relapsing inflammation that can lead to chronic abdominal pain, diarrhoea, obstruction, weight loss and an increased risk of colorectal cancer (Thia et al., 2010; Torres et al., 2017). Over time, complications such as stricture, fistulas and abscesses will occur in half of CD patients within 10 years of diagnosis, often resulting in surgery. Patients typically present with symptoms in early adulthood and disease develops as a life-long condition (Roda et al., 2020). Although primarily a disease of the GI, 24-40% of patients develop inflammation-mediated extraintestinal manifestations (EIMs). These can affect the skin, eyes, joints and liver (Bernstein et al., 2001). The most common EIMs include erythema nodosum, pyoderma gangrenosum, episcleritis, arthritis and primary sclerosing cholangitis (PSC) (Levine and Burakoff, 2011).

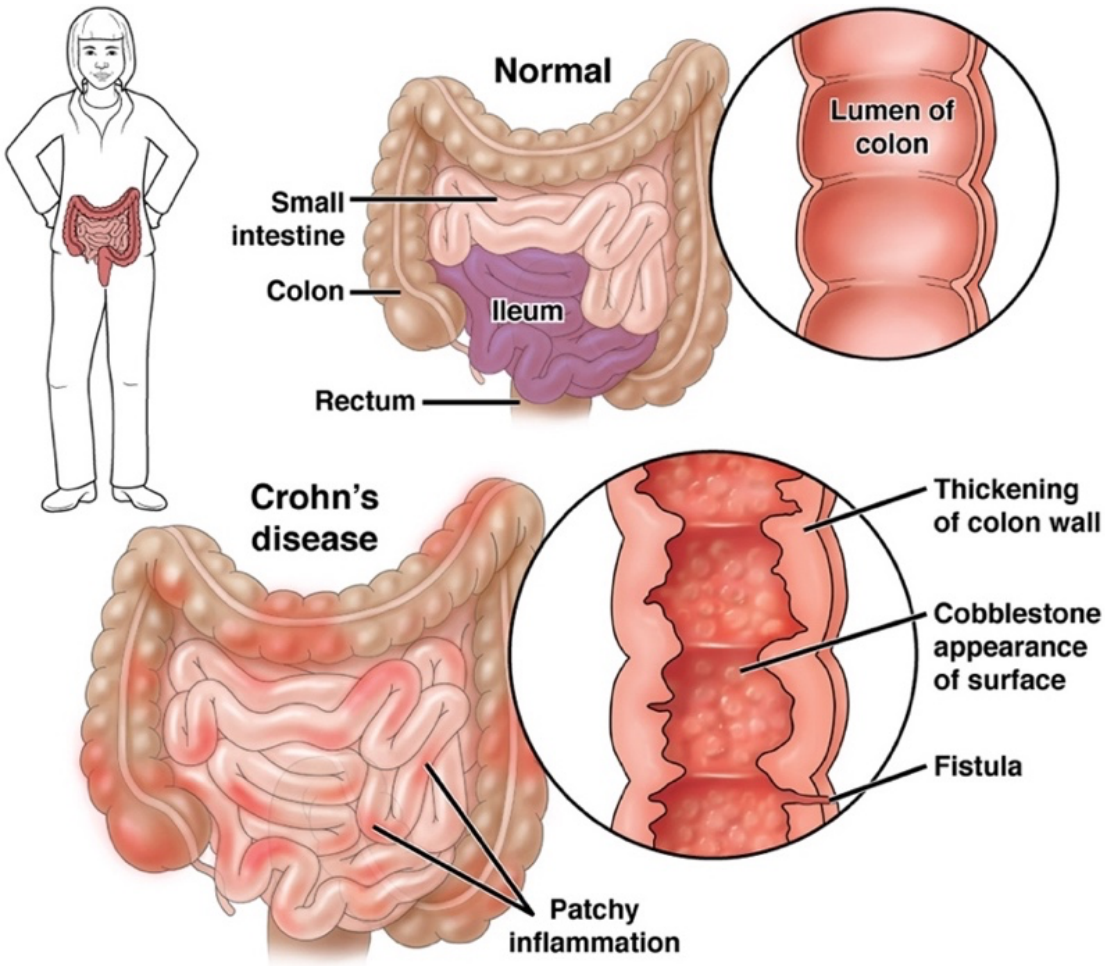

Figure 1.1. Crohn's Disease presentation. CD causes inflammation in the GI tract. The most commonly affected areas are the ileum and colon. Intestinal tissue is inflamed in patches and this can lead to thickening, stricture and fistulas (Torres, 2025).

To date, there is no curative treatment for CD. Current therapeutic strategies are broadly ameliorative, aimed at halting disease progression and preventing complications. Only symptomatic treatments, such as immunosuppressants, corticosteroids and anti-inflammatories, are used to limit the frequency of inflammatory flares (Torres et al., 2017). Steroids and tumour necrosis factor (TNF) inhibitors are highly effective in inducing remission, meanwhile medications to maintain remission include 5-aminosalicylic acid products, immunomodulators (azathioprine, 6-mercaptopurine, methotrexate) and TNF inhibitors (infliximab, adalimumab, certolizumab and golimumab). In the more severe cases requiring surgical intervention, bowel resection, stricturoplasty or abscess drainage are used (Gajendran et al., 2018). Currently, mucosal healing is the target of choice. Patients

who achieve mucosal healing have improved outcomes, a decreased risk of surgery, lower rates of relapse and an improved quality of life.

IBD incidence has increased globally since the start of the 21st century, with incidence rates differing by region. The highest incidence is reported in North America, northern and western Europe and Oceania. Incidence of CD is growing rapidly in western countries with rates varying from 1 to 20 cases per 100,000 people every year (Martinez-Medina et al., 2009a). In addition, newly industrialised countries in Asia, Africa and South America are experiencing rapidly increasing rates. For example, IBD was once considered a rare condition in China, and is now common, accounting for substantial use of hospital beds (Kaplan and Ng, 2016). These rising incidence rates may be correlated with westernised living standards and behaviours (Economou and Pappas, 2008). The economic burden of CD in the UK and across Europe is high. Direct health care costs are estimated at approximately €3500 per patient per year, and these have shifted from hospitalisation and surgery towards drug-related expenditures due to the increasing use of biologic drugs and other novel therapeutics (M. Zhao et al., 2021). With rising incidence globally, the economic burden of CD may significantly increase in the coming years.

1.2 Crohn's Disease aetiology

The aetiology of CD remains unknown, however the idea that several factors play a role in disease onset and perpetuation is widely accepted. CD is believed to be a consequence of genetic susceptibility, environmental factors, and changes in the intestinal microbiota, resulting in an abnormal mucosal immune response and compromised intestinal epithelial barrier function.

1.2.1 Genetic association in CD

Familial inheritance of CD is recognised, with concordance rates amongst monozygotic twins that are higher for CD (~50%) compared with that of UC (~15%), suggesting a role for genetic predisposition (Halfvarson et al., 2003; Torres et al., 2017). The first CD-associated locus on Chromosome 16 was identified by linkage analysis in families with multiple affected members (Hugot et al., 1996). Since then, genome-wide association studies (GWAS) in more than 700,000 individuals have identified more than 200 loci associated with CD risk, many of which encode regulatory components of the immune system, including NOD2, ATG16L1, IRGM, IL23R and LRRK2 (Sazonovs et al., 2022).

1.2.1.1 NOD2

Several genetic polymorphisms increase the risk of CD. The first identified and well-documented gene in the 200 genetic risk loci associated with IBD is *NOD2. NOD2* is expressed intracellularly in Paneth cells, monocytes, granulocytes, dendritic cells and intestinal epithelial cells (IECs) (Caruso et al., 2014). *NOD2* encodes an intracellular sensor of the Nod-like receptor (NLR) family and senses the presence of muramyl dipeptide (MDP), a component of the peptidoglycan cell wall in bacteria (Homer et al., 2010). MDP-mediated stimulation of NOD2 activates NF-κB and induces the production of various proinflammatory cytokines including IL-1, IL-6, IL-8, IL-12/23 p40 subunit and TNF-α (Kobayashi et al., 2005). NOD2 also activates

both T_H2 and T_H17 cells (Magalhaes et al., 2011, 2008; Van Beelen et al., 2007). NOD2 may also repress the T_H1 cell response by inhibiting Toll-Like Receptor 2 (TLR) signalling (Watanabe et al., 2004) and dampen T_H17 cell activity by microRNA (miRNA)-dependent IL-23 repression (Brain et al., 2013). Three mutations in *NOD2* have been extensively studied and documented to be strongly associated with CD onset. A frameshift mutation (L1007fsinsC) that results in a truncated NOD2 protein and two amino acid substitutions (R702W and G908R) are located within the leucine-rich repeat domain, which has a similar structure to the leucine-rich repeat domains of TLRs and is involved with microbial recognition (Hugot et al., 2001; Ogura et al., 2001; Strober and Watanabe, 2011). Studies in NOD2-deficient mice demonstrated IECs have impaired bacteria-killing ability, leading to perturbed interactions between the ileal microbiota and mucosal immunity (Ogura, 2003; Sidiq et al., 2016). Furthermore, CD patients with mutations in *NOD2* have decreased expression of anti-inflammatory cytokine IL-10, with alterations in mucosa-associated bacteria including increased abundance of *Escherichia* and decreased abundance of *Faecalibacterium* species (Al Nabhani et al., 2016; Swidsinski et al., 2002).

1.2.1.2 ATG16L1 and autophagy

Autophagy is one of the main degradative pathways of the immune system. In response to stress and starvation, cellular components are engulfed within an autophagosome, which fuses with lysosomes resulting in autophagolysosomal degradation to free constituents for metabolic use. However, the autophagic machinery is also used to degrade invading bacteria, a process called xenophagy. Therefore, autophagy plays a role in the maintenance of intestinal homeostasis (Baxt and Xavier, 2015).

A single-nucleotide polymorphism (SNP) in the *ATG16L1* gene resulting in the amino acid substitution of a polar threonine by a nonpolar alanine (Thr300Ala) has been identified as a risk allele for CD. This variant exhibits impaired efficiency of autophagy-mediated clearance of *Salmonella* Typhimurium and adherent-invasive

E. coli (AIEC) in human cells (Lapaquette et al., 2010). In addition, the use of siRNA to silence *ATG16L1* in human epithelial cells or macrophages leads to increased intracellular AIEC replication (Lapaquette et al., 2012, 2010). Furthermore, dendritic cells from CD individuals expressing the *ATG16L1* variant have been shown to be defective in inducing autophagy, bacterial trafficking and antigen presentation (Cooney et al., 2010).

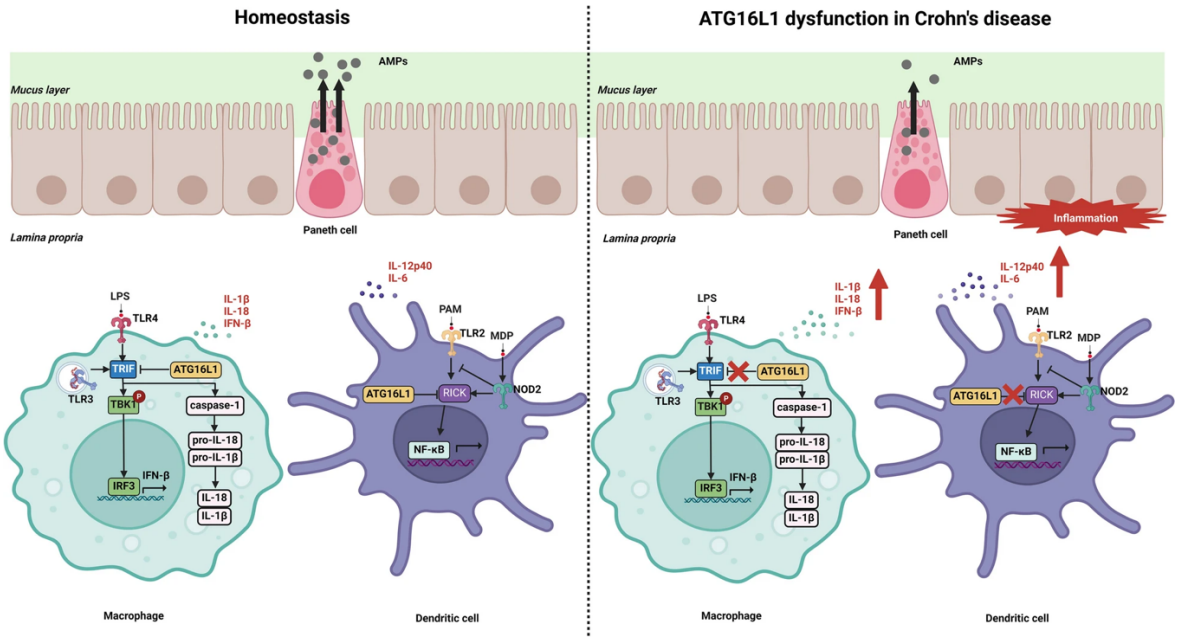

Figure 1.2. ATG16L1 dysfunction and increased risk of Crohn's inflammation. At homeostasis *in vivo* (left panel), the dense granules produced by Paneth cells are enriched with antimicrobial peptides (AMPs) and immunomodulatory proteins that control the composition of the intestinal flora. Moreover, after sensing the gut microbiota via PRRs, ATG16L1 negatively regulates TRIF- and RICK-mediated pro-inflammatory cytokine responses to maintain gut homeostasis. In the ATG16L1 dysfunctional state (right panel), AMP production by Paneth cells is reduced. This leads to increased PRRs stimulation of macrophages and DCs, which are not well regulated by ATG16L1, resulting in intestinal dysbiosis (Yuan et al., 2024).

1.2.1.3 IRGM – immune-related GTPase M

The human immunity-related GTPase M *(IRGM)* gene encodes a protein thought to play a central role in autophagy, including xenophagy, by stabilising the activation and assembly of several CD-associated core autophagy proteins and coupling them to innate immunity receptors (Chauhan et al., 2015). IRGM interacts with various essential autophagy proteins, including ULK1, Beclin 1, ATG14L and ATG16L. In infection, IRGM interacts with NOD2 in response to pathogen-associated molecular patterns (PAMPs), enhancing the K63-linked polyubiquitination of IRGM which allows IRGM to interact with ATG16L1 thus inducing xenophagy (Chauhan et al., 2015). In murine models, IRGM1-deficient mice exhibit functional abnormalities in intestinal Paneth cells and hyper-inflammation in the colon and ileum when exposed to sodium sulphate (Liu et al., 2013). In addition, IRGM1 demonstrates negative regulation of cellular inflammation in immune and epithelial cells in a CD murine model (Mehto et al., 2019). It has been speculated that AIEC infection in individuals with miR-196-dysregulated IRGM expression leads to altered antibacterial activity of IECs and abnormal persistence of CD-associated intracellular bacteria (Brest et al., 2011). Therefore, the loss of immune tolerance in the intestine and increased adaptive immunity in CD patients harbouring *ATG16L1* and *IRGM* risk alleles may be explained by this mechanism.

1.2.2 Environmental factors

1.2.2.1 Western diet and short-chain fatty acids (SCFAs)

Among environmental factors contributing to CD, a western diet is suggested to be a major risk factor in disease development. A western diet is typically comprised of an increased fat and simple carbohydrate intake, and a reduction in plant-derived complex carbohydrates (fibre). Studies have implicated a western diet in the dysbiosis of gut microbiome diversity, impairment of the epithelial immune response and the promotion of inflammation (Kang et al., 2023).

In mice, consumption of a western diet high in fat and sugar promotes dysbiosis characterised by expansion of pro-inflammatory *Proteobacteria* and *Bacteroidetes*, reduced *Firmicutes*, and increased susceptibility to AIEC colonisation and intestinal inflammation (Agus et al., 2016). This dietary shift is associated with a marked reduction in luminal short-chain fatty acid (SCFA) production, largely due to decreased dietary fibre intake (Desai et al., 2016). SCFAs are a primary energy source for colonocytes and exert immunomodulatory effects, including regulation of epithelial barrier function and inflammatory signalling pathways such as inhibiting NF-κB activation and production of pro-inflammatory cytokines (Ananthakrishnan et al., 2013; Michaudel and Sokol, 2020). However, propionic acid, a SCFA used widely in western food as a preservative, has been shown to exert distinct effects on AIEC pathogenesis. Previous work demonstrated that pre-exposure of AIEC to physiologically relevant concentrations of propionate induces metabolic reprogramming and transcriptional adaptations that enhance biofilm formation and intracellular replication within host cells (Ormsby et al., 2020). Consistent with this, clinical AIEC isolates exhibit increased expression of genes involved in SCFA uptake and utilisation, suggesting adaptation to SCFA-rich environments (Delmas et al., 2019; Elhenawy et al., 2019; Ormsby et al., 2020). Together, these findings support a model in which western diets alter both microbiota composition and SCFA availability, and in which propionate acts as an environmental cue that promotes AIEC persistence and virulence, thereby contributing to CD pathogenesis.

1.2.2.2 Microbiome

Increasing experimental and clinical evidence suggests that the intestinal microbiota plays an active role in CD. Numerous studies have acknowledged a significant difference in microbiota composition between healthy individuals and those with IBD. In patients with IBD, a decrease of beneficial bacterial groups combined with an increase in pathogenic bacteria results in a low diversity of the gut microbiota (Elatrech et al., 2015). Specifically, a depletion of symbiont bacteria, including those of the genus *Clostridium* of the Firmicutes phylum and the *Bifidobacterium* genus of the Actinobacteria phylum has been observed in CD. An increase in pathobiont *Bacteroides* has also been observed (Loh and Blaut, 2012). Specifically, amongst the Firmicutes, a decrease in *Faecalibacterium prausnitzii* is seen in CD patients (Sokol et al., 2009, 2008). *F. prausnitzii* is a commensal that inhabits the gut mucosa and mediates anti-inflammatory activities through production of an immunomodulating protein (Quévrain et al., 2016).

Furthermore, specific GI pathogens may act as environmental triggers in CD, by interacting with host genetics and disrupted microbial communities to exacerbate intestinal inflammation. Historically, *Mycobacterium avium* subsp. *paratuberculosis* (MAP) has attracted interest for its presence in ruminant Johne's disease and potential association with CD, with immune recognition of MAP antigens hypothesised to sustain chronic mucosal inflammation in genetically susceptible individuals, although causality remains debated (McNees et al., 2015). Concurrently, ectopic colonisation by oral bacteria such as *Haemophilus parainfluenzae* has been linked to CD severity, with murine models showing that specific strains from periodontal sources can drive intestinal inflammation through IFN-γ-driven $CD4^+$ T-cell responses and disruption of host metabolic pathways (Sohn et al., 2023).

1.3 The intestinal epithelial barrier

1.3.1 Mucus layer

The surface of the intestinal epithelium is covered by a protective layer of mucus, composed of mucin glycoproteins secreted by specialised goblet cells. The major glycoprotein within the intestinal mucus layer is mucin-2 (MUC2). The mucus layer is the first line of defence against invasion. Unlike the small intestine, where the mucus layer is a single layer, the colonic mucus layer can be divided into a sterile inner layer and an outer layer with bacterial colonization. The mucus layer contains antimicrobial peptides and immunoglobulins with antimicrobial and immunological effects which are secreted into the intestinal lumen by goblet cells, together with MUC2, to inhibit the adhesion and invasion of pathogenic bacteria (Yao et al., 2021). The integrity of the mucus layer is vital for intestinal health. In patients with CD, the composition and thickness of the mucus layer are significantly altered, ultimately resulting in the exposure of IECs to pathogenic bacteria, triggering an immune response. For example, a significant downregulation of MUC2 was observed in CD colonic biopsies (Moehle et al., 2006), making the mucus layer more penetrable by both pathogenic and commensal bacteria. In patients with acutely inflamed CD, significantly lower levels of MUC2 mRNA expression and lower numbers of goblet cells are observed (Hensel et al., 2015). Furthermore, Buisine et al demonstrated that the expression of MUC5AC and MUC6, which are normally restricted to the stomach, was displayed in the ileal mucosa of CD patients. This was accompanied by a disappearance of MUC2 (Buisine, 2001). Additionally, a meta-analysis of mucin gene expression in the ileal and colonic mucosa of CD patients found that total mucin levels were reduced in CD patients, with significant reductions in the expression of MUC5AC, MUC5B, and MUC7 (Niv, 2016). Interestingly, the expression of MUC2, MUC3 and MUC4 correlated with the activity of disease and the extent of inflammation in the colon, whereby the most pronounced alterations in mucin expression were observed in patients with severe CD (Dorofeyev et al., 2013).

1.3.2 Intestinal epithelium

The intestinal epithelium is composed of a single layer of columnar epithelial cells responsible for nutrient and water absorption. There are four distinct cell types categorized into two groups: secretory epithelial cells, including Paneth cells, goblet cells and enteroendocrine cells; and absorptive epithelial cells, represented by enterocytes and colonocytes in the small and large intestines, respectively (Figure 1.3). Each cell type serves an important function in barrier homeostasis. Enteroendocrine cells secrete hormones that regulate diverse physiological functions, including cholecystokinin (CCK), which stimulates pancreatic enzyme and bile release; glucose-dependent insulinotropic polypeptide (GIP) from the upper small intestine; glucagon-like peptide-1 (GLP-1), which promotes insulin secretion; and peptide YY (PYY), primarily secreted from the colon (Xie et al., 2020). Goblet cells produce glycosylated mucins which are secreted to form a layer of mucus that lines the epithelium and creates a barrier between the cell surface and contents of the intestinal lumen (See - 1.3.1 Mucus layer). Paneth cells, found only in the small intestine, are clustered at the bottom of the crypts and produce antimicrobial peptides including α and β-defensins, lysozyme and phospholipase A2, which prevent the growth and invasion of commensal and pathogenic microbes. In the colon, Paneth cells are absent and deep secretory cells are located between intestinal stem cells (ISCs) (Figure 1.3). Furthermore, Microfold cells (M cells) are located in the follicle-associated epithelium (FAE) of the Peyer's patches in the small intestine, where they actively transport luminal antigens to the underlying lymphoid follicles to initiate an immune response (Kobayashi et al., 2019). Lastly, tuft cells secrete effector molecules such as interleukin-25 (IL-25), eicosanoids, and acetylcholine that contribute to inflammation and immune regulation (Gerbe et al., 2012; Schneider et al., 2019); eicosanoids mediate innate immune responses, while acetylcholine modulates immunity and combats parasitic infection. IECs are arranged in a series of pits known as the crypts of Lieberkühn, which extend into the lumen forming finger-like villi. In addition, a constant proliferation of renewed IECs from pluripotent stem cells located at the base of the crypt occurs. After differentiation, the new epithelial cells either travel down to the base of the crypt and

reside as enteroendocrine and Paneth cells, or they travel up the crypt as enterocytes or goblet cells. Once the cell reaches the tip of the villus or the epithelium, it sloughs off the epithelium and is removed by the body, resulting in a complete renewal every 2 to 6 days (Mayhew et al., 1999).

Enterocytes and colonocytes are highly polarised, whereby the expression of membrane proteins differs between the apical and basolateral sides of the epithelial membrane (Schneeberger et al., 2018) and allows optimal transfer of nutrients, water and ions between the lumen and underlying tissue. To prevent liquids and macromolecules reaching the basolateral membrane, transmembrane protein complexes called tight junctions (TJs) bind neighbouring cells together. TJs are the most apical intercellular junctions of epithelial cells which maintain epithelial polarity and determine selective paracellular permeability properties in the epithelium. TJs are formed by different families of transmembrane TJ protein, including claudins, occludin and junctional adhesion molecules (JAMs), as well as scaffolding protein zonula occludens (ZOs) (Zhao et al., 2021).

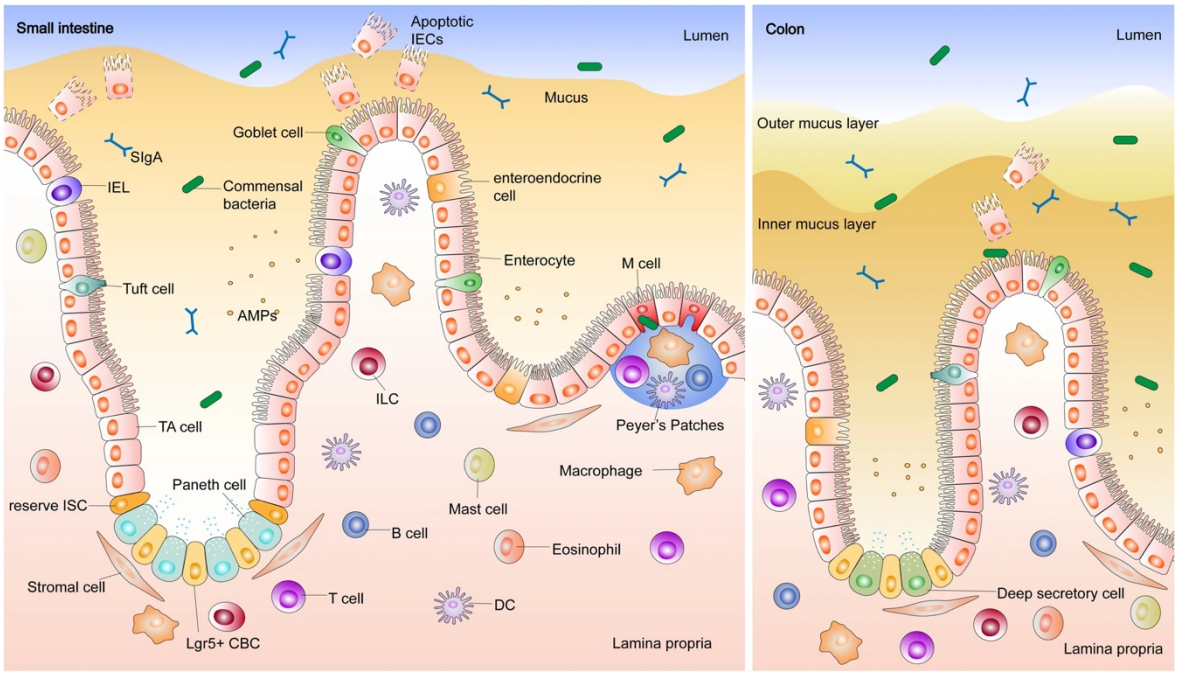

Figure 1.3. Intestinal epithelial structure and immune cell distribution. Left: Structure of the small intestine epithelium. Right: Structure of the colonic epithelium (Ma et al., 2022).

1.3.3 Cytokine-mediated reduction of barrier function

Whilst some cytokines have the properties to reinforce the epithelial barrier and promote intestinal barrier integrity, various pro-inflammatory cytokines can disrupt the epithelial barrier, promoting epithelial permeability. These can be derived from resident innate or adaptive immune cells, infiltrating inflammatory cells, or from intestinal epithelial cells themselves (Groschwitz and Hogan, 2009). For example, IL-6, TNF, IL-18, IL-1β, and IL-17 are overexpressed in the inflamed intestine and have been implicated in intestinal damage (Neurath, 2014). Specifically, TNF-α stimulation of intestinal epithelial cells has exhibited decreased protein expression of tight junction proteins claudin-1, occludin, and zonula occludens protein-1 (ZO-1), as well as inducing the rearrangement of cytoskeletal F-actin and impairing the localisation of occludin and ZO-1 (Watari et al., 2017; Ye and Sun, 2017). Furthermore, IL-22 increases intestinal epithelial permeability via changes in tight junction protein expression. Stimulation of Caco-2 cells with IL-22 *in vitro* and murine colonic epithelial cells *in vivo* demonstrated increased expression of claudin-2 which forms cation channels. As a result, IL-22 treated Caco-2 monolayers displayed decreased transepithelial electrical resistance (TEER), indicating increased paracellular ion permeability (Yaya Wang et al., 2017). In addition, interferon (IFN)-γ induced expression of the intercellular adhesion molecule-1 (ICAM-1) on the apical membrane of T84 cells, leading to increased numbers of neutrophils adhering to the apical surface in an *in vitro* model of transepithelial neutrophil migration. The ligation of ICAM-1 by neutrophils caused the phosphorylation of myosin light-chain kinase. As a result, a subsequent increase in epithelial permeability characterized by actin cytoskeletal reorganization, paracellular fluorescein isothiocyanate (FITC)–dextran flux, and a decrease in TEER was observed. Ultimately, this increase in epithelial permeability facilitated neutrophil transepithelial migration (Sumagin et al., 2014).

1.4 Immunology

1.4.1 Innate

Innate immunity is the first defence against invading microorganisms. IECs express pattern recognition receptors (PRRs) including trans-membrane TLRs and intracytoplasmic receptors such as nucleotide oligomerization domain receptors (NODs). PRRs recognise PAMPs and mediate the sensing of microbial antigens by immune cells. PRR signalling cascades result in NF-κB activation with gene transcription and production of pro-inflammatory mediators to ensure an effective innate response to pathogens (Geremia et al., 2014). The production of cytokines and chemokines by IECs recruit neutrophils, dendritic cells (DCs), monocytes, macrophages and innate lymphoid cells (ILCs).

In IBD, neutrophils phagocytose pathogens to maintain homeostasis initially, however they later accumulate within the gut epithelium and compromise epithelial barrier function, causing the release of inflammatory cytokines that perpetuate gut inflammation (De Souza and Fiocchi, 2016). In addition, neutrophil responses to attenuated *E. coli* are reduced in CD patients but not in UC, suggesting that neutrophil antimicrobial defences are defective in CD (Segal, 2018).

Altered Paneth cell distribution and function has been observed in IBD. The expression of α-defensins is reduced in patients with CD (Wehkamp et al., 2005). In addition, Paneth cells may be detected in the colonic mucosa in IBD patients resulting in α-defensin secretion in the large intestine (Wehkamp and Stange, 2020). Therefore, the reduced antimicrobial function of Paneth cells may be a primary pathogenic factor in ileal CD.

1.4.2 Adaptive

Unlike the innate immune response, the adaptive response is highly specific and adaptable. The adaptive immune response plays an important role in the pathogenesis of CD. T cells proliferate and differentiate when stimulated by the presence of antigens. Several studies have demonstrated persistent T cell immune activation in IBD (De Souza and Fiocchi, 2016). A dysregulated T cell response with abnormal development of activated T cell subsets may lead to inflammation by excessive release of cytokines and chemokines, leading to pathogenic effects. The levels of T cell-derived cytokines detected in the mucosa of IBD patients has led to an association of this dysregulation to CD (Geremia et al., 2014).

Excessive T helper 1 (T_H1) and T_H17 cell responses to pro-inflammatory cytokines produced by antigen-presenting cells and macrophages, such as IL-12, IL-18 and IL-23, are linked to CD. The T cell response leads to the secretion of proinflammatory cytokines IL-17, IFN-γ and TNF, which perpetuate inflammation by stimulating production of TNF, IL-1, IL-6, IL-8, IL-12 and IL-18 by other cells, such as macrophages, endothelial cells and monocytes (Uhlig and Powrie, 2018). Many T-cell-associated genetic risk loci are known in CD. For example, the T_H1 cell activating cytokine TNFSF15 is upregulated in CD (Bamias et al., 2003). TNFSF15 expression has been shown to initiate intestinal inflammation in mice due to T_H1 cell activation (Shih et al., 2011).

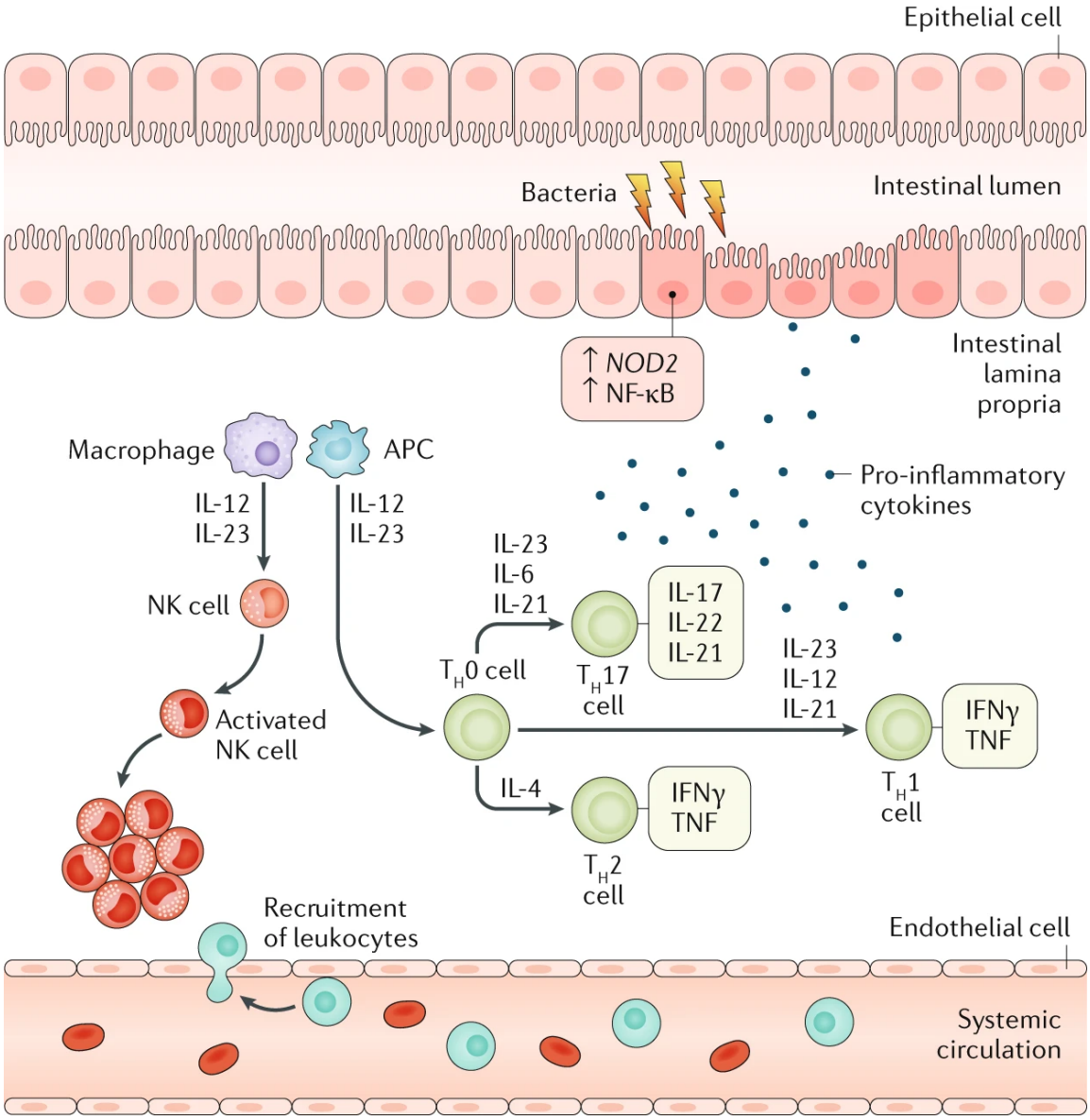

Figure 1.4. Inflammatory response in Crohn's Disease. After contact with an antigen, antigen-presenting cells (APCs) such as dendritic cells present antigen to T cells and B cells to initiate a controlled inflammatory response. In inflammatory conditions such as Crohn's disease, epithelial barrier dysfunction (owing to, for example, polymorphisms in NOD2 and nuclear factor-κB (NF-κB) signalling pathway genes) results in the luminal contents entering the lamina propria, leading to dendritic cells activating inflammatory T cell types, such as naive T helper (T_H0) cells, T helper 1 (T_H1) cells, TH17 cells and TH2 cells, which produce proinflammatory cytokines, such as IFN-γ and TNF. Furthermore, in response to luminal contents, macrophages produce the proinflammatory cytokines IL-12 and IL-23, which activate natural killer (NK) cells, resulting in perpetuation of the intestinal inflammation with production of proinflammatory cytokines. Luminal contents include dietary components and the gut microbiota. IL-4, IL-6, IL-21 and IL-22 are also produced by T_H0 cells in response to activation of dendritic cells (Roda et al., 2020).

1.5 Adherent-invasive *E. coli*

Escherichia coli is the most abundant facultative anaerobe in the GI tract, and most strains are commensals. These commensal strains coexist in humans and rarely cause disease, except in immunocompromised hosts or in cases of intestinal barrier disruption. The mucus layer of the colon acts as the niche for commensal *E. coli.* However, there are highly adapted *E. coli* strains that have acquired specific virulence attributes, increasing the ability to adapt to new niches and cause disease (Kaper et al., 2004).

Whilst no single causative microorganism has been identified, many studies have reported the potential involvement of invasive *E. coli* in CD pathogenesis. The frequent isolation of *E. coli* adhering to the inflamed ileal (Barnich et al., 2013; Darfeuille-Michaud et al., 1998; Raso et al., 2011; Rhodes, 2007) and colonic (Kotlowski et al., 2007; Prorok-Hamon et al., 2014; Sepehri et al., 2011; Swidsinski et al., 2002) mucosa of CD and UC patients led to the characterisation of several strains. The characterisation of strains isolated from the ileal mucosa of CD patients by Darfeuille-Michaud in 1998 found a lack of genes encoding virulence factors typically present in diarrhoeagenic *E. coli*, such as enterohaemorrhagic (EHEC) and enterotoxigenic *E. coli* (ETEC) (Darfeuille-Michaud et al., 1998).

Boudeau *et al* characterised the host cell interactions of *E. coli* strain LF82 isolated from an ileal biopsy of a CD patient and compared it to reference strains of well-defined pathogenic groups of *E. coli*, including EHEC and ETEC. As a result, three distinct phenotypic features were described, consisting of 1) adhesion to IECs, 2) invasion of IECs and 3) survival and replication in macrophages, without inducing cell death (Boudeau et al., 1999). As a result, a new pathogenic group of *E. coli*, named adherent-invasive *E. coli* (AIEC), was established.

1.5.1 AIEC pathogenesis

1.5.1.1 AIEC adherence to the intestinal epithelium

1.5.1.1.1 Binding of Type 1 pili to CEACAM-6

Adhesion to IECs is the first step of pathogenicity of many bacteria associated with infectious GI diseases (Eaves-Pyles et al., 2008). *FimH* codes for a mannose-binding adhesin presented at the tip of type 1 pili which are expressed on the surface of AIEC isolates. Studies to date suggest type 1 pili recognise and bind terminal mannose residues on epithelial surface glycoproteins, including carcinoembryonic antigen-related cell adhesion molecules (CEACAMs) (Leusch et al., 1991a, 1991b, 1990; Sauter et al., 1993, 1991) and TLR4 (Mossman et al., 2008). CEACAMs belong to a superfamily of immunoglobulin-like cell adhesion molecules encoded on chromosome 19 (Gray-Owen and Blumberg, 2006). They are involved in cell-cell recognition and modulate a range of cellular processes, including angiogenesis, regulation of insulin homeostasis, T-cell proliferation, tumorigenesis and also serve as pathogen receptors (Kuespert et al., 2006). For example, CEACAM expression is known to be altered in gastrointestinal cancers. Surface levels of CEACAM inversely correlated with colonocyte differentiation, supporting the suggestion that CEACAM can directly contribute to colon carcinogenesis (Ilantzis et al., 1997). Furthermore, CEACAM-5 serves as a clinical biomarker for advanced colon cancer. Of the various CEACAMs, CEACAM-1, CEACAM-5 and CEACAM-6 are expressed predominantly in the colon, but also by small intestinal epithelia, meanwhile CEACAM-7 is largely restricted to the colon (Sheikh et al., 2020).

Additionally, CEACAM-6 receptors are also present on ileal enterocytes. CEACAM-6 has previously been described as a receptor for AIEC adhesion and has been shown to be highly expressed on the apical surface of ileal epithelial cells in CD patients (Barnich et al., 2007). In a CEABAC10 transgenic mouse model, mice expressing human CEACAM receptors, including CEACAM-6, exhibited significantly reduced inflammation when AIEC *fimH* was replaced with commensal

E. coli K12 *fimH* and decreased IL-1β levels were observed (Carvalho et al., 2009; Dreux et al., 2013). Polymorphisms in the *fimH* type 1 pilus subunit sequence have been reported in AIEC strains which confer a higher adhesion ability (Dreux et al., 2013). This, combined with the overexpression of CEACAM-6 receptors in CD, has been suggested to enhance the ability of AIEC to colonise the ileal mucosa. The subsequent colonisation of AIEC promotes the secretion of IFN-γ and TNF-α by macrophages and lymphocytes, leading to an upregulation of CEACAM-6 expression (Glasser and Darfeuille-Michaud, 2008). Therefore, an amplification loop of colonisation and inflammation has been postulated, suggesting AIEC promote their own colonisation in CD (Figure 1.5).

In addition, Sheikh et al identified CEACAM-6 as a major binding receptor for ETEC. In this study, a CEACAM-6 knock-out IEC line was generated using CRISPR-Cas9, which displayed a notable decrease in ETEC adhesion. In addition, treatment of Caco-2 cells with CEACAM-5 siRNA resulted in significant decreases in adhesion, however, this was not true of CEACAM-6$^{-/-}$ cells treated with the same siRNA. Moreover, Sheikh et al showed that in the absence of *fimH* or in the presence of mannose, ETEC binding of CEACAM-6 was drastically reduced, suggesting the interaction is largely dependent on type 1 fimbriae expression and assembly. Furthermore, it was demonstrated that soluble recombinant CEACAM-6 interacted with target FimHLD, but not with FimHLD$_{Q133K}$ containing a point mutation in the mannose binding pocket (Sheikh et al., 2020).

As ETEC targets the small intestine, Sheikh et al utilised an ileal enteroid model in their studies, where transmission electron microscopy of small intestinal enterocytes demonstrated CEACAM-6 associated with microvilli and with the glycocalyx at the tips of the microvilli. Marked accumulation of CEACAM-6 surrounding sites of bacterial attachment and significantly more bacteria attached to epithelial cells exhibiting strong CEACAM-6 expression was observed (Sheikh et al., 2020). Furthermore, ETEC closely associated with apical CEACAM-6 expression and observed distinct ‘foot printing’ of CEACAM-6 surrounding adherent bacteria (Sheikh et al., 2020).

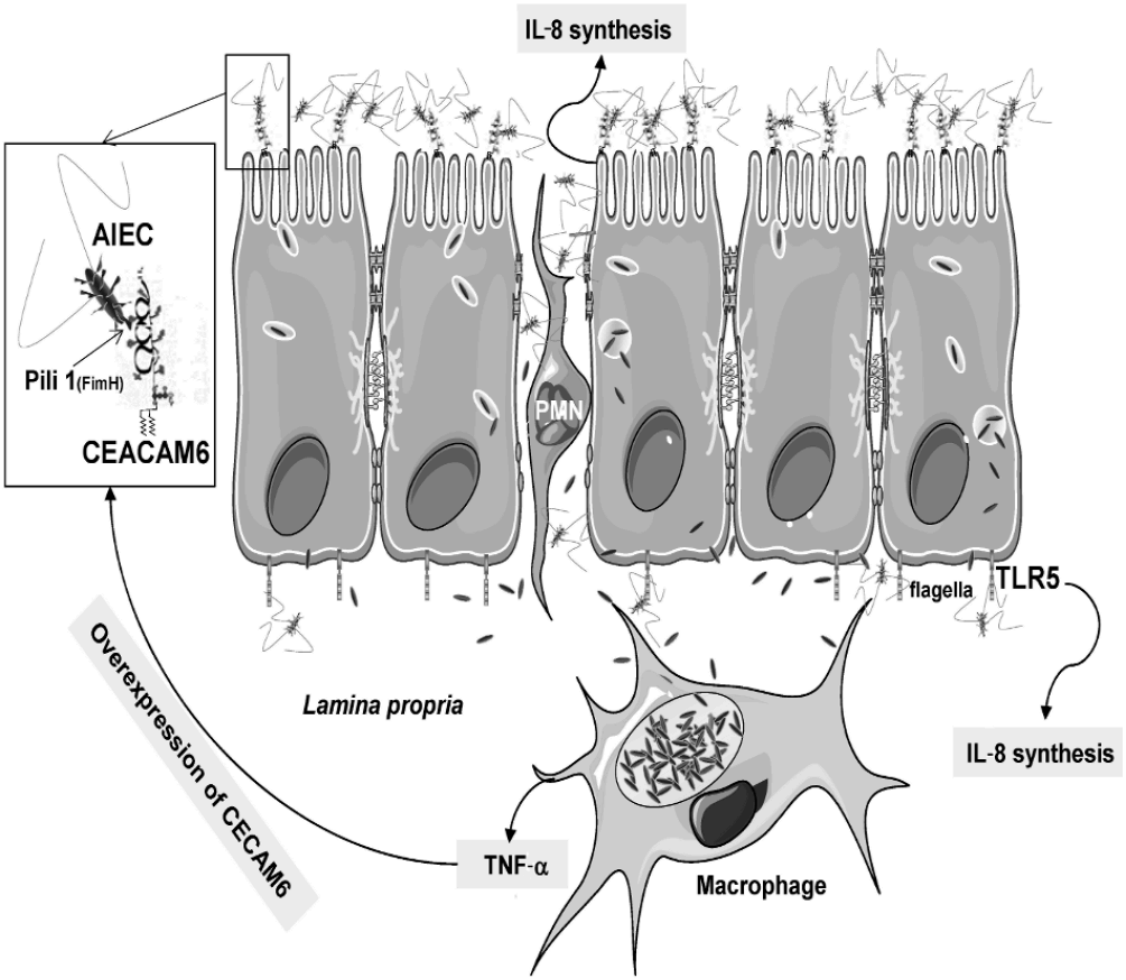

Figure 1.5. AIEC colonisation of the ileal mucosa through FimH-CEACAM-6 interaction. AIEC has previously been shown to adhere to CEACAM-6 via type 1 pili. CEACAM-6 is highly expressed by IECs of CD patients. AIEC adherence induces IL-8 secretion through signalling via flagellin and TLR5 and transmigration of polymorphonuclear leukocytes (PMNs). AIEC cross the mucosal barrier and replicate within macrophages lying beneath the epithelial barrier, inducing TNF-α secretion. Stimulation of IECs by TNF-α secretion from AIEC-infected macrophages induces the overexpression of CEACAM-6 on the ileal surface, leading to an amplification loop of colonisation and inflammation (Glasser and Darfeuille-Michaud, 2008).

1.5.1.1.2 Flagellin regulation and TLR5

In addition to type I pili, flagella have been shown to play a role in the adhesion of AIEC to IECs through motility and indirectly by regulating type 1 pili expression (Barnich et al., 2003; Nakamura and Minamino, 2019). A study by Sevrin et al used a gene reporter system to demonstrate that the *fliC* gene was upregulated in AIEC in response to bile salts and mucus. In medium supplemented with 1% bile salts, the *fliC* promoter was activated in LF82 but not in commensal *E. coli* strain HS (Sevrin et al., 2020). AIEC may therefore express flagella when they contact mucus in order to cross it.

1.5.1.1.3 Long polar fimbriae (LPF) binding to M cells

Specialised M cells are located on the follicle-associated epithelium overlying mucosa-associated lymphoid tissues, such as Peyer's Patches (PP) in the small intestine. M cells actively transport luminal antigens through the epithelium to initiate an immune response (Kobayashi et al., 2019). AIEC can interact with the host through M cells, via expression of Long Polar Fimbriae (LPF). LPF bind to transcytotic receptor GP2 which is specifically expressed on the apical plasma membrane of M cells (Hase et al., 2009). It has been shown that LPF expression is key for AIEC interaction with PP, as an *lpf*-negative AIEC mutant was highly impaired in its ability to interact with both mouse and human PP and was unable to translocate across M cells into underlying lymphoid tissue (Chassaing et al., 2013; Keita et al., 2020). In addition, the presence of bile salts is required for AIEC LPF expression under the control of the transcription factor GipA (Vazeille et al., 2016). Bile salts act as an activator of *lpf* transcription, with a dose-dependent response, subsequently promoting AIEC strain LF82 interaction with PP and M cells (Chassaing et al., 2013). Furthermore, both AIEC and *Salmonella* LPF facilitate bacterial binding to PP *in vitro* and *in vivo* (Bäumler et al., 1996; Chassaing et al., 2011), suggesting a potential ligand specific to PP.

1.5.1.1.4 ChiA-Chitinase 3-Like-1 Interaction

ChiA is another adhesin that mediates AIEC adherence to IECs. ChiA binds to inducible Chitinase 3-Like-1 (CHI3L1), an enzymatically inactive N-glycosylated chitinase within the glycohydrolase 18 family that is overexpressed in colonic epithelial cells during inflammation, including CD and UC, but is absent in normal controls (Chen et al., 2011; Mizoguchi, 2006). In mice with colitis, this interaction is mediated specifically by recognition of the N-glycosylation of asparagine 68 residue and promotes AIEC pathogenicity (Low et al., 2013). Interestingly, AIEC LF82 harbours five conserved polymorphisms in *chiA* which confer increased binding to CHI3L1 when compared with non-pathogenic *E. coli* K-12, supporting the role of ChiA in promoting AIEC virulence.

1.5.1.1.5 Biofilms

To persistently colonise the intestinal mucosa, commensal bacteria often form biofilms (Hall-Stoodley and Stoodley, 2005). These are communities of cells held together and attached to a surface by a self-produced extracellular matrix, consisting of exopolysaccharide (EPS), extracellular DNA (eDNA) and adhesive proteins such as curli and type 1 pili (Kostakioti et al., 2013). Biofilm formation is also associated with bacterial pathogenesis, allowing for increased resistance to environmental stress, antibiotics, and clearance by the immune system (Shree et al., 2023). Martinez-Medina et al. reported biofilm formation as a phenotypic feature of AIEC *in vitro*, demonstrating that AIEC have stronger biofilm formation abilities than non-AIEC strains isolated from the intestinal mucosa (Martinez-Medina et al., 2009b). Results indicated a positive correlation between adhesion, invasion and the specific biofilm forming index of AIEC, suggesting the machinery required for the AIEC phenotype, including type I pili and flagella, are shared with those required for biofilm formation. The composition of AIEC biofilms remains to be fully elucidated. Amyloid curli fibrils are produced by *Enterobacteriaceae* including resident intestinal

E. coli and invading enteric pathogens such as *Salmonella* (Ellermann and Sartor, 2018). Whilst curli contribution to the AIEC inflammatory phenotype is yet to be investigated, infectious colitis models show contrasting results. Curli reduces epithelial permeability and bacterial translocation and enhances epithelial secretion of IL-8 in *S*. Typhimurium. Meanwhile AIEC production of cellulose, a biofilm-associated extracellular polysaccharide, has been shown to increase induction of colitis in mice (Ellermann et al., 2015).

AIEC LF82 has been shown to form biofilms on the surface of IECs through activation of the σ^E stress response, which links outer membrane homeostasis to biofilm-associated persistence. The σ^E factor, also called RpoE, coordinates this response in *E. coli* by sensing perturbations in outer membrane protein (OMP) folding and assembly that arise during adherence and growth under gastrointestinal conditions. Envelope stressors such as heat shock, overexpression of outer membrane protein (OMP)-encoding genes, and mutations in genes encoding chaperones required for OMP folding, ultimately leads to the accumulation of misfolded OMPs in the periplasm. As a result, RpoE activation and transcription of the stress-adaptive regulon occurs. This includes *htrA*, encoding a periplasmic protease–chaperone that refolds or removes damaged OMPs, and *yfgL*, a component of the β-barrel assembly machinery required for efficient OMP insertion into the outer membrane, thereby sustaining envelope integrity during biofilm growth. In LF82, high osmolarity, like that of the gastrointestinal tract, increases OmpC expression, activating the σ^E pathway and promoting stable surface attachment (Rolhion et al., 2007). σ^E signalling further modulates biofilms by regulating type 1 pili and flagellar expression and is required for LF82 biofilm formation and intestinal mucosal colonisation, highlighting RpoE-mediated envelope stress adaptation as a key determinant of AIEC biofilm-associated persistence in the inflamed gut (Chassaing and Darfeuille-Michaud, 2013).

LF82 has been shown to form intracellular biofilms, also called intracellular bacterial communities (IBCs) in macrophages. Previously, IBCs have only been described in the invasion of urothelial cells lining the bladder by uropathogenic *E. coli* (UPEC),

allowing UPEC to escape host defence and persist despite treatment with antibiotics (Anderson et al., 2003; Scott et al., 2015). Prudent et al have shown that LF82 microcolonies form IBCs with an extracellular matrix composed of exopolysaccharides, and curli fibres surrounding each bacterium, inside phagolysosomes (Prudent et al., 2021). This not only indicates that LF82 can form biofilms, but also that IBCs could promote LF82 survival within macrophages. Biofilms on the epithelium provide resistance to stress, therefore IBCs confined within the phagolysosomal membrane may prevent lysosomal degradation. This may be important in the long term if macrophages die and release IBCs, which in turn may provide LF82 with protection from antibiotics or phagocytosis by another macrophage. This could explain the resurgence of AIEC in CD patients.

1.5.1.2 AIEC invasion of the intestinal epithelium

The mechanism of AIEC invasion involves macropinocytosis and vacuolization of the bacteria into IECs and macrophages. It is characterised by the elongation of membrane extensions which surround the bacteria at the site of contact where invading bacteria meet epithelial cells. AIEC then survive and replicate in the host cell cytoplasm after lysis of the endocytic vacuole (Boudeau et al., 1999).

AIEC adherence via type 1 pili and long polar fimbriae (LPF) is associated with invasion. The *ibeA* gene, present in several AIEC strains including NRG857c, UM146, KD-1, and LF82, encodes the virulence factor IbeA, an invasin that promotes host cell entry, intramacrophage survival, and heightened inflammatory responses. A deletion of *ibeA* in NRG857c confers a significant reduction in the invasion of Caco-2 cells. The mutation also decreased AIEC survival within THP-1 macrophages in the first 24 hours of infection, however adhesion was not affected (Cieza et al., 2015). This observation therefore suggests that adherence does not necessarily trigger invasion and *ibeA* may have a function in AIEC invasion and intracellular survival.

1.5.1.2.1 Outer membrane vesicles

Whilst invasion is considered to be mediated by the delivery of effector proteins to host cells, AIEC do not possess a type 3 secretion system (T3SS) which is utilised by other intracellular bacteria including *Salmonella*, *E. coli* and *Chlamydia* species. (Carabeo et al., 2002; Kim et al., 2005; Ramos-Morales, 2012; Suárez and Rüssmann, 1998). An alternative method of effector delivery includes outer membrane vesicles (OMVs), which are vesicles derived from the outer membrane and have been shown to transport bacterial effector proteins such as the *E. coli* ClyA cytolysin and *Pseudomonas aeruginosa* Cif protein (Bomberger et al., 2009; MacEachran et al., 2007). In AIEC, deletion of the *yfgL* gene which encodes an outer membrane lipoprotein involved in the synthesis and degradation of peptidoglycan, resulted in reduced release of OMVs and decreased invasion of LF82 in IECs. Notably, AIEC invasion was restored by pre-treatment of cells with OMVs, thereby suggesting OMVs are required for AIEC invasion (Rolhion et al., 2005). OmpA is the major protein on the surface of OMVs. It is a multifaceted protein with diverse roles in adhesion, invasion, and persistence of intracellular bacteria, including UPEC, EHEC and *E. coli* K-1 (Nicholson et al., 2009; Torres and Kaper, 2003; Weiser and Gotschlich, 1991). OmpA binds to the endoplasmic reticulum (ER)-localised stress response protein Gp96, which is overexpressed on the apical surface of ileal IECs in CD patients. It is suggested that the OmpA-Gp96 interaction supports OMV fusion with IECs and promotes AIEC invasion by delivering virulence factors that contribute to the invasion process into host cells (Rolhion et al., 2010). However, these virulence factors are yet to be characterised in AIEC.

Interestingly, co-localisation of Gp96 and CEACAM-6 has been observed on the apical surface of ileal epithelial cells in CD patients (Rolhion et al., 2010). As previously mentioned, CEACAM-6 acts as a receptor for type 1 pili, allowing AIEC colonisation of the ileal mucosa and promotion of inflammation. Therefore, overexpression of both CEACAM-6 and Gp96 in patients with CD should increase

AIEC virulence, as the CEACAM-6-FimH and AIEC OMV- Gp96 interactions would allow for mucosal colonisation and invasion of the ileal epithelium, respectively.

1.5.1.2.2 Translocation through M cells

Many gastrointestinal pathogens including *Salmonella*, *Shigella* and *Vibrio* species invade the intestinal epithelium by transcytosis via M cells in the follicle-associated epithelium of the small intestine. In *E. coli*, several studies have reported bacterial translocation through M cells: Enteropathogenic *E. coli* (EPEC) binds specifically to M cells in a Caco-2/Raji-B cell co-culture model (Pielage et al., 2007), and translocation is increased by the presence of M cells (Martinez-Argudo et al., 2007). Similarly, Keita et al. showed higher LF82 translocation in Caco-2/Raji-B co-cultures compared with Caco-2 monocultures, suggesting that the presence of M cells facilitates AIEC passage across the intestinal epithelium (Keita et al., 2020).

1.5.1.3 AIEC intracellular survival and replication

In addition to epithelial adherence and invasion, AIEC virulence has also been linked to their ability to survive and replicate within mucosal macrophages. Macrophages engulf bacteria within phagosomes which rapidly evolve into bactericidal phagolysosomes. During this maturation, the phagosomes acidify and interact with the endocytic pathway (Lee et al., 2020). Some intracellular pathogens including *Salmonella*, *Shigella* and *Listeria* spp. can interfere with the endocytic pathway and escape degradation by the host, having evolved different strategies to find a successful intracellular replication niche (Gutierrez and Enninga, 2022). AIEC strain LF82 can also replicate in phagolysosomes through the induction of the stress gene *htrA*, which is essential in *E. coli* for protection against high temperatures, the oxidoreductase *dsbA* gene, required for disulfide bond formation and the *gipA* gene, supporting intramacrophage replication (Bringer et al., 2005). This is despite the acidic pH, oxidative stress, proteolytic enzymes, and antimicrobial compounds.

However, the mechanism by which AIEC can resist macrophage degradation is yet to be explained. Bringer et al demonstrated that the acidic environment is required for LF82 replication within macrophages. In contrast to many other pathogens, LF82 does not escape from the endocytic pathway or infiltrate autophagy but may have evolved from non-pathogenic bacteria whereby an acidic pH acts as a key signal for the activation of virulence gene expression (Bringer et al., 2006).

1.5.1.4 AIEC and cytokine production

Given that pro-inflammatory cytokine secretion plays an important role in altered intestinal permeability, it may be associated with AIEC infection and pathogenesis. The production of cytokines is important for recruiting immune cells such as dendritic cells and neutrophils to the site of infection. Mazzarella et al showed that LF82 induced expression of TNF-α, IL-8, and IFN-γ transcripts in colonic biopsies of CD patients (Mazzarella et al., 2017). Furthermore, LF82 can activate NF-κB signalling in IECs through the phosphorylation of IkB-α, NF-κB p65 nuclear translocation and TNF-α secretion (Jarry et al., 2015). Binding of flagella to TLR5 on IECs induces production of hypoxia-inducible factor-1α (HIF1α) and activates the NF-κB pathway and IL-8 secretion, increasing the inflammatory response (Mimouna et al., 2011). Furthermore, significantly increased levels of IL-1β, IL-6, and IL-17 mRNAs (5.5-fold, 3.4-fold, and 6.1-fold, respectively) and significantly decreased levels of IL-10 mRNAs (5.6-fold) were observed in colonic specimens of CEABAC10 mice infected with AIEC LF82 compared with those of noninfected mice, mediated by type 1 pili and flagella expression (Carvalho et al., 2009, 2008). In addition, AIEC infection has demonstrated increased IL-8 secretion by Caco-2 cells (Sasaki et al., 2007) and T84 cells (Elatrech et al., 2015). Mossman et al. also observed FimH stimulation of TLR4 leads to potent TNF-α and IL-8 secretion *in vitro* (Mossman et al., 2008). Finally, AIEC promoted release of IL-6, IL-8 and TNF-α from T84 cells by stimulating TLR4 expression (Guo et al., 2018).

1.5.1.5 AIEC disruption to epithelial barrier function

In CD patients, deficient barrier function is frequently observed, with abnormalities in tight junctions documented in several studies (See - 1.3.3 Cytokine-mediated reduction of barrier function) (Lee, 2015). Interestingly, infection of IECs with AIEC decreased the transepithelial electrical resistance by delocalizing the tight junction protein ZO-1 (Sasaki et al., 2007; Wine et al., 2009). In addition, one of the effectors of IBD inflammation, TNF-α, may modulate the transcription of tight junction proteins. TNF-α promotes epithelial permeability by inducing apoptosis of enterocytes, increasing their shedding rate, and obstructing the redistribution of tight junctions (Michielan and D'Incà, 2015).

Notably, a CEABAC10 mouse model indicates that the overexpression of CEACAM genes is associated with increased intestinal permeability (Denizot et al., 2012). As previously described, increased expression of CEACAMs in the ileal mucosa of CD patients has been noted. AIEC may therefore take advantage of the disrupted intestinal barrier in CD patients which facilitates bacterial penetration of the epithelial barrier.

1.5.1.6 Interaction of AIEC with the mucus layer

Elatrech et al demonstrated that AIEC LF82 inhibited mucin gene expression of MUC2 and MUC5A in T84 cells (Elatrech et al., 2015). AIEC LF82 has also been shown to exhibit mucinolytic activity. The viscosity of mucus was decreased by the Vat-AIEC mucinase, rendering the mucus layer more permeable to AIEC infection (Gibold et al., 2016). In addition, upregulation of Vat-AIEC mucinase expression by bile salts and mucus enhanced AIEC colonisation in a CEACAM-overexpressing mouse model of CD (Carvalho et al., 2009)

1.5.1.7 Resistance to antimicrobial peptides

Antimicrobial peptides (AMPs) are secreted by IECs and regulate host-microbe homeostasis by killing bacteria. Predominant AMPs include α- and β-defensins, cathelicidins, RegIII family antimicrobial lectins and lysozyme which diffuse into the mucus layer, following a concentration gradient (Bevins and Salzman, 2011). To cross the mucus layer, AIEC must either develop resistance to AMPs or capitalise on deficiencies in AMP production in CD patients. McPhee et al have shown that AMP resistance contributes to host colonisation by AIEC in CD. They identified a plasmid-encoded genomic island (PI-6) in AIEC strain NRG857c which confers high-level resistance to α- and β-defensins. In particular, *arlA* which encodes a Mig-14 family protein is implicated in defensin resistance, and *arlC*, an OmpT family outer membrane protease confers host defense peptide resistance. Deletion of PI-6 rendered AIEC NRG857c sensitive to α- and β-defensins and reduced its competitive fitness in a mouse infection model (McPhee et al., 2014).

1.6 Type VI Secretion System

Although AIEC LF82 does not encode any T3SS, the presence of two Type VI Secretion Systems (T6SS) has been shown (Massier et al., 2015). The T6SS is a specialised secretion system harboured by Gram-negative bacteria that delivers toxins into both eukaryotic and prokaryotic cells. It is a nanomachine with a bacteriophage tail-like structure that assembles to release effector proteins into the environment or target cells for competitive survival for the same colonizing niche or pathogenicity (Hernandez et al., 2020; Lazzaro et al., 2017; Lien and Lai, 2017). The T6SS is expressed in multi-species environments including the gut, for example the antibacterial T6SS in *Salmonella* Typhimurium helps establish infection by killing commensal bacteria to successfully colonise the host gut (Sana et al., 2016).

The genes encoding T6SS components and toxins are typically grouped and clustered into genetic islands. These islands have a different GC content than the core genome, suggesting they have been acquired by horizontal gene transfer (Bingle et al., 2008; Boyer et al., 2009; Cascales, 2008). In *E. coli*, T6SS gene clusters are categorised into three distinct phylogenetic groups: T6SS-1, T6SS-2 and T6SS-3 (Journet and Cascales, 2016). AIEC LF82 encodes two T6SSs including one T6SS-1 and one T6SS-3 (Miquel et al., 2010; Nash et al., 2010).

1.6.1 Structure of the T6SS

The T6SS is a multiprotein machine that uses a spring-like mechanism to inject effectors into target cells (Figure 1.6). The trans-envelope core TssJLM complex is bound to the membrane and anchors the injection system. It orientates towards the cell exterior and has a 79 Å pore, where the TssD (Hcp) needle is fired through to puncture the target cell. A contractile tail tube/sheath complex is built on an inner membrane bound TssEFGK baseplate. The needle, or inner tube, is topped by the spike complex consisting of TssI (VgrG) and a PAAR-domain protein and is

propelled outside of the cell by contraction of the TssBC sheath, which surrounds the needle. Effector proteins are loaded within the inner tube or on the spike complex prior to firing, targeting either prokaryotic and/or eukaryotic cells. Following firing of effectors, the TssBC sheath is disassembled by TssH, allowing the system to reassemble and fire in a new location (Cherrak et al., 2019).

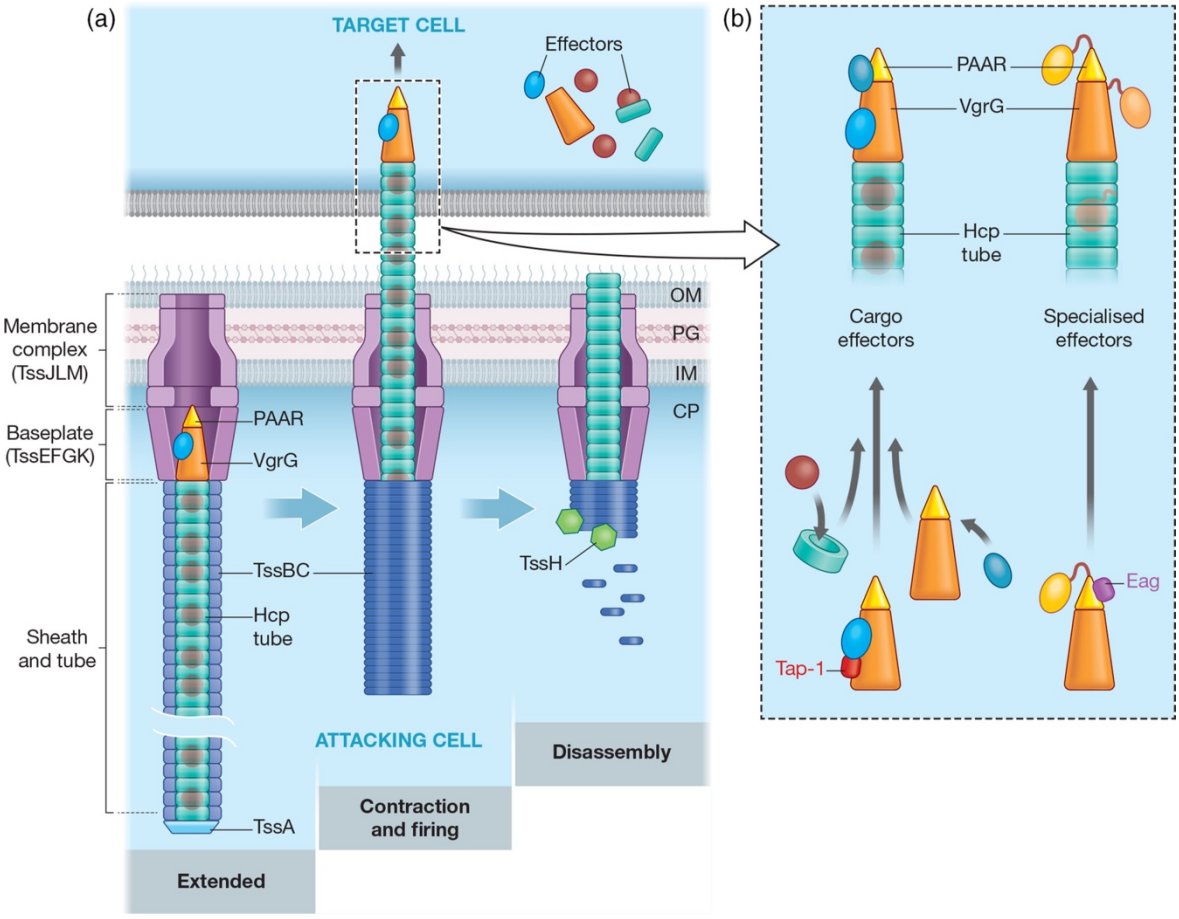

Figure 1.6. Schematic representation of T6SS assembly, firing and disassembly and the different modes of T6SS effector delivery. (a) Schematic representation of assembly, firing and disassembly of the T6SS. CP, cytoplasm; IM, inner membrane; OM, outer membrane; PG, peptidoglycan cell wall. (b) Schematic representation of the different modes of delivery of T6SS effectors. Effectors delivered by the T6SS can be classified as either “cargo” or “specialised” effectors, based on their interaction with the components of the puncturing structure (Hcp, VgrG or PAAR) (Hernandez et al., 2020).

1.6.2 T6SS and AIEC Invasion

Studies into the role of a T6SS in AIEC invasion are limited and have shown conflicting results. Massier et al demonstrated that deletion of one or both T6SS-encoding pathogenicity islands (PAI) in LF82 decreased invasion of T84 cells (Massier et al., 2015). However, the results also described decreased motility in LF82 T6SS mutants, which may explain the reduction in host cell invasion. Meanwhile, LF82 mutants in the structural *tssE1* gene (*ΔtssE1*) showed increased invasion levels compared to the wild-type, whilst no difference was observed for *ΔtssE3*, suggesting that LF82 T6SS-3 has no role in invasion, whilst T6SS-1 inhibits invasion (Cogger-Ward, 2020). In addition, no AIEC specific T6SS effector proteins have been characterised, however various pathogens utilise T6SS effectors, suggesting a T6SS may play a role in other methods of pathogenesis.

1.6.3 T6SS Effectors

1.6.3.1 Anti-eukaryotic effectors

The T6SS can deliver effectors that target numerous cellular processes and structures in eukaryotic cells. Such effectors may assist host cell invasion by resisting phagocytosis, promoting intracellular survival, replication and thus, pathogenesis.

1.6.3.1.1 Disruption of the actin cytoskeleton

Many anti-eukaryotic T6SS effectors target the actin cytoskeleton of host cells. An example is seen in *Aeromonas hydrophila*, whereby VgrG1 employs actin ADP-ribosylase activity, preventing actin polymerisation and inducing caspase 9-mediated apoptosis (Suarez et al., 2010). Meanwhile, in *Vibrio cholerae*, VgrG1 has

an actin crosslinking domain which inhibits cytoskeleton rearrangement and phagocytosis, facilitating intracellular survival and causing inflammatory diarrhoea *in vivo* (Ma and Mekalanos, 2010). Furthermore, TecA in *Burkholderia cenocepacia* disrupts the actin cytoskeleton of macrophages by deamidating Rho GTPases, triggering inflammation through activation of the Pyrin inflammasome (Aubert et al., 2016). In *Vibrio proteolyticus*, the effector Vpr01570 induces cytoskeleton rearrangements in macrophages (Ray et al., 2017).

1.6.3.1.2 Host cell invasion

In addition to cytoskeletal disruption, other T6SS effectors have been demonstrated to promote bacterial internalisation, intramacrophage growth and phagosomal escape to effectively invade the host. In *P. aeruginosa*, the effector domain of VgrG2b is delivered into epithelial cells, where it interacts with the γ-tubulin ring complex of microtubules to promote internalisation by non-phagocytic cells (Sana et al., 2015). In addition, phospholipase effectors PldA and PldB in *P. aeruginosa* promote host cell invasion via the activation of the PI3K/Akt signalling pathway (Jiang et al., 2014). Lastly, *B. pseudomallei* employs the VgrG5 phospholipase to induce host cell fusion and cell-to-cell spread of bacteria, where the C-terminal domain inserts into the host cell membrane to mediate a fusion event and multinucleated giant cell formation in infected macrophages and HEK293 cells (Schwarz et al., 2014; Toesca et al., 2014).

1.6.3.2 Anti-fungal effectors

Recent studies have also identified two T6SS effectors specifically targeting fungal cells by *Serratia marcescens*. Tfe1 and Tfe2 are anti-fungal effectors that cause plasma membrane depolarisation and disruption to nutrient transport and metabolism respectively. Ultimately, this leads to fungal cell death or the induction of autophagy as a starvation response (Trunk et al., 2018). Such T6SS effectors are

likely present across the microbial community and may influence gut colonisation, which could be significant in the context of CD-associated microbiome changes and AIEC infection.

1.6.3.3 Anti-bacterial effectors

The majority of T6SS effectors have been associated with anti-bacterial activity. The T6SS can deliver various anti-bacterial effectors with a diverse range of functions into neighbouring bacterial cells to induce lysis or growth inhibition (Hernandez et al., 2020). Several T6SS anti-bacterial effectors have been identified in *E. coli* species. For example, the Tle1 phospholipase in enteroaggregative *E. coli* (EAEC) and ETEC can mediate competition *in vitro* by disrupting the cell membrane of competing bacteria, leading to growth inhibition (Flaugnatti et al., 2016; Ma et al., 2017). In EHEC, T6SS-mediated HNH-DNase activity inhibits bacterial growth of related *Enterobacteriaceae* species (Ma et al., 2017). Meanwhile, in *Salmonella* Typhimurium, the T6SS Tae4 amidase promotes niche establishment in a mouse model by eliminating competing members of the microbiota (Sana et al., 2016). Whilst Tae and Tge toxins are antibacterial only, members of the Tle and Tde toxin families target both eukaryotic and prokaryotic cells (Navarro-Garcia et al., 2019). It has previously been described that the T6SS-1 cluster of AIEC LF82 carries putative phospholipases of the Tle3 family (Journet and Cascales, 2016), therefore the T6SS in LF82 may have anti-bacterial effects that facilitate niche establishment in the gut as seen in *Salmonella* Typhimurium.

1.7 AIEC therapeutic targets

1.7.1 Antibiotics

Due to the increasing prevalence of multidrug-resistant bacteria, promotion of pathogenic bacterial growth and the dysbiosis of the intestinal microbiome, antibiotics are a less popular therapeutic option (Nitzan, 2016). In IBD, antibiotics have shown poor efficacy and are typically only used to treat complications such as bacterial infection post-surgery (Gionchetti et al., 2017). A systematic review suggests that certain antibiotic therapies could be useful in inducing and maintaining remission, such as clarithromycin and rifampin. However, Martinez-Medina et al. demonstrated that antibiotic resistance in AIEC differs between strains, therefore identification of AIEC and characterisation of antimicrobial resistance profiles could be critical in preventing poor clinical outcomes in CD patients (Martinez-Medina et al., 2020). Therefore, antibiotics should be used with caution and alternative therapies explored.

1.7.2 Anti-adhesive molecules

Given the well-characterised CEACAM-6-FimH interaction in the adherence of AIEC to IECs, the use of anti-adhesive compounds against AIEC is an attractive therapeutic option. FimH antagonists have been developed, whereby small glycomimetic molecules saturate the carbohydrate recognition domain (CRD) of FimH, mimicking a ligand. By blocking the CRD, AIEC are unable to bind to the epithelium and are removed from the gut (Alvarez Dorta et al., 2016; Brument et al., 2013; Chalopin et al., 2016; Sivignon et al., 2015b). In addition, blocking FimH has the potential to prevent an inflammatory reaction from IECs and macrophages as a result of AIEC interaction with TLR4 (Mossman et al., 2008).

A specific FimH blocker, TAK-018, inhibits adhesion of AIEC strains LF82 and NRG857c to T84 cells and primary ileal cells in a dose-dependent manner and prevents inflammation, preserving mucosal integrity (Chevalier et al., 2021). TAK-018 is currently undergoing clinical trials. The advantage of such FimH antagonists is that AIEC can be cleared without disturbing the intestinal microbiome.

1.7.3 Dietary interventions

Given that a western diet influences microbiome changes, dietary interventions could help control disease and target AIEC. *E. coli* adhesion to IECs can be inhibited with fibre such as soluble plantain non-starch polysaccharide (Martin et al., 2004). In addition, studies have shown that Vitamin D-deficient dextran sodium sulfate (DSS)-treated mice exhibited epithelial barrier dysfunction, colonic injury and greater susceptibility to AIEC colonisation. Additionally, pre-incubation of Caco-2 cells with Vitamin D protected against AIEC-induced barrier disruption, including TEER and tight junction integrity (Assa et al., 2015). Therefore, vitamin D supplementation may reduce risk of AIEC infection.

1.7.4 Probiotics and postbiotics

Probiotics present a potential therapeutic option to control AIEC-mediated intestinal inflammation. A study by Sivignon et al. showed that *Saccharomyces cerevisiae* CNCM I-3856 inhibited LF82 epithelial adhesion and reduced inflammation and colitis in CEABAC10 mice (Sivignon et al., 2015a). Furthermore, AIEC survival and growth was reduced during co-culture with *Lactobacillus rhamnosus* GG and *Lactobacillus reuteri* 1063 (Van Den Abbeele et al., 2016). However, there have been reports of increased inflammation in IBD mucosal explants exposed to probiotics due to bacterial translocation into the mucosa (Tsilingiri et al., 2012). Further studies into the safety and efficacy of probiotics are therefore required in patients with IBD.

Probiotic bacteria produce soluble factors which could provide an alternative therapeutic option. Bacteriocins, such as colicins, are postbiotic proteins that are effective against specific species of bacteria. Colicins E1 and E9 have been shown to kill AIEC strains LF82, HM95, HM419 and HM615 effectively in comparison with metronidazole and ciprofloxacin and did not induce damage to IECs or macrophages (Brown et al., 2015). Whilst colicins present potential in targeting AIEC due to their selectivity without harming the remaining microbiome, further *in vivo* studies are required to determine their efficacy and side effects.

1.7.5 Faecal microbiota transplantation (FMT)

Faecal microbiota transplantation (FMT) is a method of modifying the composition of the microbiota and has demonstrated high efficacy in treating recurrent *Clostridium difficile* infection (Brandt et al., 2012). In theory, FMT could restore a 'healthy' intestinal microbiota and reverse the changes and immune mucosal stimulation seen in CD, which could create an environment less suitable for AIEC colonisation (Agus et al., 2014). Studies using FMT as a therapeutic intervention in IBD have shown inconclusive results, however this could be due to different methods, donors and disease status (Colman and Rubin, 2014; Moayyedi et al., 2015; Rossen et al., 2015). One study in DSS-induced colitis mice demonstrated that AIEC exacerbated gut dysbiosis and led to resistance to restoring the normal gut microbiota by FMT (Xu et al., 2021). Therefore, the presence of AIEC may impact the efficacy of FMT by preventing colonisation of donor-derived bacteria, however further studies into the impact of FMT on AIEC colonisation are required.

1.7.6 Phage Therapy

Bacteriophages are viruses which infect bacteria and are found in a range of environments including the human GI tract. An advantage of bacteriophages is that they are highly specific and can be targeted to distinct bacterial strains. This is beneficial as it restricts their impact on microbiome composition, as opposed to antibiotic use which results in non-specific bacterial killing (Kakasis and Panitsa, 2019).

The potential of bacteriophages to decrease AIEC colonisation of the intestine has been demonstrated, whereby a cocktail of three bacteriophages isolated from wastewater, LF82_P2, LF82_P6 and LF82_P8, significantly decreased the number of AIEC in faeces and in the adherent flora of intestinal sections in CEABAC10 transgenic mice. In addition, the cocktail reduced ileal and colonic colonisation of AIEC LF82 and decreased symptoms of DSS-induced colitis in mice (Galtier et al., 2017). Currently, a clinical trial is underway aimed at using an AIEC-specific bacteriophage cocktail (EcoActive) to target AIEC load, levels of inflammatory markers CRP and faecal calprotectin, and disease activity in 30 CD patients (NCT03808103).

1.7.7 Induction of autophagy

When functional, autophagy limits intracellular replication of AIEC, thus reducing their persistence. However, as described previously (See - 1.2.1 Genetic association in CD) genetic variants in autophagy-related genes are associated with CD, particularly *ATG16L, IRGM* and *NOD2*. Lapaquette et al. showed that pharmacological induction of autophagy with rapamycin and physiological induction with starvation significantly decreased the number of intracellular AIEC and secretion of pro-inflammatory cytokines in *NOD2*$^{-/-}$ murine macrophages (Lapaquette et al., 2012). This presents an opportunity for therapies targeted at

inducing autophagy to reduce AIEC colonisation. However, the efficacy of autophagy activation in CD patients harbouring defective autophagy genes would need to be evaluated.

1.8 Intestinal model systems

Human gut physiology is highly dynamic and complex, due to the various cell types of the epithelium and exogenous factors such as oxygen concentration, pH, mucus density, peristalsis, epithelial morphology and barrier function. Furthermore, the gut is inhabited by large microbial communities which contribute to intestinal homeostasis by playing key roles in SCFA and vitamin K production. Various *in vitro* and *ex vivo* models have been developed over recent years to model gut physiology, intestinal barrier function and host-microbe interaction in healthy and diseased conditions to allow for the study of gastrointestinal diseases (Rahman et al., 2021).

1.8.1 Cell culture

Cell culture has been extensively used in the study of host-pathogen interactions in GI diseases. Cell lines commonly used as models of the intestinal epithelial barrier are Caco-2, HT-29 and T84 human colon carcinoma cells. In culture, Caco-2 and HT-29 cells undergo spontaneous differentiation to form a monolayer reminiscent of enterocytes, with properties including an apical brush border of microvilli like that of the epithelium of the small intestine (Sambuy et al., 2005). In contrast, T84 cells resemble colonocytes, displaying significantly shorter microvilli and retaining their original colonic characteristics throughout differentiation (Devriese et al., 2017). The polarised orientation of these cell lines is especially useful for permeability and transport studies, which require the separation of the apical and basolateral sides. Caco-2 and T84 cells can be grown on Transwell inserts that are placed in a multi-well tissue culture plate, establishing a two-chamber system separated by the permeable membrane of the insert. Using these inserts further differentiates the cell monolayer and allows investigation of barrier function of cells by measurement of

TEER. Polarisation of cells is important when studying functional responses of the epithelium, as many cell surface receptors are distributed asymmetrically on apical and basolateral membranes. In addition, Caco-2, HT-29 and T84 cells express TLRs, making them useful for studying host-microbe interactions (Furrie et al., 2005).

Previous studies of AIEC interactions with human intestinal epithelia have used Caco-2 and T84 cell lines. For example, Boudeau et al. characterised AIEC adherence and invasion in Caco-2 cells (Boudeau et al., 1999). T84 cells have been used to demonstrate that AIEC induce reactive oxygen species (ROS) production by intestinal NADPH and alter mucin and IL-8 expression, leading to inflammation in CD (Elatrech et al., 2015).

Despite the advantages of human cell lines, including cost-effectiveness and ease of use, they exhibit limitations. They only represent one cell type of the intestinal epithelium (i.e. absorptive enterocyte/colonocyte), lack a mucus layer and harbour considerable genetic and phenotypic changes, which is likely to affect their response and interaction with the microbiota (Vogelstein and Kinzler, 2004). The cancerous origin of Caco-2, HT-29 and T84 cells and lack of epithelium-specific functions seen *in vivo* exemplify the need for more physiologically relevant models.

1.8.2 Microaerobic model systems

When studying host-microbe interactions in the intestine, microaerobic conditions are important environmental cues for GI pathogens. Therefore, various microaerobic systems have been developed to allow IEC culture in a physiologically relevant apical anaerobic environment (Von Martels et al., 2017). These involve compartmentalisation of the apical and basal environment surrounding IECs, allowing the maintenance of low-oxygen on the apical side whilst supplying the host cells with oxygen on the basal side. Each model system achieves this at different levels of complexity depending on the goal of the research. For example, the Human-Microbe crosstalk model (HuMiX) is a dynamic fluid system with artificial

physical separation between host cells and bacteria (Shah et al., 2016). Meanwhile, the Gut Microbiome physiomimetic platform (GuMi) uses colonoids grown on Transwells and utilises an artificially generated vacuum to drive the flow of anaerobic medium at the apical surface of cells (Zhang et al., 2021). Furthermore, the anaerobic gut-on-a-chip model places microfluidic chips into a chamber composed of gas-permeable plastic perfused with anaerobic gas (Jalili-Firoozinezhad et al., 2019; Kim et al., 2012).

1.8.2.1 The Vertical Diffusion Chamber (VDC) System

In addition to the systems described above, the Schüller lab has established a vertical diffusion chamber (VDC) which creates an environment that mimics the microaerobic conditions at the luminal side of the intestinal mucosa. In this model, polarised T84 cells on Snapwell filters are mounted between the two half chambers, resulting in an apical and basolateral separation of the epithelium (Figure 1.7). Each compartment can be filled with specific cell culture media and perfused with either anaerobic or aerobic gas mixtures.

The VDC provides a suitable model system to study AIEC interaction with intestinal epithelial cells due to its many features. Firstly, the use of polarised IECs is crucial in studying AIEC pathogenesis. Polarisation influences apical receptor expression, such as CEACAMs and TLRs, and allows for the formation of tight junctions (Madara et al., 1987). In addition, the system enables direct interaction between bacteria and host cells with differing conditions on either side of the epithelium. The VDC has been utilised previously to study various GI pathogens (McGrath et al., 2022; Mills et al., 2012; Naz et al., 2013). For example, attaching and effacing (A/E) lesion-forming *E. coli* display enhanced adherence under microaerobic conditions due to the stimulation of T3SS expression (Schüller and Phillips, 2010). In addition, infection of T84 and Caco-2 cells with *Campylobacter jejuni* in the VDC demonstrated increased epithelial association and invasion of host cells under microaerobic versus aerobic conditions (Mills et al., 2012; Naz et al., 2013). Meanwhile, *Clostridioides difficile* infection of T84 cells in a VDC resulted in

increased pro-inflammatory gene expression including IL-8 and TNF-α in microaerobic conditions (Jafari et al., 2016).

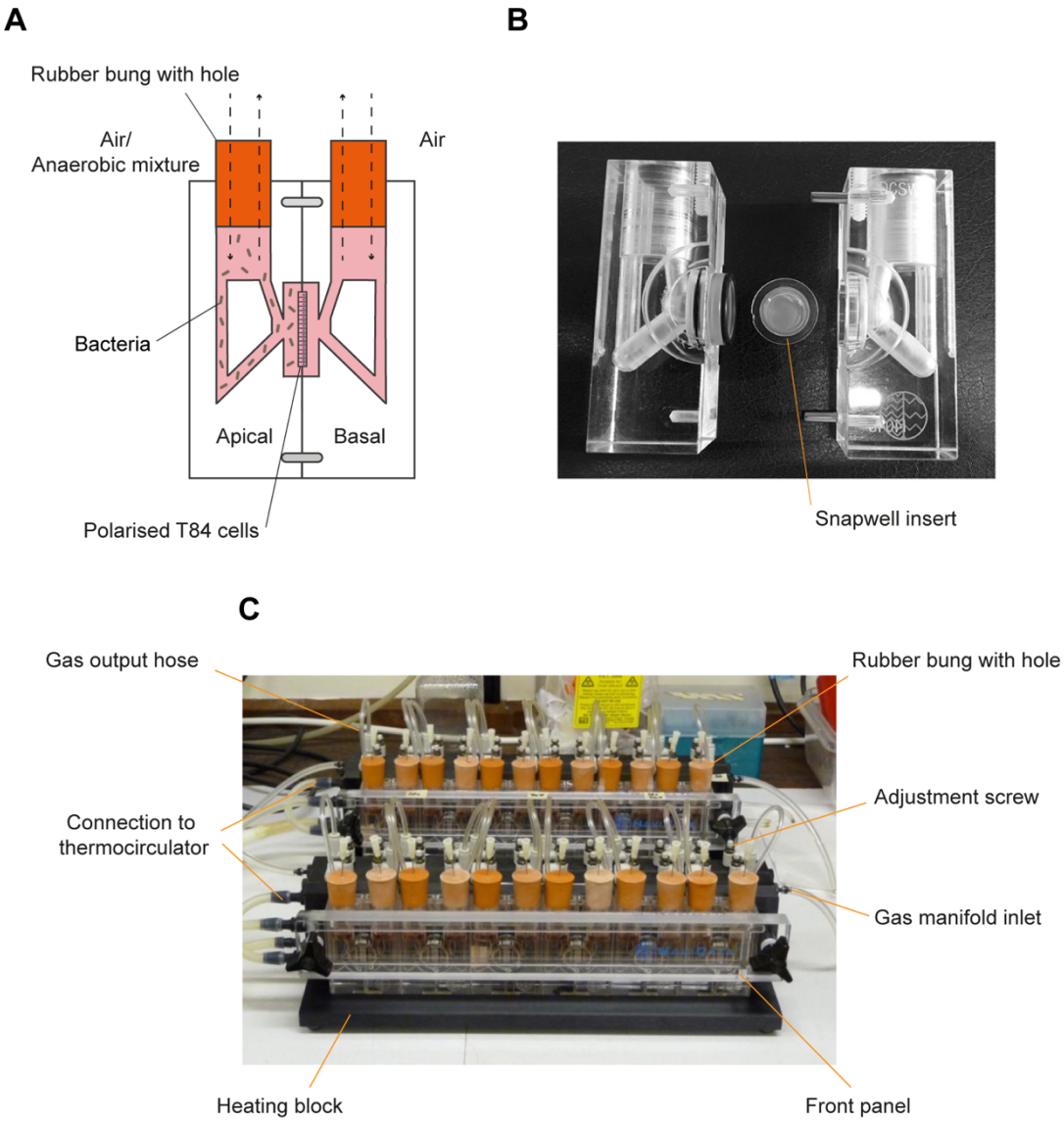

Figure 1.7. Set-up of the VDC system. Schematic representation of an assembled VDC unit with a T84 monolayer in the middle of two chambers. The apical medium can be gassed with either air or an anaerobic mixture and inoculated with bacteria. The basal medium is gassed with air to support oxygen supply to the epithelium. Two half chambers connect and rubber bungs with a central hole are used to maintain gas levels and reduce evaporation (**A**). Photograph of two VDC half chambers with a Snapwell filter insert in the middle to make up one unit (**B**). VDC units (up to 6) are placed in a heating manifold to maintain temperatures at 37°C which are connected to the gas supply (**C**) (McGrath and Schüller, 2021).

1.8.3 Mouse models

At the whole organism level, many mouse models have been generated to study human IBD mechanistically, playing a pivotal role in studying pathogenesis, drug efficacy and pharmacological mechanisms. These include chemically-induced inflammation with DSS or trinitrobenzene sulfonic acid (TNBS) (Chassaing et al., 2014; Wirtz et al., 2017). Meanwhile, genetically modified mice, such as the IL-10 KO mouse, develop spontaneous colitis mediated by T_H1 cells (Berg et al., 1996). Mouse models have also been employed in researching the role of AIEC in IBD. AIEC have demonstrated colonisation in the humanized carcinoembryonic antigen bacterial artificial chromosome 10 (CEABAC10) transgenic mouse model encoding four genes of the CEACAM family, including human CEACAM-6 , and *eif2ak4*$^{-/-}$ mice exhibiting defective autophagy in response to AIEC infection (Bretin et al., 2018). Although mouse models are suitable for replicating complex disease mechanisms in a whole organism, they bear limited relevance to human disease due to different GI tract anatomy, physiology, and microbiota composition (Hugenholtz and de Vos, 2018). In addition, the use of mice raises significant ethical concerns due to the potential for pain and suffering. The development of intestinal organoids circumvents these problems.

1.8.4 Organoids

The introduction of organoids into research has provided an advanced tool to study intestinal function and disease in more physiologically relevant conditions. Human intestinal organoids can be derived from the differentiation of pluripotent stem cells (PSCs) or by culture of adult stem cells (ASCs) from isolated intestinal crypts (Aguirre Garcia et al., 2022). Under specific culture conditions, including the provision of the growth factors Wnt3a, R-spondin and Noggin, intestinal stem cells proliferate and differentiate, generating three-dimensional structures containing all major cell types of the intestinal epithelium (Paneth cells, enteroendocrine cells, goblet cells, and enterocytes) (d'Aldebert et al., 2020). Intestinal organoids can be established from the tissue of the small intestine (enteroids) or the colon (colonoids) (Zachos et al., 2016). These three-dimensional structures form a sphere, whereby epithelial cells are orientated with their apical side toward the lumen.

The advantage of using organoids from intestinal ASCs include genetic and epigenetic stability relative to the site of origin. Organoid cultures can be generated from the human small intestine and the colon, retaining the transcriptional and epigenetic profiles specific to the location from which they are from, even following prolonged culture (Kraiczy et al., 2019; Middendorp et al., 2014). Furthermore, as ASC-derived organoids are genetically stable, they present an advantage over the use of organoids derived from induced pluripotent stem cells (iPSCs), which can acquire genetic and epigenetic changes during the reprogramming process (Liang and Zhang, 2013). ASC-derived organoids can also give rise to the less represented cells that populate the intestinal crypt (Sato et al., 2009), including enteroendocrine, tuft and M cells, which are important in modelling IBD as several different epithelial cell types are implicated in IBD disease progression.

The use of organoids from intestinal crypts has been employed in various IBD studies. For example, Dicarlo et al demonstrated small intestinal organoids from UC murine models retain the chronic intestinal inflammatory features characteristic of the parental tissue (Dicarlo et al., 2019). Meanwhile, Lee et al showed TNF-α

induces intestinal stem cell expansion in healthy enteroids, however TNF-α-induced expansion of LGR5+ stem cells is impaired in CD patient-derived enteroids, resulting in decreased organoid-forming efficiency and delayed wound healing (Lee et al., 2022). Interestingly, organoids from UC inflamed tissue lose the inflammatory phenotype after 1 week of culture, resembling that of non-inflamed controls. However, inflammation could be re-induced by addition of TNF-α, IL-1β and flagellin, returning to a phenotype observed in inflamed crypts (Arnauts et al., 2019). Various studies have described conflicting results regarding barrier function in CD organoids. For example, 3D colonoids from CD tissue demonstrate exclusion of FITC-dextran, suggesting an effective intestinal barrier (Xu et al., 2018). On the other hand, 2D colonoids from CD patients have displayed disrupted ZO-1 baseline staining (Sayed et al., 2020) and reduced TEER compared to non-IBD controls (Angus et al., 2022).

Although organoid culture is a major advancement for the *in vitro* study of the intestinal epithelium, the 3D spheroidal structure prevents bacterial access to the apical side. A solution to this is to 'unfold' 3D organoids to produce a polarised 2D monolayer (Moon et al., 2014; Yuli Wang et al., 2017). Organoids can be fragmented and plated into Transwell filters to generate intestinal monolayers that facilitate sampling at the apical and basolateral side. These 2D organoid cultures have been used previously to explore the interaction of EHEC, ETEC and *C. difficile* with intestinal epithelium (In et al., 2016; Karve et al., 2017; Leslie et al., 2015).

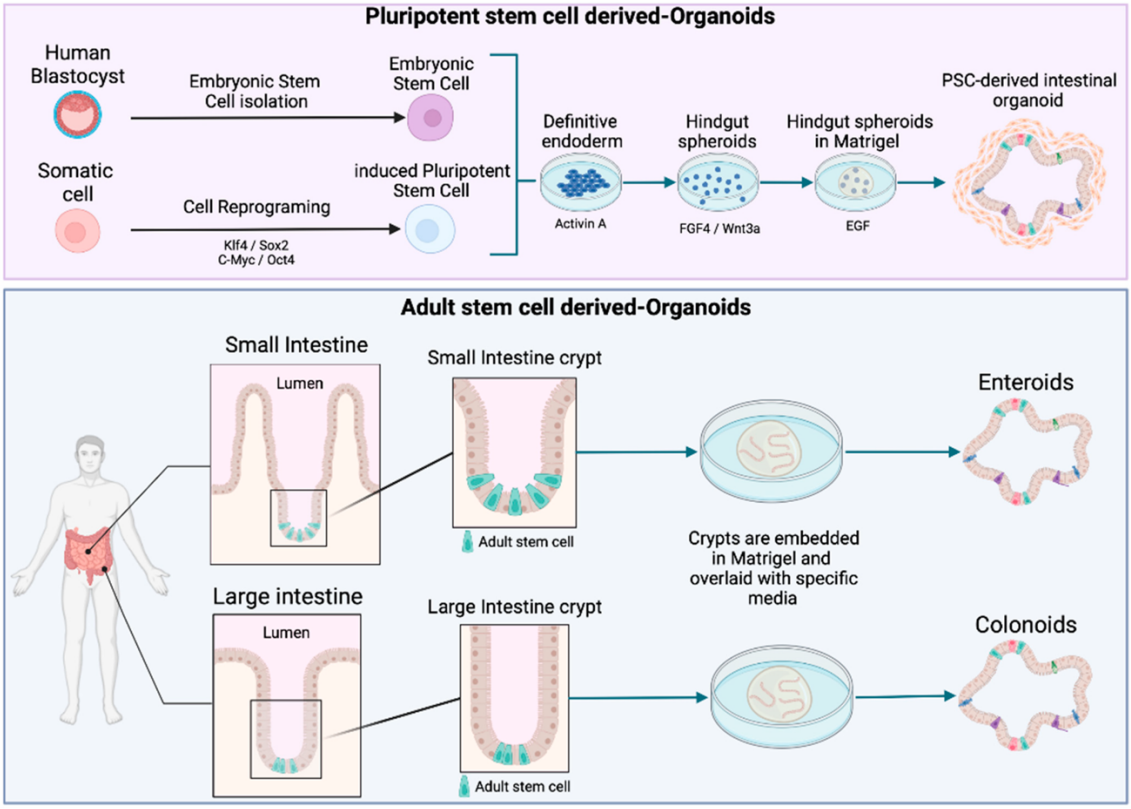

Figure 1.8. Schematic diagram of intestinal organoid, enteroid, and colonoid generation. Organoids can be derived from pluripotent stem cells (PSCs), including either induced pluripotent stem cells (iPSC) or embryonic stem cells (ESC). Enteroids and colonoids can be grown from the adult stem cells (ASC) isolated from intestinal crypts (Aguirre Garcia et al., 2022).

1.9 Project Aims

The overarching aim of this research was to investigate the interaction of AIEC with human colonic epithelium to determine whether AIEC infection can cause epithelial dysfunction, or if CD-derived epithelia are more susceptible to AIEC invasion and replication. This was achieved by:

1. Investigating AIEC interaction with colonic cell lines T84 and Caco-2 by evaluating adherence, invasion, intracellular replication, host receptor expression, cytotoxicity and secretion of pro-inflammatory cytokines.
2. Determining the influence of cell differentiation status and oxygen on AIEC pathogenesis by using polarised IECs and a microaerobic VDC system.
3. Characterising organoid monolayers derived from CD and non-IBD tissue and evaluating AIEC interactions.

Understanding the interactions between AIEC and the intestinal epithelium will provide crucial insight into CD progression and inform the development of novel therapeutics.

Chapter 2. Materials and Methods

2.1 Bacterial strains

2.1.1 Bacterial strains and culture conditions

Bacterial strains (Table 2.1) were stored as 15% (v/v) glycerol stocks at -80°C. Strains were grown statically in Lennox Lysogeny broth (LB) for liquid cultures, or LB agar for plate cultures, at 37°C overnight. Liquid cultures were prepared by inoculating bacteria directly from a streak plate into LB broth. Streak plates were stored up to 1 month at 4°C, after which fresh streak plates were prepared. Every 3 months, streak plates were prepared from original frozen glycerol stocks to prevent the accumulation of mutations.

Table 2.1. Information of bacterial strains used in this study.

***E. coli* Strain**	**Serotype**	**Pathotype**	**Phylogroup**	**Description**	**Source/Reference**
LF82	O83:H1	AIEC	B2	Ileal CD isolate	Darfeuille-Michaud (1999)
LF82 Δ*tssE1*	O83:H1	AIEC	B2	LF82 with 341 bases of the LF82_025 CDS deleted	Collins (2016)
LF82 Δ*tssE3*	O83:H1	AIEC	B2	LF82 with 396 bases of the LF82_445 CDS deleted	Collins (2016)
LF82 Δ*tssE1* Δ*tssE3*	O83:H1	AIEC	B2	LF82 with 341 bases of the LF82_025 CDS and 396 bases of the LF82_445 CDS deleted	Collins (2016)
NRG857c	O83:H1	AIEC	B2	Clinical ileal CD isolate	Eaves-Pyles *et al.* (2007)
HM615	Not determined	AIEC	B2	Colonic CD isolate	Martin *et al*. (2004)
HM605	O1:H7	AIEC	B2	Colonic CD isolate	Martin *et al*. (2004)
HM580	O45:H7	AIEC	D	Colonic CD isolate	Martin *et al*. (2004)
MG1655 (K-12)	OR:H48:K-	Commensal	A	*E. coli* K-12 lab strain derivative	Blattner *et al*. (1997)

2.2 Cell culture

2.2.1 Cell lines and culture conditions

Human colon carcinoma T84 cells (PHE/ECACC) were cultured in Dulbecco's Modified Eagle's Medium/Nutrient F-12 Ham (1:1) (DMEM/F-12) medium (Gibco, 21331020) supplemented with 10% foetal bovine serum (FBS) (Sigma, F7524), 2.5 mM L-glutamine (Sigma, G7513) and penicillin (100 units/ml) /streptomycin (100 µg/ml) (P/S) (Sigma, P0781). Human colon carcinoma Caco-2 cells (ATCC HTB-37) were cultured in Dulbecco's Modified Eagle's Medium (DMEM) (Sigma, D5671) supplemented with 10% FBS, 4 mM L-glutamine and 1% P/S. Cells were used up to passage 65. Cells were grown in 25 cm^2 culture flasks (Sarstedt) and passaged at full confluency. To passage cells, cell culture medium was removed from culture flasks and the cell monolayer was washed with 4 ml sterile phosphate-buffered saline (PBS) to remove residual FBS. Cells were rinsed with 0.5 ml 0.25% (w/v) trypsin/ 0.02% (w/v) ethylenediaminetetraacetic acid (EDTA) (Sigma, T4049) and incubated in 0.5 ml fresh trypsin-EDTA solution at 37°C, 5% CO_2 until cell detachment from the base of the flask was observed (10-15 min for Caco-2 and 20-30 min for T84 cells). Detached cells were resuspended in 5 ml fresh cell culture medium to neutralise trypsin activity and transferred to new culture flasks at a ratio of 1:5 for T84 and 1:10 for Caco-2 cells. Cells were maintained at 37°C in a 5% CO_2 atmosphere.

2.2.2 Cell seeding for plate culture or polarisation

During the passaging process, cells were seeded for experimental use. Following trypsinisation and resuspension in fresh medium, 40 µl of resuspended cells was diluted 1:1 with 0.4% (w/v) Trypan Blue solution (Sigma, T8154) and loaded into a Neubauer cytometer (0.1 mm depth) for cell counting. Viable cells (distinguishable by lack of Trypan Blue staining) were counted from at least two quadrants of the cytometer (Figure 2.1). The number of cells per ml was calculated using the following equation:

$$\text{Total cells/ml} = \frac{(\text{Total cells counted x dilution factor x } 10^4)}{\text{Number of quadrants counted}}$$

For plate culture, cells were seeded into 24-well plates (Sarstedt) at a density of 1.2 x 10^5 cells/well for T84 and 1 x 10^5 cells/well for Caco-2 cells in 1 ml of cell culture medium per well. Cultures used for immunofluorescent staining were grown in wells containing sterile circular coverslips (13 mm diameter, 0.13-0.16 mm thickness, Academy).

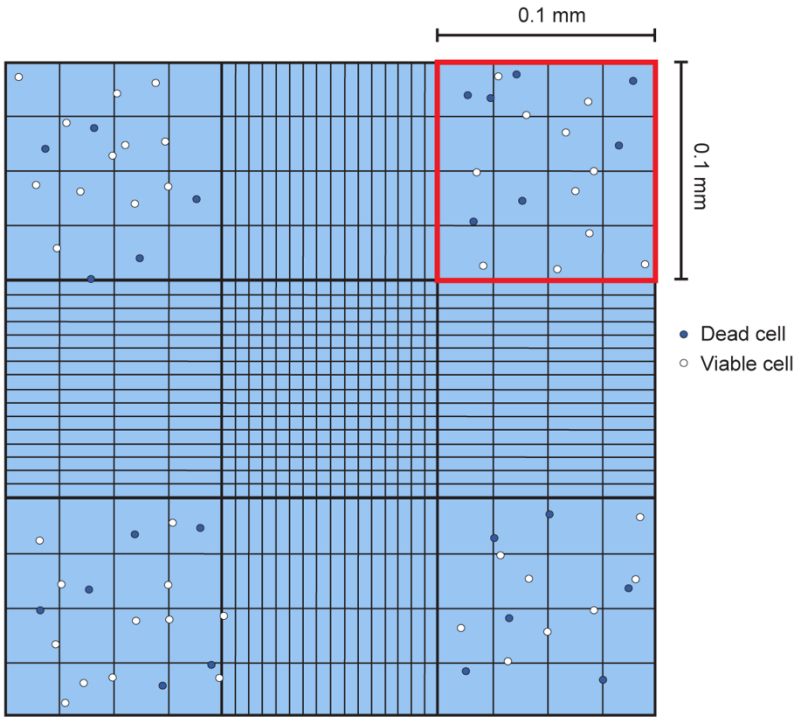

Figure 2.1. Neubauer cell counting chamber. Red box indicates counting region with area of 0.1mm^3 i.e. 10^{-4} mL volume of cell suspension.

For experiments using polarised cells, 5 x 10^5 T84 cells were seeded onto collagen coated polyester Snapwell (12 mm diameter, 0.4 µm pore, Corning 3801) or Transwell (12mm diameter, 0.4 µm pore, Corning 3460) filter inserts. To coat filters with collagen, a stock solution was prepared by dissolving rat tail collagen type I (Merck, C7661) at a concentration of 1.25 mg/ml in 0.1 N acetic acid on a tube rotator for 4 hr. The stock solution was diluted to 50 µg/ml in 60% (v/v) ethanol, and 200 µl (i.e., 10 µg) was added to each membrane. Filters were dried in a microbiology safety cabinet until the solution had evaporated and stored at room temperature until use. Cells seeded on filter inserts were maintained in cell culture medium with medium exchange after four days of seeding and every two days thereafter. Medium was changed to P/S-free medium on the day before an experiment. Polarisation of cells was monitored by determining the trans-epithelial electrical resistance (TEER) of monolayers using an EVOM resistance meter and EndOhm electrode (World Precision Instruments). T84 cells were considered polarised and used for experiments when the TEER reached >500 Ω x cm^2.

2.2.3 Cryopreservation and thawing of cells

Long term storage of eukaryotic cells was achieved by cryopreservation in liquid nitrogen. Cells were trypsinised and resuspended in 5 ml supplemented cell culture medium. Cell suspension concentrations were determined using a cytometer and adjusted to 2-4 x 10^6 cells/ml in 950 µl in culture medium plus 50 µl dimethyl sulfoxide (DMSO) (5% v/v) and added to a 1 ml cryovial. Cryovials were placed in a freezing container (Mr Frosty, Nalgene) containing 250 ml isopropanol and stored overnight at -80°C for gradual freezing. Frozen cryovials were transferred to liquid nitrogen storage the following day for long term preservation.

2.3 Quantification of bacterial adhesion, invasion and replication

2.3.1 Gentamicin invasion assay

Unless otherwise stated, 10 µl AIEC LF82 and *E. coli* MG1655 were inoculated into 1 ml/well DMEM/F-12 or DMEM without supplements at 2 x 10^7 colony forming units/ml (CFU/ml) to yield a multiplicity of infection (MOI) value of 10 and added to T84 or Caco-2 cell monolayers respectively. Plates were incubated for 3 hr at 37°C, 5% CO_2. Cells were subsequently washed 3 times with 1 ml sterile PBS to remove non-adherent bacteria. To measure bacterial invasion and intracellular replication, cell culture medium containing 50 µg/ml gentamicin (Gibco) was added to kill extracellular bacteria and plates were incubated at 37°C, 5% CO_2 for a further 1 hr or 21 hr respectively. For quantification of adherence, cells were lysed before addition of antibiotic-containing medium. At indicated time points, cells were washed 3 times with 1 ml sterile PBS and lysed with 1% Triton X-100 (Sigma) in PBS for 5 min at room temperature. After incubation, cells were carefully scraped from the plate using a sterile P1000 tip and homogenised by pipetting. Serial dilutions of cell lysates were prepared in sterile PBS and 10 µl spot plated in triplicate on LB agar. Plates were incubated at 37°C overnight and CFUs quantified the following day by counting colonies. Bacterial adhesion, invasion and replication values were standardised against the bacterial inoculum of each experiment.

2.3.2 Blocking of CEACAM receptors

Inhibition adhesion assays were performed in the presence of either 0.5% (w/v) D-mannose in cell culture medium (DMEM for Caco-2, DMEM/F-12 for T84), or after 1 hr pre-treatment with 100 µl of cell culture medium containing various antibodies at 37°C. Bacteria were inoculated and adhesion assays performed as described previously (See - 2.3.1 Gentamicin invasion assay). For the 1 hr blocking experiment, antibodies remained in the cell culture medium during inoculation and cells were incubated with bacteria for 1 hr. The following antibodies were used: anti-

CEACAM1, anti-CEACAM5, anti-CEACAM6, anti-CEACAM7 (Santa Cruz) and anti-CEACAM6 (Invitrogen). Antibodies (Table 2.6) were used at a 1:100 dilution in cell culture medium.

2.3.3 Apical/basolateral infection assay

For apical and basolateral infection assays, T84 and Caco-2 cells were seeded at 1.7 x 10^5 onto collagen coated Transwell inserts (6.5 mm diameter, 0.3 µm pore, Corning Falcon 353096). Filters were inoculated with 75 µl cell culture medium containing 10 µl of LF82 ONC into the apical compartment or added as a droplet onto the basolateral side of the inverted filter (Figure 2.2) and incubated for 3 hr. After incubation, filters infected basolaterally were returned to an upright position and 100 µl fresh DMEM or DMEM/F-12 containing 50 µg/ml gentamicin was added to the apical compartment, 600 µl to the basal compartment and cells were incubated for a further 1 hr. Afterwards, cells were washed in PBS, lysed in 1% Triton-X-100 and plated for CFU as described above.

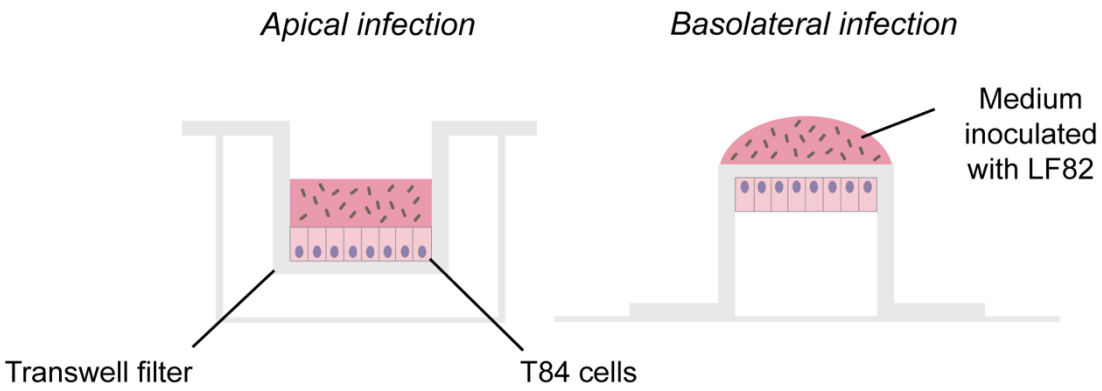

Figure 2.2. Schematic diagram of apical and basolateral infection of T84 cells on Transwell filters. Medium containing LF82 was added to the apical insert of the Transwell, or the Transwell was inverted, and medium added as a droplet onto the basolateral side of the filter.

2.3.4 Vertical Diffusion Chamber

For experiments with polarised cells in an aerobic or microaerobic environment, a VDC unit (Harvard Apparatus) composed of two half chambers separated by an epithelial cell monolayer was used (McGrath and Schüller, 2021). Polarised T84 cells grown on Snapwell filter inserts (12 mm, 0.4 µm pore, Corning 3801) were mounted between apical and basal chambers (Figure 2.3). Each half-chamber was filled with 4 ml DMEM/F-12. The basal chamber was perfused with an aerobic gas mixture (95% air, 5% CO_2), whilst the apical chamber was perfused with either an anaerobic gas mixture (90% N_2, 5% H_2, 5% CO_2) or aerobic gas mixture (95% air, 5% CO_2) for microaerobic or aerobic conditions respectively. For VDC experiments without eukaryotic cells, empty Snapwell inserts were used between the chambers and 8 ml DMEM/F-12 added to the VDC. The chambers were perfused with either an aerobic or anaerobic gas mixture to both apical and basal outlets.

Unless otherwise stated, AIEC LF82 and *E. coli* MG1655 were inoculated into the apical medium at 2 x 10^7 colony forming units/mL (CFU/mL) to yield a multiplicity of infection (MOI) value of 10. Chambers were mounted in a central heating block maintained by a thermocirculator and incubated at 37°C. For invasion assays, chambers were incubated for 3 hr followed by either 1 hr or 21 hr incubation in DMEM/F-12 containing 50 µg/mL gentamicin. To determine bacterial growth during the incubation, OD_{600} measurements were taken using a spectrophotometer.

Following completion of experiments, VDC components were disassembled and cleaned by disinfecting in 2 L dH_2O containing 5g Presept (Johnson & Johnson) for 24 hr. The components were rinsed with dH_2O the following day to remove residual disinfectant, air dried and stored in a plastic box until next use.

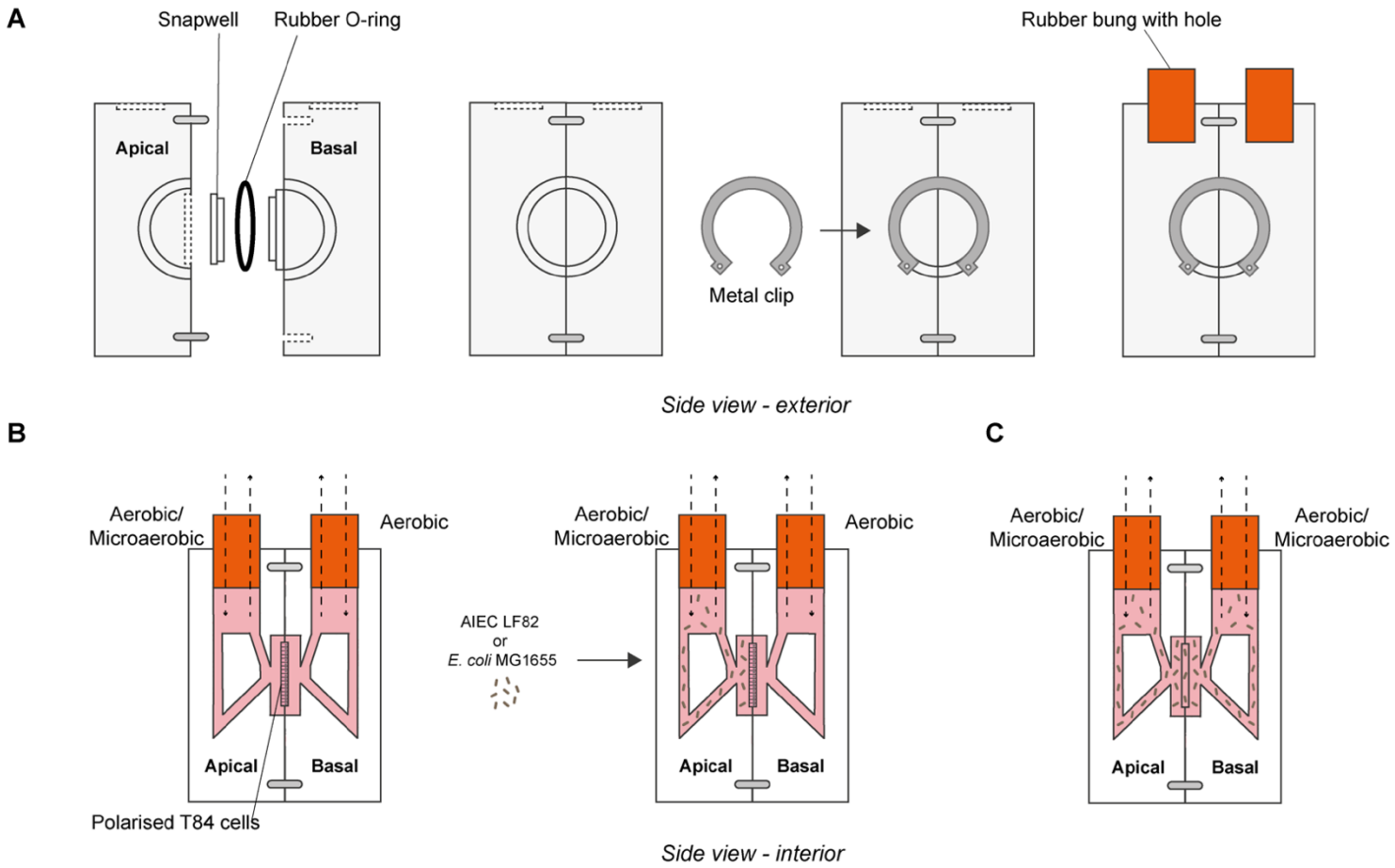

Figure 2.3. Schematic diagram of VDC assembly. Snapwell filter with polarised cells mounted between two half chambers secured by a metal clip. Rubber bungs with holes are used to control gas release (**A**). Cell culture media is added to each half chamber and the apical side inoculated with bacteria (**B**). VDC units can be used without cells to measure bacterial growth only (**C**).

2.4 Intestinal organoid culture

2.4.1 Preparation of noggin- and R-spondin-conditioned media

293T-Noggin-FC or 293T-HA-Rspo1-FC cells were cultured in Dulbecco's Modified Eagle's Medium (DMEM) supplemented with 10% FBS, 2 mM L-glutamine and puromycin (10 µg/ml) or zeocin (300 µg/ml), respectively. Cells were grown in 25 cm^2 culture flasks at 37°C, 5% CO_2 until confluency and split into three 75 cm^2 flasks and one 25 cm^2 flask. The 25 cm^2 flask was maintained in growth medium with antibiotics for propagation. Cells in the three 75 cm^2 flasks were grown in DMEM supplemented with 10% FBS without antibiotics. Once confluent, cells were distributed into nine 75 cm^2 flasks in conditioning medium (Table 2.2). Flasks were incubated at 37°C, 5% CO_2 for 7 days without medium change. The medium from each flask was collected and centrifuged at 1000 x g for 10 min at 20°C. Supernatants were sterile filtered using a 0.22 µm filter, aliquoted and stored at -70°C.

2.4.2 Preparation of Wnt3a-conditioned media

L-Wnt3A cells were cultured in Dulbecco's Modified Eagle's Medium (DMEM) supplemented with 10% FBS, 2 mM L-glutamine and G418 (400 µg/ml). Cells were grown in 25 cm^2 culture flasks at 37°C, 5% CO_2 and split into three 75 cm^2 flasks and one 25 cm^2 flask at confluency. The 25 cm^2 flask was maintained in expansion media (Table 2.2) for propagation. Cells in the three 75 cm^2 flasks were grown in DMEM supplemented with 10% FBS without antibiotics. Once confluent, cells were distributed into nine 75 cm^2 flasks in conditioning medium (Table 2.2). Flasks were incubated at 37°C, 5% CO2 for 4 days without medium change. After 4 days, the medium from each flask was collected and stored at 4°C. 10 ml of conditioning media (Table 2.2) was added to each of the same flasks and incubated at 37°C, 5% CO_2 for a further 3 days without medium change. On day 7, the medium from each flask was collected and combined with the medium from day 4. The media was

centrifuged at 1000 x g for 10 min at 20°C. Supernatants were sterile filtered using a 0.22 µm filter, aliquoted and stored at -70°C.

Table 2.2. Expansion and conditioning media for 293T-Noggin-FC, 293T-HA-Rspo1-FC and L-Wnt3a cells.

Expansion medium	Conditioning medium ($CMGF^-$)
DMEM	Advanced DMEM/F-12
10% FBS	10 mM HEPES
2mM L-glutamine	2 mM Glutamax
10 µg/ml puromycin (Noggin)	10% FBS
300 µg/ml zeocin (R-spondin)	
400 µg/ml G418 (Wnt)	

2.4.3 Thawing and passaging of colonic organoids

Vials of frozen organoid stocks (organoids generated from normal and CD human transverse colon – Table 2.3) were rapidly thawed by partial submersion in 37°C water. The organoid suspension was transferred into 5 ml $CMGF^-$. The organoid solution was centrifuged at 240 x g for 10 min at 4°C and the cell pellet resuspended in *UltiMatrix* Reduced Growth Factor Basement Membrane Extract (Cultrex) on ice. The Matrigel-organoid suspension was dispensed (40 µl per dome) into the centre of wells of a pre-warmed 24-well plate and incubated at 37°C, 5% CO2 for 4 min. The plate was then inverted for 30 min to prevent organoids collecting at the base of the Matrigel dome. After 30 min, 500 µl of $CMGF^+$ (Table 2.4) containing 10 µM Y-27632 (ROCK inhibitor) was added to each well and the plate returned to the incubator at 37°C, 5% CO_2. After 48 hr, inhibitors were removed from the medium and organoids incubated for 5-7 days with medium change every 2-3 days thereafter and maintained at 37°C, 5% CO_2.

For passaging, medium was removed from organoids in Matrigel and 800 µl of Gentle Cell Dissociation Reagent (Stem Cell Technologies) added to each well at room temperature. The Matrigel was dissolved by pipetting and the plate was incubated on a rocking platform for 10 min at room temperature. Organoids were fragmented by pipetting and observed by microscopy. Once fragmented, the organoid solution in each well was collected and 2 volumes of $CMGF^-$ added. The protocol then follows from centrifugation at 240 x g for 10 min at 4°C and the cell pellet resuspended in Matrigel on ice as described above.

Table 2.3. Patient information for transverse colonic organoids.

Organoid line	Age	Sex	Diagnosis	Status
TCC-2	53	Male	CD in descending colon	In remission
TCC-6	71	Male	CD in terminal ileum	In remission
TCC-7	20	Female	Colonic CD	In remission
TCN-1	60	Male	Routine Bowel screening	n/a
TCN-2	74	Male	Adenocarcinoma ascending colon	n/a
TCN-4	53	Female	Caecal cancer	n/a

2.4.4 Culture of 2D organoid monolayers on Transwell inserts

To establish two-dimensional organoid monolayer cultures, fragmented organoids were seeded onto collagen coated polyester Transwell filter inserts (6.5 mm diameter, 0.4 µm pore, Corning 3470). Filters were coated with 100 µl human type IV collagen in water (35 µg/ml from a stock solution of 1 mg/ml; Sigma C5533) and incubated at room temperature overnight. The collagen solution was removed, and filters washed with 200 µl $CMGF^-$ to remove excess collagen. Pelleted organoids were resuspended in $CMGF^+$ (100 µl per filter) and the organoid suspension added to the apical compartment of the Transwell filter. In the basal compartment, 600 µl of $CMGF^+$ was added. The organoid monolayers were incubated at 37°C, 5% CO_2 until confluency, with medium exchange 48 hr after seeding to remove ROCK inhibitor from the medium, with medium exchange every 2-3 days thereafter.

2.4.4.1 Differentiation of 2D organoid monolayers

Once the organoid monolayers reached confluence, TEER was determined to assess barrier formation using an EVOM resistance meter and EndOhm STX electrode (World Precision Instruments). Differentiation of organoid monolayers was achieved by withdrawal of Wnt3a-conditioned medium, R-spondin1 conditioned medium and SB202190 (p38 MAPkinase inhibitor). Differentiation medium was exchanged every 48 hr for 4 days and organoid monolayers were maintained at 37°C, 5% CO_2.

Table 2.4. Reagents for expansion medium (CMGF+).

Name	Description	Stock solution concentration	Working concentration in media
B27	supplement for small intestines	50 x	1 x
N- acetylcysteine	antioxidant/anti-apoptosis	500mM	1mM
EGF, human	epithelial growth factor	50 µg/ml	50 ng/ml
[Leu- 15] gastrin human	GI mitogenic factor	10 µM	10 nM
A83-01	TGF β inhibitor; Alk4/5/7 inhibitor	500 µM	500 nM
SB202190	p38 MAPkinase inhibitor	10 mM	10 µM
Penicillin/Streptomycin	Antibiotic	100 x	1 x
Nicotinamide	Improves culture efficiency and life span of human colonoids	1 M	10 mM
Y-27632	ROCK inhibitor	10 mM	10 µM
	GSK3β inhibitor	10 mM	10 µM
Noggin conditioned medium	Noggin protein	-	10% (v/v)
R-spondin1 conditioned medium	RSPO1 protein	-	20% (v/v)
Wnt3A conditioned medium	Wnt3a protein	-	50% (v/v)
$CMGF^-$ (Table 2.2).	Conditioning medium	-	

Table 2.5. Reagents for differentiation medium.

Name	Description	Stock solution concentration	Working concentration in media
B27	supplement for small intestines	50 x	1 x
N- acetylcysteine	antioxidant/anti-apoptosis	500mM	1mM
EGF, human	epithelial growth factor	50 µg/ml	50 ng/ml
[Leu- 15] gastrin human	GI mitogenic factor	10 µM	10 nM
A83-01	TGF β inhibitor; Alk4/5/7 inhibitor	500 µM	500 nM
Noggin conditioned medium	Noggin protein	-	10% (v/v)
CMGF$^-$	Conditioning medium		

2.5 Immunofluorescence staining and microscopy

Table 2.6. Primary and secondary antibodies and fluorescent stains.

Antigen	Host species	Working Conc.	Source	Product code
E. coli	Goat	1:200	Abcam	Ab13627
E. coli OK antigens	Rabbit	1:200	US Biological	E3500-06C
CEACAM-1	Mouse	1:200	Santa Cruz	sc-16645
CEACAM-5	Mouse	1:200	Santa Cruz	sc-23928
CEACAM-6	Mouse	1:200	Santa Cruz	sc-59899
CEACAM-6	Rabbit	1:200	Invitrogen	MA5-29144
CEACAM-7	Mouse	1:200	Santa Cruz	sc-59946
MUC2 (H-300)	Rabbit	1:250	Santa Cruz	sc-15334
MUC2	Mouse	1:250	Santa Cruz	sc-7314
Occludin	Rabbit	1:200	Invitrogen	40-4700
DAPI	n/a	1:4000	Merck	
Phalloidin-Atto 488	n/a	1:200	Sigma	49409
Calcofluor	n/a	1:50	Merck	
Propidium Iodide	n/a			
Alexa Fluor™ Plus 647 Phalloidin	n/a	1:400	Invitrogen	A30107
Alexa Fluor™ 488 anti-rabbit	Donkey	1:400	Invitrogen	A21206
Alexa Fluor™ 568 anti-mouse	Donkey	1:400	Invitrogen	A10037
Alexa Fluor™ 568 anti-rabbit	Donkey	1:400	Invitrogen	A10042
Alexa Fluor™ 488 anti-mouse	Donkey	1:400	Invitrogen	A21202
Alexa Fluor™ 568 anti-goat	Donkey	1:400	Invitrogen	A11057

Cell monolayers on coverslips, Snapwell or Transwell filters were fixed in 3.7% (v/v) formaldehyde (Acros Organics) in PBS for 20 min at room temperature, washed with PBS and stored at 4°C until use. Fixed cells were blocked and permeabilised with 0.1% (v/v) Triton X-100, 0.5% (w/v) bovine serum albumin (BSA) in PBS for 20 min at room temperature. Primary antibodies (Table 2.6) were diluted in 0.5% (w/v) BSA in PBS. Samples were incubated with primary antibodies for 1 hr at room temperature. Following incubation, samples were washed with PBS on a rocking platform for 10 min followed by incubation with respective secondary antibody (Table 2.6) for 30 min in the dark at room temperature. For counterstaining, 4',6-diamidino-2-phenylindole (DAPI) and fluorescein isothiocyanate-labelled phalloidin (FITC-phalloidin) were used to stain DNA and filamentous actin, respectively, for 30 min in the dark at room temperature. Samples were washed with PBS in the dark on a rocking platform for 30 min, mounted onto glass microscopy slides using Vectashield mountant (Vector Laboratories) to prevent photo-bleaching and stored at 4°C in the dark. For occludin staining, cell monolayers were pre-extracted in 0.2% (v/v) Triton X-100 in PBS for 2 min on ice, washed with PBS, fixed in 3.7% (v/v) formaldehyde in PBS for 20 min at room temperature, washed with PBS and stored at 4°C until used for IFS. For MUC2 staining, cells were fixed in ice cold methanol/acetone (1:1) for 4 min on ice to preserve mucus, washed with PBS and stored at 4°C until used for IFS.

2.6 Growth curve analysis

Growth curves were generated by diluting bacterial overnight cultures to an optical density of 0.1 at 600nm in 200 µl/well Lysogeny broth, DMEM or DMEM/F-12 cell culture medium in 96-well plates. Plates were cultured at 37°C in aerobic conditions, and OD_{600} measurements taken using a FLUOstar Optima microplate reader (BMG) every 30 min. Data was analysed using the MARS data analysis software.

2.7 Yeast agglutination assay for FimH expression

Bacterial overnight cultures were grown statically in 2 ml LB, DMEM or DMEM/F-12. Cultures were washed and resuspended in PBS at 0.5 OD_{600}. Bacterial suspensions were serially diluted up to 1:32 in PBS and 50 µl of each deposited in a 96-well plate. Commercial bakers' yeast (*Saccharomyces cerevisiae*) was suspended in PBS (20 mg/ml) and 50 µl of yeast cell suspension was added to each well. Agglutination was monitored visually, and the titre recorded as the last bacterial dilution giving a positive reaction.

2.8 Crystal Violet staining for biofilm formation

Bacterial overnight cultures (ONCs) were diluted to an optical density of 1.0 at 600nm in Lysogeny broth, followed by dilution at 1:100 in 100 µl/well DMEM or DMEM/F-12 cell culture medium in 96-well plates. Plates were incubated at 37°C in aerobic conditions for 24 or 48 hr. Medium was removed, plates were washed with 200 µl/well dH_2O 2 times and stained with 125 µl/well 0.1% (w/v) crystal violet in ethanol for 10 min at room temperature. Plates were washed with dH_2O to remove excess stain and left to air dry at room temperature. The stain was solubilised in 30% (v/v) acetic acid and absorbance measured at OD_{595} using a FLUOstar Optima microplate reader (BMG). Data was analysed using the MARS data analysis software.

2.9 Trypan Blue staining for cytotoxicity

To quantify cell death, cell monolayers were stained with 300 µl 0.05% (w/v) Trypan Blue for 15 min at room temperature. Plates were washed with PBS 2 times to remove unbound dye. Cells were lysed in 400 µl 1% (w/v) sodium dodecyl sulfate (SDS) to release internalised dye and absorbance measured at OD_{590} using a FLUOstar Optima microplate reader (BMG). Data was analysed using the MARS data analysis software.

2.9.1 Effects of bacterial adhesion on T84 cytotoxicity

AIEC LF82 and *E. coli* MG1655 were inoculated into DMEM/F-12 at 2 x 10^7 colony forming units/ml (CFU/ml) to yield a multiplicity of infection (MOI) value of 10 and added to T84 cell monolayers. Plates were incubated for 3 hr at 37°C, 5% CO_2. After 3 hr, supernatants from infected cells were collected, centrifuged at 14000 x g for 5 min at room temperature and stored at 4°C until required. Supernatants were added to fresh T84 monolayers for 21 hr and a cytotoxicity assay performed as previously described (See - 2.9 Trypan Blue staining for cytotoxicity).

2.9.2 Effects of inhibiting bacterial invasion on T84 cytotoxicity

T84 cells were pre-incubated for 30 min with DMEM/F-12 devoid of antibiotics containing either 1 µg/ml cytochalasin D (Enzo) or 0.5 µg/ml colchicine (Acros Organics). Bacteria were subsequently added as described in (See - 2.3.1 Gentamicin invasion assay) and incubated 3 hr followed by 21 hr gentamicin treatment. After 21 hr, cell culture medium was removed, cells washed with PBS and cytotoxicity evaluated as previously described (See - 2.9 Trypan Blue staining for cytotoxicity).

2.10 Cytokine enzyme-linked immunosorbent assay (ELISA)

Experiments were performed as per (See - 2.3.1 Gentamicin invasion assay). Apical and basolateral cell culture medium was sampled, and bacteria removed by centrifugation at 14000 x g for 5 min at room temperature. Supernatants were stored at -20°C until required.

IL-8 was quantified using a human IL-8 ELISA kit (PeproTech) according to the manufacturer's instructions. IL-6, IL-1β and TNF-α were quantified using human IL-6, IL-1β and TNF-α uncoated ELISA kits (Invitrogen) respectively, according to manufacturer's instructions. For horseradish peroxidase (HRP) detection and colour

development, 2,2'-Azinobis [3-ethylbenzothiazoline-6-sulfonic acid]-diammonium salt (ABTS) was used for IL-8 and 3,3',5,5'-tetramethylbenzidine (TMB) used for IL-6, IL-1β and TNF-α.

All ELISAs were performed in NUNC Maxisorb immunoassay 96-well plates (ThermoFisher Scientific). All samples were used undiluted, except for LF82-infected cell supernatants for IL-8 quantification, which were diluted 1:2 in DMEM/F-12. For washes, 200 µl per well of 0.05% Tween-20 in PBS was used. Optical density readings were taken using a FLUOstar Optima microplate reader (BMG). Standard curves were generated, and data was analysed using the MARS data analysis software.

2.11 Statistical analysis

Data was displayed and analysed using GraphPad Prism Version 10 software. Bar graphs show individual data points plus a bar at the mean value, unless otherwise stated. Error bars are indicative of standard deviation. For the comparison of two groups, parametric student's t-test was used. Three or more groups were compared using parametric one-way analysis of variance (One-way ANOVA) with either Tukey's or Dunnett's multiple comparison post-test. For all data analysis, a P value of < 0.05 was considered statistically significant, and degrees of statistical significance are presented as follows: * = $P < 0.05$; ** = $P < 0.01$; *** = $P < 0.001$; **** = $P < 0.0001$.

Chapter 3. AIEC interaction with intestinal epithelial cell lines T84 and Caco-2

3.1 Background

AIEC are implicated in the pathogenesis of CD. The AIEC strain LF82 was initially characterised as a CD-associated, non-diarrhoeagenic intestinal *E. coli* pathotype, with a pathogenicity phenotype of adherence to and invasion of intestinal epithelial cells followed by intracellular survival and replication within IECs and macrophages (Boudeau et al., 1999; Bringer et al., 2006; Darfeuille-Michaud et al., 1998). AIEC adherence has previously been shown to be mediated by the binding of FimH, located at the tip of type 1 pili, to the mannosylated host cell receptor CEACAM-6 (Barnich et al., 2007). To date, the current understanding of AIEC pathogenesis has been obtained from studies using non-confluent, undifferentiated carcinoma-derived cell lines and mouse models.

In this study, the interaction of AIEC LF82 with intestinal epithelium was re-examined by the characterisation of LF82 adherence, invasion and intracellular replication in T84 and Caco-2 cells. In addition, biofilm formation, interactions with established receptor CEACAM-6, LF82 effect on cell viability and secretion of pro-inflammatory cytokines were determined. Furthermore, experiments were extended to additional AIEC strains NRG857c (ileal isolate) and HM615, HM605 and HM580 (colonic isolates) to gain a better understanding of AIEC pathogenesis in the human colon.

3.2 Results

3.2.1 AIEC LF82 adherence, invasion and intracellular replication is cell line dependent

Early AIEC studies characterised LF82 invasion in intestinal epithelial cell lines. Boudeau et al demonstrated a 4% invasion rate of LF82 in Caco-2 cells (Boudeau et al., 1999), meanwhile a 1% invasion rate of LF82 was shown in T84 cells by Elatrech et al (Elatrech et al., 2015). Initial experiments focused on characterising AIEC LF82 adherence, invasion and replication in T84 and Caco-2 cells. Cells were seeded in 24-well plates and onto coverslips at a low cell density (1.2×10^5/ml) and cultured for 48 hours to approximately 70% confluency. Cell monolayers were incubated with AIEC LF82 or MG1655 for 3 hr, followed by either 1 hr or 21 hr treatment with gentamicin to determine invasion and replication respectively. For CFU quantification, monolayers were lysed and plated, and for microscopy, coverslips were fixed and stained.

Following a 3 hr infection period, LF82 showed significantly more adherence to T84 and Caco-2 cells than the non-invasive lab strain MG1655, with higher adherence observed in T84 cells (Figure 3.1A). Given that *E. coli* have a doubling time of 20 minutes, it is plausible that increased adherence could be due to a growth advantage over the 3 hr infection period. The growth of LF82 and MG1655 in DMEM and DMEM/F-12 medium was therefore monitored by a conventional growth curve at OD_{600} (Figure 3.1B). No significant difference was observed between the growth curves of the two strains in each medium, suggesting equivalent growth rates and thus unlikely to account for the adherence advantage seen by LF82.

Addition of gentamicin for 1 hr or 21 hr to determine invasion and intracellular replication, respectively, indicated significantly higher LF82 invasion compared to MG1655 in both cell lines and this was more pronounced in Caco-2 cells (Figure 3.1C). However, when numbers of invaded bacteria were normalised to numbers of adherent *E. coli* to calculate invasion rates (%), non-invasive MG1655 invasion

frequency was significantly higher than LF82 in both T84 and Caco-2 cells (Figure 3.1E). In addition, numbers of intracellular LF82 after 24 hr were significantly higher than MG1655 in both cell lines, which was more pronounced in T84 cells (Figure 3.1D).

As for the percentage of intracellular bacteria after 24 hr compared to 1 hr (replication rate), LF82 intracellular replication was significantly higher than MG1655 in T84 cells, yet there was no significant difference between strains in Caco-2 cells. Notably, the replication rate of both strains was below 100% in Caco-2 cells, with overall LF82 CFU numbers decreasing after 21 hours (~11,000 CFU after 1hr compared to ~2000 CFU after 21hr) (Figure 3.1C, D and F).

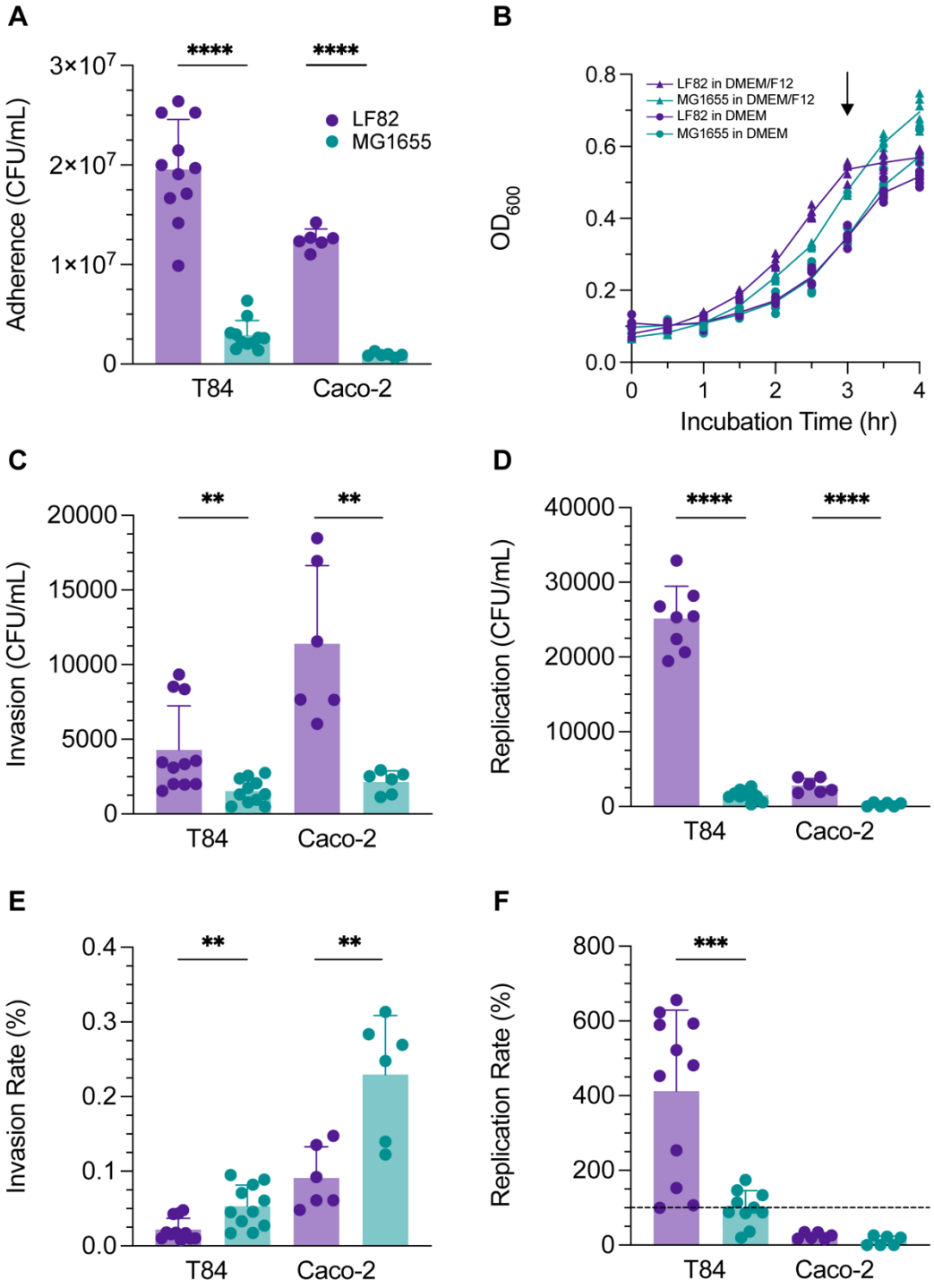

Figure 3.1. Adherence, invasion and intracellular replication of AIEC LF82 and non-invasive *E. coli* MG1655 in non-confluent T84 and Caco-2 cells. Cells were grown for 48 hr and incubated with bacteria for 3 hr, followed by 1 hr or 21 hr of gentamicin to kill extracellular bacteria. Adherent bacteria were determined after 3 hr by CFUs (**A**). Bacterial growth of both strains was determined by quantification at OD600. The arrow depicts the 3 hr incubation with bacteria before gentamicin treatment (**B**). Invasion (**C**) and intracellular replication (**D**) was determined after 1 hr or 21 hr of gentamicin treatment and plating out cell lysates for CFUs respectively. Results were normalised to an inoculum of 10^7 bacteria.

Invasion (**E**) and replication rates (**F**) were calculated relative to adherent and invaded bacteria respectively. Data shown as the mean +- SD. Significance was calculated using a student's unpaired t-test (**p<0.01; ***p<0.001; ****p<0.0001).

Invasion assays were repeated in confluent monolayers. This is because confluent monolayers exhibit a polarised distribution of cell surface receptors and are therefore more physiologically relevant to differentiated epithelium. Cells were seeded in 24-well plates and onto coverslips at a low cell density (1.2 x 10^5/ml) as described above, but instead cultured for 7 days to allow for the establishment of a confluent monolayer.

Following a 3 hr infection period, LF82 showed significantly more adherence to confluent T84 and Caco-2 cells than MG1655 (Figure 3.2A). The number of adherent CFU in confluent cells was approximately half the value of that observed in non-confluent cells. Addition of gentamicin for 1 hr indicated significantly higher LF82 invasion compared to MG1655 in both cell lines and this was more pronounced in Caco-2 cells, as previously described in non-confluent cells (Figure 3.2B). However, when invasion rates (%) were calculated, non-invasive MG1655 invasion frequency was significantly higher than LF82 in T84 cells only (Figure 3.2D). Although LF82 invasion was approximately 2-fold higher in non-confluent T84 cells in comparison to confluent cells, overall invasion rates were still low at ~0.02%. Similarly, LF82 exhibited higher invasion rates in non-confluent Caco-2 cells compared to confluent (~0.1% vs 0.03%) (Figure 3.2D). Low invasion rates observed in these experiments are therefore not due to cell confluency.

In addition, numbers of intracellular bacteria after 24 hr indicated no significant difference between the two strains in T84 cells, but numbers of intracellular LF82 after 24 hr were significantly higher in Caco-2 cells (Figure 3.2C). Interestingly, numbers of intracellular CFU in non-confluent T84 cells was approximately 2.5-fold higher than confluent T84s, whereas non-confluent Caco-2 cells exhibited 3.3-fold higher CFU in comparison to the confluent equivalent.

As for the percentage of intracellular bacteria after 21 hr compared to 1 hr (replication rate), there was no significant difference between strains in either cell line, however MG1655 showed higher replication rates than LF82 in T84 cells. Notably, replication rates of both strains was below 100% in Caco-2 cells, with overall LF82 CFU numbers decreasing after 21 hours (~3000 CFU after 1hr compared to ~2000 CFU after 21hr) (Figure 3.2E).

Interestingly, replication rates after 21 hr differed between cell lines and cell confluency. LF82 replication rate doubled in non-confluent cells compared with confluent, however MG1655 replication halved. Meanwhile, in Caco-2 cells, the replication rate of both strains was below 100% after 21 hr in both non-confluent and confluent cells (Figure 3.2E).

Subsequent experiments were performed using fully-confluent cells.

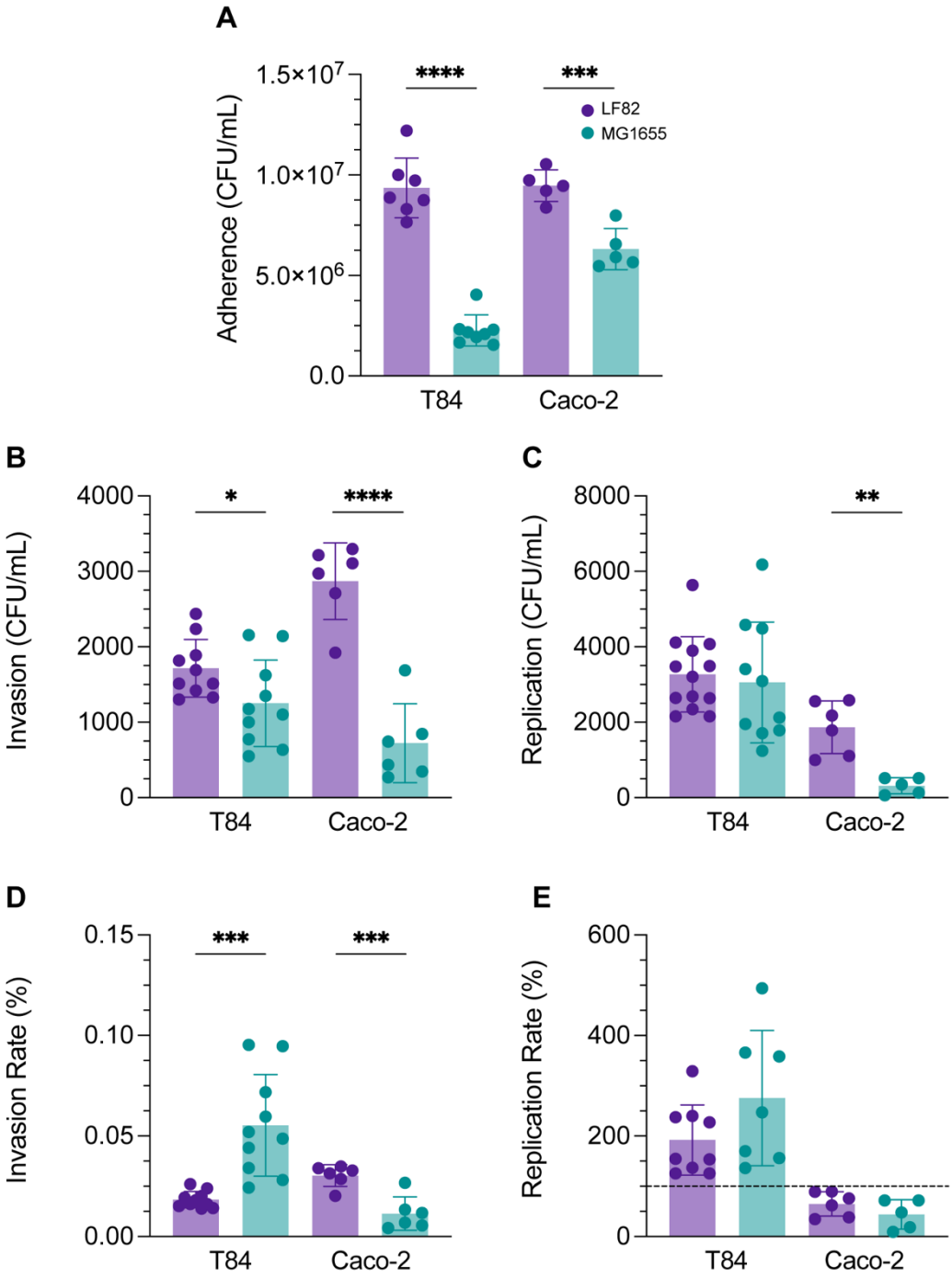

Figure 3.2. Adherence, invasion and intracellular replication of AIEC LF82 and non-invasive *E. coli* MG1655 in T84 and Caco-2 cells. Confluent cells were incubated with bacteria for 3 hr, followed by 1 hr or 21 hr of gentamicin treatment to kill extracellular bacteria. Adherent bacteria were determined after 3 hr by CFUs (**A**). Invasion (**B**) and intracellular replication (**C**) was determined after 1 hr or 21 hr of gentamicin treatment respectively and cell lysates plated for CFUs. Results were normalised to an inoculum of 10^7 bacteria. Invasion (**D**) and replication rates (**E**) were calculated relative to adherent and invaded bacteria respectively. Data shown as the mean +- SD. Significance was calculated using a student's unpaired t-test (*p<0.05; **p<0.01; ***p<0.001; ****p<0.0001).

3.2.2 AIEC LF82 forms biofilms on T84 and Caco-2 cells

To visualise bacterial association and host cell integrity, T84 and Caco-2 cells infected with LF82 and MG1655 were stained for *E. coli* and F-actin and evaluated by fluorescence microscopy. AIEC LF82 demonstrated extensive adherence to both T84 and Caco-2 cells, whereby chain-like structures of bacteria and potential filamentation were seen. In comparison, few MG1655 adherent bacteria were observed (Figure 3.3A and B). Interestingly, when observing immunofluorescence staining, there appeared to be a discrepancy whereby CFUs observed in quantification were lower than the extensive adherence seen visually under the microscope.

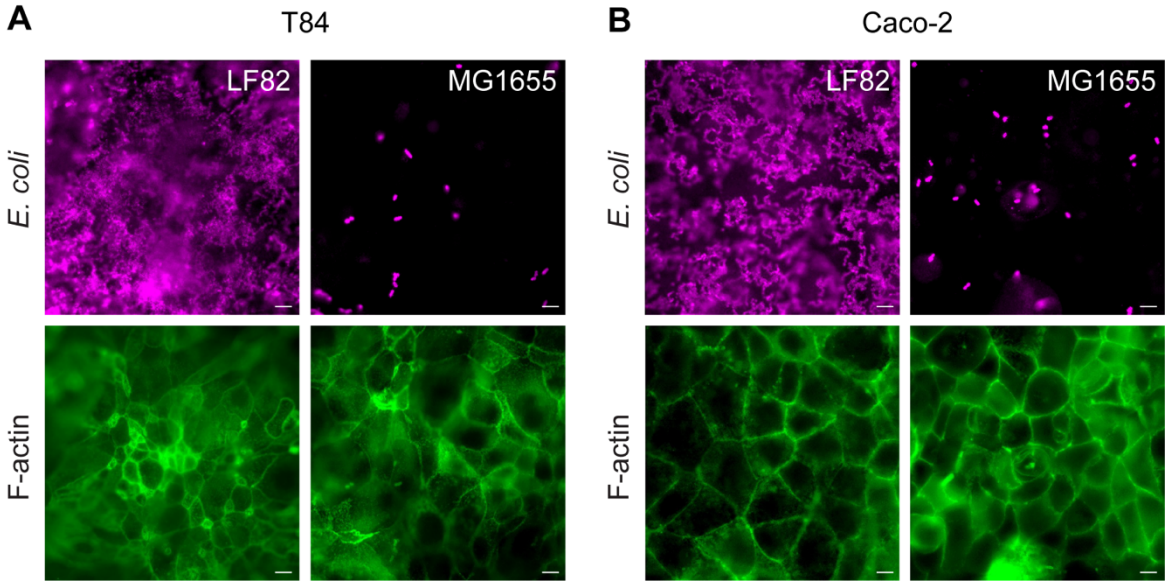

Figure 3.3. Adherence of LF82 and MG1655 to confluent T84 (A) and Caco-2 (B) cells. Cells were incubated with AIEC LF82 or non-invasive *E. coli* MG1655 for 3 hr. Epithelia were stained for *E. coli* (magenta) and F-actin (green). Scale bar = 10 μm.

To determine if this discrepancy was due to the presence of dead bacteria, T84 monolayers infected with LF82 or MG1655 were stained with Propidium Iodide (PI). PI is a fluorescent DNA stain which penetrates the cell membrane of dead cells but is excluded from viable cells. As seen in Figure 3.4, a high proportion of LF82 was

not stained with PI, suggesting the discrepancy was not due to bacterial death (Figure 3.4).

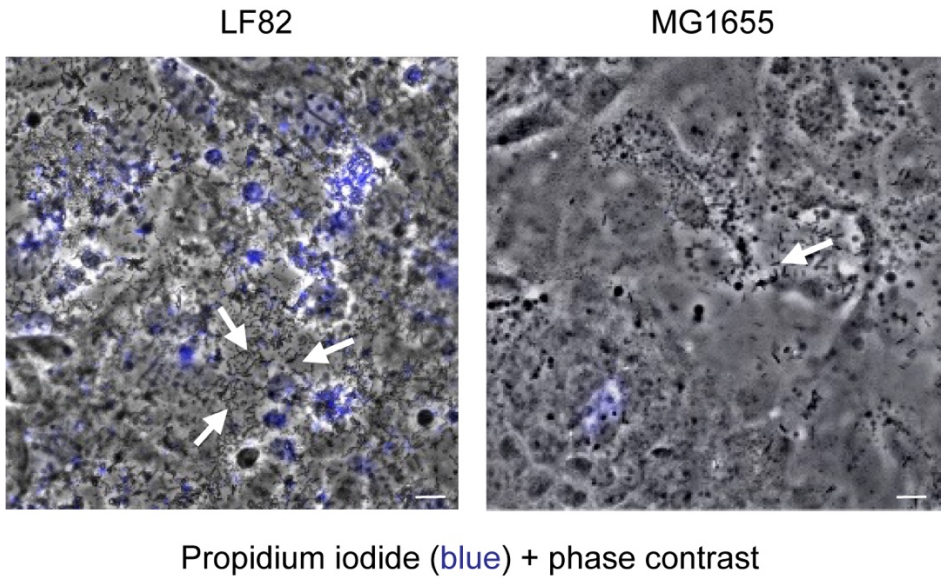

Figure 3.4. Extensive AIEC LF82 adherence is not due to dead bacteria. Confluent T84 cells were incubated with AIEC LF82 or non-invasive *E. coli* MG1655 for 3 hr. Dead bacteria were stained with propidium iodide (blue). Epithelia and total bacteria were visualised by phase contrast (grey). White arrows indicate areas with live bacteria (unstained). Scale bar = 10 μm.

It was hypothesised that the extensive adherence of LF82 observed by microscopy may represent biofilm formation. Biofilm formation is a phenotypic feature of both commensal and pathogenic bacteria to persistently colonise the intestinal mucosa. For example, enteroaggregative *E. coli* (EAEC) form thick biofilms that adhere to the apical side of enterocytes in their pathogenesis (Sheikh et al., 2001). AIEC LF82 has previously been shown to form stronger biofilms than other *E. coli* strains isolated from the intestinal mucosa (Martinez-Medina et al., 2009). Several exopolysaccharides are found in *E. coli* biofilms, one of which is cellulose, known to play a structural role by providing a matrix that protects and supports biofilm growth (Limoli et al., 2015). Therefore, initial investigations into biofilm formation focussed on staining infected monolayers for cellulose by using the fluorochrome calcofluor-white which allows the visualisation of cellulose fibres by fluorescence microscopy.

Biofilm formation was confirmed by calcofluor staining which indicated cellulose fibre-like structures between bacteria on LF82-infected T84 and Caco-2 cells which were not present in MG1655-infected cells (Figure 3.5A and B). Biofilm formation of each strain was further determined on abiotic surfaces by crystal violent staining. AIEC LF82 and MG1655 were incubated in T84 and Caco-2 cell culture medium (DMEM/F-12 or DMEM, respectively) for 24 or 48 hr in 96-well plates and stained with crystal violet solution. AIEC LF82 biofilm formation was significantly higher than that of MG1655 in both DMEM and DMEM/F-12 (Figure 3.5C and D).

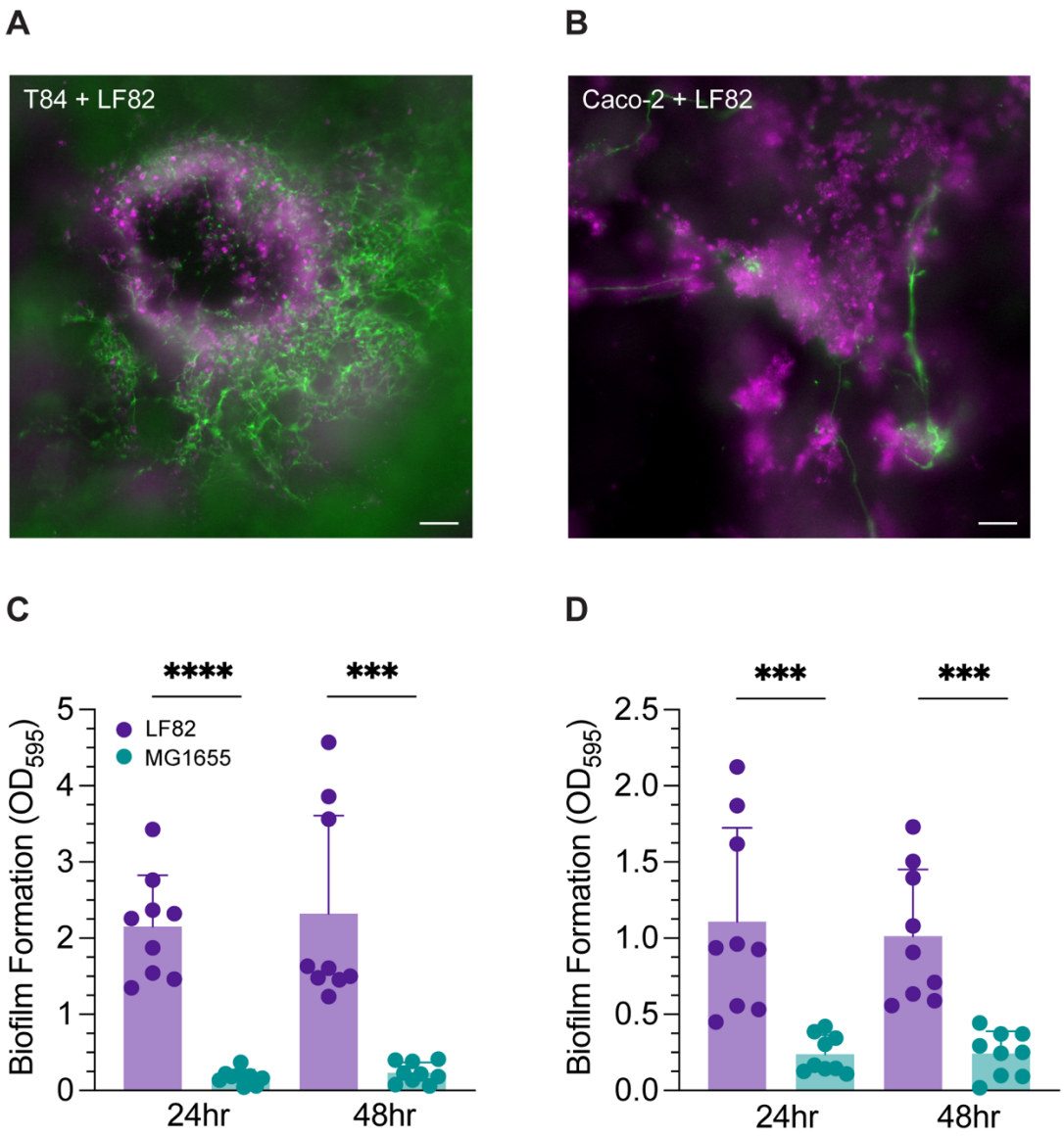

Figure 3.5. AIEC LF82 forms biofilms on T84 (A) and Caco-2 cells (B). Confluent T84 and Caco-2 cells were incubated with LF82 or MG1655 for 3 hr and stained for E. coli (magenta) and cellulose (green). Scale bar = 10 μm. Biofilm formation in DMEM/F-12 (**C**) and DMEM (**D**) on 96-well plates was quantified after 24 or 48 hr by crystal violet staining . Data shown as the mean +- SD. Significance was calculated using a student's unpaired t-test (***p<0.001;****p<0.0001).

3.2.3 T84 cells show heterogenous CEACAM-5 and CEACAM-6 expression which is not associated with LF82 adherence

CEACAM-6 has previously been identified as a receptor for AIEC adhesion to isolated ileal enterocytes from CD patients (Barnich et al., 2007). Of the CEACAM family, CEACAM-1, CEACAM-5 and CEACAM-6 are expressed in the colon and small intestine, while CEACAM-7 is restricted to the colon (Sheikh et al., 2020). Given the association between CEACAMs and the pathogenesis of various *E. coli* pathovars (Sheikh and Fleckenstein, 2023), CEACAM expression and AIEC LF82 binding was investigated in T84 and Caco-2 cells.

T84 monolayers infected with LF82 or MG1655 were stained for *E. coli* and CEACAM-1, 5, 6 or 7 and evaluated by fluorescence microscopy. T84 cells demonstrated heterogenous expression of CEACAM-6, whereby some cells exhibited high CEACAM-6 expression whereas others lacked receptor expression entirely (Figure 3.6A). T84 cells lacked CEACAM-1 and CEACAM-7 expression, but showed heterogenous CEACAM-5 expression, similar to CEACAM-6 (Figure 3.6A). In addition, infected Caco-2 monolayers were also stained for *E. coli* and CEACAM-6. Caco-2 cells exhibited a similar heterogenous pattern of CEACAM-6 expression, as seen in T84 cells (Figure 3.6B).

Interestingly, there was no evident association between adherent LF82 and CEACAM-6 in either cell line (Figure 3.6A and B). LF82 adherence was not localised to areas of high CEACAM-6 expression and instead appeared scattered with no preferential binding, suggesting LF82 binding to confluent T84 and Caco-2 cells may be mediated by a different host receptor. Non-infected T84 monolayers exhibited similar CEACAM-6 expression as those infected with LF82 (Figure 3.6C).

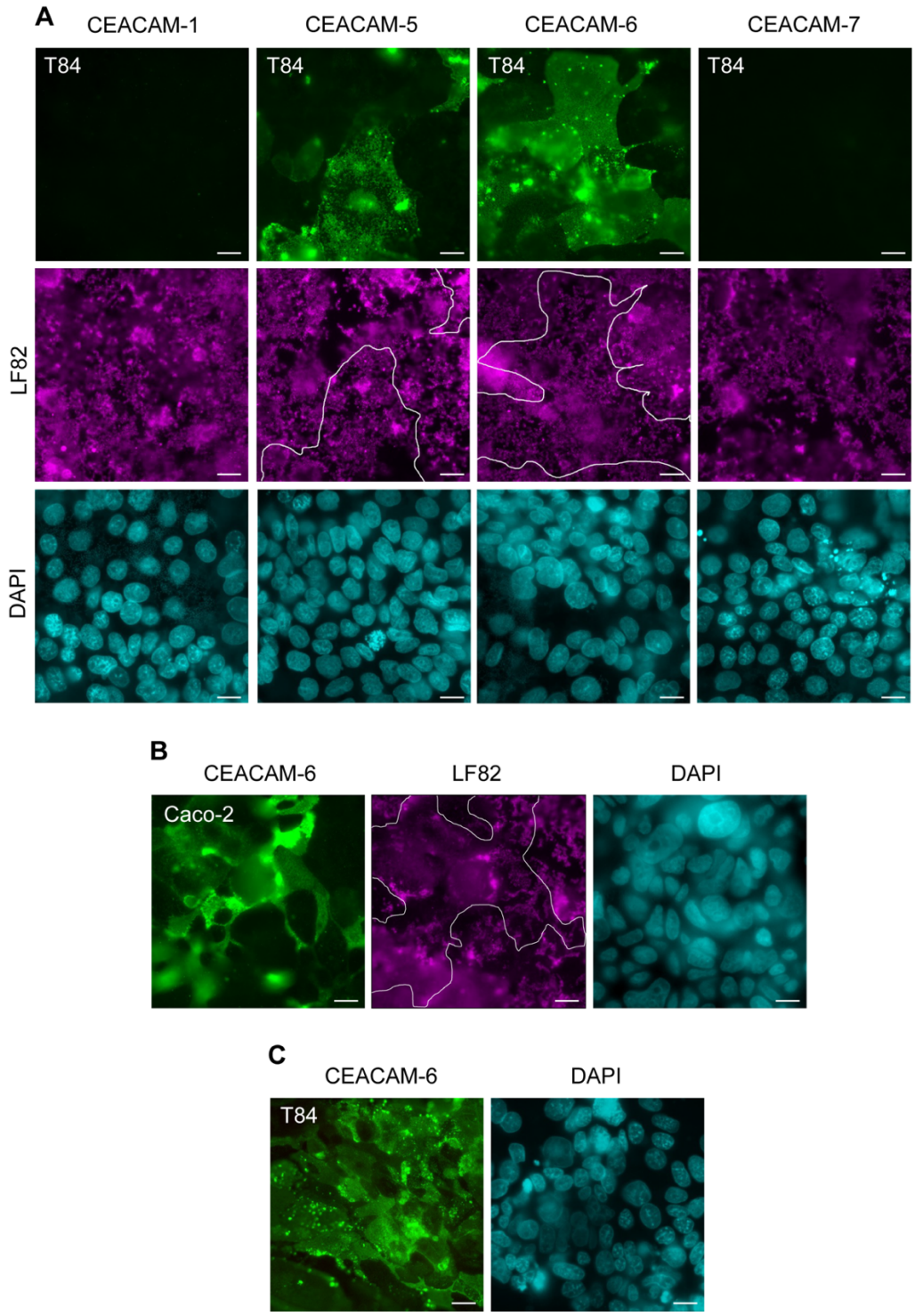

Figure 3.6. T84 cells do not express CEACAM-1 or CEACAM-7, meanwhile CEACAM-5 and CEACAM-6 expression is heterogenous and AIEC LF82 does not bind preferentially to either receptor. Caco-2 cells also display heterogenous CEACAM-6 expression and LF82 does not bind preferentially to CEACAM-6-rich cells. Confluent T84 (**A**) or Caco-2 (**B**) cells were incubated with AIEC LF82 for 3 hr and stained for *E. coli* (magenta), CEACAM-1,5,6 or 7 (green) and DAPI (cyan). Cells with high CEACAM expression are outlined in white. Non-infected T84 cells were stained for CEACAM-6 (green) and DAPI (cyan) (**C**). Scale bar = 10 μm.

3.2.4 LF82 adherence is mediated by a mannosylated receptor that is not CEACAM-6

Previous studies have demonstrated that adherence of AIEC LF82 involves binding of type 1 pili to CEACAM-6 expressed on the apical side of primary ileal enterocytes (Barnich et al., 2007). Given that LF82 did not appear to preferentially bind to CEACAM-6 expressed in T84 and Caco-2 cells when evaluated by microscopy, experiments to inhibit LF82 adherence were performed using CEACAM-specific antibodies. T84 or Caco-2 cells were pre-treated with anti-CEACAM-1, -CEACAM-5, -CEACAM-6 and -CEACAM-7 monoclonal antibodies for 1 hr followed by medium change and subsequent incubation with LF82 for 3 hr. In addition, incubations were performed in the presence of 0.5% D-mannose to block FimH binding to mannose. To evaluate LF82 adherence, monolayers were either fixed, stained for *E. coli* and analysed by microscopy, or lysed and plated for CFU quantification as previously described (See - 2.3.1 Gentamicin invasion assay).

Whilst pre-treatment of T84 or Caco-2 cells with anti-CEACAM-1, -CEACAM-5, -CEACAM-6 and -CEACAM-7 monoclonal antibodies had no significant effect on LF82 adherence (Figure 3.7A and B), adherence was reduced in the presence of 0.5% D-mannose. This was also observed by microscopy (Figure 3.7D).

Given the lack of influence of CEACAM-blocking on LF82 binding, the protocol was modified, and antibodies were retained in the media during bacterial infection. In addition, incubations were shortened to 1 hr to reduce bacterial burden. However, similar results were obtained showing no effect of antibody blocking on LF82 adhesion (Figure 3.7C).

Taken together, these data suggest that the binding of LF82 to colon carcinoma cells occurs via a mannosylated receptor expressed on the apical cell surface other than CEACAM-1, CEACAM-5, CEACAM-6 or CEACAM-7.

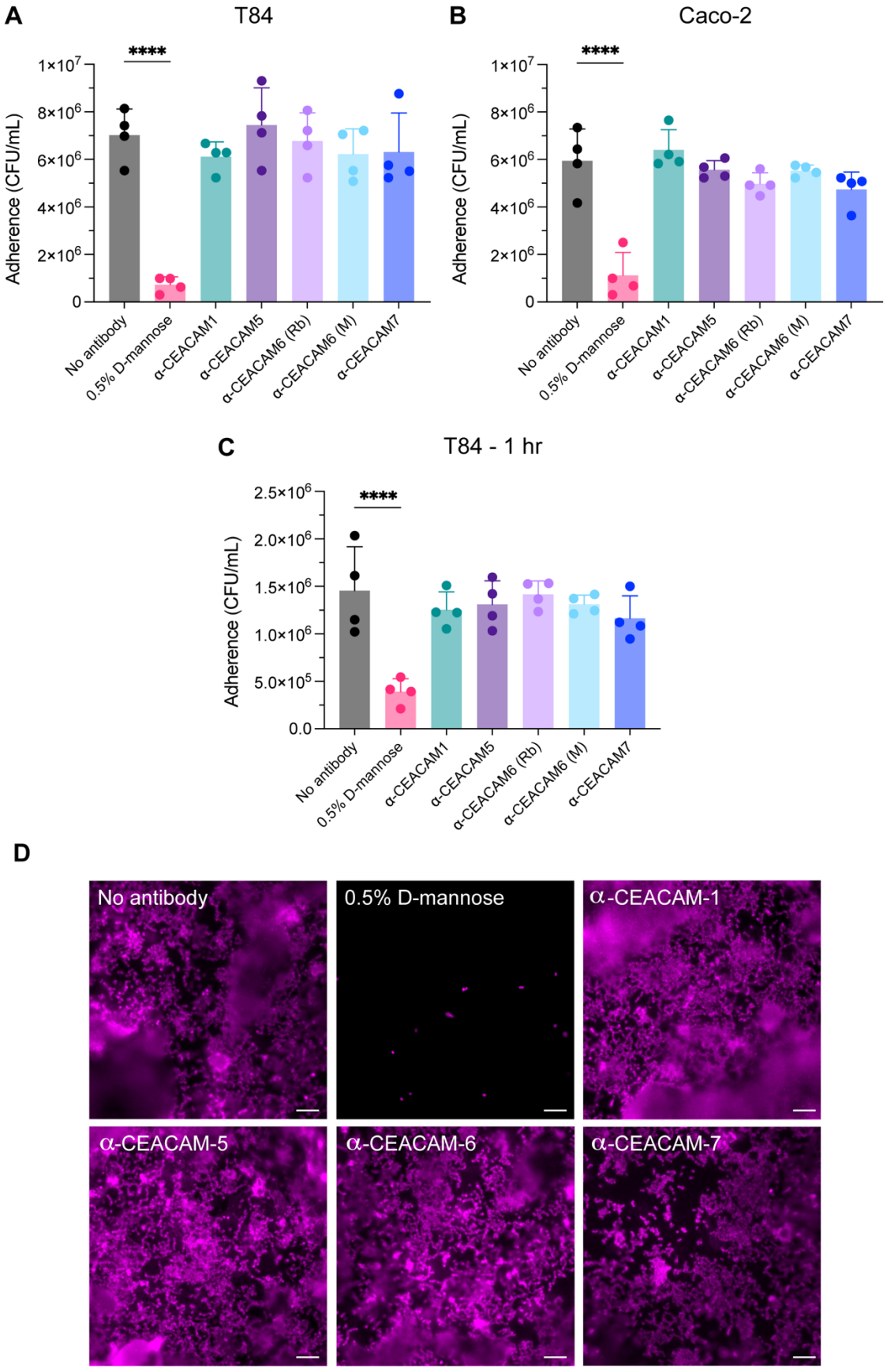

Figure 3.7. LF82 adherence is inhibited by D-mannose, but not by CEACAM antibodies. T84 (**A**) and Caco-2 (**B**) cells were incubated with LF82 for 3 hr. Experiments in T84 cells were also performed using a 1 hr incubation with LF82 without antibody removal

(**C**). Immunofluorescence staining of adherent LF82 on treated T84 cells incubated for 3 hr (**D**). Cell culture media contained either 0.5% D-mannose, antibodies against CEACAMs 1, 5, 6 and 7 or were left untreated (no antibody). For CEACAM-6, a rabbit (Rb) and a mouse antibody (M) were applied. For IFS, the CEACAM-6 mouse antibody was used. Data shown as the mean +- SD. Significance was calculated using a one-way ANOVA test with Dunnett's post-test comparison to no antibody (****$p<0.0001$). Scale bar = 10 μm.

To ascertain that LF82 expresses FimH in cell culture medium, a yeast agglutination assay was performed (Migliore et al., 2018). When present, FimH binds to the mannose receptors on the cell membrane of *Saccharomyces cerevisiae* and agglutination occurs. Bacterial ONCs of LF82 and MG1655 in LB, DMEM or DMEM/F-12 were diluted and mixed with *S. cerevisiae*. Yeast agglutination was determined visually, with a positive reaction forming a sheet, and a negative reaction forming a pellet. LF82 expressed FimH in all conditions, whilst MG1655 only expressed FimH in LB medium (Figure 3.8). In addition, LF82 FimH expression was higher in LB than in DMEM or DMEM/F-12, as agglutination occurred at a higher dilution (Figure 3.8).

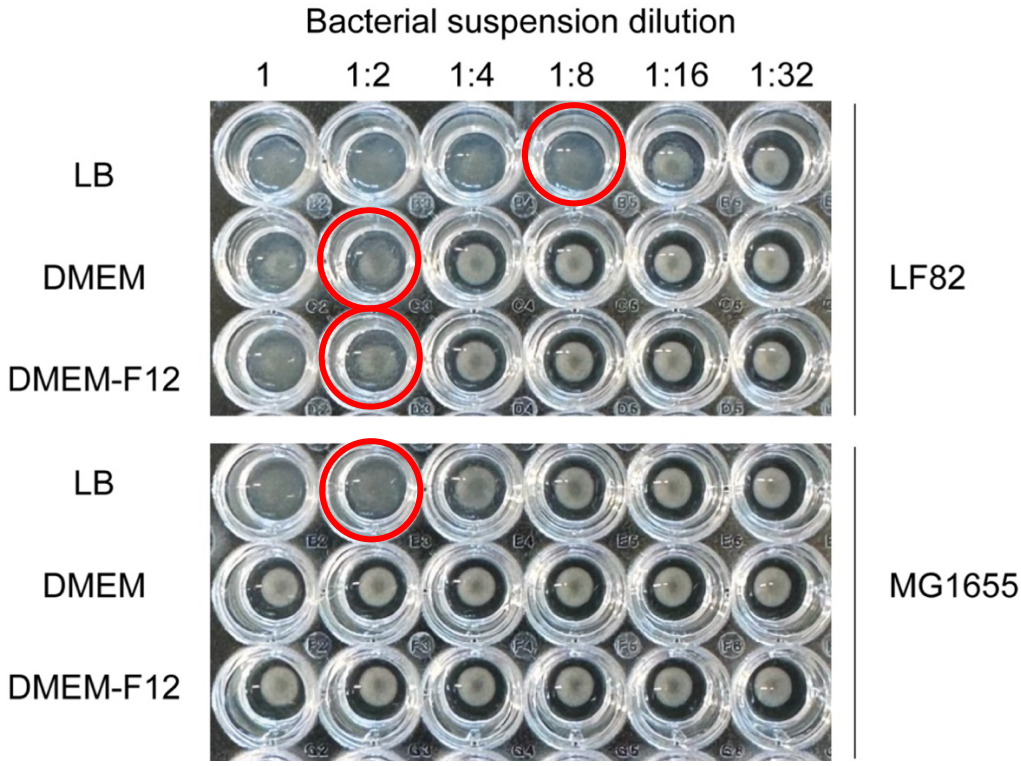

Figure 3.8. AIEC LF82 expresses FimH in cell culture media. Bacterial overnight cultures of LF82 and MG1655 were serially diluted from 1 to 1:32 in LB, DMEM or DMEM/F-12 medium. Commercial baker's yeast (*Saccharomyces cerevisiae*) was added, and agglutination determined visually. The highest dilution giving a positive reaction in each condition is circled in red. Image representative of three experimental repeats.

3.2.5 AIEC LF82 is cytotoxic to T84 and Caco-2 cells

During the invasion assays described previously (See - 3.2.1 AIEC LF82 adherence, invasion and intracellular replication is cell line dependent), cell morphology was visualised by immunofluorescence staining and phase contrast microscopy. Upon examination of infected T84 cell monolayers, changes in cell morphology were observed. LF82-infected T84 cells occasionally exhibited cell elongation and formation of 'holes' in the monolayers (Figure 3.9A). This effect was not observed in Caco-2 cells or MG1655-infected monolayers (Figure 3.9B). Therefore, cytotoxicity was evaluated by Trypan Blue staining which only penetrates dead cells and can be quantified by absorbance at 590 nm (OD_{590}). Trypan Blue staining showed that LF82 induced cytotoxicity in both T84 and Caco-2 cells after 24 hr incubation (3 hr followed by 21 hr gentamicin treatment) (Figure 3.9C and D), with the cytotoxic effect apparent after only 4 hr in T84 cells (Figure 3.9C). Interestingly, cytotoxicity was present in Caco-2 cells after 24 hr although the morphological changes occasionally observed in T84 cells were not evident.

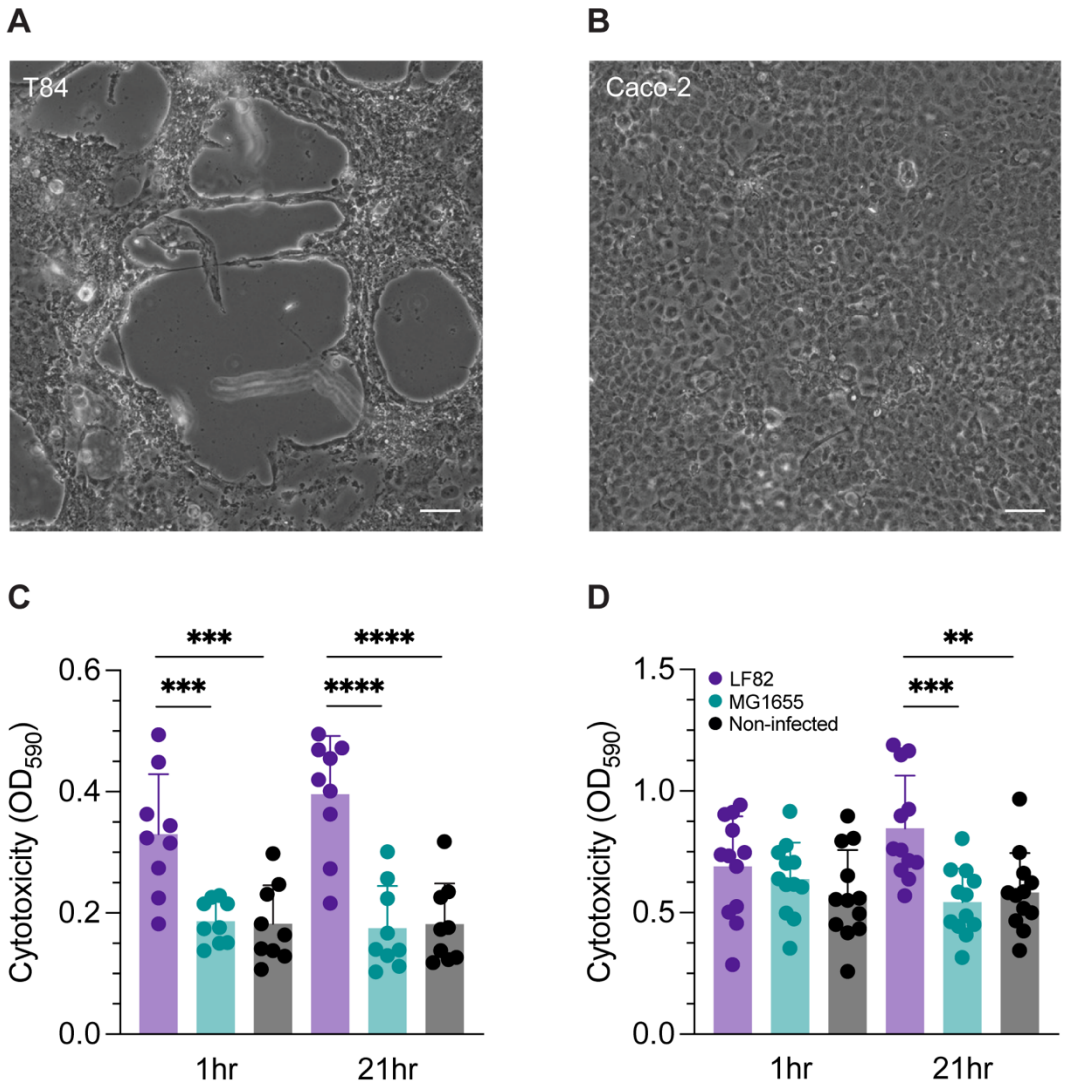

Figure 3.9. AIEC LF82 is cytotoxic to T84 and Caco-2 cells. Confluent T84 and Caco-2 cells were incubated with AIEC LF82 or non-invasive *E. coli* MG1655 or left non-infected for 3 hr, followed by 1 or 21 hr treatment with gentamicin to kill extracellular bacteria (**A**, **B**). Cell morphology was evaluated by light microscopy at 21 hr post gentamicin treatment. Scale bar = 50 μm (**C**, **D**). Cytotoxicity was measured by Trypan Blue staining and quantification at OD_{590}. Data shown as the mean +- SD. Significance was calculated using a one-way ANOVA test with Tukey's post-test comparison (**p<0.01; ***p<0.001; ****p<0.0001).

3.2.5.1 LF82-induced cytotoxicity is not mediated by secreted factors

As secretion of toxins is a common feature in bacterial pathogenesis (Erkmen and Bozoglu, 2016), we determined whether LF82-induced cytotoxicity was mediated by secreted factors. To this aim, T84 cells were incubated with conditioned medium generated from cells incubated with LF82, MG1655 or left non-infected for 24 hr. Results showed that a cytotoxic effect was only detected in LF82-infected cells but not in cells incubated with conditioned media (Figure 3.10).

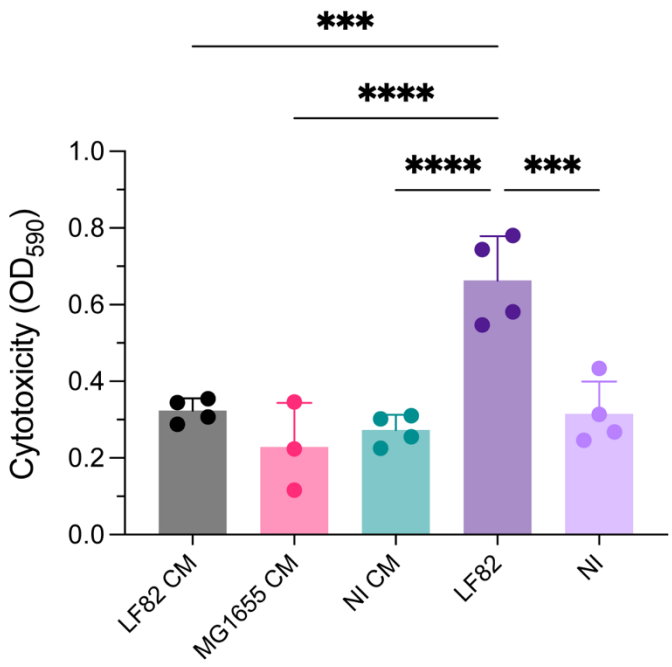

Figure 3.10. AIEC cytotoxicity in T84 cells is contact-dependent. Conditioned media from T84 cells incubated with AIEC LF82, MG1655 or left non-infected for 3 hr were collected and added to fresh T84 cells for a further 21 hr to determine if cytotoxicity was due to secreted factors. Cells incubated with AIEC LF82 or left non-infected for 3 hr plus 21 hr gentamicin treatment were used as a positive and negative control, respectively. Data shown as the mean +- SD. Significance was calculated using a one-way ANOVA test with Dunnett's post-test in comparison to LF82 (***p<0.001; ****p<0.0001).

3.2.5.2 LF82-induced cytotoxicity is independent of bacterial invasion

Additionally, it was investigated whether bacterial invasion was required for host cytotoxicity. It has previously been shown that LF82 invasion of Hep-2 cells is mediated by both an actin microfilament-dependent mechanism and microtubule involvement (Boudeau et al., 1999). The use of cytochalasin D and colchicine can disrupt actin and microtubule involvement, respectively, therefore blocking bacterial invasion. To determine if LF82-induced T84 cytotoxicity was dependent on LF82 invasion, T84 cells were treated with either cytochalasin D, colchicine or left untreated and incubated with LF82 for 3 hr followed by 21 hr gentamicin treatment and cytotoxicity was quantified by Trypan Blue staining. In addition, non-infected controls containing either cytochalasin D or colchicine were included to check for any potential drug-induced cell damage during the assay.

Results indicated no difference in cytotoxicity between LF82-infected cells that were left untreated or treated with either drug. Additionally, cytochalasin D and colchicine did not cause a cytotoxic effect on non-infected cells (Figure 3.11). Therefore, it was concluded that bacterial invasion was not required for cytotoxicity.

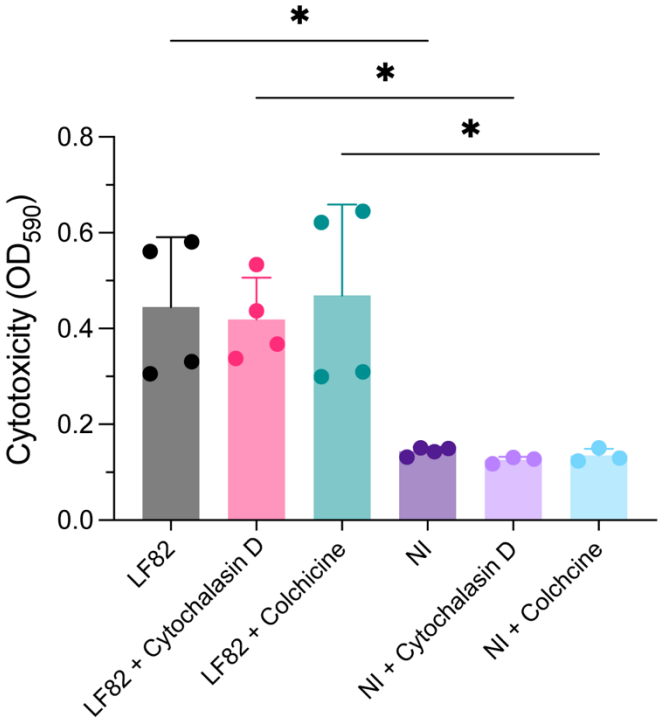

Figure 3.11. AIEC cytotoxicity in T84 cells is independent of invasion. T84 cells were incubated with AIEC LF82 for 3 hr plus 21 hr gentamicin treatment in the presence or absence of cytoskeletal inhibitors cytochalasin D and colchicine. Non-infected controls containing both drugs were included. Data shown as the mean +- SD. Significance was calculated using a one-way ANOVA test with Tukey's post-test comparison (*p<0.05).

3.2.5.3 LF82-induced cytotoxicity is not mediated by T6SS effector proteins

Unlike enteropathogenic and enterohaemorrhagic *E. coli*, AIEC do not harbour a Type 3 Secretion System. However, AIEC strain LF82 possess two Type VI Secretion Systems (T6SS-1 and T6SS-3), encoded by the pathogenicity islands PAI-1 and PAI-3, respectively (Miquel et al., 2010). T6SSs can kill bacterial or eukaryotic target cells by delivering enzymatic effectors (Hernandez et al., 2020). It has previously been suggested that the T6SSs in AIEC LF82 may mediate adherence to and invasion of IECs (Massier et al., 2015). However, studies have shown that T6SS-3 played no role in invasion, whilst inactivation of T6SS-1 increased LF82 invasion (Cogger-Ward, 2019).

To assess whether T6SS effector proteins were responsible for the cytotoxicity observed in LF82-infected T84 cells, cytotoxicity assays were performed with LF82 T6SS functional knockout strains LF82 Δ*tssE1*, LF82 Δ*tssE3* and LF82 Δ*tssE1* Δ*tssE3.* These strains were generated by deletion of TssE subunit genes from T6SS-1 (Δ*tssE1*), T6SS-3 (Δ*tssE*3) or both T6SSs (Δ*tssE1* Δ*tssE3*) (Collins, 2016) and kindly provided by Alan Huett (University of Nottingham).

As before, T84 cells were incubated with bacteria for 3 hr followed by 21 hr gentamicin treatment and cytotoxicity was quantified by Trypan Blue staining. LF82 wildtype was included as a positive control. There was no difference in LF82-induced cytotoxicity between the wildtype and T6SS-knockout strains (Figure 3.12), with all conditions exhibiting higher cytotoxicity than in non-infected cells. This suggests that T6S of effector proteins is not responsible for LF82-induced cell death in T84 cells.

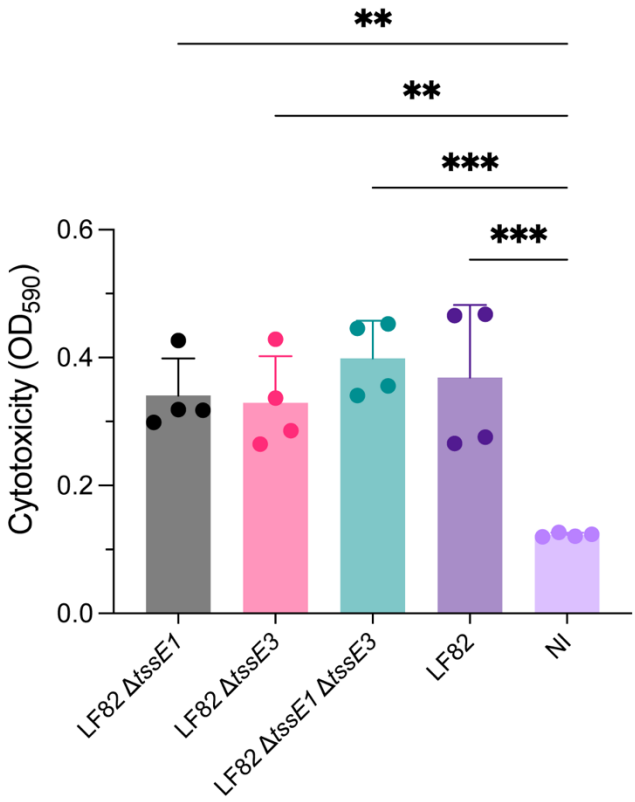

Figure 3.12. LF82-induced cytotoxicity is not mediated by T6SS effector proteins. Confluent cells were incubated with AIEC LF82, LF82 Δ*tssE1*, LF82 Δ*tssE3*, LF82 Δ*tssE1* Δ*tssE3* or left non-infected (NI) for 3 hr, followed by 21 hr treatment with gentamicin. Cytotoxicity was measured by Trypan Blue staining and quantification at OD_{590}. Data shown as the mean +- SD. Significance was calculated using a one-way ANOVA test with Dunnett's post-test in comparison to NI (**p<0.01; ***p<0.001).

3.2.6 AIEC LF82 induces secretion of pro-inflammatory cytokines from T84 cells

The cytokine response has a crucial role in the pathogenesis of CD, as cytokines act as upstream facilitators and downstream mediators of inflammation. Cytokines not only drive intestinal inflammation and diarrhoea in CD but may also regulate systemic effects and drive complications such as intestinal stenosis and fistula formation. Such cytokines include TNF-α, IL-8, IL-6 and IL-1β (Strober and Fuss, 2011).

Therefore, the T84 cell response to LF82 infection was evaluated here by quantification of TNF-α, IL-8, IL-6 and IL-1β release by sandwich ELISA. Non-invasive MG1655 and a non-infected control were included for comparison. Cells were incubated with LF82, MG1655 or left non-infected for 3 hr followed by 21 hr treatment with gentamicin. Cell supernatants were sampled and used for quantification of secreted cytokines. TNF-α levels were significantly higher in supernatants of LF82-infected T84 cells compared to MG1655-infected and non-infected cells (Figure 3.13A). Similarly, IL-8 was significantly higher in LF82-infected cells compared to non-infected controls (Figure 3.13B). MG1655 also induced a higher IL-8 response in comparison to non-infected cells, however this did not reach significance. Additionally, IL-1β levels were significantly higher in LF82-infected cells compared to MG1655 and non-infected samples, however quantities were very low (~8 pg/ml for LF82 infected) (Figure 3.13D). In contrast, there was no significant difference in IL-6 release between LF82, MG1655 and non-infected cells (Figure 3.13C).

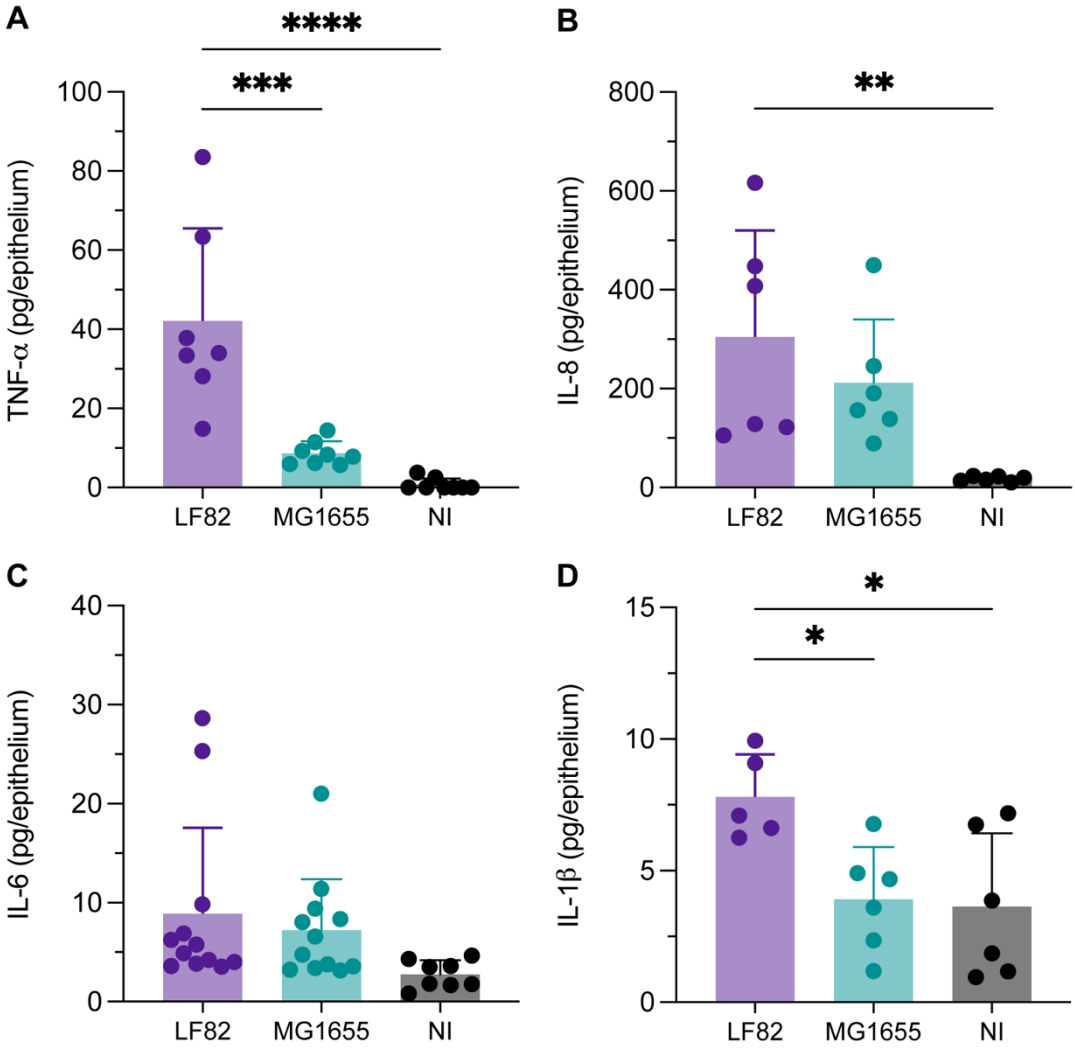

Figure 3.13. LF82 induces pro-inflammatory cytokine release in T84 cells. T84 cells were incubated with LF82, MG1655 or left non-infected for 3 hr followed by 21 hr gentamicin treatment. Cytokines TNF-α (**A**), IL-8 (**B**), IL-6 (**C**) and IL-1β (**D**) in cell supernatants were quantified by ELISA. Data shown as the mean +- SD. Significance was calculated using a one-way ANOVA test with Tukey's post-test comparison (*p<0.05; **p<0.01; ***p<0.001; ****p<0.0001).

3.2.7 AIEC interaction with colonic cells is strain-specific

The prototype AIEC strains LF82 and NRG857c were originally isolated from the ileal mucosa of CD patients (Boudeau et al., 1999; Eaves-Pyles et al., 2008). Other studies have isolated AIEC from colonic CD specimens (Martin et al., 2004). Similar to ileal LF82 and NRG857c, colonic strains HM615, HM605 and HM580 have been shown to adhere to and invade intestinal cell lines Caco-2 and HT29, and HeLa cell-derived I407. Given the low invasion rates of LF82 and the lack of preferential binding to CEACAM-6, our studies on AIEC interaction with T84 cells was expanded to other AIEC isolates.

3.2.7.1 AIEC adherence, invasion and intracellular replication is strain-specific

To determine the adherence, invasion and intracellular replication of additional AIEC isolates, gentamicin assays were performed as previously described (See - 2.3.1 Gentamicin invasion assay). Following a 3 hr infection of T84 cells, NRG857c, HM615 and HM605 demonstrated similar levels of adherence as LF82, meanwhile HM580 showed significantly higher adherence (Figure 3.14A). A growth curve of all strains showed that NRG857c, HM615, HM605 and HM580 demonstrated higher growth than LF82 after 3 hr (Figure 3.14B). Numbers of intracellular bacteria after 1 hr were similar between LF82, NRG857c, HM615 and HM605, however numbers of intracellular HM580 were significantly higher compared to LF82. Interestingly, numbers of intracellular NRG857c and HM580 after 21 hr were significantly higher compared to LF82 (Figure 3.14D). Calculation of invasion rates demonstrated that NRG857c was significantly more invasive than LF82, meanwhile HM615, HM605 and HM580 invasion rates were similar to that of LF82 (Figure 3.14E). Furthermore, replication rates demonstrated that NRG857c also had the highest replication rate (Figure 3.14F) and interestingly, HM580 replication was also significantly higher than that of LF82 despite showing a similar invasion rate. The replication rate of HM615 was below 100%, suggesting it is cleared from T84 cells.

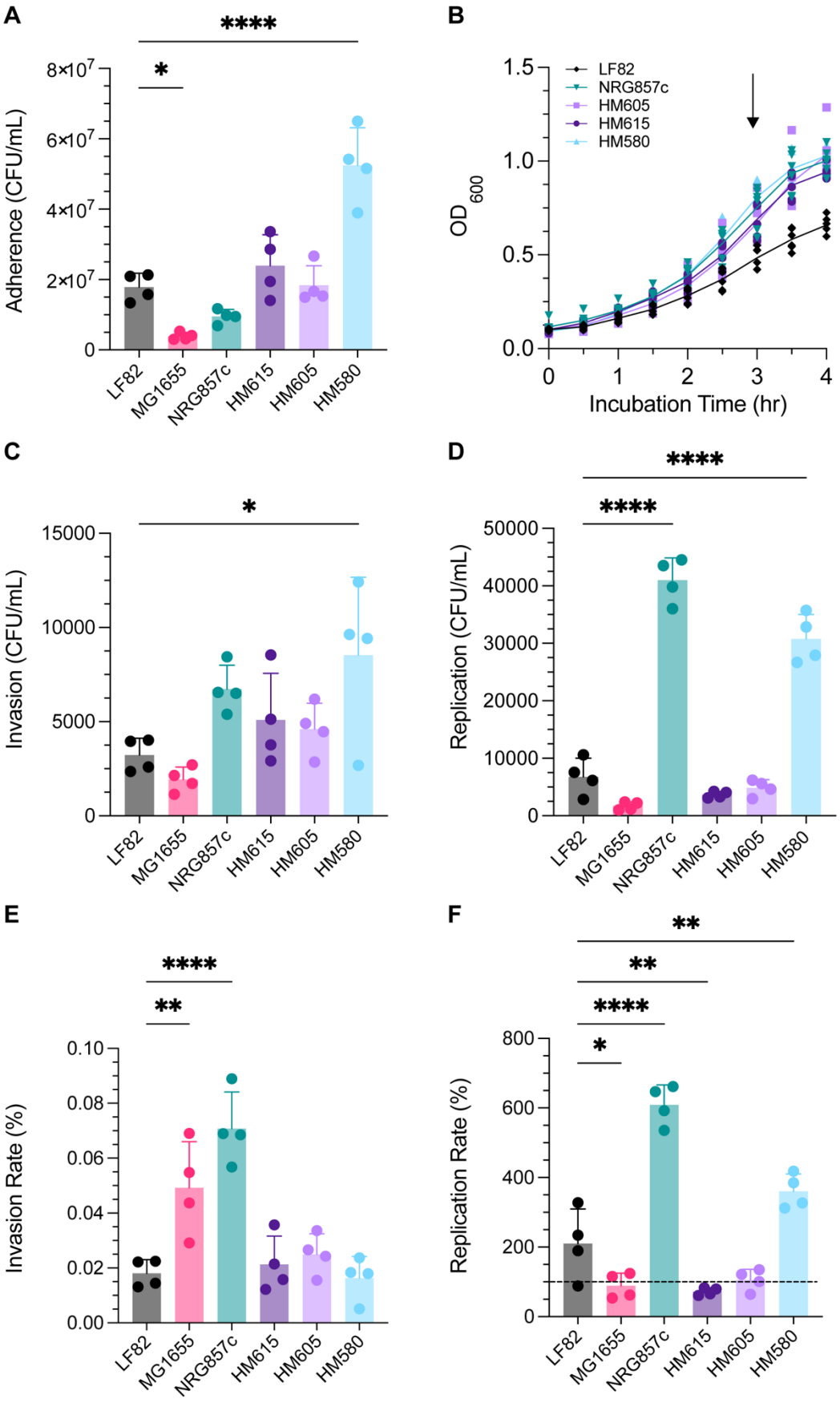

Figure 3.14. Adherence, invasion and intracellular replication of AIEC LF82, NRG857c, HM615, HM605 and HM580 and *E. coli* MG1655 in T84 cells. Confluent cells

were incubated with each strain for 3 hr, followed by 1 hr or 21 hr of gentamicin to kill extracellular bacteria. Numbers of adherent bacteria were determined after 3 hr by CFUs (**A**). Bacterial growth of all strains was determined by quantification at OD_{600} with the arrow indicating the 3 hr adherence timepoint (**B**). Invasion (**C**) and intracellular replication (**D**) was determined after 1 hr or 21 hr of gentamicin treatment, respectively, and cell lysates plated for CFUs. Results were normalised to an inoculum of 10^7 bacteria. Invasion rates (**E**) and replication rates (**F**) were calculated relative to adherent and invaded bacteria respectively. Data shown as the mean +- SD. Significance was calculated using a one-way ANOVA test with Dunnett's post-test in comparison to LF82 (*p<0.05; **p<0.01; ****p<0.0001).

To determine whether binding of AIEC strains NRG857c, HM615, HM605 and HM580 was associated with CEACAM-6 localisation, IFS was performed. Initially, T84 infected for 3 hr were stained with the rabbit *E. coli* OK antibody and DAPI to determine antibody reactivity with the different AIEC strains. Whilst *E. coli* OK stained most bacteria of strains LF82, NRG857c, HM615 or HM605, detection of HM580 was poor (Figure 3.15). Therefore, DAPI was used to visualise adherent HM580. Subsequent co-staining of infected T84 cells for CEACAM-6 did not show any evident association between adherent AIEC NRG857c, HM615, HM605 or HM580 with CEACAM-6 (Figure 3.16).

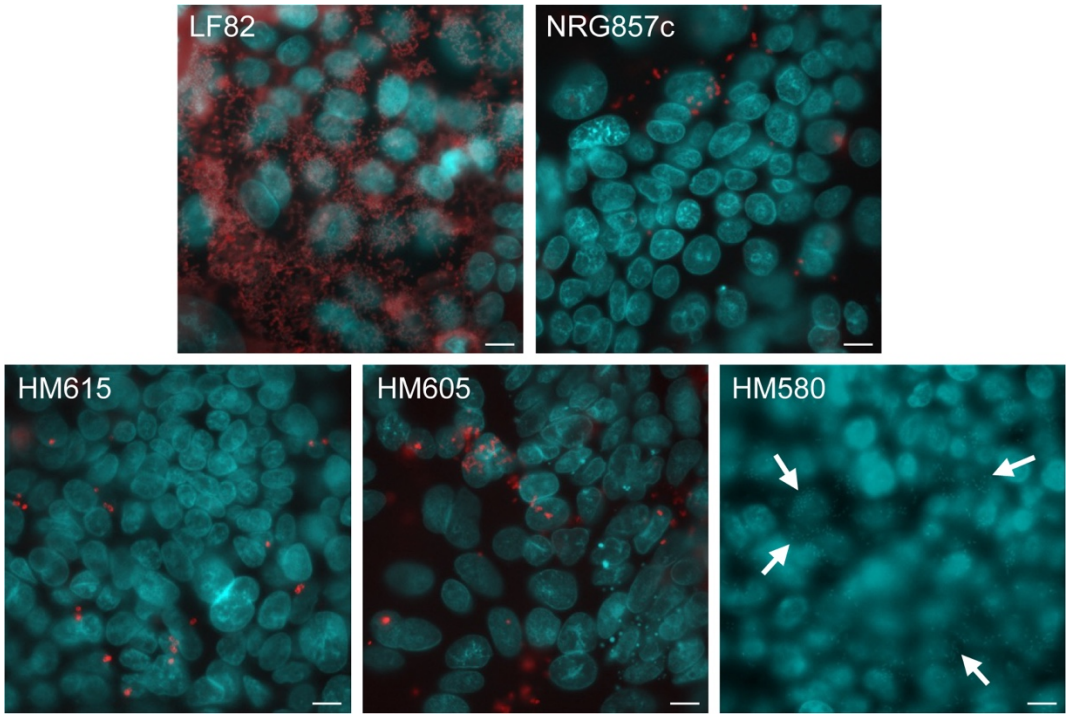

Figure 3.15. AIEC strains LF82, NRG857c, HM615, HM605 but not HM580 were detected by the rabbit *E. coli* OK antibody. Confluent T84 cells were incubated with AIEC LF82, NRG857c, HM615, HM605 or HM580 for 3 hr and stained for *E. coli* (red) and DAPI (cyan). White arrows indicate areas with DAPI-stained HM580 bacteria (Scale bar = 10 μm).

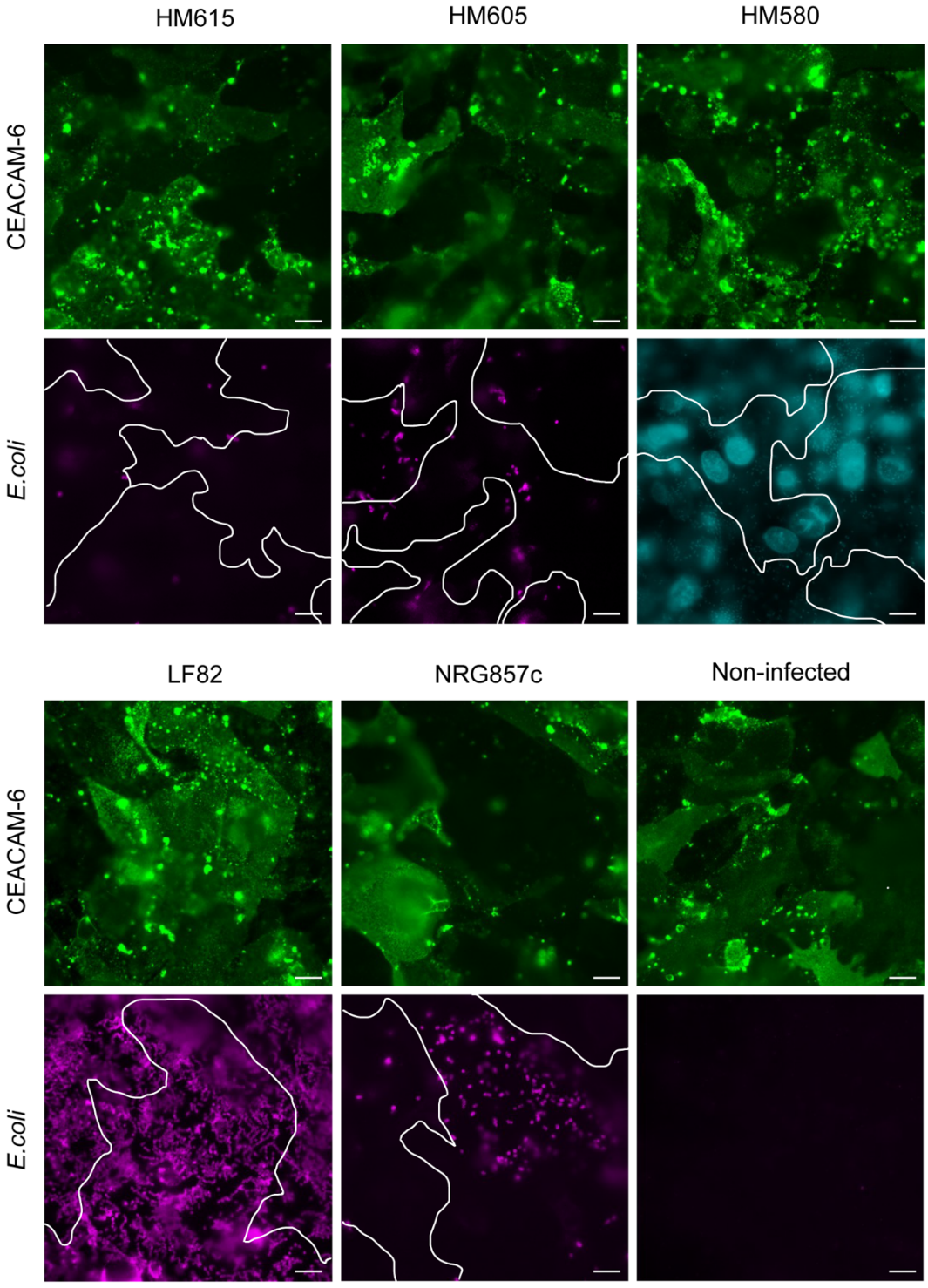

Figure 3.16. Adherence of AIEC strains HM615, HM605, HM580, LF82 and NRG857c to T84 cells. Confluent T84 cells were incubated with AIEC HM615, HM605, HM580, LF82, NRG857c or left non-infected for 3 hr and stained for *E. coli* (magenta) and CEACAM-6 (green). Cells with high CEACAM-6 expression are outlined in white. For HM580, DAPI staining is shown as the *E. coli* OK Ab did not stain the majority of bacteria. Scale bar = 10 μm.

3.2.7.2 The AIEC LF82 cytotoxicity phenotype is not present in other AIEC strains

To determine whether the cytotoxicity mediated by LF82 is shared amongst other AIEC strains, T84 cells were infected with strains NRG857c, HM615, HM605 and HM580 for 3 hr followed by 21 hr gentamicin treatment and cytotoxicity was determined. LF82-infected and non-infected cells were included as positive and negative controls, respectively. Results indicated that HM615, HM605, HM580 and NRG857c did not induce cytotoxicity in T84 cells and cytotoxicity was comparable to the levels seen in non-infected cells (Figure 3.17). Only LF82 showed significantly higher levels of cell death compared to non-infected controls (Figure 3.17).

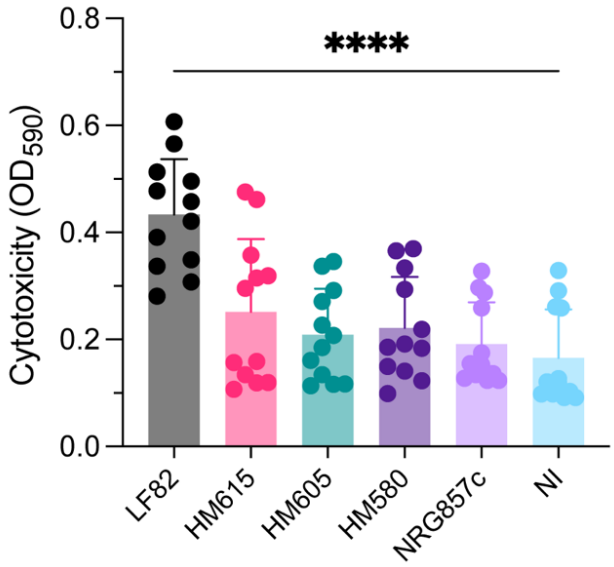

Figure 3.17. AIEC LF82-mediated cytotoxicity is not exhibited by colonic strains HM615, HM605 and HM580 or ileal strain NRG857c in T84 cells. Confluent T84 cells were incubated with AIEC LF82, HM615, HM605, HM580, NRG857c or left non-infected (NI) for 3 hr, followed by 21 hr treatment with gentamicin. Cytotoxicity was measured by Trypan Blue staining and quantification at OD_{590}. Data shown as the mean +- SD. Significance was calculated using a one-way ANOVA test with Dunnett's post-test comparison to NI (****p<0.0001).

3.2.8 Summary

Overall, the results of this study showed that AIEC LF82 adherence and biofilm formation was significantly increased compared to non-pathogenic *E. coli* MG1655, meanwhile invasion and intracellular replication were comparable in both strains. Notably, LF82 binding was mediated by fimbriae but occurred independently of the established ileal AIEC receptor CEACAM-6. Despite low invasion and intracellular replication, infection with LF82 resulted in cytotoxicity which was dependent on bacterial contact but not invasion or type VI secretion of effector proteins. In addition, LF82-infected T84 cells exhibited increased release of pro-inflammatory TNF-α, IL-6 and IL-8. Extension of our studies to additional ileal and colonic AIEC isolates demonstrated highly divergent infection strategies between strains. Therefore, these results suggest that LF82 pathogenesis in the human colon is strain-specific and mediated by the formation of stress-resistant biofilms, contact-dependent cytotoxicity and pro-inflammatory cytokine secretion.

3.3 Discussion

3.3.1 AIEC LF82 adherence, invasion and replication is cell-line dependent

Early experiments by Boudeau and colleagues characterised the invasive ability of LF82 using a gentamicin protection assay, whereby the membrane-impermeable antibiotic gentamicin is utilised to kill extracellular bacteria whilst having no effect on the host cell (Boudeau et al., 1999). As a result, intracellular CFU can be accurately determined by plating out dilutions of infected lysed cells. These early studies used intestinal epithelial cell lines Intestine-407, HCT-8 and Caco-2, whereby cells were grown for 48 hours. This time frame is not long enough to allow a confluent, polarised monolayer to form, therefore affecting cell height and distribution of cell surface receptors (Langerholc et al., 2011). Additionally, cell line Intestine-407, whilst initially thought to be derived from normal embryonic intestinal tissue, was later identified as a contaminant of the cervical cancer-derived cell line HeLa and is therefore not representative of intestinal epithelial cells (Korch and Capes-Davis, 2021).

In this investigation, experiments were initially repeated using non-confluent T84 and Caco-2 colon carcinoma cells. Whilst LF82 exhibited extensive adherence compared to MG1655, invasion rates were unexpectedly low when invaded bacteria were calculated as a percentage of adherent bacteria. Although MG1655 invasion was higher than LF82, it is important to note overall LF82 invasion rates were low (~0.2% in T84 cells, ~0.1% in Caco-2) compared to similar studies in the literature, where a 1% invasion rate of T84 cells (Elatrech et al., 2015) and 4% invasion of Caco-2 cells (Boudeau et al., 1999) has previously been observed. Furthermore, the invasion % calculated in the studies by Boudeau et al were calculated as a percentage of the inoculum surviving gentamicin treatment, whereas in our studies the percentage of invasion was standardised to levels of adherent bacteria. These experiments were repeated in cells grown to confluence, and displayed similarly low invasion rates. Interestingly, the replication of LF82 in T84 cells was approximately 4-fold in non-confluent and 2-fold in confluent cells, meanwhile, in Caco-2 cells,

replication rates were below 100% in both states. This indicates a potential mechanism of clearance in Caco-2 cells that is not present in T84 cells and demonstrates intracellular replication of AIEC LF82 differs between cell lines. Interestingly, studies by Larabi et al demonstrated that upon AIEC LF82 infection, miR-30c and miR-130a were packaged in exosomes and transferred to recipient T84 cells, in which they inhibit ATG5 and ATG16L1 expression and suppress autophagy using qRT-PCR analysis (Larabi et al., 2020). In addition, AIEC have been shown to inhibit autophagy by impairing host SUMOylation leading to increases in AIEC intracellular replication *in vitro* (Bretin et al., 2016; Dalmasso et al., 2019; Nguyen et al., 2014). This could therefore explain the higher replication observed in T84 cells in comparison to Caco-2. In contrast, Dalmasso et al showed that a functional siderophore yersiniabactin is implicated in the activation of autophagy upon infection with AIEC in T84 cells (Dalmasso et al., 2021). Whilst yersiniabactin is an advantage for AIEC survival and growth in an iron-restricted environment, presence of the siderophore in AIEC activated Hif-1α, leading to autophagy activation and consequently a better host control of AIEC intracellular replication (Dalmasso et al., 2021).

The intrinsic heterogeneity of Caco-2 cells is also important to consider, given that several clones have been isolated from the parental line (Sambuy et al., 2005), therefore making it difficult to compare results in the literature when the sub-type of Caco-2 cells has not been specified. As a result, the sub-clones may display different morphological and functional characteristics which may affect the results described in these studies. In addition, Caco-2 cells have demonstrated increased division rate, decreased expression of cell surface receptors and altered membrane permeability at higher passage numbers (Yu et al., 1997). This could explain differences between results in the literature due to selection of fast-growing sub-populations during passaging.

3.3.2 LF82 forms biofilms on T84 and Caco-2 cells

Biofilms are a community of bacteria living within an extracellular polymeric substance (EPS) matrix, produced by the bacteria, and adhere to each other on either living or non-living surfaces (Gupta et al., 2016; Zhao et al., 2023). Bacteria employ biofilm formation under environmental cues to develop a relationship with the host, display resistance in harsh conditions or to survive antibiotic and host response-mediated stress (Castiblanco and Sundin, 2016). As a result, biofilm formation contributes towards the development of antibiotic resistance and the persistence of infections (Pang et al., 2019).

E. coli biofilm formation is a well-characterised and defined process, present amongst both commensal and pathogenic *E. coli* (Reisner et al., 2006). However, the wide range of environmental niches in which *E. coli* can thrive combined with the genomic variability amongst strains suggests varying biofilm formation strategies which are underexplored. Commensal GI *E. coli* typically reside in the outer mucus layer of the colon without contacting the underlying epithelium (Conway and Cohen, 2015), establishing biofilms by formation of an ECM consisting of curli and cellulose (Hufnagel et al., 2015). In addition, AIEC have been shown to be higher biofilm producers than non-AIEC strains, where adhesion and invasion correlated with biofilm formation capabilities (Martinez-Medina et al., 2009b). Given that increased AIEC has been observed in intestinal biopsy specimens of IBD patients (Darfeuille-Michaud et al., 2004), the ability to form biofilms could contribute to IBD aetiology and is thus gaining interest in AIEC and IBD research.

Previous research demonstrated that AIEC deposited cellulose in microcolonies on Caco-2 cells, promoted by a T4SS (Elhenawy et al., 2021). Furthermore, Prudent et al found that intracellular LF82 produced an extrabacterial matrix that acts as a biofilm and controls the formation of LF82 intracellular bacterial communties (IBCs) (Prudent et al., 2021). In our study, extensive LF82 adherence was initially observed on confluent Caco-2 and T84 cells and biofilm formation was subsequently confirmed by detection of cellulose fibres inbetween bacteria. However, quantification of cellular biofilm formation was problematic due to a lack of distinctive

E. coli antibody labelling. This could be circumvented by GFP labelling of bacteria. Instead, quantification of abiotic biofilms in 96-well plates confirmed our findings and indicated strong biofilm formation by LF82. This is in agreement with earlier studies by Martinez-Medina et al which demonstrated AIEC strains, including LF82, are strong biofilm-producers and associated with pathogenesis and colonisation of the ileal mucosa in CD (Martinez-Medina et al., 2009b).

With distinct bacterial labelling and a strong signal, biofilms on biotic surfaces can be quantified by imaging and automated cell counting (Wilson et al., 2017). In addition to a lack of labelling in our studies, LF82 was found to form chain-like structures, making it difficult to isolate single bacterial cells for counting. Another method of biofilm quantification includes flow cytometry, or FACS analysis, which would provide a value of adherent bacterial cells (Ambriz-Aviña et al., 2014). This method would also require a strong bacterial signal and lack of aggregation. Additionally, this comes with limitations in that staining may pick up host cell debris, affecting output.

In contrast to LF82, AIEC strains NRG857c, HM580, HM605 and HM615 did not form biofilms on confluent T84 cells. Although this was not confirmed by cellulose staining, AIEC binding was diffuse or restricted to very few adhering bacteria (HM605). This agrees with previous studies (Vejborg et al., 2011) which demonstrated that HM580 and HM605 did not form biofilms in 96-well plates while HM615 biofilm fomation was significantly reduced compared with LF82. Interestingly, Vejborg et al found potential AIEC virulence genes to be strain-specific and not shared between isolates, thus making it difficult to identify specific markers (Vejborg et al., 2011). Amongst these were a number of biofilm-related genes including *fim*, *flu* and *csg* genes encoding type 1 fimbriae, Ag43 (autotransporter protein) and curli, respectively. In addition, isolates from IBD patients did not display any consistently better biofilm-forming capacity *in vitro* compared to isolates from healthy controls (Vejborg et al., 2011), suggesting genes are not shared between strains and other factors are required for pathogenesis in IBD. This contributes to the hypothesis that AIEC are a diverse group and each strain may potentially have

its own virulence strategy. Whilst LF82 is regarded as the AIEC prototype strain, its virulence traits displayed here, including extensive adherence and cytotoxicity, do not apply to the other strains tested, highlighting the need to revise the criteria used to define AIEC.

3.3.3 LF82 adherence to Caco-2 and T84 cells is mannose-dependent but not mediated by CEACAM-6

Various adhesins that mediate AIEC adherence to IECs have been described. For example, ChiA binds to inducible CHI3L1, which is overexpressed in colonic epithelial cells during inflammation (Chen et al., 2011; Mizoguchi, 2006). Meanwhile, the OmpA-Gp96 interaction supports OMV fusion with IECs and promotes AIEC invasion (Rolhion et al., 2010). Previous studies have implicated CEACAM-6 as a receptor for AIEC LF82 binding by FimH (Barnich et al., 2007). The studies by Barnich et al utilised ileal biopsies to determine CEACAM-6 expression and interaction with LF82. Their results demonstrated AIEC adhere to the brush border of primary ileal enterocytes isolated from CD patients but not to healthy controls. In addition, blocking of CEACAM-6 with a monoclonal antibody reduced LF82 binding, and CEACAM-6 expression was elevated in ileal epithelial cells of CD patients versus non-IBD controls. Interestingly, expression of CEACAM-6 was also increased after infection with AIEC, suggesting AIEC can promote its own colonisation in CD.

In contrast, the results of our study showed that LF82 adherence is not mediated by CEACAM-6 binding in the colonic epithelium. Immunofluorescent staining of LF82-infected T84 cells indicated LF82 binding was independent of CEACAM-6 expression. The use of CEACAM monoclonal antibodies to block LF82 binding demonstrated no change in LF82 adhesion compared to non-treated controls. Interestingly, some of these results aligned with those of Barnich et al., whereby blocking CEACAM-1 and 5 had no effect on LF82 adhesion, however our results conflicted with the blocking of CEACAM-6. In this investigation, CEACAM-6 antibodies did not block LF82 adherence to T84 cells, whereas Barnich et al demonstrated a significant reduction in LF82 adherence to ileal IECs using the same

antibody (clone 9A6, Santa Cruz) and blocking protocol. This discrepancy could be due to differences in intestinal binding sites (ileum versus colon) as no upregulation of CEACAM-6 expression was observed in the colonic mucosa of CD patients (Barnich et al., 2007). In addition, AIEC access was restricted to the apical cell surface in our experiments whereas bacteria were exposed to isolated ileal IECs in the Barnich study, thereby allowing basolateral membrane binding. Furthermore, our results showed similar CEACAM-6 expression in non-infected T84 monolayers and those infected with LF82 although this was not quantified by Western Blot or ImageJ analysis. Therefore, increased CEACAM-6 expression observed after infection with AIEC in ileal enterocytes (Barnich et al., 2007) might not be reflected in T84 cells.

Whilst the same monocolonal antibody (clone 9A6) was used in our investigations as those by Barnich et al, it is important to consider that monoclonal antibodies are not guaranteed to block AIEC binding if the epitope is located outside of the binding site. In addition, the lack of a positive control, such as ETEC which has been confirmed to bind via CEACAM-6, is a limitation to our studies. Sheikh et al confirmed ETEC binding to CEACAM-6, whereby a CRISPR-Cas9 deletion of CEACAM-6 in intestinal epithelial cells led to a marked decrease in bacterial adhesion by wildtype ETEC (Sheikh et al., 2020). Additionally, the study showed interaction of recombinant CEACAM-6 with the mannose-binding lectin domain of FimH (Sheikh et al., 2020).

Our studies demonstrated that LF82 adherence was dependent on FimH binding to mannose, given that in the presence of 0.5% D-mannose, LF82 binding to T84 and Caco-2 cells was significantly reduced. It is important to consider any potential effects of D-mannose and its mechanism of action on *E. coli* physiology. Whilst our study did not investigate whether D-mannose has any toxic activity on AIEC LF82, multiple studies in uropathogenic *E. coli* (UPEC) demonstrate that D-mannose, even at relatively high concentrations, does not alter bacterial growth, viability or morphology, indicating that it lacks bacteriostatic or bactericidal activity against *E. coli* strains *in vitro*. In the prototype UPEC strain CFT073, high concentrations of D-

mannose had no detectable effect on colony formation or growth dynamics on solid media or in broth, and did not influence bacterial motility or morphology compared with untreated cells (Scribano et al., 2020). Systematic reviews of the use of D-mannose in urinary tract infection prevention similarly conclude that it interferes with type 1 fimbriae–mediated adhesion without affecting bacterial metabolism or growth, and that its action does not involve direct effects on bacterial or host cellular processes (Scaglione et al., 2021). Therefore, this supports the interpretation that D-mannose is not inherently toxic to AIEC, but instead acts as an anti-adhesive. Collectively, these results suggest that the upregulation and binding of AIEC to CEACAM-6 is specific to the ileal segment in CD while different mannosylated host cell receptors are likely to play a role in AIEC colonisation of the colon.

This could be due to differential gene expression and environmental changes along different areas of the gastrointestinal tract. For example, in the GI tract, *S*. Typhimurium Std fimbriae (Suwandi et al., 2019) and *Bacillus subtilis* YesU (Tiralongo et al., 2018) use abundant fucosylated glycans to adhere to and colonise the gut. *Vibrio cholerae* adhesins, including *V. cholerae* cytolysin (VCC) and RbmC, bind complex-type N-linked glycans expressed on intestinal epithelial cells to support colonisation (De et al., 2018). Meanwhile, ETEC adhesin EtpA binds blood group A glycans to adhere and deliver toxins (Kumar et al., 2018). Although beyond the scope of this thesis, this could potentially be explored by the use of glycan arrays or mass spectrometry analysis of LF82-infected colonic epithelia in future studies to identify the mannosylated receptor. For example, the use of a shotgun carbohydrate microarray to identify receptors for ETEC fimbrial adhesins demonstrated that the blood group A type 1 hexasaccharide acts as a receptor for the FedF lectin domain and remarkably also for F18-fimbriated *E. coli* in livestock (Lonardi et al., 2013). A shotgun approach could thus help in identifying AIEC receptors *in vivo*. Current strategies to block AIEC binding include approaches to block the receptor CEACAM-6 or to interfere with CEACAM-6 glycosylation (Sivignon et al., 2022; Sun et al., 2020). However, based on the results of this thesis, these strategies would only be applicable in the small intestine and not the colon. Meanwhile, approaches to block

FimH, and thus bacterial adhesion, using a specific FimH antagonist (TAK-018) may be more suitable (Chevalier et al., 2021).

3.3.4 AIEC adherence, invasion and intracellular replication is strain-specific

Whilst increased numbers of AIEC have been reported in the ileum of CD patients, there is also evidence of *E. coli* associated with the colonic mucosa (Martinez-Medina et al., 2009a). In addition, mucosa-associated *E. coli* that resisted gentamicin treatment and were assumed to be intracellular have been located within the histologically normal regions of the colonic mucosa in colon cancer patients (Swidsinski et al., 1998). Studies by Martin et al demonstrated the presence of increased numbers of adherent, hemagglutinin-expressing *E. coli* on and within CD mucosae which are able to induce IL-8 release from IEC lines I407 and HT29 (Martin et al., 2004). Strains HM580, HM605 and HM615 used in our study were isolated from the colonic mucosa of CD patients. In addition to LF82, NRG857c is also an AIEC strain isolated from the ileum of a CD patient. NRG857c belongs to the same serogroup as LF82 and shows high sequence similarity, whereby 35 genomic islands in NRG857c are highly orthologous in LF82 (Nash et al., 2010).

The low invasion rates of LF82 and lack of preferential binding to CEACAM-6 led to extension of our studies to include ileal strain NRG857c and colonic strains HM615, HM605 and HM580. Our results suggest that adherence, invasion and intracellular replication of AIEC to colonic cells is strain-specific. Of all strains investigated, HM580 displayed significantly higher adherence. Interestingly, the adherence of HM580 to T84 cells in our study (5.2×10^7 CFU/well) was much higher than described previously, whereby 2.7×10^5 and 3.54×10^4 CFU/well adherence to I407 and HT29 cells respectively was shown (Martin et al., 2004). Although higher than LF82, the growth of HM580 was similar to other strains and therefore may not be responsible for the increase in adherence. Interestingly, whilst HM580 showed higher adherence, it has previously been described that HM580 does not form biofilms like LF82 (Vejborg et al., 2011). Therefore, the mechanism of adherence of HM580 and LF82 may differ. Similarly, NRG857c has been shown to adhere to and

invade Caco-2 cells, whereby 3 x 10^6 and 2.6 x 10^3 CFU were recovered following adherence and invasion respectively (Cieza et al., 2015).

With respect to invasion, colonic strains HM615, HM605 and HM580 showed similar rates to LF82. This is in contrast to results in HT29 cells, where HM580 demonstrated significantly less invasion compared with LF82 (1.98% versus 12.36%), whereas strains HM605 and HM615 showed no viable intracellular bacteria after 1 hr gentamicin treatment at all (Martin et al., 2004). In addition, ileal isolate NRG857c invasion into T84 cells was significantly higher than LF82. Given that both LF82 and NRG857c are ileal isolates and have previously been suggested to be similar characteristically, the difference is surprising. However, the overall invasion rate (0.08%) of NRG857c in our studies is still a fraction of what has previously been described by Cieza et al, where a 1.22% invasion rate of Caco-2 cells was observed (Cieza et al., 2015). Interestingly, Mancini et al demonstrated significantly higher LF82 invasion in comparison to NRG857c in T84 cells, however infection parameters differed, where only a 2 hr infection incubation period was used (Mancini et al., 2021). Furthermore, genomic studies by Vejborg et al demonstrated several AIEC isolates do not share virulence genes. These include genes related to invasion, namely *ibeA*, *invA* and *tia* (Vejborg et al., 2011). Therefore, NRG857c may harbour virulence genes related to invasion that are not shared with other isolates which could be investigated by functional genomic studies.

3.3.5 AIEC LF82 is cytotoxic to T84 and Caco-2 cells

In this study, cytotoxicity was a key feature of LF82 pathogenesis across both T84 and Caco-2 cells. Given that AIEC LF82 has been shown to disrupt epithelial barrier function by direct targeting of TJ protein ZO-1 (Wine et al., 2009), it may also be speculated that LF82 induces cell damage that ultimately leads to a leaky gut barrier in CD. Given that LF82-induced cytotoxicity in our study was not mediated by secreted factors and was independent of bacterial invasion, it can be hypothesised that LF82 adherence to the host cell mediates cell death. Interestingly, epithelia exposed to LF82 deficient in type 1 pili, which are critical for adhesion, had mitochondrial networks similar to noninfected epithelia (Mancini et al., 2021). This was in addition to a lack of effect observed when using dead LF82, indicating that the attachment of viable bacteria to the epithelium caused fragmentation of the mitochondrial network.

Furthermore, it was hypothesised that the cell death observed in LF82-infected IECs could be due to the secretion of T6SS effector proteins. T6SSs can deliver enzymatic effectors into both prokaryotic and eukaryotic hosts to destroy them (Massier et al., 2015). AIEC LF82 harbours two Type VI Secretion Systems (T6SS), T6SS-1 and T6SS-3. However, infections with mutant strains LF82 Δ*tssE1*, LF82 Δ*tssE3* and LF82 Δ*tssE1* Δ*tssE3* did not diminish cell death in T84 cells. Previous studies have also shown that T6SS-1 and T6SS-3 were not involved in LF82 invasion (Cogger-Ward, 2019). Therefore, alternative virulence factors mediate LF82 host cytotoxicity. For example, *Brucella melitensis* cytotoxicity in macrophages is dependent on a T4SS (Pei et al., 2008). Interestingly, a T4SS has been identified in AIEC NRG857c which is required for intestinal biofilm formation in C57BL/6 mice. Notably, the T4SS is enriched among *E. coli* isolates from CD patients compared to healthy controls suggesting a role in pathogenesis (Elhenawy et al., 2021). As LF82 formed biofilms and promoted contact-dependent cytotoxicity in our study, exploring the role of a T4SS in LF82 cytotoxicity would be an interesting avenue of future research.

Whilst the underlying mechanisms of LF82-mediated cytotoxicity were not identified in this study, it can be hypothesised that this may be a result of reactive oxygen species (ROS) production and mitochondrial damage. ROS production can be induced by microbial pathogens and can lead to the damage of mitochondrial proteins, membranes and DNA in the host, leading to impaired mitochondrial function and thus cell death (McKay et al., 2020). A study by Mancini et al investigated the effect of AIEC LF82 on mitochondrial function, demonstrating that LF82 significantly affected epithelial expression of approximately 8600 genes in T84 cells, many of which relate to mitochondrial function. Furthermore, LF82-infected T84 epithelia revealed swollen mitochondria, reduced mitochondrial membrane potential and adenosine triphosphate, and fragmentation of the mitochondrial network, which were not observed with dead LF82, medium from bacterial cultures, or commensal *E. coli*-HB101 (Mancini et al., 2021). This fragmentation occurred at early time points after infection (2-4 hr), while loss of mitochondrial fusion protein OPA1-L was observed by 16 hr after infection. Thus, fragmentation of the mitochondrial network was shown as a novel aspect of LF82 epithelial interaction that could explain the cytotoxicity demonstrated here. This may have implications for barrier function that could be relevant to AIEC triggering initiation or disease relapse in IBD.

Interestingly, host cell cytotoxicity was restricted to LF82 and not observed in isolates NRG857c, HM615, HM605 or HM580. As these strains also did not form biofilms, this would support a role of the T4SS as suggested above. In addition, previous studies have shown that ROS-mediated mitochondrial damage in T84 cells during LF82 infection was not shared among other AIEC strains from CD patients (Elatrech et al., 2015) and that strain NRG857c caused little mitochondrial fragmentation (Mancini et al., 2021). Although this suggests that LF82-induced T84 cell death might be mediated via ROS production, the results by Elatrech et al indicated a strong ROS response reaches its maximum after 3 hr, which they suggested to be coinciding with the invasion of LF82 in T84 cells (Elatrech et al., 2015). In our studies, cytotoxicity was observed after 4 and 24 hrs in T84 cells but was independent of LF82 invasion. Therefore, prolonged ROS exposure as a result

of extensive LF82 adherence could be studied to gain a better insight into LF82-induced cytotoxicity in IECs.

Furthermore, differences in T84 and Caco-2 cell lines are likely to substantially influence the epithelial cell death pathways activated following AIEC infection. T84 cells model a crypt-like colonic epithelium, exhibit innate immunity signalling, are highly depenedent on tight junction integrity and active autophagic flux, therefore are more likely to undergo regulated cell death in response to intracellular AIEC and inflammatory stress (Eckmann et al., 1993; Larabi et al., 2020; Madara et al., 1987). Consistent with this, infection of T84 monolayers with AIEC LF82 in this study resulted in the formation of gaps within the epithelial monolayer (Figure 3.9A), indicative of a loss in barrier integrity. This barrier disruption is predicted to promote intrinsic apoptotic signalling, characterised by caspase-3 activation and PARP cleavage when autophagic clearance mechanisms are overwhelmed (Elhenawy et al., 2019; Larabi et al., 2020). In contrast, Caco-2 cells displayed preserved monolayer integrity following LF82 infection when observed by microscopy (Figure 3.9B). This may be explained by attenuated innate immune responses and increased tolerance of intracellular bacteria (Barnich et al., 2007; Pinto et al., 1983). Such a reduced response may limit activation of apoptotic or pyroptotic pathways in Caco-2 cells and instead permit intracellular persistence of AIEC with less prominent epithelial damage, thus Caco-2 cells may underestimate cytotoxic effects of AIEC infection.

3.3.6 AIEC LF82 induces secretion of pro-inflammatory cytokines from T84 cells

Increased release of pro-inflammatory cytokines is a key feature of CD and results in perpetuation of intestinal inflammation (De Souza and Fiocchi, 2016). The observation that LF82 induces secretion of pro-inflammatory cytokines from IECs highlights the potential pathogenesis of AIEC in CD. Results of our studies indicated a significantly higher release of IL-8, TNF-α and IL-6 from cells incubated with LF82 compared with non-infected controls. Similarly, Elatrech et al demonstrated that LF82 induced IL-8 mRNA expression in T84 cells, which, interestingly, occurred as a result of LF82-induced ROS production (Elatrech et al., 2015). Given the cytotoxicity described previously, and the potential link to ROS production, a mechanism whereby LF82 extensively adheres to IECs, inducing ROS production and subsequent IL-8 release could be proposed for the cell death observed.

Whilst LF82 exhibited increased release of IL-8, non-invasive MG1655 also elicited an IL-8 response in T84 cells. This is not unexpected, as it has previously been described that flagellin released by commensal *E. coli* strains can induce a pro-inflammatory response in enterocytes. For example, MG1655 induced IL-8 release after 16 hr incubation in HT-29 and Caco-2 cells due to activation of the TLR5 signalling pathway (Bambou et al., 2004). This raises the important question of how gut homeostasis is maintained and inappropriate inflammation avoided in the presence of the bacterial microbiota. Haller et al suggested that the intestine may rapidly produce immunoregulatory cytokines to counteract the pro-inflammatory effect of commensal bacteria. For example TGF-β1 secreted from enterocytes inhibits *Bacteroides vulfgatus*-induced NF-κB recruitment to the IL-6 promoter by histone acetylation (Haller et al., 2002). Instead, it is also possible that other gut microbiota may reduce the IEC pro-inflammatory response. For example, *Bacteroides thetaiotaomicron* has been shown to inhibit inflammatory responses induced by *Salmonella in vitro* and *in vivo* (Kelly et al., 2004). Furthermore, flagellin expression in commensal bacteria might be downregulated under intestinal conditions as shown for *E. coli* (Sevrin et al., 2020).

Chapter 4. Investigating AIEC LF82 interaction with polarised IECs and the influence of oxygen using a Vertical Diffusion Chamber (VDC) model system

4.1 Background

The intestinal environment is highly complex, with factors such as oxygen availability, epithelial morphology, and barrier integrity playing critical roles in host–pathogen interactions. To mimic this *in vitro*, colonocyte-like T84 cells were polarised on permeable Transwell membranes enabling full differentiation into microvillous epithelial monolayers with intact tight junctions. This is particularly relevant to CD, where increased epithelial permeability is a hallmark of pathology, and AIEC strain LF82 has been shown to disrupt tight junction proteins (Wine et al., 2009).

Polarised T84 epithelia grown on membrane filters can be incorporated into a vertical diffusion chamber (VDC), allowing maintenance of a low-oxygen apical environment that more accurately reflects conditions in the distal gastrointestinal tract, where oxygen levels are typically below 1% (Friedman et al., 2018). Oxygen availability is increasingly recognised as a critical determinant of bacterial virulence. Work by Marteyn *et al.* demonstrated that intestinal oxygen gradients directly regulate pathogen behaviour through the oxygen-responsive transcription factor FNR, enabling spatial control of virulence gene expression *in vivo*. In *Shigella flexneri*, active FNR under anaerobic luminal conditions represses type III secretion, while oxygen diffusion near the epithelial surface inactivates FNR, triggering effector secretion precisely at the site of host cell contact (Marteyn et al., 2010).

Microaerobic conditions may therefore act as a cue for AIEC to upregulate adhesins, invasion-associated factors, and intracellular survival mechanisms, facilitating epithelial colonisation and persistence. Consistent with this model, A/E lesion-forming *E. coli* display enhanced adherence under microaerobic conditions due to the stimulation of T3SS expression (Schüller and Phillips, 2010), and AIEC virulence has similarly been shown to be sensitive to environmental cues encountered at the epithelial interface. Similarly, infection of T84 and Caco-2 cells with *Campylobacter jejuni* in the VDC demonstrated increased epithelial association and invasion of host cells under microaerobic versus aerobic conditions (Mills et al., 2012; Naz et al.,

2013). In addition, *Clostridioides difficile* infection of T84 cells under microaerobic conditions results in heightened pro-inflammatory responses, including increased IL-8 and TNF-α expression, alongside a more pronounced loss of epithelial barrier resistance (Anonye et al., 2019; Jafari et al., 2016).

Despite this, the majority of AIEC studies to date have relied on non-polarised carcinoma cell lines such as Caco-2, HT-29, and T84 cultured under atmospheric oxygen conditions. Building on the findings presented in Chapter 3, the interaction between AIEC LF82 and intestinal epithelial cells was therefore re-examined using fully polarised T84 monolayers within the VDC system, enabling assessment of host–pathogen interactions under physiologically relevant microaerobic conditions that more accurately reflect the *in vivo* intestinal niche.

4.2 Results

4.2.1 Establishment of polarised T84 monolayers

For this study, polarised T84 cell monolayers were used as they are more physiologically relevant than non-polarised cells, whereby the cells develop a tall, column-shaped morphology and have a polarised distribution of cell surface receptors which is of critical importance when investigating host-pathogen interactions (Madara et al., 1987; Tran et al., 2014). Polarised T84 monolayers were obtained by culturing cells on permeable collagen-coated Snapwell or Transwell filters. T84 cells were seeded onto filter inserts at 5 x 10^5 cells per filter and cultured for 14 days. From day 4 post-seeding, Trans-epithelial electrical resistance (TEER) was determined to monitor epithelial barrier function. Epithelial structure was determined by immunofluorescence staining for the microvillous actin, and the tight junction protein occludin. By day 8, T84 monolayers developed a strong resistance, with TEER values peaking around 2000 Ω x cm^2, and then stabilised over the following 6 days to approximately 1000 Ω x cm^2 (Figure 4.1A). When evaluating immunofluorescence staining by microscopy, T84 cells exhibited other hallmarks of polarisation, including a tall, column-shaped morphology with an apical microvillous brush border and intact tight junctions between cells (Figure 4.1B).

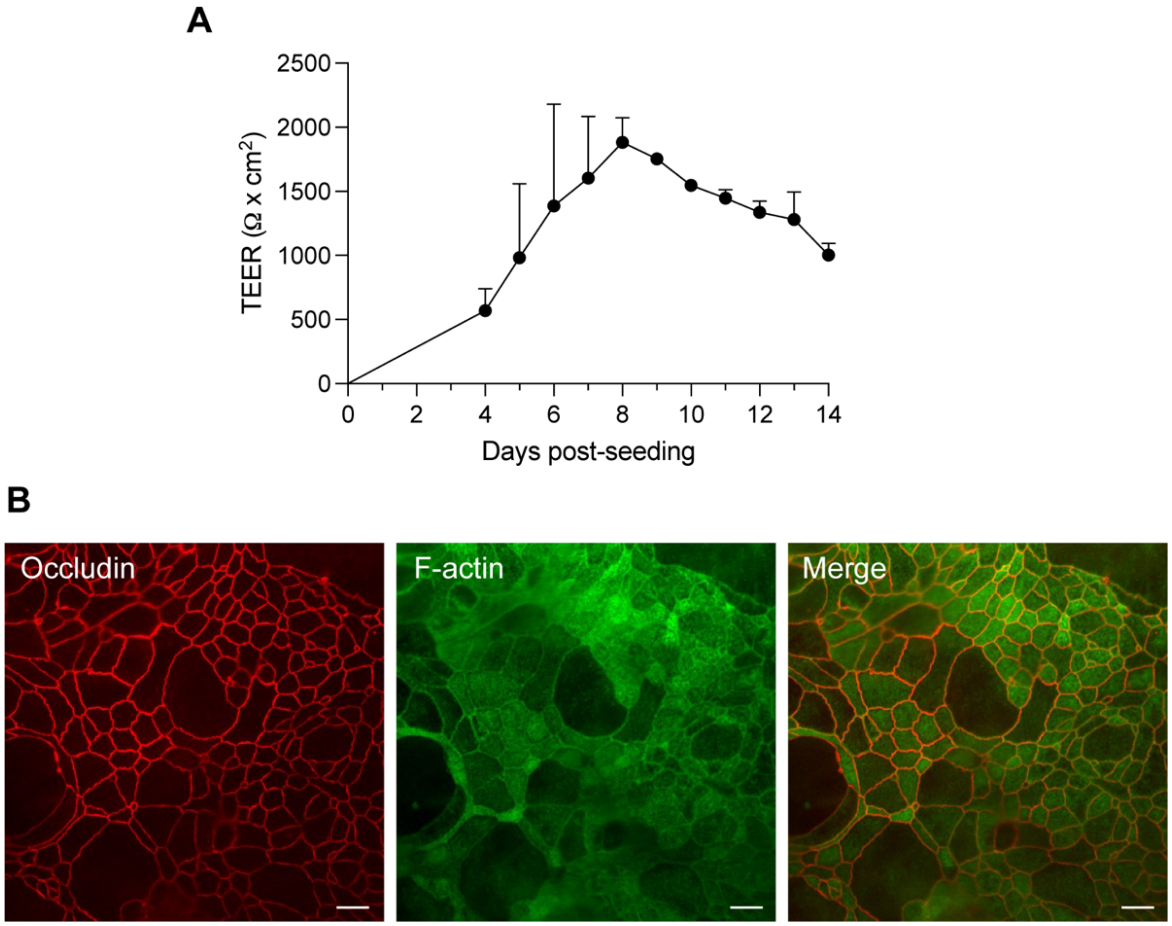

Figure 4.1. Polarised T84 cells have a high epithelial resistance, a microvillus brush border and form tight junctions. T84 cells were cultured in Transwell inserts for 14 days and transepithelial electrical resistance (TEER) monitored every 2 days from day 4 post-seeding (**A**). Data shown as the mean +- SD from 3 experiments. Monolayers cultured for 14 days were stained for occludin (red) and F-actin (green) (**B**). Scale bar = 10μm.

4.2.2 AIEC LF82 adherence, invasion and intracellular replication in polarised T84 cells

Given the low invasion and high adhesion of LF82 in non-polarised T84 and Caco-2 cells, the adherence, invasion and intracellular replication of AIEC LF82 and non-invasive MG1655 was determined in polarised T84 monolayers. T84 cells on Transwell filters were incubated with either LF82 or MG1655 and adherence, invasion and replication was determined as described previously (See - 2.3.1 Gentamicin invasion assay). LF82 adherence was higher than that of MG1655 but this did not reach significance (Figure 4.2A). Numbers of intracellular LF82 after 1hr and 21hr were significantly higher compared with MG1655 (Figure 4.2B). LF82 invasion and replication rates were higher than MG1655, however this also did not reach significance (Figure 4.2C and 4.2D).

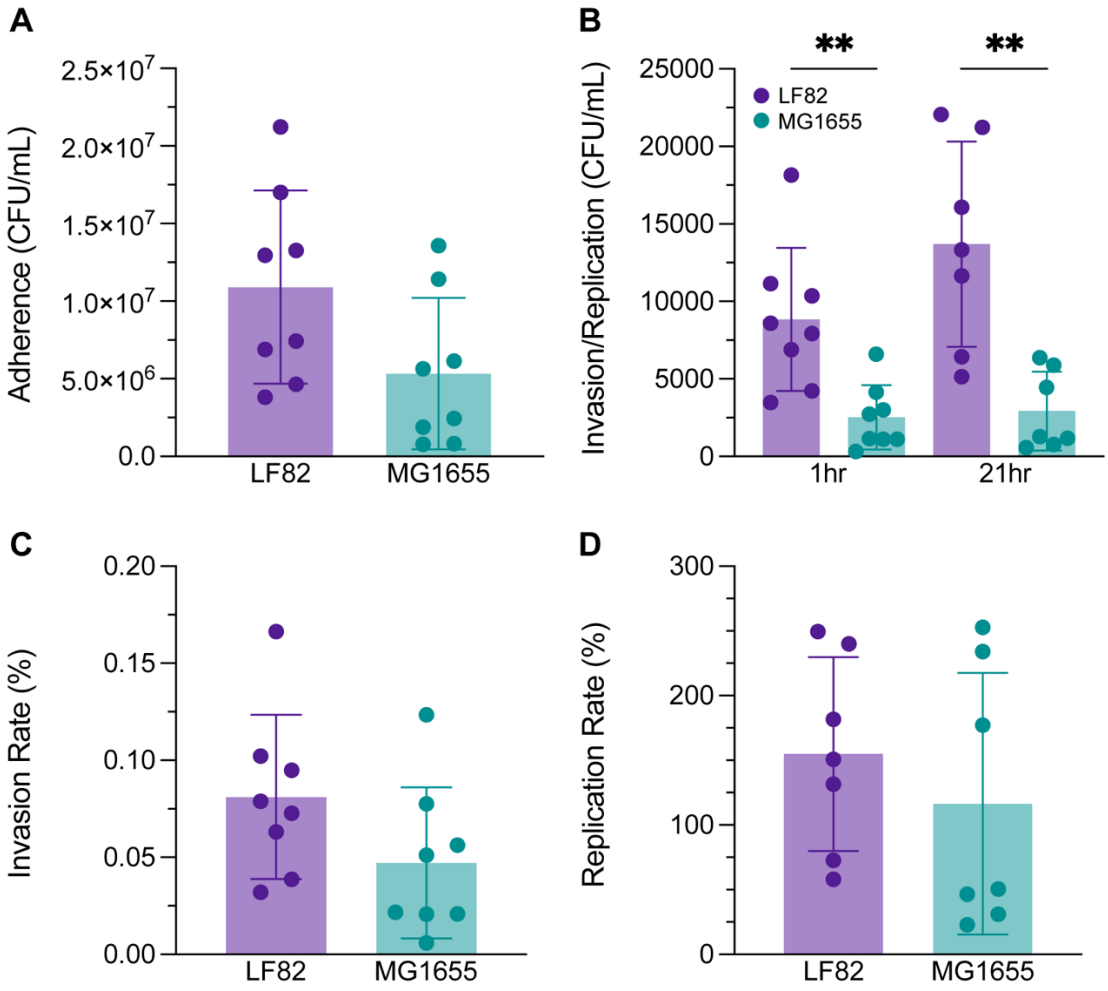

Figure 4.2. Adherence, invasion and intracellular replication of AIEC LF82 and *E. coli* MG1655 in polarised T84 cells. T84 cells were polarised on Transwell filters. Cells were incubated with bacteria for 3 hr, followed by 1 hr or 21 hr of gentamicin to kill extracellular bacteria. Adherent bacteria were determined after 3 hr by CFUs (**A**). Invasion and intracellular replication (**B**) was determined after 1 hr or 21 hr of gentamicin treatment, respectively, and cell lysates plated for CFUs. Results were normalised to an inoculum of 10^7 bacteria. Invasion rates (**C**) and replication rates (**D**) were calculated relative to numbers of adherent and invaded bacteria, respectively. Data shown as the mean +- SD. Significance was calculated using a student's unpaired t-test (**p<0.01).

4.2.3 Apical invasion of AIEC LF82 is predominant in Caco-2 but not T84 cells

Given the low invasion rates of LF82 in T84 and Caco-2 cells, it was hypothesised that AIEC invasion occurred via the basolateral side of the epithelium. This strategy is employed by the gastrointestinal pathogen *Shigella flexneri* where invasion was significantly higher from the basolateral versus apical surface in in differentiated enteroid monolayers (Ranganathan et al., 2019). Additionally, previous studies have demonstrated increased TEER reduction in polarised T84 cells infected with AIEC LF82 via the basolateral versus apical surface (Wine et al., 2009) indicating a preferential interaction with the basolateral side.

To determine if LF82 invades via the basolateral membrane of polarised IECs, T84 and Caco-2 cells were grown on Transwell filters and incubated with LF82 on either the apical or basolateral side for 3 hr followed by 1 hr of gentamicin treatment. To prevent bias due to the impact of gravity, filters were inverted for basolateral invasion. Results showed similar CFU numbers for apical and basolateral invasion in T84 cells (Figure 4.3A) whereas LF82 preferentially invaded the apical surface of Caco-2 cells (Figure 4.3B). Therefore, low invasion rates in earlier experiments are likely not due to preferential invasion from the basolateral side.

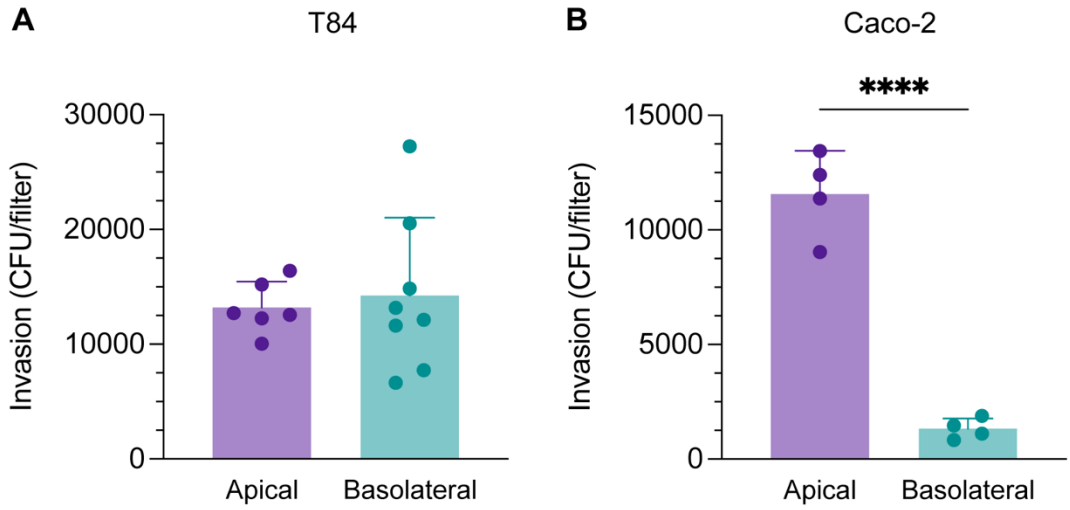

Figure 4.3. AIEC LF82 invasion in T84 and Caco-2 cells infected from the apical or basolateral side of the epithelium. T84 (**A**) or Caco-2 (**B**) cells were polarised on Transwell filters and incubated with AIEC LF82 for 3 hr followed by 1 hr treatment with gentamicin. Invasion was determined by plating out cell lysates for CFUs. Results were normalised to an inoculum of 10^7 bacteria. Data shown as the mean +- SD. Significance was calculated using a student's unpaired t-test (****$p<0.0001$).

4.2.4 AIEC LF82 is cytotoxic to polarised T84 cells and disrupts epithelial barrier function

Given the LF82-induced cell death observed in confluent T84 cells, cytotoxicity in polarised T84 cells was investigated. Polarised T84 monolayers were incubated with AIEC LF82, MG1655 or left non-infected for 3 hr followed by 21 hr gentamicin treatment and cytotoxicity was determined by Trypan Blue staining. In addition, TEER was measured before and after 21 hr of incubation to determine changes in epithelial barrier function as a result of infection. LF82 induced significantly higher cytotoxicity in polarised T84 cells compared to MG1655 and non-infected controls (Figure 4.4). While non-infected polarised T84 cells maintained approximately 80% of barrier function, incubation with MG1655 and LF82 significantly decreased barrier function to 60% and 25%, respectively (Figure 4.4). The decrease in TEER correlates with increases in cytotoxicity observed during LF82 infection.

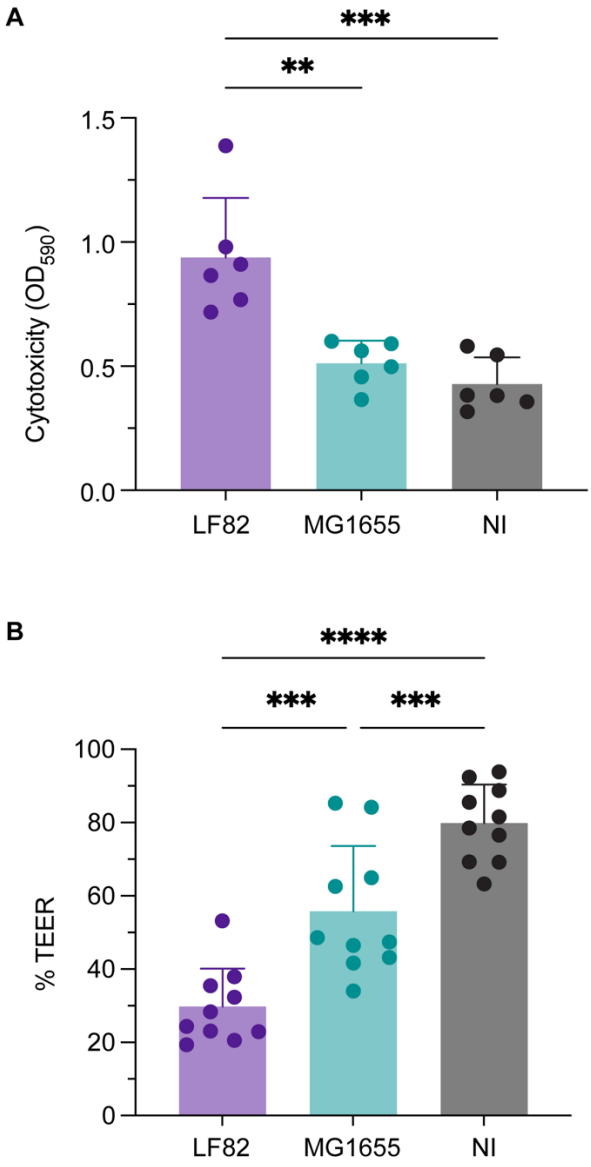

Figure 4.4. LF82 is cytotoxic to polarised T84 cells and significantly reduces barrier function. Polarised T84 cells were incubated with AIEC LF82 or non-invasive *E. coli* MG1655 or left non-infected for 3 hr, followed by 21 hr treatment with gentamicin to kill extracellular bacteria. Cytotoxicity was measured by Trypan Blue staining and quantification at OD_{590} (**A**). Barrier function was determined by measuring TEER (**B**). TEER data shown as % TEER relative to barrier function before infection. All data shown as the mean +- SD. Significance was calculated using a one-way ANOVA test with Tukey's post-test comparison (**p<0.01; ***p<0.001; ****p<0.0001).

4.2.5 AIEC LF82 induces predominant pro-inflammatory cytokine secretion from the apical side of the epithelium

As previously shown, confluent T84 cells secrete the pro-inflammatory cytokines TNF-α and IL-8 in response to LF82 infection (See - 3.2.6 AIEC LF82 induces secretion of pro-inflammatory cytokines from T84 cells). Polarising cells on Transwell filters additionally allows to determine the direction of cytokine secretion (i.e. apical versus basolateral). Apical cytokine secretion would suggest that cytokines may be secreted into the lumen during infection. Earlier studies have demonstrated IL-8 secretion from polarised T84 cells to be primarily basolateral following apical infection with *Salmonella* Typhimurium, leading to neutrophil migration across the epithelium (Kucharzik, 2005; McCormick et al., 1995). However, previous studies in the Schüller group demonstrated predominant apical IL-8 secretion in EPEC-infected T84 cells (McGrath et al., 2022).

Samples were collected after 3 hr incubation with bacteria followed by 21 hr gentamicin treatment and TNF-α, IL-8, IL-6 and IL-1β in apical and basal supernatants was quantified by sandwich ELISA. IL-8 release into the apical compartment was significantly higher in LF82 and MG1655-infected cells compared with non-infected controls (Figure 4.5A). This was mirrored in basal compartments but only reached significance for LF82. Notably, *E. coli*-induced IL-8 secretion was higher in apical versus basal supernatants (Figure 4.5A). In addition, TNF-α release was also primarily apical and significantly higher in LF82-infected cells compared to non-infected controls. Whilst basal TNF-α release also appeared higher than MG1655 and non-infected cells, this did not reach significance (Figure 4.5B). Cytokines IL-6 and IL-1β were not detected.

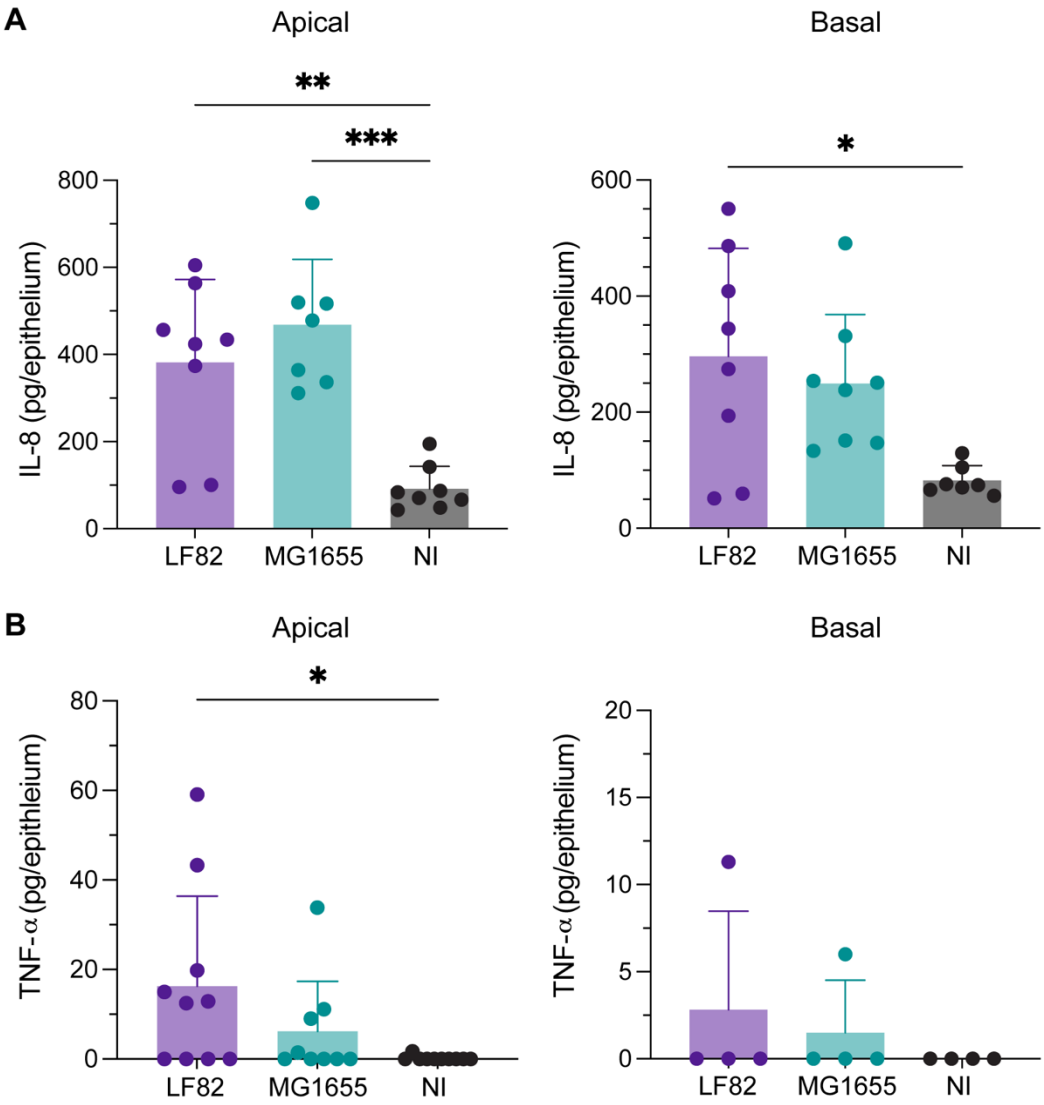

Figure 4.5. Exposure to AIEC LF82 and *E. coli* MG1655 induces IL-8 secretion and LF82 induces TNF-α secretion in polarised T84 cells. T84 cells polarised on Transwell filters were incubated with LF82, MG1655 or non-infected for 3 hr followed by 21 hr gentamicin treatment. IL-8 (**A**) and TNF-α (**B**) release was quantified in apical and basal supernatants by ELISA. Data shown as the mean +- SD. Significance was calculated using a one-way ANOVA test with Tukey's post-test comparison (*p<0.05; **p<0.01; ***p<0.001).

4.2.6 Investigating the influence of oxygen on AIEC LF82 pathogenesis using a Vertical Diffusion Chamber (VDC) system

To investigate AIEC interaction with polarised T84 cells in aerobic and microaerobic conditions, a vertical diffusion chamber model system was used. The apical medium was inoculated with bacteria for 3 hr to allow bacterial adherence and replaced with media containing gentamicin for 1 hr or 21 hr to quantify invasion and replication, respectively.

4.2.6.1 AIEC LF82 adherence, invasion and intracellular replication in aerobic and microaerobic conditions

LF82 adherence to polarised T84 cells was significantly higher in aerobic vs microaerobic conditions (Figure 4.6A). This was not due to enhanced microbial replication in the presence of oxygen as LF82 growth was similar in aerobic and microaerobic conditions when cultured in the VDC without the presence of host cells (Figure 4.6B). Regarding LF82 invasion and intracellular replication, there was no significant difference between aerobic and microaerobic conditions (Figure 4.6C and D). When invasion and replication rates were calculated, there was no significant difference between the two conditions (Figure 4.6E and F).

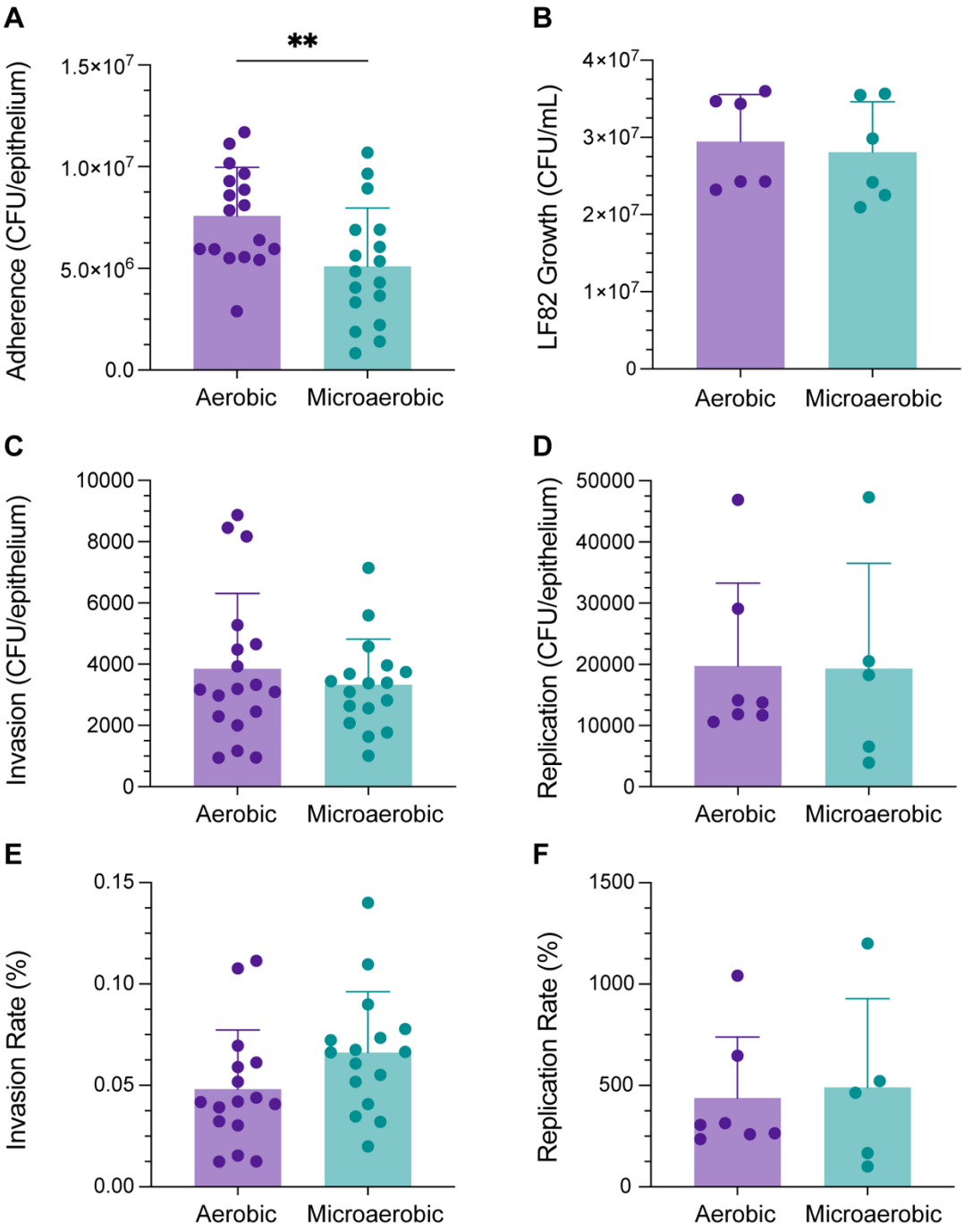

Figure 4.6. Adherence, invasion and intracellular replication of AIEC LF82 in polarised T84 cells under aerobic and microaerobic conditions. Cells were incubated in the VDC with AIEC LF82 for 3 hr, followed by 1 hr or 21 hr of gentamicin to kill extracellular bacteria. Adherent bacteria were determined after 3 hr by CFUs (**A**). Bacterial growth of LF82 in each condition without host cells was determined after 3 hr by CFUs (**B**). Invasion (**C**) and intracellular replication (**D**) was determined after 1 hr or 21 hr of gentamicin treatment respectively and cell lysates plated for CFUs. Results were normalised to an inoculum of 10^7 bacteria. Invasion (**E**) and replication rates (**F**) were calculated relative to adherent and invaded bacteria, respectively. Data shown as the mean +- SD. Significance was calculated using a student's unpaired t-test (**p<0.01).

4.2.6.2 Polarised T84 cells do not maintain barrier function in the VDC

To investigate the effect of LF82 infection on epithelial permeability in aerobic and microaerobic conditions, barrier function in T84 cells infected with LF82, MG1655 or left non-infected was determined after 24 hr. Previous studies in the Schüller group have successfully used T84 cells in the VDC whilst barrier function was maintained (McGrath et al., 2022). Unexpectedly, TEER values dropped by about 80% even in non-infected controls suggesting loss of epithelial integrity during the 24 hr incubation in the VDC (Figure 4.7). To determine if this was due to the lack of FCS in the culture medium, T84 cells were incubated in DMEM/F-12 medium containing 1, 5 or 10% FCS or no FCS (0%). However, this did not restore barrier function (Figure 4.8). Additionally, immunofluorescence staining for occludin indicates tight junctions are less intact in lower FCS concentrations (Figure 4.9).

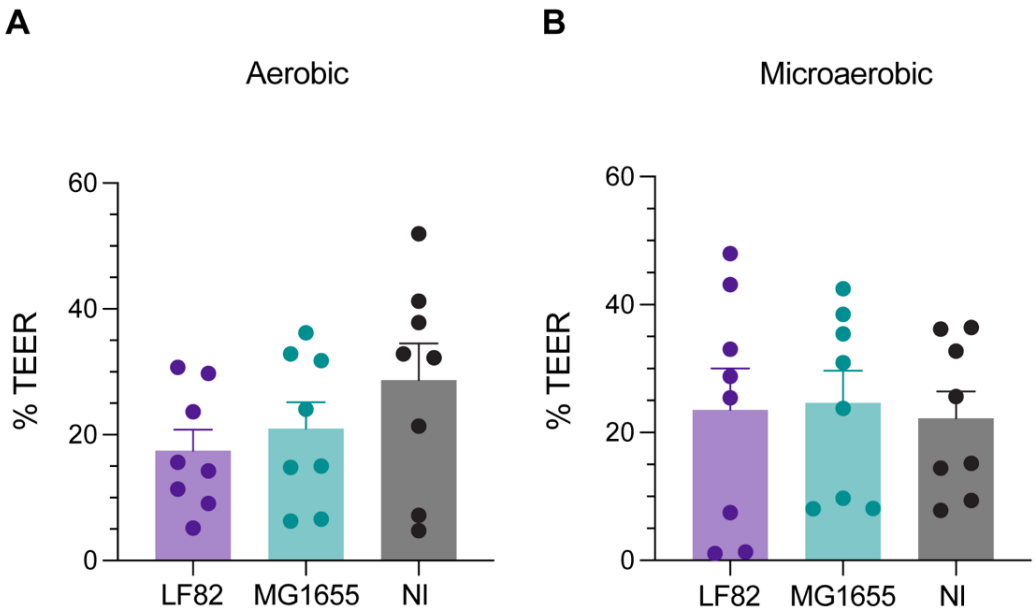

Figure 4. 7. Barrier function of T84 cells under aerobic (A) and microaerobic (B) conditions in the VDC. Polarised T84 cells were incubated with AIEC LF82, *E. coli* MG1655 or left non-infected (NI) for 3 hr, followed by 21 hr treatment with gentamicin to kill extracellular bacteria. Barrier function was determined by measuring TEER. Data shown as % TEER relative to barrier function before infection. Data shown as the mean +- SD.

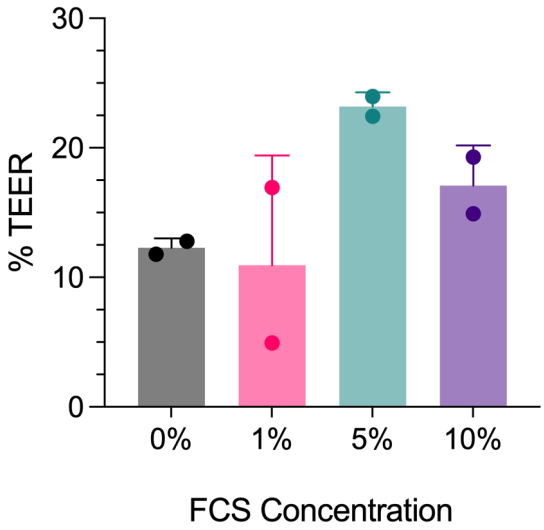

Figure 4.8. Reduced barrier function after VDC incubation is not caused by a lack of FCS. Polarised T84 cells were maintained in the VDC under aerobic conditions in DMEM/F-12 medium supplemented with 1%, 5% or 10% FCS or no FCS (0%). Barrier function was determined by measuring TEER after 24 hr. Data shown as % TEER relative to barrier function before incubation. Data shown as the mean +- SD.

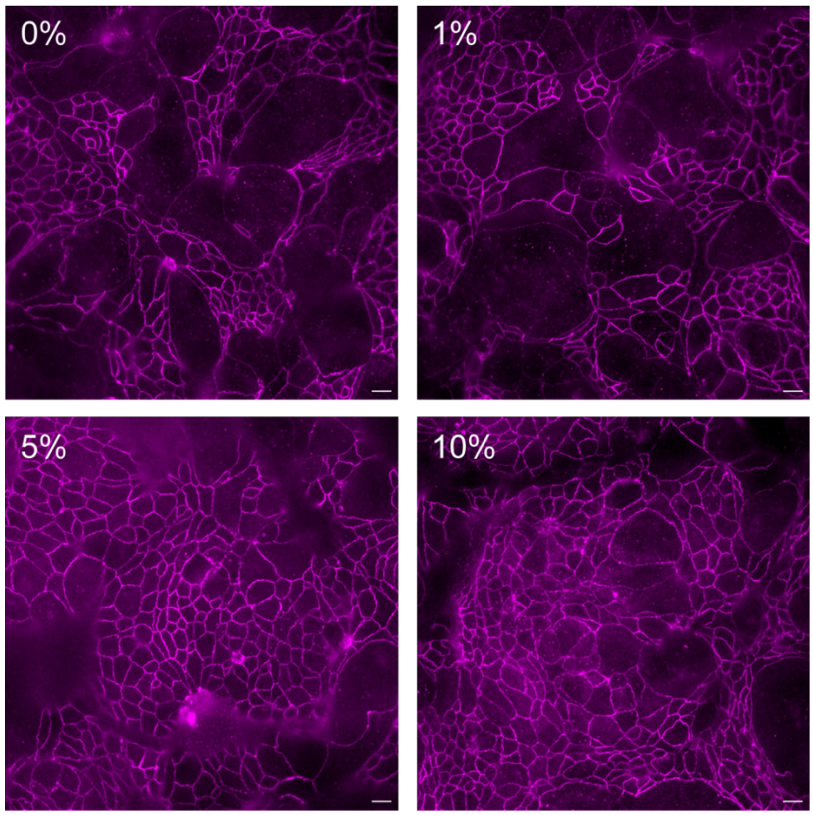

Figure 4.9. Occludin staining indicates intact tight junctions despite low TEER. Scale bar = 10 µm.

4.2.6.3 AIEC LF82-induced pro-inflammatory cytokine release is primarily apical and lower in microaerobic conditions

To determine LF82-induced pro-inflammatory cytokine release in aerobic and microaerobic conditions, apical and basal supernatants from T84 cells incubated with LF82, MG1655 or non-infected in the VDC were collected after 24 hrs and TNF-α, IL-8, IL-6 and IL-1β was quantified by sandwich ELISA. LF82 induced a significantly higher apical and basolateral IL-8 release compared to non-infected cells in both aerobic and microaerobic conditions (Figure 4.10). As previously described in polarised T84 cells (See - 4.2.5 AIEC LF82 induces predominant pro-inflammatory cytokine secretion from the apical side of the epithelium), IL-8 release was higher from the apical versus the basal side. Similarly, MG1655 also elicited an IL-8 response, although this was lower than that of LF82. Similarly, IL-1β release was higher in apical versus basal supernatants in LF82-infected cells. There was no significant difference between IL-1β release in LF82-infected cells compared with MG1655 or non-infected in either aerobic or microaerobic environments, however high variation between samples was observed (Figure 4.10). In addition, concentrations of TNF-α and IL-6 were below detection levels of the ELISA kit.

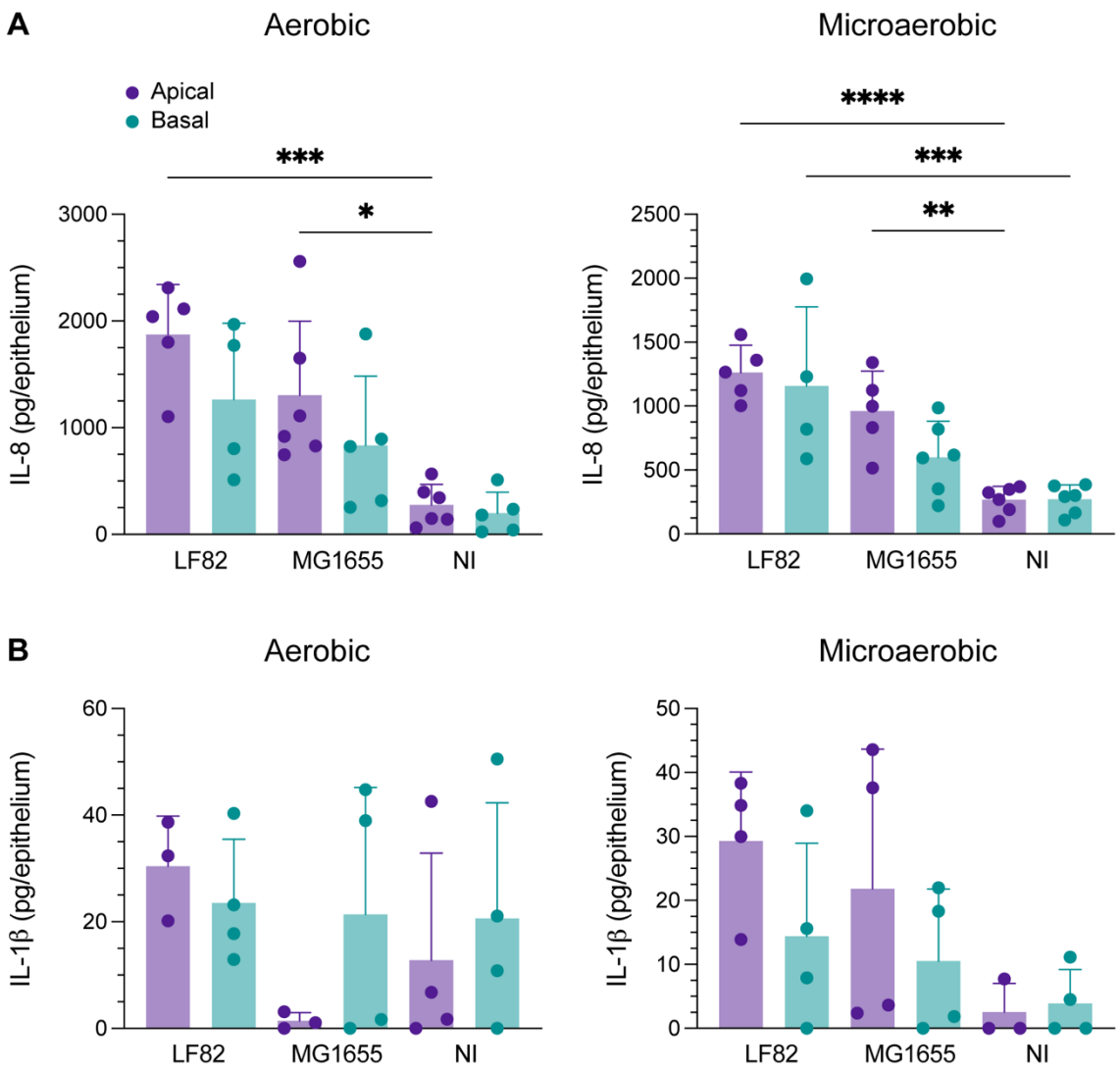

Figure 4.10. LF82 and MG1655 induce IL-8 release in polarised T84 cells under aerobic and microaerobic conditions. Polarised T84 cells were incubated in the VDC with LF82, MG1655 or left non-infected (NI) for 3 hr followed by 21 hr gentamicin treatment. IL-8 (**A**) and IL-1β secretion (**B**) in apical and basal supernatants were quantified by ELISA. Data shown as the mean +- SD. Significance was calculated using a one-way ANOVA test with Tukey's post-test comparison (*p<0.05; **p<0.01; ***p<0.001; ****p<0.0001).

4.2.7 Summary

In this study, the adherence, invasion and intracellular replication of AIEC LF82 was determined in fully polarised T84 cells and compared with MG1655. LF82 adherence, invasion and intracellular replication was higher than MG1655. Interestingly, LF82 invasion and replication rates were higher than MG1655, which differed from non-polarised cells, however these did not reach significance. Given these low invasion rates, investigations into basolateral invasion showed that LF82 invasion of T84 cells was similar to apical invasion, meanwhile apical invasion was significantly higher than basolateral in Caco-2 cells. Therefore, there was no preferential binding to the basolateral side. As in Chapter 3, LF82 also induced significantly higher cytotoxicity in polarised T84 cells compared to MG1655 and non-infected controls. The polarisation on Transwells allowed TEER to be determined, showing that LF82 decreased barrier function. Furthermore, evaluation of pro-inflammatory cytokine secretion showed that polarised T84 cells released IL-8 and TNF-α primarily from the apical side which was higher when incubated with LF82. Use of the VDC allowed investigations into the effects of a microaerobic environment on LF82 pathogenesis. Interestingly, LF82 adherence to T84 cells was higher under aerobic conditions compared to microaerobic, and there was no difference in invasion or replication across the two conditions. Unexpectedly, T84 cells did not tolerate the VDC as barrier function decreased in all conditions, which was not due to lack of FCS in the cell culture media. Finally, secretion of IL-8 and IL-1β was higher in LF82-infected cells compared to MG1655 and non-infected. Interestingly, levels of secreted cytokines were lower in microaerobic conditions compared to aerobic. Meanwhile, TNF-α and IL-6 were not detected.

4.3 Discussion

4.3.1 AIEC LF82 adherence, invasion and replication in polarised T84 cells

Colon carcinoma cell lines are frequently used due to their highly proliferative nature and ease of culture, making them a useful tool for mechanistic studies and toxicology assays (Creff et al., 2021). Whilst T84 and Caco-2 cells spontaneously differentiate into a polarised epithelium upon reaching confluence, these cells can be polarised further by culture on collagen coated membranes. As a result, T84 cells display characteristics similar to colonocytes, including apical brush borders, tight junctions, desmosomes, taller height and apical/basolateral polarisation of cell surface receptors (Madara et al., 1987; Tran et al., 2014). Therefore a more accurate representation of *in vivo* gastrointestinal pathogenesis can be studied *in vitro*. In this study, evaluation of adherence, invasion and replication in polarised T84 cells showed higher LF82 adherence in comparison to MG1655, however this did not reach significance. Numbers of intracellular bacteria after 1 hr and 21 hr were significantly higher than MG1655. In addition, LF82 had a higher invasion rate than MG1655, in contrast to non-polarised T84 cells, where MG1655 had a higher rate. However, it is important to consider the spread of data, and the overall invasion rate was still low and comparable to that of non-polarised cells (0.08%).

Whilst many common intestinal pathogens including *Salmonella*, *Campylobacter* and other pathogenic *E. coli* primarily invade the colonic epithelium through the apical surface, the low invasion rates observed prompted investigations into whether LF82 uses basolateral invasion in its pathogenesis. This strategy is employed by the gastrointestinal pathogen *Shigella flexneri*, whereby bacteria invade through the basolateral pole of Caco-2 cells (Marteyn et al., 2010). Additionally, previous studies have demonstrated increased TEER reduction in polarised T84 cells infected with AIEC LF82 via the basolateral versus apical surface (Wine et al., 2009) indicating a preferential interaction with the basolateral side. In

this study, LF82 invasion was similar between the apical and basolateral sides of T84 cells. Meanwhile, apical invasion of LF82 was predominant in Caco-2 cells.

4.3.2 AIEC LF82 adherence, invasion and intracellular replication in aerobic and microaerobic conditions

The low oxygen conditions of the intestinal environment are of critical importance in host-pathogen interaction (Marteyn et al., 2011). As described above, LF82 adherence was significantly higher under aerobic compared to microaerobic conditions. This was not due to higher replication in the aerobic environment, as bacterial growth was comparable between the two conditions. This is interesting, as adherence of gastrointestinal pathogens is typically expected to be higher in a microaerobic environment due to being specially adapted to the luminal conditions of the gut. This is observed in *Campylobacter jejuni*, whereby epithelial association and invasion of host cells is increased under microaerobic conditions in comparison to aerobic (Mills et al., 2012; Naz et al., 2013). In addition, *H. pylori* exhibits increased adherence to Caco-2 cells in microaerobic conditions, whereby numbers of adherent bacteria were more than 20 times higher after 4 hr incubation when compared with aerobic conditions (Cottet et al., 2002). Similar results were also seen with EHEC, where adherence to T84 cells was increased under microaerobic conditions (Schüller and Phillips, 2010). Furthermore, a VDC was employed to culture *C. difficile* with T84 cells and an anaerobic environment induced enhanced *C. difficile*-induced cytokine secretion compared to the aerobic equivalent (Jafari et al., 2016). Whilst many gastrointestinal pathogens exhibit increased virulence in a microaerobic environment, it has previously been demonstrated that a zone of relative oxygenation adjacent to the GI tract mucosa exists. This is caused by diffusion from the capillary network at the tips of villi, which has been shown to reverse the anaerobic block of Ipa secretion in *Shigella flexneri*, allowing T3SS activation and thus enhancing invasion and virulence (Marteyn et al., 2010). In CD, observations of gut microbiota dysbiosis include a decrease in anaerobes of the Firmicutes phylum and an increase in facultative anaerobes, such as *E. coli*. This shift is suggestive of a disruption in anaerobiosis and thus a role for oxygen. It has

been suggested that disruption to the microvasculature of the intestinal tissue during inflammation may influence both tissue oxygenation and release of oxygen in the intestinal lumen (Binion and Rafiee, 2009; Chidlow et al., 2007; Deban et al., 2008). Meanwhile, recent studies in a DSS colitis-induced mouse model showed intestinal injury reduces intestinal tissue oxygenation and increases the flux of oxygen from the tissue into the intestinal lumen, altering microbiome composition (Zong et al., 2024). The higher LF82 adherence observed in an oxygenated environment compared to microaerobic in our studies may therefore be due to LF82 adapting to higher oxygen levels based on the leaky gut phenotype typically associated with CD. Given that pathogens need to regulate their virulence gene expression to maximize their fitness, and use environmental cues to do this, such as oxygen, pH and nutrient availability, it is plausible that LF82 may harbour virulence factors that are switched on in an aerobic environment. For example, in Shiga toxin-producing *E. coli* (STEC), these cues influence T3SS expression in the colon (Ando et al., 2007; Carlson-Banning and Sperandio, 2016; Schüller and Phillips, 2010). Interestingly, AIEC LF82 flagellum expression is enhanced in the presence of bile acids and mucins in contrast to commensal *E. coli* (HS) (Sevrin et al., 2020). Therefore, LF82 virulence modulation in response to available oxygen would be an interesting potential avenue of future AIEC research.

4.3.3 Cytotoxicity and reduced barrier function in polarised T84 monolayers

In addition to cell death, we determined the TEER in LF82-infected polarised T84 compared to MG1655- and non-infected controls. Results demonstrated reduced barrier function in LF82-infected cells, whereby TEER was ~30% of the pre-infected value in T84 cells. Similar results were observed in a separate study, whereby apical LF82 infection of polarised T84 cells caused a 46% reduction in TEER when compared with uninfected controls (Wine et al., 2009). In addition, LF82 infection of the basolateral side exhibited an 81% reduction in TEER (Wine et al., 2009). It could be hypothesised that the reduced TEER following basolateral infection could be due to increased LF82 adherence or invasion of the basolateral side. Whilst TEER was not determined following basolateral infection in this project, our results

indicated similar levels of LF82 invasion from the apical and basolateral side of polarised T84 cells. Therefore, reduced TEER is unlikely caused by increased invasion. Interestingly, Wine et al. described that live bacteria were required, as a drop in TEER was not observed with either heat-inactivated or formaldehyde treated LF82 (Wine et al., 2009). In our investigations, a significant reduction in TEER was observed in polarised T84 cells infected with LF82, which correlated with increasing cytotoxicity. Therefore LF82-induced cytotoxicity may be a cause of decreased barrier function.

4.3.3 Polarised T84 cells do not maintain barrier function in the VDC

Previous work in the Schüller group utilised the VDC system with T84 cells for studies on the pathogenesis of diarrhoeagenic *E. coli*. During 22 hr incubations, morphology and integrity of cell monolayers remained intact (McGrath et al., 2022; Schüller and Phillips, 2010). Unexpectedly, T84 cells did not maintain epithelial barrier function in our experiments, and a significant reduction in TEER was observed after 24 hr of incubation even in the absence of bacteria. This was not due to a lack of FCS in the cell culture medium. Notably, T84 cells used in this study were sourced from the European Collection of Authenticated Cell Cultures (ECACC), while previous studies in the Schüller group utilised T84 cells from the American Type Culture Collection (ATCC). Both cell lines exhibited different cell morphology and growth kinetics (data not shown), suggesting intrinsic differences between T84 cell line clones from ECACC and ATCC repositories which may have affected cell viability.

4.3.4 AIEC LF82 induces apical IL-8 secretion in polarised T84 cells

Polarised T84 cells exhibit highly directional cytokine secretion in response to bacterial infection, with IL-8 release occurring predominantly from the basolateral surface under most conditions. This is thought to reflect physiological signalling towards the lamina propria to promote neutrophil recruitment during infection (Kucharzik, 2005; McCormick et al., 1995), and has been consistently observed following apical infection with enteric pathogens, including *Campylobacter jejuni* (Zheng et al., 2008). In addition, attachment of *S*. Typhimurium to the apical membrane of T84 monolayers cultured on filter inserts stimulated basolateral secretion of IL-8 and resulted in neutrophil migration across an intact epithelial monolayer (McCormick et al., 1995). In contrast, apical IL-8 release from T84 cells is influenced by epithelial polarity, receptor localisation, and the nature of the bacterial stimulus. Engagement of pattern recognition receptors that are preferentially localised to the basolateral membrane, such as TLR5 and TLR4, results in more robust NF-κB activation and IL-8 secretion than apical stimulation alone (Gribar et al., 2008). Nevertheless, apical IL-8 secretion has been reported in response to certain pathogens and PAMPs, including flagellin and enterohaemorrhagic *E. coli*, suggesting that epithelial cells retain the capacity to signal into the lumen under specific conditions (Lewis et al., 2016). In our study, IL-8 secretion occurred mainly from the apical side of the T84 monolayer. This confirms more recent studies on EHEC and EPEC showing predominant apical IL-8 release in T84 cells (Lewis et al., 2016; McGrath et al., 2022). The functional role of apical IL-8 remains less defined, but may contribute to local autocrine signalling or luminal neutrophil recruitment during severe or sustained infection. Together, these studies indicate that while basolateral IL-8 secretion represents the dominant and physiologically relevant response of polarised T84 cells to bacterial challenge, apical IL-8 release can occur in a pathogen- and context-dependent manner and should be interpreted with consideration of epithelial polarity and barrier integrity.

Many gastrointestinal pathogens induce a pro-inflammatory cytokine response in microaerobic conditions, for example *Clostridium difficile* infection increased gene expression of IL-8 and TNF-α in T84 cells in a VDC model (Jafari et al., 2016). In our studies, T84 cells incubated with LF82 in the VDC showed a higher release of apical IL-8 in aerobic compared to microaerobic conditions. Interestingly, this correlates with increased LF82 adherence observed in aerobic conditions. In contrast to experiments in confluent T84 cells (Chapter 3), TNF-α and IL-6 were not detected in VDC supernatants. This is likely due to higher medium volumes in VDC compartments (4 ml) compared with 24-well plates (1 ml) resulting in dilution of cytokine concentrations below detection levels.

Chapter 5. AIEC LF82 interaction with human colonoids

5.1 Background

As previously described, a prevalent approach to modelling human intestinal infections has been the use of colon carcinoma cells. Widely used cell lines, including T84 and Caco-2 (used in Chapters 3 and 4), and HT-29, are cost-effective and readily available, but represent only one single cell type (i.e. enterocyte/colonocyte) of the intestinal epithelium and generally do not produce mucus (Navabi et al., 2013). Whilst Caco-2 cells display characteristics of the small intestine, T84 cells more resemble colonic crypt cells (Liévin-Le Moal and Servin, 2013). In addition, carcinoma-derived cell lines have a mutational profile which is very different in comparison to healthy IECs, or the specific mutations present in CD (Sazonovs et al., 2022). Whilst animal models provide an alternative and have advantages in modelling the systemic development of diseases, they are expensive, time consuming and raise ethical issues. Furthermore, AIEC do not efficiently colonise the mouse gut in the presence of a native microbiota and efficient immune response (Sivignon et al., 2022). The development of human intestinal organoid models circumvents these problems and provides a powerful tool for studying the role of AIEC in CD.

As organoids maintain the genetic background of the tissue from which they are derived, organoids with CD-specific mutations can be generated from biopsies of CD patients. In addition, they display all the major cell types of the gut, produce a mucus layer and can also be polarised to present apical basolateral polarisation. In culture, organoids are closed 3D structures, with the apical membrane facing inwards towards the lumen, and the basolateral surface facing outward. More recently, ‘apical-out’ organoids have been developed for access to the apical membrane to reflect *in vivo* interactions with the intestinal lumen (Han et al., 2021). Alternatively, monolayers can be generated, whereby organoid fragments are seeded onto Transwell membranes coated with extracellular matrix (ECM) proteins and cultured in media containing essential growth factors for expansion and differentiation (In et al., 2016). This allows assessment of barrier function by

determining TEER, and the sampling of apical and basal supernatants for evaluation of pro-inflammatory cytokine secretion.

In this study, organoids were cultured from endoscopic biopsies from CD patients in remission (CD) or resection samples from tumour excisions (non-IBD) (See - 2.4 Intestinal organoid culture). All tissues were derived from the transverse colon; therefore, organoids were referred to as colonoids from this point onwards. Characteristics of CD mucosa include increased mucus production, discontinuous inflammation and a disrupted epithelial barrier (Kang et al., 2022). Therefore, initial studies focussed on characterising colonoids derived from CD or non-IBD tissue, by assessing MUC2 production, cytokine secretion, CEACAM-6 expression and barrier function. Following this, colonoid monolayers were used to investigate AIEC interaction with the epithelium by evaluating adherence and invasion, barrier function, cell viability and pro-inflammatory cytokine secretion.

5.2 Results

5.2.1 Colonoid culture and differentiation

For this study, colonoid monolayers were used as they form a polarised monolayer with an apical brush border, allowing bacterial access to the apical side of the epithelium. To generate 2D polarised colonoid monolayers, 3D colonoids in expansion were fragmented and seeded onto permeable collagen-coated Transwell filters (Figure 5.1). Once confluent, monolayers were differentiated by withdrawal of Wnt3a, R-spondin and SB202190 in differentiation medium for 4 days thereafter. The TEER of each monolayer was determined to confirm barrier function before and after differentiation. Colonoids derived from non-IBD tissue were named ‘TCN’, whilst colonoids from CD tissue were named ‘TCC’.

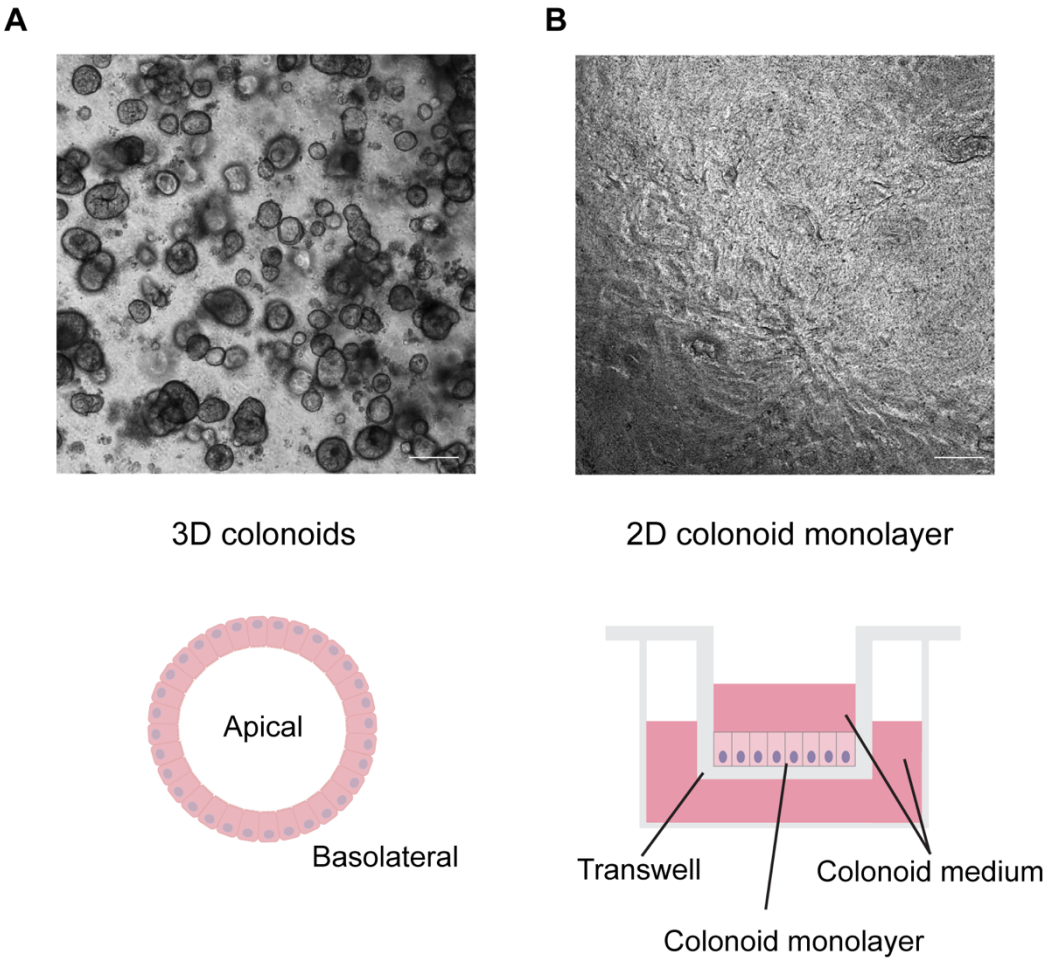

Figure 5.1. Phase contrast micrographs of 3D colonoids in expansion (A) and 2D colonoid monolayers (B). Scale bar = 50 µm.

Epithelial structure and the presence of mucus was determined by immunofluorescence staining for microvillous actin, MUC2 and cell nuclei. When evaluating immunofluorescence staining by confocal microscopy, colonoid monolayers exhibited hallmarks of polarisation and differentiation, including a tall, column-shaped morphology, with an apical microvillous brush border and the presence of goblet cells (Figure 5.2A and B).

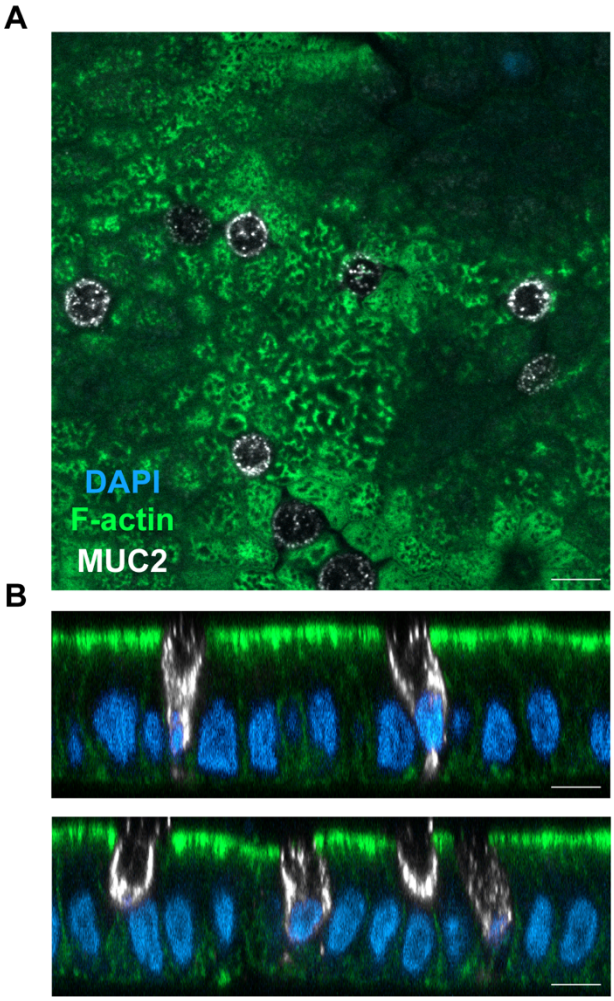

Figure 5.2. Differentiated TCN-1 colonoid monolayer on Transwell filter. Confocal laser microscopy image of TCN-1 monolayers stained for F-actin (colonocytes, green), MUC2 (goblet cells, white) and cell nuclei (blue). XY scan of apical cell surface (**A**). Selected XZ scans (**B**). Scale bar = 10 µm.

5.2.2 Colonoid characteristics differ between patients

5.2.2.1 Barrier function is different between colonoid lines

Given that reduced barrier function is a typical feature in CD patients (Hollander et al., 1986), barrier function of 2D organoid monolayers derived from CD or non-IBD tissue was determined and compared.

To determine colonoid barrier function before and after differentiation, TEER was measured before and 4 days post differentiation. Barrier function increased after differentiation in all organoid lines except TCC-7 (Figure 5.3). Overall, barrier function after differentiation was significantly lower in TCN-4, TCC-6 and TCC-7 compared to other colonoid lines, with TCN-4 displaying the lowest TEER (Figure 5.3). Although there were significant differences in barrier function between colonoid lines, this was not dependent on patient status (CD vs non-IBD) (Figure 5.3).

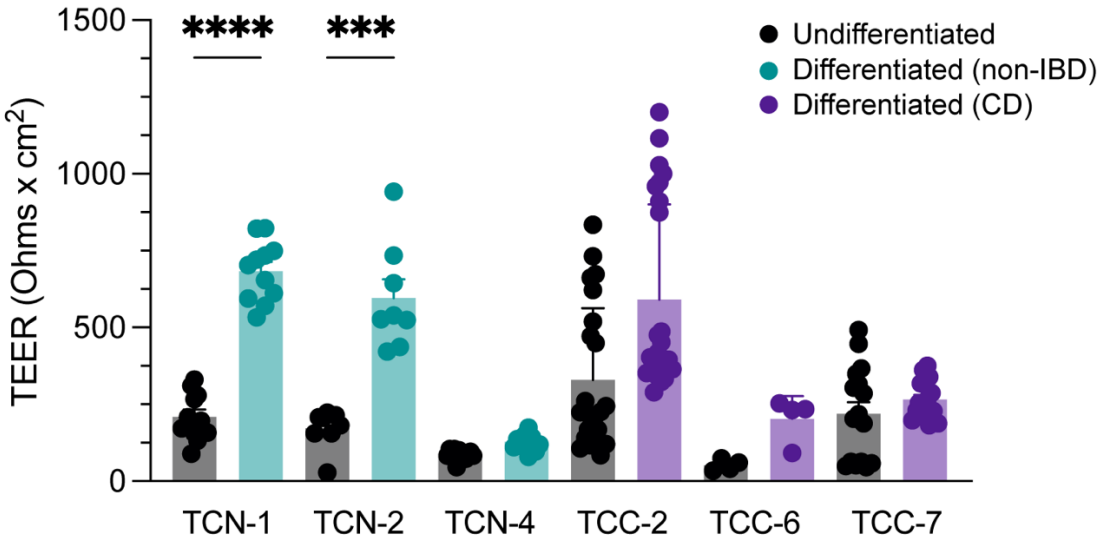

Figure 5.3. Organoid barrier function differs between lines. Barrier function was determined before and after differentiation by measuring TEER. Data shown as the mean +- SD. Significance was calculated using a one-way ANOVA test with Tukey's post-test comparison (*p<0.05; **p<0.01; ***p<0.001; ****p<0.0001).

5.2.2.2 Colonoid IL-8 secretion is primarily apical and cytokine secretion differs between colonoid lines

To evaluate whether the inflammatory signature of CD was retained in colonoids generated from patient samples, the baseline levels of pro-inflammatory cytokine secretion in differentiated non-IBD colonoid lines TCN-1 and TCN-2, and CD colonoid lines TCC-6 and TCC-7, were evaluated by quantification of TNF-α, IL-8, IL-6 and IL-1β release by sandwich ELISA. On day 4, apical and basal supernatants were sampled and used for cytokine analysis. Overall, IL-8 secretion was higher in apical versus basal compartments although this did not reach significance for TCC-6 (Figure 5.4A) where apical IL-8 secretion was lower compared with other organoid lines. In contrast, IL-6 levels were very low for all colonoid lines, with no apparent correlation between non-IBD or CD-derived colonoids observed (Figure 5.4B). In addition, concentrations of TNF-α and IL-1β were below detection levels (4 pg/ml and 2 pg/ml, respectively).

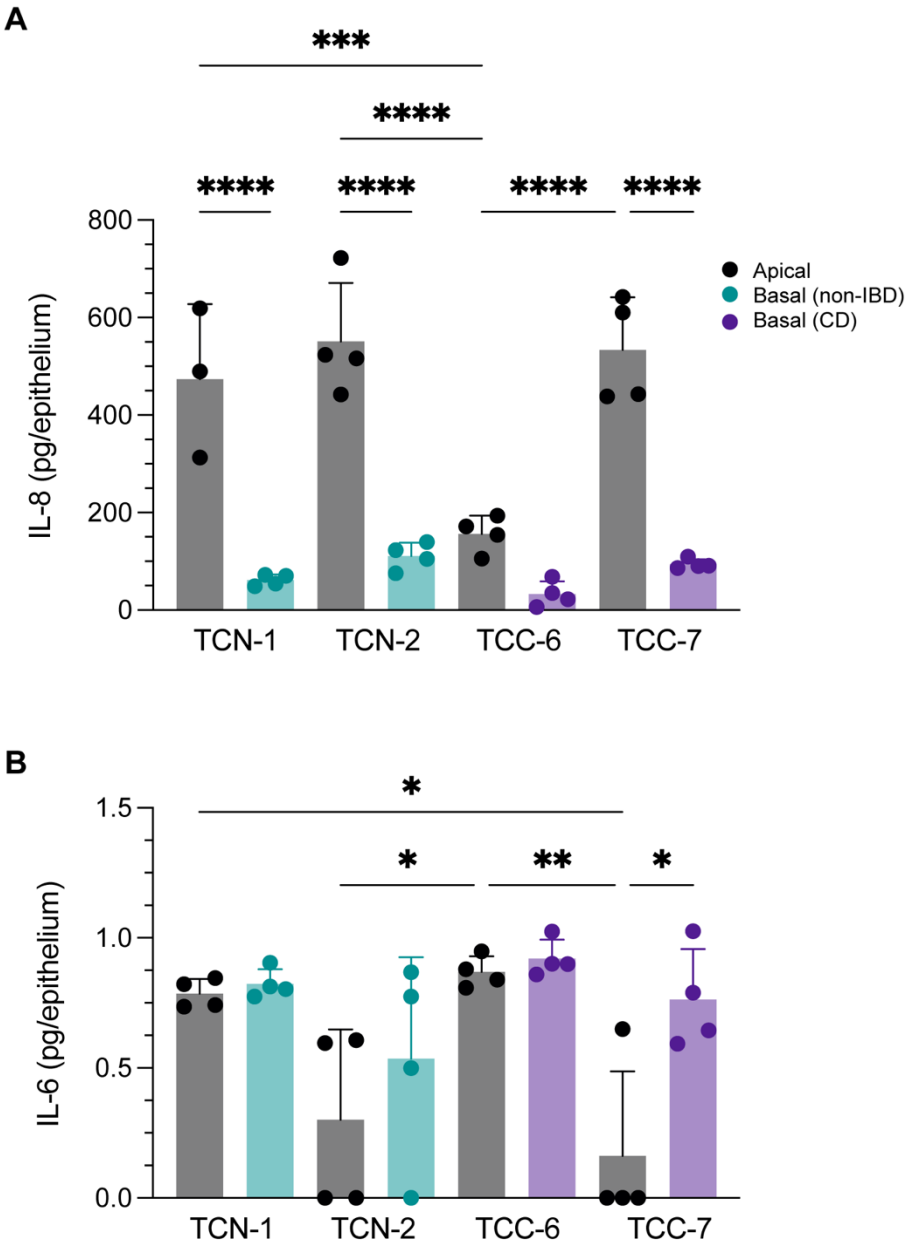

Figure 5.4. **Baseline cytokine secretion of differentiated colonoids. A**) IL-8 and **B**) IL-6 secretion in apical and basal supernatants were quantified by ELISA. Data shown as the mean +- SD. Significance was calculated using a one-way ANOVA test with Tukey's post-test comparison (*p<0.05; ****p<0.0001).

5.2.2.3 MUC2 expression is different between colonoid lines

To determine if MUC2 expression differed between non-IBD and CD-derived colonoids, differentiated colonoids were fixed for immunofluorescence staining for MUC2. IFS staining was evaluated by microscopy at x 20 magnification and the integrated density was quantified with ImageJ. Upon observation by microscopy, TCN-1, TCN-2 and TCC-7 showed small patches of overlaying MUC2, which was more extensive in TCN-1. In contrast, TCC-6 produced a confluent sheet of MUC2 (Figure 5.5). When quantified with ImageJ, levels of MUC2 were significantly different between organoid lines, where TCC-6 displayed the highest levels of MUC2. There was no correlation between MUC2 levels and CD status of the donor (Figure 5.5A and B).

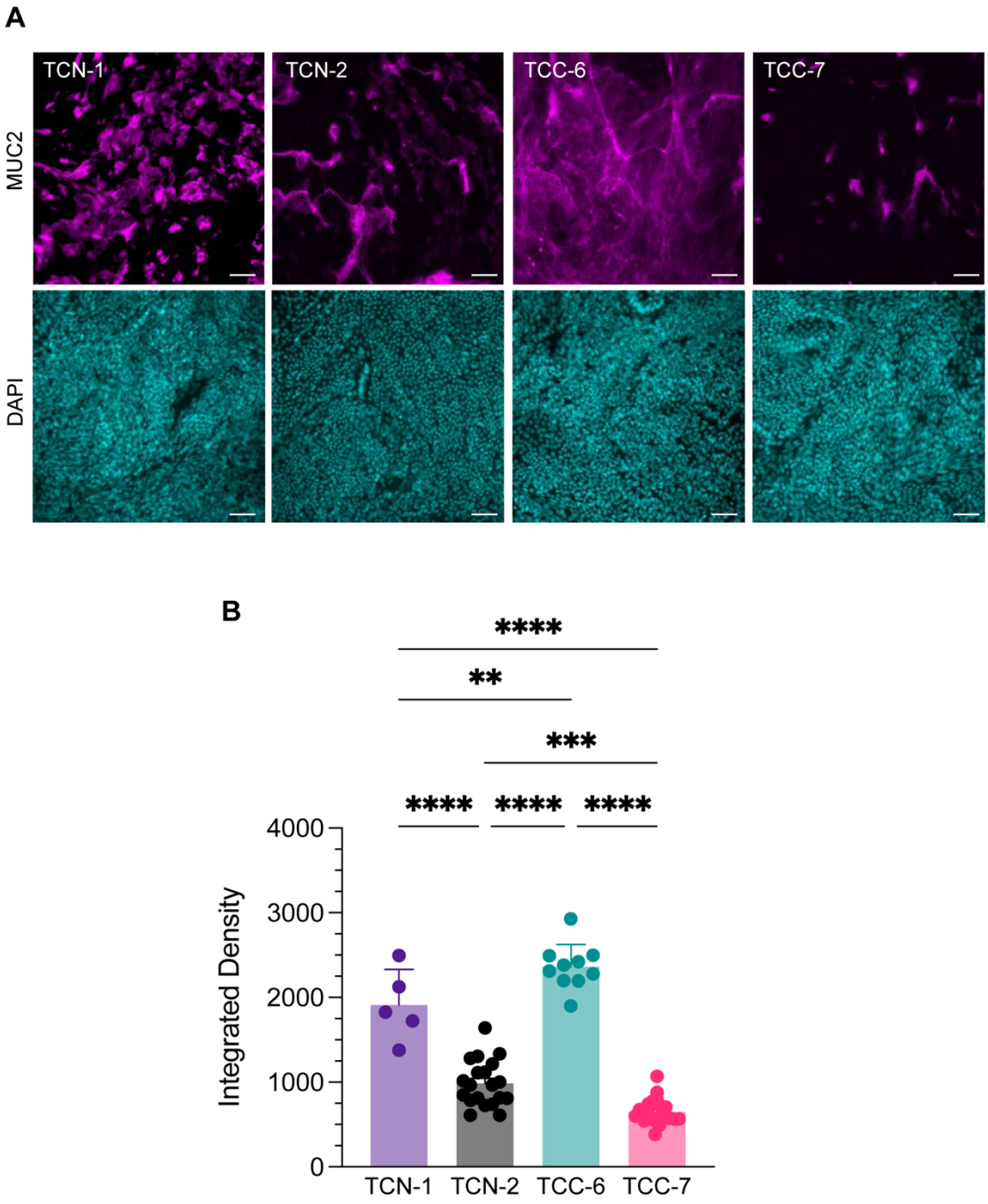

Figure 5.5. MUC2 levels differ between colonoid lines. Colonoid monolayers on Transwells were differentiated and stained for MUC2 (magenta) and cell nuclei (cyan). Scale bar = 50 µm (**A**). MUC2 was quantified by calculating the integrated density (**B**). Data shown as the mean +- SD. Significance was calculated using a one-way ANOVA test with Tukey's post-test comparison (**p<0.01; ***p<0.001; ****p<0.0001).

5.2.2.4 CEACAM-6 expression is heterogenous and differs between colonoid lines

To determine if CEACAM-6 expression differed between non-IBD and CD-derived colonoids, differentiated colonoids were fixed for immunofluorescence staining for CEACAM-6. IFS staining was evaluated by microscopy at x 20 magnification and the integrated density was quantified with ImageJ. Evaluation of CEACAM-6 staining in colonoids demonstrated heterogenous expression, whereby some cells expressed high CEACAM-6 levels and others none. Upon quantification with ImageJ, CEACAM-6 expression in TCN-1 was significantly higher than in TCN-2, TCC-6 and TCC-7 (Figure 5.6A and B). Like MUC2, there was no correlation between CEACAM-6 levels and organoids derived from normal or CD tissue.

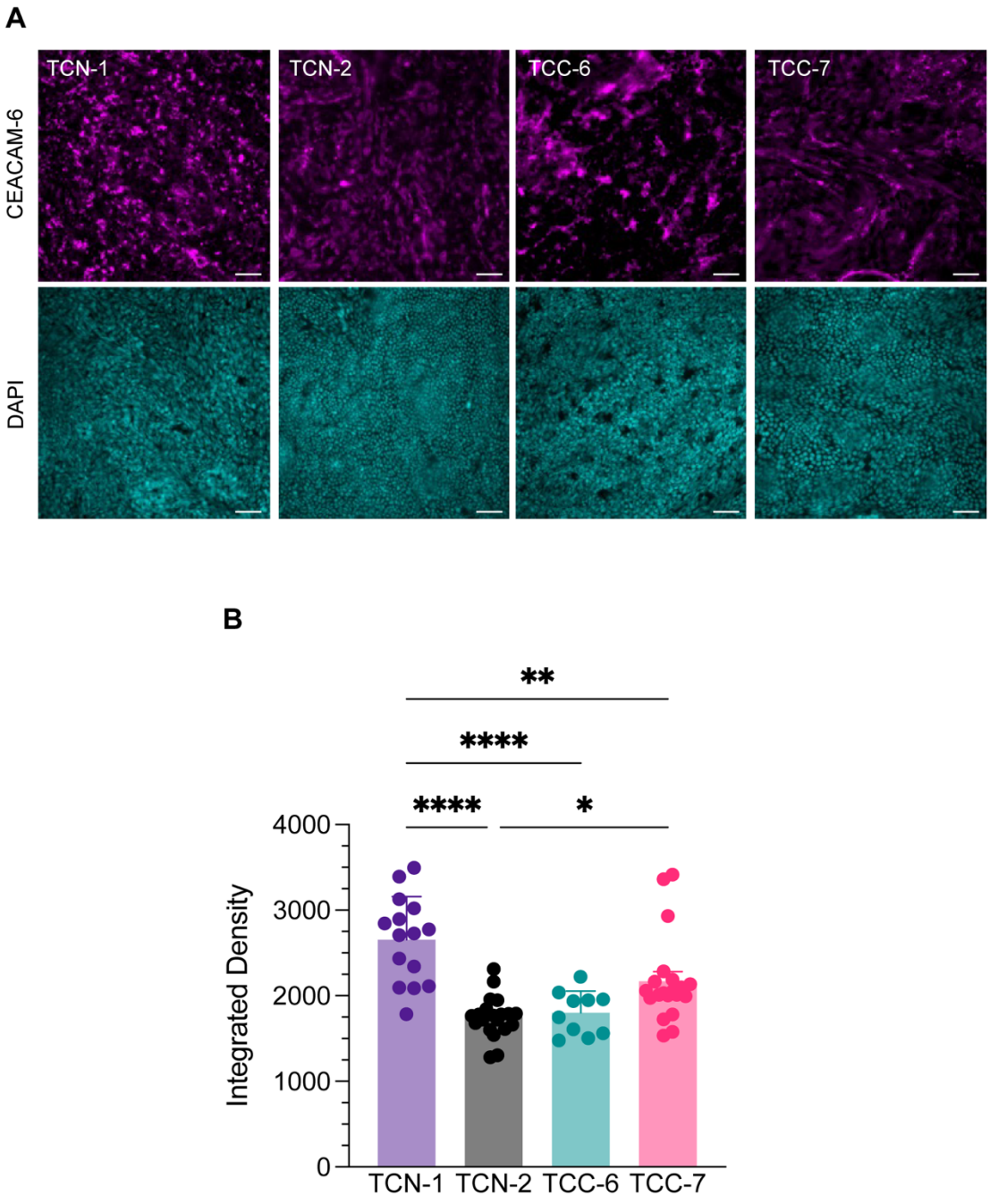

Figure 5.6. **CEACAM-6 expression varies between colonoid lines.** Colonoid monolayers on Transwells were differentiated and stained for CEACAM-6 (magenta) and cell nuclei (cyan). Scale bar = 50 µm (**A**). CEACAM-6 was quantified by calculating the integrated density (**B**). Data shown as the mean +- SD. Significance was calculated using a one-way ANOVA test with Tukey's post-test comparison (*p<0.05; **p<0.01; ****p<0.0001).

5.2.3 AIEC interaction with differentiated colonoids

5.2.3.1 AIEC LF82 adherence and invasion of colonoid monolayers

To determine adherence and invasion of AIEC LF82 in colonoids, invasion assays were performed as described previously (See - 2.3.1 Gentamicin invasion assay). Colonoid lines TCC-2 (CD) and TCN-4 (non-IBD) were used. Differentiated colonoid monolayers were incubated with LF82 or non-invasive MG1655 for 3 hr followed by 1 hr treatment with gentamicin to determine adherence and invasion, respectively. For CFU quantification, monolayers were lysed and plated, and for microscopy, monolayers were fixed and stained.

Following a 3 hr infection period, LF82 showed higher adherence to TCC-2 and TCN-4 compared to MG1655, although this did not reach significance. Additionally, LF82 adherence was similar between TCC-2 and TCN-4 organoids (Figure 5.7A). Addition of gentamicin for 1 hr to determine bacterial invasion indicated higher numbers of intracellular bacteria for LF82 compared with MG1655, although this was not significant (Figure 5.7B). Similarly, LF82 invasion was comparable between TCC-2 and TCN-4. When numbers of invaded bacteria were normalised to numbers of adherent *E. coli* to calculate invasion rates (%), LF82 invasion was higher than MG1655 in TCC-2, however this did not reach significance. Meanwhile, LF82 and MG1655 invasion rates were comparable in TCN-4 (Figure 5.7C).

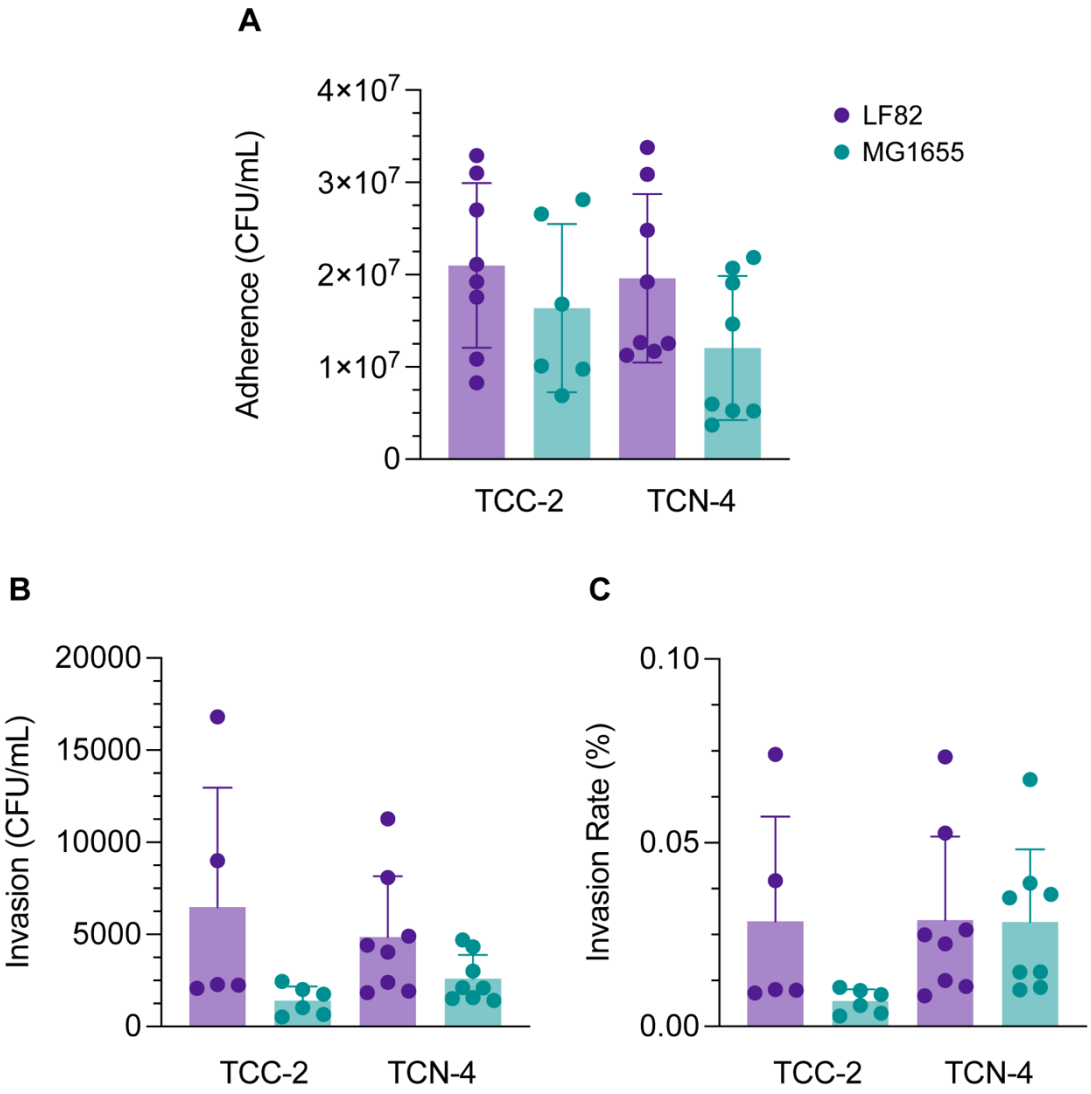

Figure 5.7. Adherence and invasion of AIEC LF82 and *E. coli* MG1655 in TCC-2 and TCN-4 colonoid monolayers. Colonoid monolayers were polarised on Transwell filters, grown to confluence and differentiated. Monolayers were incubated with bacteria for 3 hr, followed by 1 hr of gentamicin treatment to kill extracellular bacteria. Adherent bacteria were determined after 3 hr by CFUs (**A**). Invasion (**B**) was determined after 1 hr of gentamicin treatment and cell lysates plated for CFUs. Results were normalised to an inoculum of 10^7 bacteria. Invasion rates (**C**) were calculated relative to adherent bacteria. Data shown as the mean +- SD. Significance was calculated using a student's unpaired t-test.

To visualise bacterial association with colonoids, TCN-1 monolayers incubated with LF82, MG1655 or left non-infected were stained for *E. coli*, F-actin, DAPI and either MUC2 or CEACAM-6. Microscopy indicated aggregates of LF82 on the colonoid surface, meanwhile few single bacteria were observed for MG1655 (Figure 5.8A and B). In addition, CEACAM-6 appeared to be located on shed vesicles with subsequent LF82 binding (Figure 5.9A and B).

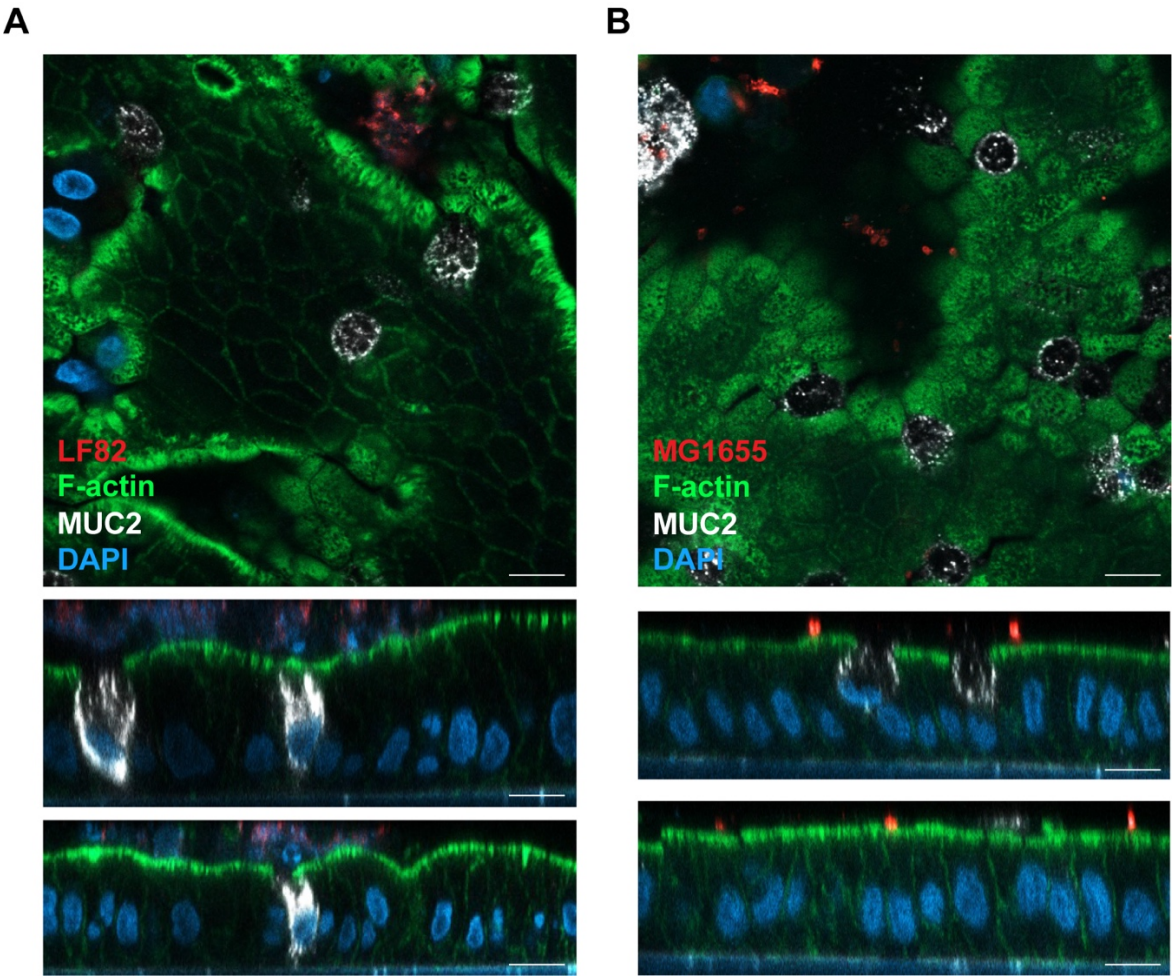

Figure 5.8. TCN-1 colonoid monolayer infected with LF82 (A) and MG1655 (B). Confocal laser microscopy image of TCN-1 monolayers stained for *E. coli* (red), F-actin (colonocytes, green), MUC2 (goblet cells, white) and cell nuclei (blue). XY scan of apical cell surface and selected XZ scans shown. Scale bar = 10 µm.

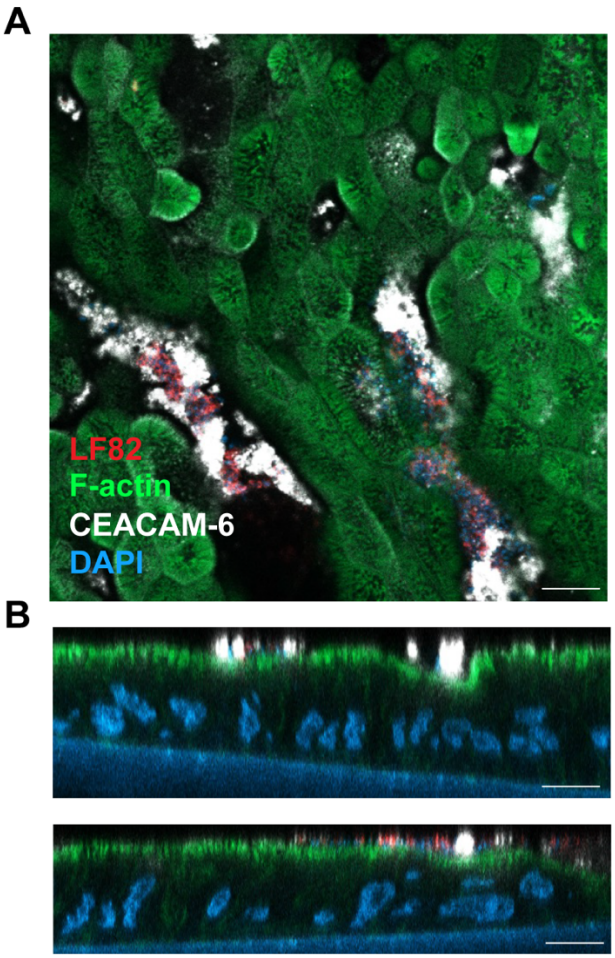

Figure 5.9. TCN-1 colonoid monolayer infected with LF82. Confocal laser microscopy image of TCN-1 monolayers stained for *E. coli* (red), F-actin (colonocytes, green), CEACAM-6 (white) and cell nuclei (blue). XY scan of apical cell surface (**A**) and selected XZ scans shown (**B**). Scale bar = 10 µm.

5.2.3.2 AIEC LF82 induces cytotoxicity in colonoids

Given the cytotoxicity observed in LF82-infected T84 cells (See - 3.2.5 AIEC LF82 is cytotoxic to T84 and Caco-2 cells), barrier integrity and cell death were also evaluated in colonoid monolayers. Differentiated colonoid lines TCN-4 (non-IBD) and TCC-7 (CD) were incubated with LF82, MG1655 or left non-infected for 3 hr followed by 21 hr gentamicin treatment. Cytotoxicity was determined by Trypan Blue staining and quantification at OD_{590}. To determine the effect of bacteria on barrier function, TEER was measured before and after incubation and end values presented as % TEER relative to before incubation. Trypan Blue staining showed that cytotoxicity in LF82-infected colonoids was significantly higher than in non-infected controls in TCN-4, and significantly higher than in MG1655- and non-infected cells in TCC-7 (Figure 5.10A). Although TEER was reduced after incubation with LF82 in TCN-4 and TCC-7, this was not statistically significantly different compared with MG1655 or non-infected controls (Figure 5.10B).

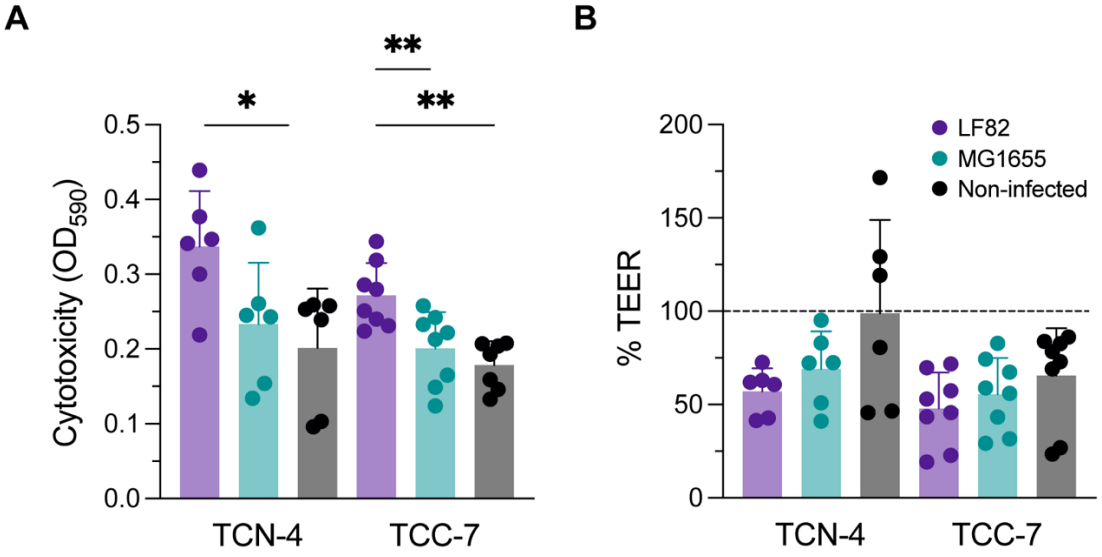

Figure 5.10. AIEC LF82 is cytotoxic and reduces barrier function in TCN-4 and TCC-7 colonoids. Colonoid monolayers were incubated with AIEC LF82, non-invasive *E. coli* MG1655 or left non-infected for 3 hr, followed by 21 hr treatment with gentamicin to kill extracellular bacteria. Cytotoxicity was measured by Trypan Blue staining and quantification at OD_{590} (**A**). Barrier function was determined by measuring TEER (**B**). Data shown as % TEER relative to barrier function before infection. Data shown as the mean +- SD. Significance was calculated using a one-way ANOVA test with Tukey's post-test comparison (*p<0.05; **p<0.01).

5.2.3.3 AIEC LF82 does not induce considerable IL-8 secretion

As IL-8 was the most highly secreted cytokine in LF82-infected T84 cells, the pro-inflammatory response of TCN-1 (non-IBD) and TCC-2 (CD-derived) colonoid monolayers to LF82 infection was measured by quantification of IL-8 release after 3 hr plus 21 hr gentamicin incubation. Apical and basal supernatants were collected from colonoids incubated with LF82, MG1655 or left non-infected and IL-8 was quantified by sandwich ELISA. Although IL-8 release into the apical compartment was higher in LF82- and MG1655-infected TCN-1 and TCC-2 monolayers compared with non-infected controls, this did not reach significance due to restricted sample numbers (Figure 5.11). This was mirrored in basal compartments in TCN-1, while basal IL-8 secretion in LF82-infected TCC-2 colonoids was lower compared with non-infected controls. Interestingly, MG1655 induced the highest IL-8 secretion whilst LF82-induced IL-8 release was only marginally higher compared to non-infected colonoids. Notably, *E. coli*-induced IL-8 secretion was higher in apical versus basal supernatants. In addition, IL-8 levels were generally higher in TCN-1 versus TCC-2 (Figure 5.11).

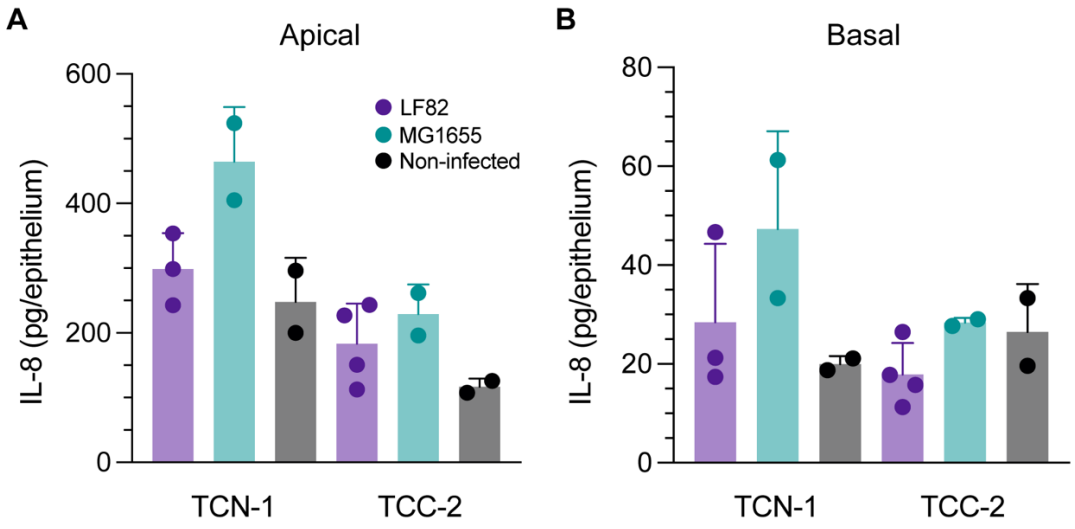

Figure 5.11. Exposure to AIEC LF82 and *E. coli* MG1655 induces IL-8 secretion in TCN-1 and TCC-2 organoid monolayers. Organoid monolayers on Transwell filters were incubated with LF82, MG1655 or left non-infected for 3 hr followed by 21 hr gentamicin treatment. IL-8 release was quantified in apical (**A**) and basal (**B**) supernatants by ELISA. Data shown as the mean +- SD. Significance was calculated using a one-way ANOVA test with Tukey's post-test comparison.

5.2.4 Summary

Overall, characterisation of different colonoid lines derived from non-IBD and CD tissue suggests that all characteristics tested are donor-dependent. This includes barrier function, MUC2 and CEACAM-6 expression and base-line pro-inflammatory cytokine secretion. When infected with AIEC LF82 and non-invasive MG1655, LF82 adherence and invasion appeared to be higher than that of MG1655 in both colonoid lines although this did not reach statistical significance due to high variation. The calculation of invasion rates demonstrated comparable levels between LF82 and MG1655 in TCN-4, but higher LF82 invasion in TCC-2, although again this was not statistically significant. The invasion rates of LF82 overall were even lower than those observed in T84 cells. Additionally, confocal microscopy of infected colonoid epithelia showed a lack of intracellular bacteria. Instead, aggregates of LF82 were observed on the surface. Furthermore, LF82 induced significant cytotoxicity in both colonoid lines. Interestingly, IL-8 secretion was higher in MG1655-infected than in LF82-infected colonoids. As observed in T84 cells, IL-8 was predominantly released from the apical membrane.

5.3 Discussion

5.3.1 Colonoid characteristics differ between patients

In contrast to colon cancer-derived cell lines, which represent only one IEC type (mostly colonocytes), organoids include the all major cell types of the gut, maintain the crypt-villi structure of the intestine, produce mucus and retain the region-specific genetic background and transcriptional and epigenetic characteristics of the gastrointestinal tract from which they derive (Cramer et al., 2015; Kraiczy et al., 2019; Middendorp et al., 2014). Organoids generated from CD patients maintain altered gene expression profiles associated with absorptive and secretory functions (d'Aldebert et al., 2020; Dotti et al., 2017). However, the acute transcriptional inflammatory phenotype is lost during organoid culture (Arnauts et al., 2020), although this can be induced with subsequent inflammatory stimulation such as addition of cytokines (Middendorp et al., 2014). Cytokines play a critical role in driving inflammation and tissue injury in the intestine. As such, biological therapies targeting inflammatory cytokines and the cells that produce them, such as anti-TNF agents and IL-12/IL-23 inhibitors (Xue et al., 2025), have led to progress in treating IBD, yet sustained remission in CD patients is rarely achieved.

The establishment and characterisation of morphological and functional phenotypes of control (non-IBD) organoids and organoids derived from IBD patients has been performed by different researchers. Previous studies have demonstrated that intestinal organoids derived from IBD patients display similar expression levels of several IBD-marker genes when compared to the tissue from which they were derived (Dotti et al., 2017). Genes encoding TJ proteins, such as *ZO-1*, *OCLN* and *CTNNB*, exhibited similar expression levels in intestinal crypts from CD-patients and derived organoids (Dotti et al., 2017). Meanwhile, studies by d'Aldebert et al demonstrated an inflammatory phenotype, decreased size and budding capacity, increased cell death and luminal debris, decreased tight junction formation and an inverted polarisation in IBD organoids (d'Aldebert et al., 2020). As for the inflammatory phenotype of IBD colonoids, mRNA expression of MCP1, IL-8 and IP-

10 was similar in colonoids from IBD patients and controls. Notably, stimulation with an inflammatory cocktail of IL-1, TNF-α and IL-6, induced significant mRNA overexpression of MCP-1 and IL-8, whilst also significantly decreasing expression of TJ proteins ZO-1 and Occludin, but not Claudin-1 in non-IBD organoids compared to unstimulated controls (d'Aldebert et al., 2020). These results agree with our findings which show that colonoids derived from normal and IBD tissue exhibited no difference in the secretion of pro-inflammatory cytokines. Hibiya et al demonstrated that murine colonoid exposure to a mixture of cytokines and bacterial components over 60 continuous weeks led to significant induction of target genes for the NF-κB pathway, which remained elevated 11 weeks after withdrawal of all cytokines (Hibiya et al., 2016). Therefore, the regulation of inflammatory gene expression may be a result of the acute inflammatory response in IBD as opposed to gene mutation. Interestingly, Özkan et al demonstrated that IBD fibroblasts are a key driver in IBD inflammation using a CD organ-on-a-chip model (Özkan et al., 2024). Studies by Pavlidis et al observed significant enrichment of IFN-γ and IL-17a responsive transcriptional signatures in colonic biopsies from patients with active colonic CD compared to healthy controls (Pavlidis et al., 2022). In addition, there was a concordance in IBD enrichment of cytokine-regulated transcriptional responses between the epithelium and the whole biopsy (Pavlidis et al., 2022). Epigenetic variations have been identified in tissues from IBD patients (Kellermayer, 2012; McGovern et al., 2015), therefore exposure of the epithelium to inflammatory mediators may result in epigenetic changes that could be conserved in organoid cultures. On the other hand, organoid co-culture models with immune cells or fibroblasts could be employed (Staab et al., 2023). It is also important to consider that immune cells are not present in our model. The inflammation in CD may be due to an excessive immune response to intestinal microbiota, with increased phagocytic activity and secretion of cytokines observed by gut resident macrophages in IBD patients (Lu et al., 2022). Co-culture models of organoid monolayers with macrophages and monocytes have been utilised to investigate the epithelium and underlying immune response. In our results, it is important to consider that secreted cytokines are derived from the epithelium itself. It is also interesting to consider whether the inflammatory state of a colonoid is affected by

the disease state of the patient biopsy it was derived from, for example if the patient was in remission or had active disease.

Similar to our results in polarised T84 cells (See - 4.2.5 AIEC LF82 induces predominant pro-inflammatory cytokine secretion from the apical side of the epithelium), IL-8 was secreted predominantly from the apical surface in colonoid monolayers. This agrees with studies on enteroid monolayers where IL-8 was mainly released apically (Zachos et al., 2016). Furthermore, Zachos et al demonstrated that IL-1β and TNF-α were undetectable or present at levels below 1 pg/ml. Meanwhile, IL-6 was secreted from both apical and basal surfaces and at quantities below 50 pg/epithelium (Zachos et al., 2016). This is in concordance with our results, whereby IL-6 secretion was below 1 pg/epithelium, meanwhile IL-1β and TNF-α were below detection levels (2 pg/ml and 4 pg/ml, respectively).

The culture of 2D colonoid monolayers on Transwell filters allowed barrier function to be assessed before and after differentiation by measuring TEER. Previous studies have described contradictory results on CD organoid barrier function. Studies by d'Aldebert et al showed a significant decrease in the expression of TJ proteins ZO-1, occludin and claudin-1 in colonoids from IBD compared to controls by western blot analysis (d'Aldebert et al., 2020). In addition, 2D colonoids from CD patients have displayed disrupted ZO-1 baseline staining (Sayed et al., 2020) and reduced TEER compared to non-IBD controls (Angus et al., 2022). On the other hand, 3D colonoids from CD tissue demonstrate exclusion of FITC-dextran, suggesting an effective intestinal barrier (Xu et al., 2018). However, in our studies, we generally did not observe a lower TEER in CD colonoids in comparison to non-IBD controls. Instead, TEER values were characteristic for each donor.

As previously described, Barnich et al demonstrated higher CEACAM-6 expression in ileal biopsies from CD patients compared to healthy controls (Barnich et al., 2007). In addition, CEACAM-6 is generally upregulated in inflamed tissues, including various cancers such as pancreatic adenocarcinoma (Kurlinkus et al., 2021; Pandey et al., 2019; Yan et al., 2016), gastric cancer (Roy et al., 2016) and

colon cancer (Ilantzis et al., 2002). In gastric cancer, it is suggested that *Helicobacter pylori* may infect the stomach through interactions with CEACAM-6, which in turn promotes gastric expression of CEACAM-6; exacerbating the infection and promoting inflammation (Behrens et al., 2020). A similar feedback loop has been suggested for AIEC and CEACAM-6, whereby AIEC promotes its own colonisation in CD. This is due to overexpression of CEACAM-6 in CD tissue leading to AIEC colonisation, which in turn promotes secretion of IFN-γ and TNF-α by macrophages and lymphocytes, resulting in upregulated CEACAM-6 expression (Glasser and Darfeuille-Michaud, 2008).

In contrast, our results showed that CEACAM-6 expression was not higher in organoids derived from CD versus control tissue although this was not quantified by Western blotting. Therefore, higher CEACAM-6 expression may not be retained in colonoids, which could be due to the loss of inflammatory stimulus from non-epithelial cells described above.

Finally, MUC2 levels in CD and non-IBD colonoids differed between colonoid lines but were independent of disease status (CD versus non-IBD). This is in agreement with studies by d'Aldebert which showed similar expression of MUC2 in colonoids from IBD donors and controls (d'Aldebert et al., 2020). Interestingly, mRNA expression analysis to characterise IBD and non-IBD organoids demonstrated no difference in MUC2 expression in undifferentiated IBD vs non-IBD organoids. However, MUC2 mRNA expression was significantly reduced in differentiated CD organoids compared to UC and non-IBD controls (Noben et al., 2017). Further analysis of the colonoids generated in this study could benefit from quantification of MUC2 by western blot or ELISA.

5.3.2 AIEC LF82 interaction with human colonoids

Given that carcinoma-derived cell lines lack some physiological characteristics including epithelium architecture, patient-specific variability and location-specific attributes of the intestine, human colonoids from patient biopsies provide a promising strategy for studying the epithelial response to and pathogenicity mechanisms of AIEC infection in a CD-specific background. Mayorgas et al showed that LF82 was able to invade differentiated colonoid monolayers, where 0.2% LF82 invasion at MOI 20 after 4 hr infection was observed (Mayorgas et al., 2021). A kinetic infection analysis demonstrated that over time, increasing amounts of invasive bacteria were detected at MOI 20 and 100. In contrast, our results demonstrated a much lower invasion rate of 0.03% in both colonoid lines tested, which showed no difference between CD-derived and non-IBD colonoids. Although it is important to note that an MOI of 10 was used in our studies, whereas Mayorgas et al used MOI 20. In addition, confocal microscopy indicated that LF82 did not form epithelial biofilms on colonoids as seen in T84 cells but localise in the mucus layer. Studies in CEABAC10 mice on a high fat and high sugar diet demonstrated increased AIEC colonisation of the intestinal mucosa with an associated decrease in MUC2 expression (Martinez-Medina et al., 2014). Investigating the effect of LF82 infection on MUC2 levels in CD and non-IBD colonoids by ELISA or WB was beyond the time restraint of this thesis but could be determined in future studies.

Additionally, Sayed et al used enteroid monolayers co-cultured with monocytes on the basal side to investigate host immune responses to AIEC LF82 infection. Enteroid monolayers from non-IBD controls displayed disrupted TJs after infection with LF82, meanwhile enteroids derived from CD patients showed disrupted TJs before infection (Sayed et al., 2020). Interestingly, CD-derived enteroids showed increased occludin levels upon infection with LF82, indicating a potential host mechanism in response to infection that prevents TJ collapse. However, this was assessed by immunofluorescence staining for occludin and was not quantified.

Interestingly, Mayorgas et al showed infected cells remained viable over time using the CellTox Green assay (Mayorgas et al., 2021). This is in contrast to the results of our study, which indicated cytotoxicity was induced by LF82 following infection. However, the methods employed by Mayorgas et al reached a maximum 7 hr incubation with LF82, whereas our investigation observed cytotoxicity after 24 hr. Therefore, cytotoxicity may be induced in colonoids only at later time points.

5.3.3 Rationale for patient selection for future colonoid studies

Given that organoids retain key genetic, epigenetic, and functional characteristics of the donor epithelium (Dotti and Salas, 2018), careful patient selection is essential to ensure that epithelial responses reflect clinically relevant host–pathogen interactions. Selection criteria commonly consider disease subtype (CD vs UC), location, disease activity at the time of sample collection and treatment history, as each of these variables can influence epithelial behaviour, barrier function and innate immune responses (Jeshvaghani et al., 2025). Importantly, organoids derived from inflamed and non-inflamed regions of the same patient can exhibit distinct phenotypes, providing an opportunity to dissect inflammation-associated epithelial changes while controlling for host genetic background (Arnauts et al., 2020). Therefore, future studies should include a large population of donors classified into disease status and age at diagnosis, with control groups including healthy donors. Various studies include individuals diagnosed with non-IBD GI diseases as healthy controls, therefore it is important to obtain resections from non-inflammatory zones to prevent the introduction of unwanted genetic mutations (d'Aldebert et al., 2020).

Chapter 6. Conclusions and Future Work

6.1 Final conclusions

In this study, the interaction of AIEC LF82 with human colonic epithelia was investigated using confluent and polarised carcinoma cell lines and differentiated human colonic organoid monolayers. Whilst earlier studies found a 4.8% invasion rate of LF82 in non-confluent Caco-2 cells, our results demonstrated a considerably lower invasion rate below 0.1%, displaying no significant difference compared with non-invasive MG1655. Such a discrepancy is likely to be a result of differences in cell polarity, whereby polarised cells form intact tight junctions and cell surface receptors are segregated apically and basolaterally. This polarity restricts LF82 to the binding receptors expressed on the apical surface. Given that intestinal pathogens such as *Shigella flexneri* bind to the basolateral surface via M cells or through disrupted tight junctions (Marteyn et al., 2010), it was plausible that this may explain the low invasion rates observed with AIEC LF82. However, LF82 did not show preferential binding to the basolateral side. Whilst invasion rates were lower than previously described in the literature, LF82 displayed distinct biofilm formation in T84 cells which was not shared amongst AIEC ileal strain NRG857c and colonic strains HM615, HM605 and HM580. Interestingly, LF82 biofilm formation was not observed on colonoid epithelia. Instead, LF82 appeared to adhere predominantly to the colonoid mucus layer rather than the exposed cell surface.

In addition, LF82 appeared to bind to a mannosylated receptor independent of the established fimbrial receptor CEACAM-6. LF82 expressed type I fimbriae and adherence to T84 cells was inhibited by D-mannose, but did not co-localise with CEACAM-6 expressing cells. The use of CEACAM-6 antibodies also did not inhibit LF82 binding, which differs from the work of Barnich et al, whereby LF82 adhered specifically to CEACAM-6 in ileal enterocytes from CD patients (Barnich et al., 2007). Given that the same antibody (mouse monoclonal 9A6) was used for blocking studies, it can be suggested that LF82 may bind to different cell surface receptors in human colonic epithelial cells.

A key finding across LF82-infected cell models was cytotoxicity that was dependent on bacterial contact and independent of secreted factors. Whilst LF82 has two identified T6SSs (T6SS-1 and T6SS-3), it is yet to be determined whether effector proteins with virulence functions are present. Given that T6SS-deficient LF82 mutants did not reduce cytotoxicity in T84 cells, this indicates other mechanisms of contact-dependent cytotoxicity. In addition, LF82 significantly reduced TEER in polarised T84 cells when compared with MG1655-infected and non-infected controls, suggesting disruption to epithelial barrier function. A similar pattern was observed in colonoids; however, TEER reduction did not reach significance. Furthermore, the secretion of pro-inflammatory cytokines TNF-α, IL-8, IL-6 and IL-1β suggests AIEC may exacerbate inflammation observed in CD.

The use of colonoids derived from CD patients and non-IBD controls showed MUC2 production and CEACAM-6 expression in colonoids was independent of disease status. Rather, these phenotypes were patient-specific. Whilst this is unexpected given that reduced MUC2 secretion and increased CEACAM-6 expression have been reported in CD tissue, it is important to consider our studies were limited to four colonoid lines. In addition, colonoids from UC patients have previously been shown to lose their inflammatory signature. Therefore, it remains to be investigated whether colonoids retain these phenotypes and are comparable to that of the original tissue from which they were derived. As a result, LF82 infection displayed a similar phenotype in both CD and non-IBD colonoids.

In summary, we demonstrated that LF82 pathogenesis in the human colon is strain-specific and mediated by the formation of biofilms, contact-dependent cytotoxicity, epithelial permeability, and pro-inflammatory cytokine secretion. This has been shown in both polarised carcinoma cell lines and human colonic organoids, however more studies using the latter are required to gain more insight into AIEC pathogenesis in colonoids. These data further extend the characteristics of AIEC LF82 which may perpetuate chronic inflammation observed in CD.

6.2. Future directions

To further develop the findings of this thesis, infection of colonic organoids within a VDC system would permit simultaneous control of oxygen gradients while preserving the mucus layer, enabling investigation of LF82 pathogenesis under microaerobic conditions that more closely reflect the colonic lumen. Such approaches would provide important insight into the environmental cues that regulate AIEC localisation, persistence, and epithelial interactions. In parallel, further studies are required to define the bacterial and host mechanisms underlying LF82-mediated epithelial damage and barrier disruption.

The present study confirmed that LF82 adherence to the colonic epithelium is mannose-dependent and does not involve CEACAM-6 binding, highlighting a significant gap in the current understanding of colonic-specific AIEC receptors. This could be addressed using approaches such as shotgun carbohydrate microarrays or mass spectrometry-based glycomics to identify mannosylated host glycans that mediate LF82 binding in the colon. Identification of such interactions would be critical for the development of anti-adhesive therapeutic strategies with efficacy in the colonic environment.

Future work should also focus on strategies to limit LF82 persistence, including disruption of biofilm formation and mucus-associated colonisation. Given the heterogeneity within the AIEC pathovar, it will be essential to extend these analyses beyond LF82 to a broader panel of clinical isolates. Evaluation of multiple AIEC strains in complex intestinal models, such as colonic organoids, will be necessary to distinguish conserved pathogenic mechanisms from isolate-specific traits and to enhance the translational relevance of experimental findings to CD pathogenesis.

Bibliography

Aguirre Garcia, M., Hillion, K., Cappelier, J.-M., Neunlist, M., Mahe, M.M., Haddad, N., 2022. Intestinal Organoids: New Tools to Comprehend the Virulence of Bacterial Foodborne Pathogens. Foods 11, 108. https://doi.org/10.3390/foods11010108

Agus, A., Denizot, J., Thévenot, J., Martinez-Medina, M., Massier, S., Sauvanet, P., Bernalier-Donadille, A., Denis, S., Hofman, P., Bonnet, R., Billard, E., Barnich, N., 2016. Western diet induces a shift in microbiota composition enhancing susceptibility to Adherent-Invasive E. coli infection and intestinal inflammation. Sci Rep 6, 19032. https://doi.org/10.1038/srep19032

Agus, A., Massier, S., Darfeuille-Michaud, A., Billard, E., Barnich, N., 2014. Understanding Host-Adherent-Invasive *Escherichia coli* Interaction in Crohn's Disease: Opening Up New Therapeutic Strategies. BioMed Research International 2014, 1–16. https://doi.org/10.1155/2014/567929

Al Nabhani, Z., Lepage, P., Mauny, P., Montcuquet, N., Roy, M., Le Roux, K., Dussaillant, M., Berrebi, D., Hugot, J.-P., Barreau, F., 2016. *Nod2* Deficiency Leads to a Specific and Transmissible Mucosa-associated Microbial Dysbiosis Which Is Independent of the Mucosal Barrier Defect. ECCOJC 10, 1428–1436. https://doi.org/10.1093/ecco-jcc/jjw095

Alvarez Dorta, D., Sivignon, A., Chalopin, T., Dumych, T.I., Roos, G., Bilyy, R.O., Deniaud, D., Krammer, E., de Ruyck, J., Lensink, M.F., Bouckaert, J., Barnich, N., Gouin, S.G., 2016. The Antiadhesive Strategy in Crohn′s Disease: Orally Active Mannosides to Decolonize Pathogenic *Escherichia coli* from the Gut. ChemBioChem 17, 936–952. https://doi.org/10.1002/cbic.201600018

Ambriz-Aviña, V., Contreras-Garduño, J.A., Pedraza-Reyes, M., 2014. Applications of Flow Cytometry to Characterize Bacterial Physiological Responses. BioMed Research International 2014, 1–14. https://doi.org/10.1155/2014/461941

Ananthakrishnan, A.N., Khalili, H., Konijeti, G.G., Higuchi, L.M., De Silva, P., Korzenik, J.R., Fuchs, C.S., Willett, W.C., Richter, J.M., Chan, A.T., 2013. A Prospective Study of Long-term Intake of Dietary Fiber and Risk of Crohn's Disease and Ulcerative Colitis. Gastroenterology 145, 970–977. https://doi.org/10.1053/j.gastro.2013.07.050

Anderson, G.G., Palermo, J.J., Schilling, J.D., Roth, R., Heuser, J., Hultgren, S.J., 2003. Intracellular Bacterial Biofilm-Like Pods in Urinary Tract Infections. Science 301, 105–107. https://doi.org/10.1126/science.1084550

Ando, Hiroki., Abe, Hiroyuki., Sugimoto, Nakaba., Tobe, Toru., 2007. Maturation of functional type III secretion machinery by activation of anaerobic respiration in enterohaemorrhagic Escherichia coli. Microbiology 153, 464–473. https://doi.org/10.1099/mic.0.2006/000893-0

Angus, H.C., Urbano, P.C., Laws, G.A., Fan, S., Gadeock, S., Schultz, M., Butt, G., Highton, A.J., Kemp, R.A., 2022. An autologous colonic organoid-derived monolayer model to study immune: bacterial interactions in Crohn's disease patients. Clin Transl Immunology 11, e1407. https://doi.org/10.1002/cti2.1407

Anonye, B.O., Hassall, J., Patient, J., Detamornrat, U., Aladdad, A.M., Schüller, S., Rose, F.R.A.J., Unnikrishnan, M., 2019. Probing Clostridium difficile Infection in Complex Human Gut Cellular Models. Front. Microbiol. 10, 879. https://doi.org/10.3389/fmicb.2019.00879

Arnauts, K., Verstockt, B., Ramalho, A.S., Vermeire, S., Verfaillie, C., Ferrante, M., 2020. Ex Vivo Mimicking of Inflammation in Organoids Derived From Patients With Ulcerative Colitis. Gastroenterology 159, 1564–1567. https://doi.org/10.1053/j.gastro.2020.05.064

Arnauts, K., Verstockt, B., Vancamelbeke, M., Vermeire, S., Verfaillie, C., Ferrante, M., 2019. OP11 Organoids derived from inflamed intestinal biopsies of patients with ulcerative colitis lose their inflammatory phenotype during *ex vivo* culture. Journal of Crohn's and Colitis 13, S007–S007. https://doi.org/10.1093/ecco-jcc/jjy222.010

Assa, A., Vong, L., Pinnell, L.J., Rautava, J., Avitzur, N., Johnson-Henry, K.C., Sherman, P.M., 2015. Vitamin D Deficiency Predisposes to Adherent-invasive Escherichia coli-induced Barrier Dysfunction and Experimental Colonic Injury: Inflammatory Bowel Diseases 21, 297–306. https://doi.org/10.1097/MIB.0000000000000282

Aubert, D.F., Xu, H., Yang, J., Shi, X., Gao, W., Li, L., Bisaro, F., Chen, S., Valvano, M.A., Shao, F., 2016. A Burkholderia Type VI Effector Deamidates Rho GTPases to Activate the Pyrin Inflammasome and Trigger Inflammation. Cell Host Microbe 19, 664–674. https://doi.org/10.1016/j.chom.2016.04.004

Bambou, J.-C., Giraud, A., Menard, S., Begue, B., Rakotobe, S., Heyman, M., Taddei, F., Cerf-Bensussan, N., Gaboriau-Routhiau, V., 2004. In Vitro and ex Vivo Activation of the TLR5 Signaling Pathway in Intestinal Epithelial Cells by a Commensal Escherichia coli Strain. Journal of Biological Chemistry 279, 42984–42992. https://doi.org/10.1074/jbc.M405410200

Bamias, G., Martin, C., Marini, M., Hoang, S., Mishina, M., Ross, W.G., Sachedina, M.A., Friel, C.M., Mize, J., Bickston, S.J., Pizarro, T.T., Wei, P., Cominelli, F., 2003. Expression, Localization, and Functional Activity of TL1A, a Novel Th1-Polarizing Cytokine in Inflammatory Bowel Disease. The Journal of Immunology 171, 4868–4874. https://doi.org/10.4049/jimmunol.171.9.4868

Barnich, N., Boudeau, J., Claret, L., Darfeuille-Michaud, A., 2003. Regulatory and functional co-operation of flagella and type 1 pili in adhesive and invasive abilities of AIEC strain LF82 isolated from a patient with Crohn's disease: Flagella and adherent-invasive E. coli. Molecular Microbiology 48, 781–794. https://doi.org/10.1046/j.1365-2958.2003.03468.x

Barnich, N., Carvalho, F.A., Glasser, A.-L., Darcha, C., Jantscheff, P., Allez, M., Peeters, H., Bommelaer, G., Desreumaux, P., Colombel, J.-F., Darfeuille-Michaud, A., 2007. CEACAM6 acts as a receptor for adherent-invasive E. coli, supporting ileal mucosa colonization in Crohn disease. J. Clin. Invest. 117, 1566–1574. https://doi.org/10.1172/JCI30504

Barnich, N., Denizot, J., Darfeuille-Michaud, A., 2013. E. coli-mediated gut inflammation in genetically predisposed Crohn's disease patients. Pathologie Biologie 61, e65–e69. https://doi.org/10.1016/j.patbio.2010.01.004

Bäumler, A.J., Tsolis, R.M., Heffron, F., 1996. The lpf fimbrial operon mediates adhesion of Salmonella typhimurium to murine Peyer's patches. Proc Natl Acad Sci U S A 93, 279–283. https://doi.org/10.1073/pnas.93.1.279

Baxt, L.A., Xavier, R.J., 2015. Role of Autophagy in the Maintenance of Intestinal Homeostasis. Gastroenterology 149, 553–562. https://doi.org/10.1053/j.gastro.2015.06.046

Behrens, I.-K., Busch, B., Ishikawa-Ankerhold, H., Palamides, P., Shively, J.E., Stanners, C., Chan, C., Leung, N., Gray-Owen, S., Haas, R., 2020. The HopQ-CEACAM Interaction Controls CagA Translocation, Phosphorylation, and Phagocytosis of *Helicobacter pylori* in Neutrophils. mBio 11, e03256-19. https://doi.org/10.1128/mBio.03256-19

Berg, D.J., Davidson, N., Kühn, R., Müller, W., Menon, S., Holland, G., Thompson-Snipes, L., Leach, M.W., Rennick, D., 1996. Enterocolitis and colon cancer in interleukin-10-deficient mice are associated with aberrant cytokine production and CD4(+) TH1-like responses. J. Clin. Invest. 98, 1010–1020. https://doi.org/10.1172/JCI118861

Bernstein, C.N., Blanchard, J.F., Rawsthorne, P., Yu, N., 2001. The Prevalence of Extraintestinal Diseases in Inflammatory Bowel Disease: A Population-Based Study: American Journal of Gastroenterology 96, 1116–1122. https://doi.org/10.1111/j.1572-0241.2001.03756.x

Bevins, C.L., Salzman, N.H., 2011. Paneth cells, antimicrobial peptides and maintenance of intestinal homeostasis. Nat Rev Microbiol 9, 356–368. https://doi.org/10.1038/nrmicro2546

Bingle, L.E., Bailey, C.M., Pallen, M.J., 2008. Type VI secretion: a beginner's guide. Current Opinion in Microbiology 11, 3–8. https://doi.org/10.1016/j.mib.2008.01.006

Binion, D.G., Rafiee, P., 2009. Is Inflammatory Bowel Disease a Vascular Disease? Targeting Angiogenesis Improves Chronic Inflammation in Inflammatory Bowel Disease. Gastroenterology 136, 400–403. https://doi.org/10.1053/j.gastro.2008.12.029

Bomberger, J.M., MacEachran, D.P., Coutermarsh, B.A., Ye, S., O'Toole, G.A., Stanton, B.A., 2009. Long-Distance Delivery of Bacterial Virulence Factors

by Pseudomonas aeruginosa Outer Membrane Vesicles. PLoS Pathog 5, e1000382. https://doi.org/10.1371/journal.ppat.1000382

Boudeau, J., Glasser, A.-L., Masseret, E., Joly, B., Darfeuille-Michaud, A., 1999. Invasive Ability of an *Escherichia coli* Strain Isolated from the Ileal Mucosa of a Patient with Crohn's Disease. Infect Immun 67, 4499–4509. https://doi.org/10.1128/IAI.67.9.4499-4509.1999

Boyer, F., Fichant, G., Berthod, J., Vandenbrouck, Y., Attree, I., 2009. Dissecting the bacterial type VI secretion system by a genome wide in silico analysis: what can be learned from available microbial genomic resources? BMC Genomics 10, 104. https://doi.org/10.1186/1471-2164-10-104

Brain, O., Owens, B.M.J., Pichulik, T., Allan, P., Khatamzas, E., Leslie, A., Steevels, T., Sharma, S., Mayer, A., Catuneanu, A.M., Morton, V., Sun, M.-Y., Jewell, D., Coccia, M., Harrison, O., Maloy, K., Schönefeldt, S., Bornschein, S., Liston, A., Simmons, A., 2013. The Intracellular Sensor NOD2 Induces MicroRNA-29 Expression in Human Dendritic Cells to Limit IL-23 Release. Immunity 39, 521–536. https://doi.org/10.1016/j.immuni.2013.08.035

Brandt, L.J., Aroniadis, O.C., Mellow, M., Kanatzar, A., Kelly, C., Park, T., Stollman, N., Rohlke, F., Surawicz, C., 2012. Long-Term Follow-Up of Colonoscopic Fecal Microbiota Transplant for Recurrent Clostridium difficile Infection. American Journal of Gastroenterology 107, 1079–1087. https://doi.org/10.1038/ajg.2012.60

Brest, P., Lapaquette, P., Souidi, M., Lebrigand, K., Cesaro, A., Vouret-Craviari, V., Mari, B., Barbry, P., Mosnier, J.-F., Hébuterne, X., Harel-Bellan, A., Mograbi, B., Darfeuille-Michaud, A., Hofman, P., 2011. A synonymous variant in IRGM alters a binding site for miR-196 and causes deregulation of IRGM-dependent xenophagy in Crohn's disease. Nat Genet 43, 242–245. https://doi.org/10.1038/ng.762

Bretin, A., Carrière, J., Dalmasso, G., Bergougnoux, A., B'chir, W., Maurin, A.-C., Müller, S., Seibold, F., Barnich, N., Bruhat, A., Darfeuille-Michaud, A., Nguyen, H.T.T., 2016. Activation of the EIF2AK4-EIF2A/eIF2α-ATF4 pathway triggers autophagy response to Crohn disease-associated adherent-invasive *Escherichia coli* infection. Autophagy 12, 770–783. https://doi.org/10.1080/15548627.2016.1156823

Bretin, A., Lucas, C., Larabi, A., Dalmasso, G., Billard, E., Barnich, N., Bonnet, R., Nguyen, H.T.T., 2018. AIEC infection triggers modification of gut microbiota composition in genetically predisposed mice, contributing to intestinal inflammation. Sci Rep 8, 12301. https://doi.org/10.1038/s41598-018-30055-y

Bringer, M.-A., Glasser, A.-L., Tung, C.-H., Meresse, S., Darfeuille-Michaud, A., 2006. The Crohn's disease-associated adherent-invasive Escherichia coli strain LF82 replicates in mature phagolysosomes within J774 macrophages. Cell Microbiol 8, 471–484. https://doi.org/10.1111/j.1462-5822.2005.00639.x

Brown, C.L., Smith, K., Wall, D.M., Walker, D., 2015. Activity of Species-specific Antibiotics Against Crohn's Disease–Associated Adherent-invasive Escherichia coli: Inflammatory Bowel Diseases 1. https://doi.org/10.1097/MIB.0000000000000488

Brument, S., Sivignon, A., Dumych, T.I., Moreau, N., Roos, G., Guérardel, Y., Chalopin, T., Deniaud, D., Bilyy, R.O., Darfeuille-Michaud, A., Bouckaert, J., Gouin, S.G., 2013. Thiazolylaminomannosides As Potent Antiadhesives of Type 1 Piliated Escherichia coli Isolated from Crohn's Disease Patients. J. Med. Chem. 56, 5395–5406. https://doi.org/10.1021/jm400723n

Buisine, M.-P., 2001. Mucin gene expression in intestinal epithelial cells in Crohn's disease. Gut 49, 544–551. https://doi.org/10.1136/gut.49.4.544

Carabeo, R.A., Grieshaber, S.S., Fischer, E., Hackstadt, T., 2002. Chlamydia trachomatis induces remodeling of the actin cytoskeleton during attachment and entry into HeLa cells. Infect Immun 70, 3793–3803. https://doi.org/10.1128/IAI.70.7.3793-3803.2002

Carlson-Banning, K.M., Sperandio, V., 2016. Catabolite and Oxygen Regulation of Enterohemorrhagic Escherichia coli Virulence. mBio 7, e01852-16. https://doi.org/10.1128/mBio.01852-16

Caruso, R., Warner, N., Inohara, N., Núñez, G., 2014. NOD1 and NOD2: Signaling, Host Defense, and Inflammatory Disease. Immunity 41, 898–908. https://doi.org/10.1016/j.immuni.2014.12.010

Carvalho, F.A., Barnich, N., Sauvanet, P., Darcha, C., Gelot, A., Darfeuille-Michaud, A., 2008. Crohn's disease-associated Escherichia coli LF82 aggravates colitis in injured mouse colon via signaling by flagellin: Inflammatory Bowel Diseases 14, 1051–1060. https://doi.org/10.1002/ibd.20423

Carvalho, F.A., Barnich, N., Sivignon, A., Darcha, C., Chan, C.H.F., Stanners, C.P., Darfeuille-Michaud, A., 2009. Crohn's disease adherent-invasive Escherichia coli colonize and induce strong gut inflammation in transgenic mice expressing human CEACAM. Journal of Experimental Medicine 206, 2179–2189. https://doi.org/10.1084/jem.20090741

Cascales, E., 2008. The type VI secretion toolkit. EMBO Reports 9, 735–741. https://doi.org/10.1038/embor.2008.131

Castiblanco, L.F., Sundin, G.W., 2016. New insights on molecular regulation of biofilm formation in plant-associated bacteria. JIPB 58, 362–372. https://doi.org/10.1111/jipb.12428

Chalopin, T., Alvarez Dorta, D., Sivignon, A., Caudan, M., Dumych, T.I., Bilyy, R.O., Deniaud, D., Barnich, N., Bouckaert, J., Gouin, S.G., 2016. Second generation of thiazolylmannosides, FimH antagonists for E. coli-induced Crohn's disease. Org. Biomol. Chem. 14, 3913–3925. https://doi.org/10.1039/C6OB00424E

Chassaing, B., Aitken, J.D., Malleshappa, M., Vijay-Kumar, M., 2014. Dextran Sulfate Sodium (DSS)-Induced Colitis in Mice. CP in Immunology 104. https://doi.org/10.1002/0471142735.im1525s104

Chassaing, B., Darfeuille-Michaud, A., 2013. The σ^{E} Pathway Is Involved in Biofilm Formation by Crohn's Disease-Associated Adherent-Invasive Escherichia coli. J Bacteriol 195, 76–84. https://doi.org/10.1128/JB.01079-12

Chassaing, B., Etienne-Mesmin, L., Bonnet, R., Darfeuille-Michaud, A., 2013. Bile salts induce long polar fimbriae expression favouring Crohn's disease-associated adherent-invasive *Escherichia coli* interaction with Peyer's patches: LPF regulation by bile salts in AIEC strains. Environ Microbiol 15, 355–371. https://doi.org/10.1111/j.1462-2920.2012.02824.x

Chassaing, B., Rolhion, N., Vallée, A. de, Salim, S.Y., Prorok-Hamon, M., Neut, C., Campbell, B.J., Söderholm, J.D., Hugot, J.-P., Colombel, J.-F., Darfeuille-Michaud, A., 2011. Crohn disease–associated adherent-invasive E. coli bacteria target mouse and human Peyer's patches via long polar fimbriae. J. Clin. Invest. 121, 966–975. https://doi.org/10.1172/JCI44632

Chauhan, S., Mandell, M.A., Deretic, V., 2015. IRGM Governs the Core Autophagy Machinery to Conduct Antimicrobial Defense. Molecular Cell 58, 507–521. https://doi.org/10.1016/j.molcel.2015.03.020

Chen, C.-C., Pekow, J., Llado, V., Kanneganti, M., Lau, C.W., Mizoguchi, A., Mino-Kenudson, M., Bissonnette, M., Mizoguchi, E., 2011. Chitinase 3-Like-1 Expression in Colonic Epithelial Cells as a Potentially Novel Marker for Colitis-Associated Neoplasia. The American Journal of Pathology 179, 1494–1503. https://doi.org/10.1016/j.ajpath.2011.05.038

Cherrak, Y., Flaugnatti, N., Durand, E., Journet, L., Cascales, E., 2019. Structure and Activity of the Type VI Secretion System. Microbiol Spectr 7, 7.4.11. https://doi.org/10.1128/microbiolspec.PSIB-0031-2019

Chevalier, G., Laveissière, A., Desachy, G., Barnich, N., Sivignon, A., Maresca, M., Nicoletti, C., Di Pasquale, E., Martinez-Medina, M., Simpson, K.W., Yajnik, V., Sokol, H., MOBIDIC Study Investigators, Adegbamigbe, T., Ahmad, T., Arnott, I., Bouhnik, Y., Carbonnel, F., Colombel, J.-F., Doherty, G., Cummings, J.R.F., Hébuterne, X., Herfarth, H., Kevans, D., de Chambrun, G.P., Nachury, M., Nancey, S., Roblin, X., Tremelling, M.A.W., Plassais, J., Strozzi, F., Cervino, A., Morra, R., Bonny, C., 2021. Blockage of bacterial FimH prevents mucosal inflammation associated with Crohn's disease. Microbiome 9, 176. https://doi.org/10.1186/s40168-021-01135-5

Chidlow, J.H., Shukla, D., Grisham, M.B., Kevil, C.G., 2007. Pathogenic angiogenesis in IBD and experimental colitis: new ideas and therapeutic avenues. American Journal of Physiology-Gastrointestinal and Liver Physiology 293, G5–G18. https://doi.org/10.1152/ajpgi.00107.2007

Cieza, R.J., Hu, J., Ross, B.N., Sbrana, E., Torres, A.G., 2015. The IbeA Invasin of Adherent-Invasive Escherichia coli Mediates Interaction with Intestinal

Epithelia and Macrophages. Infect Immun 83, 1904–1918. https://doi.org/10.1128/IAI.03003-14

Cogger-Ward, R., 2020. Characterisation of putative virulence factors in Adherent-Invasive Escherichia coli. University of Nottingham.

Colman, R.J., Rubin, D.T., 2014. Fecal microbiota transplantation as therapy for inflammatory bowel disease: A systematic review and meta-analysis. Journal of Crohn's and Colitis 8, 1569–1581. https://doi.org/10.1016/j.crohns.2014.08.006

Conway, T., Cohen, P.S., 2015. Commensal and Pathogenic *Escherichia coli* Metabolism in the Gut. Microbiol Spectr 3, 3.3.24. https://doi.org/10.1128/microbiolspec.MBP-0006-2014

Cooney, R., Baker, J., Brain, O., Danis, B., Pichulik, T., Allan, P., Ferguson, D.J.P., Campbell, B.J., Jewell, D., Simmons, A., 2010. NOD2 stimulation induces autophagy in dendritic cells influencing bacterial handling and antigen presentation. Nat Med 16, 90–97. https://doi.org/10.1038/nm.2069

Cottet, S., Cortheásy-Theulaz, I., Spertini, F., Cortheásy, B., 2002. Microaerophilic Conditions Permit to Mimic in VitroEvents Occurring during in Vivo Helicobacter pylori Infection and to Identify Rho/Ras-associated Proteins in Cellular Signaling. Journal of Biological Chemistry 277, 33978–33986. https://doi.org/10.1074/jbc.M201726200

Cramer, J.M., Thompson, T., Geskin, A., LaFramboise, W., Lagasse, E., 2015. Distinct Human Stem Cell Populations in Small and Large Intestine. PLoS ONE 10, e0118792. https://doi.org/10.1371/journal.pone.0118792

Creff, J., Malaquin, L., Besson, A., 2021. In vitro models of intestinal epithelium: Toward bioengineered systems. J Tissue Eng 12, 2041731420985202. https://doi.org/10.1177/2041731420985202

d'Aldebert, E., Quaranta, M., Sébert, M., Bonnet, D., Kirzin, S., Portier, G., Duffas, J.-P., Chabot, S., Lluel, P., Allart, S., Ferrand, A., Alric, L., Racaud-Sultan, C., Mas, E., Deraison, C., Vergnolle, N., 2020. Characterization of Human Colon Organoids From Inflammatory Bowel Disease Patients. Front. Cell Dev. Biol. 8, 363. https://doi.org/10.3389/fcell.2020.00363

Dalmasso, G., Nguyen, H.T.T., Faïs, T., Massier, S., Barnich, N., Delmas, J., Bonnet, R., 2019. Crohn's Disease-Associated Adherent-Invasive Escherichia coli Manipulate Host Autophagy by Impairing SUMOylation. Cells 8, 35. https://doi.org/10.3390/cells8010035

Dalmasso, G., Nguyen, H.T.T., Faïs, T., Massier, S., Chevarin, C., Vazeille, E., Barnich, N., Delmas, J., Bonnet, R., 2021. Yersiniabactin Siderophore of Crohn's Disease-Associated Adherent-Invasive Escherichia coli Is Involved in Autophagy Activation in Host Cells. IJMS 22, 3512. https://doi.org/10.3390/ijms22073512

Darfeuille-Michaud, A., Boudeau, J., Bulois, P., Neut, C., Glasser, A.-L., Barnich, N., Bringer, M.-A., Swidsinski, A., Beaugerie, L., Colombel, J.-F., 2004. High prevalence of adherent-invasive Escherichia coli associated with ileal mucosa in Crohn's disease. Gastroenterology 127, 412–421. https://doi.org/10.1053/j.gastro.2004.04.061

Darfeuille-Michaud, A., Neut, C., Barnich, N., Lederman, E., Di Martino, P., Desreumaux, P., Gambiez, L., Joly, B., Cortot, A., Colombel, J.-F., 1998. Presence of adherent Escherichia coli strains in ileal mucosa of patients with Crohn's disease. Gastroenterology 115, 1405–1413. https://doi.org/10.1016/S0016-5085(98)70019-8

De, S., Kaus, K., Sinclair, S., Case, B.C., Olson, R., 2018. Structural basis of mammalian glycan targeting by Vibrio cholerae cytolysin and biofilm proteins. PLoS Pathog 14, e1006841. https://doi.org/10.1371/journal.ppat.1006841

De Souza, H.S.P., Fiocchi, C., 2016. Immunopathogenesis of IBD: current state of the art. Nat Rev Gastroenterol Hepatol 13, 13–27. https://doi.org/10.1038/nrgastro.2015.186

Deban, L., Correale, C., Vetrano, S., Malesci, A., Danese, S., 2008. Multiple Pathogenic Roles of Microvasculature in Inflammatory Bowel Disease: A Jack of All Trades. The American Journal of Pathology 172, 1457–1466. https://doi.org/10.2353/ajpath.2008.070593

Delmas, J., Gibold, L., Faïs, T., Batista, S., Leremboure, M., Sinel, C., Vazeille, E., Cattoir, V., Buisson, A., Barnich, N., Dalmasso, G., Bonnet, R., 2019. Metabolic adaptation of adherent-invasive Escherichia coli to exposure to bile salts. Sci Rep 9, 2175. https://doi.org/10.1038/s41598-019-38628-1

Denizot, J., Sivignon, A., Barreau, F., Darcha, C., Chan, C.H.F., Stanners, C.P., Hofman, P., Darfeuille-Michaud, A., Barnich, N., 2012. Adherent-Invasive Escherichia coli Induce Claudin-2 Expression and Barrier Defect in CEABAC10 Mice and Crohn's Disease Patients§: Inflammatory Bowel Diseases 18, 294–304. https://doi.org/10.1002/ibd.21787

Desai, M.S., Seekatz, A.M., Koropatkin, N.M., Kamada, N., Hickey, C.A., Wolter, M., Pudlo, N.A., Kitamoto, S., Terrapon, N., Muller, A., Young, V.B., Henrissat, B., Wilmes, P., Stappenbeck, T.S., Núñez, G., Martens, E.C., 2016. A Dietary Fiber-Deprived Gut Microbiota Degrades the Colonic Mucus Barrier and Enhances Pathogen Susceptibility. Cell 167, 1339-1353.e21. https://doi.org/10.1016/j.cell.2016.10.043

Devriese, S., Van den Bossche, L., Van Welden, S., Holvoet, T., Pinheiro, I., Hindryckx, P., De Vos, M., Laukens, D., 2017. T84 monolayers are superior to Caco-2 as a model system of colonocytes. Histochem Cell Biol 148, 85–93. https://doi.org/10.1007/s00418-017-1539-7

Dicarlo, M., Teti, G., Verna, G., Liso, M., Cavalcanti, E., Sila, A., Raveenthiraraj, S., Mastronardi, M., Santino, A., Serino, G., Lippolis, A., Sobolewski, A., Falconi, M., Chieppa, M., 2019. Quercetin Exposure Suppresses the Inflammatory

Pathway in Intestinal Organoids from Winnie Mice. IJMS 20, 5771. https://doi.org/10.3390/ijms20225771

Dorofeyev, A.E., Vasilenko, I.V., Rassokhina, O.A., Kondratiuk, R.B., 2013. Mucosal Barrier in Ulcerative Colitis and Crohn's Disease. Gastroenterology Research and Practice 2013, 1–9. https://doi.org/10.1155/2013/431231

Dotti, I., Mora-Buch, R., Ferrer-Picón, E., Planell, N., Jung, P., Masamunt, M.C., Leal, R.F., Martín De Carpi, J., Llach, J., Ordás, I., Batlle, E., Panés, J., Salas, A., 2017. Alterations in the epithelial stem cell compartment could contribute to permanent changes in the mucosa of patients with ulcerative colitis. Gut 66, 2069–2079. https://doi.org/10.1136/gutjnl-2016-312609

Dotti, I., Salas, A., 2018. Potential Use of Human Stem Cell-Derived Intestinal Organoids to Study Inflammatory Bowel Diseases. Inflamm Bowel Dis 24, 2501–2509. https://doi.org/10.1093/ibd/izy275

Dreux, N., Denizot, J., Martinez-Medina, M., Mellmann, A., Billig, M., Kisiela, D., Chattopadhyay, S., Sokurenko, E., Neut, C., Gower-Rousseau, C., Colombel, J.-F., Bonnet, R., Darfeuille-Michaud, A., Barnich, N., 2013. Point Mutations in FimH Adhesin of Crohn's Disease-Associated Adherent-Invasive Escherichia coli Enhance Intestinal Inflammatory Response. PLoS Pathog 9, e1003141. https://doi.org/10.1371/journal.ppat.1003141

Eaves-Pyles, T., Allen, C.A., Taormina, J., Swidsinski, A., Tutt, C.B., Eric Jezek, G., Islas-Islas, M., Torres, A.G., 2008. Escherichia coli isolated from a Crohn's disease patient adheres, invades, and induces inflammatory responses in polarized intestinal epithelial cells. International Journal of Medical Microbiology 298, 397–409. https://doi.org/10.1016/j.ijmm.2007.05.011

Eckmann, L., Jung, H.C., Schürer-Maly, C., Panja, A., Morzycka-Wroblewska, E., Kagnoff, M.F., 1993. Differential cytokine expression by human intestinal epithelial cell lines: Regulated expression of interleukin 8. Gastroenterology 105, 1689–1697. https://doi.org/10.1016/0016-5085(93)91064-O

Economou, M., Pappas, G., 2008. New global map of Crohn's disease: Genetic, environmental, and socioeconomic correlations: Inflammatory Bowel Diseases 14, 709–720. https://doi.org/10.1002/ibd.20352

Elatrech, I., Marzaioli, V., Boukemara, H., Bournier, O., Neut, C., Darfeuille-Michaud, A., Luis, J., Dubuquoy, L., El-Benna, J., My-Chan Dang, P., Marie, J.-C., 2015. Escherichia coli LF82 Differentially Regulates ROS Production and Mucin Expression in Intestinal Epithelial T84 Cells: Implication of NOX1. Inflammatory Bowel Diseases 21, 1018–1026. https://doi.org/10.1097/MIB.0000000000000365

Elhenawy, W., Hordienko, S., Gould, S., Oberc, A.M., Tsai, C.N., Hubbard, T.P., Waldor, M.K., Coombes, B.K., 2021. High-throughput fitness screening and transcriptomics identify a role for a type IV secretion system in the pathogenesis of Crohn's disease-associated Escherichia coli. Nat Commun 12, 2032. https://doi.org/10.1038/s41467-021-22306-w

Elhenawy, W., Tsai, C.N., Coombes, B.K., 2019. Host-Specific Adaptive Diversification of Crohn's Disease-Associated Adherent-Invasive Escherichia coli. Cell Host & Microbe 25, 301-312.e5. https://doi.org/10.1016/j.chom.2018.12.010

Ellermann, M., Huh, E.Y., Liu, B., Carroll, I.M., Tamayo, R., Sartor, R.B., 2015. Adherent-Invasive Escherichia coli Production of Cellulose Influences Iron-Induced Bacterial Aggregation, Phagocytosis, and Induction of Colitis. Infect Immun 83, 4068–4080. https://doi.org/10.1128/IAI.00904-15

Ellermann, M., Sartor, R.B., 2018. Intestinal bacterial biofilms modulate mucosal immune responses. J Immunol Sci 2, 13–18.

Erkmen, O., Bozoglu, T.F. (Eds.), 2016. Bacterial Pathogenicity and Microbial Toxins, in: Food Microbiology: Principles into Practice. Wiley, pp. 126–137. https://doi.org/10.1002/9781119237860.ch7

Flaugnatti, N., Le, T.T.H., Canaan, S., Aschtgen, M., Nguyen, V.S., Blangy, S., Kellenberger, C., Roussel, A., Cambillau, C., Cascales, E., Journet, L., 2016. A phospholipase A $_1$ antibacterial Type VI secretion effector interacts directly with the C-terminal domain of the VgrG spike protein for delivery. Molecular Microbiology 99, 1099–1118. https://doi.org/10.1111/mmi.13292

Friedman, E.S., Bittinger, K., Esipova, T.V., Hou, L., Chau, L., Jiang, J., Mesaros, C., Lund, P.J., Liang, X., FitzGerald, G.A., Goulian, M., Lee, D., Garcia, B.A., Blair, I.A., Vinogradov, S.A., Wu, G.D., 2018. Microbes vs. chemistry in the origin of the anaerobic gut lumen. Proc. Natl. Acad. Sci. U.S.A. 115, 4170–4175. https://doi.org/10.1073/pnas.1718635115

Furrie, E., Macfarlane, S., Thomson, G., Macfarlane, G.T., Microbiology & Gut Biology Group, Tayside Tissue & Tumour Bank, 2005. Toll-like receptors-2, -3 and -4 expression patterns on human colon and their regulation by mucosal-associated bacteria. Immunology 115, 565–574. https://doi.org/10.1111/j.1365-2567.2005.02200.x

Gajendran, M., Loganathan, P., Catinella, A.P., Hashash, J.G., 2018. A comprehensive review and update on Crohn's disease. Disease-a-Month 64, 20–57. https://doi.org/10.1016/j.disamonth.2017.07.001

Galtier, M., De Sordi, L., Sivignon, A., De Vallée, A., Maura, D., Neut, C., Rahmouni, O., Wannerberger, K., Darfeuille-Michaud, A., Desreumaux, P., Barnich, N., Debarbieux, L., 2017. Bacteriophages targeting adherent invasive *Escherichia coli* strains as a promising new treatment for Crohn's disease. ECCOJC jjw224. https://doi.org/10.1093/ecco-jcc/jjw224

Geremia, A., Biancheri, P., Allan, P., Corazza, G.R., Di Sabatino, A., 2014. Innate and adaptive immunity in inflammatory bowel disease. Autoimmunity Reviews 13, 3–10. https://doi.org/10.1016/j.autrev.2013.06.004

Gibold, L., Garenaux, E., Dalmasso, G., Gallucci, C., Cia, D., Mottet-Auselo, B., Faïs, T., Darfeuille-Michaud, A., Nguyen, H.T.T., Barnich, N., Bonnet, R.,

Delmas, J., 2016. The Vat-AIEC protease promotes crossing of the intestinal mucus layer by Crohn's disease-associated *Escherichia coli*: Vat-AIEC Favours Mucus Layer's Crossing by LF82 E. coli. Cellular Microbiology 18, 617–631. https://doi.org/10.1111/cmi.12539

Gionchetti, P., Dignass, A., Danese, S., Magro Dias, F.J., Rogler, G., Lakatos, P.L., Adamina, M., Ardizzone, S., Buskens, C.J., Sebastian, S., Laureti, S., Sampietro, G.M., Vucelic, B., Van Der Woude, C.J., Barreiro-de Acosta, M., Maaser, C., Portela, F., Vavricka, S.R., Gomollón, F., on behalf of ECCO, 2017. 3rd European Evidence-based Consensus on the Diagnosis and Management of Crohn's Disease 2016: Part 2: Surgical Management and Special Situations. Journal of Crohn's and Colitis 11, 135–149. https://doi.org/10.1093/ecco-jcc/jjw169

Glasser, A.-L., Darfeuille-Michaud, A., 2008. Abnormalities in the handling of intracellular bacteria in Crohn's disease: a link between infectious etiology and host genetic susceptibility. Arch. Immunol. Ther. Exp. 56, 237–244. https://doi.org/10.1007/s00005-008-0026-1

Gray-Owen, S.D., Blumberg, R.S., 2006. CEACAM1: contact-dependent control of immunity. Nat Rev Immunol 6, 433–446. https://doi.org/10.1038/nri1864

Gribar, S.C., Richardson, W.M., Sodhi, C.P., Hackam, D.J., 2008. No Longer an Innocent Bystander: Epithelial Toll-Like Receptor Signaling in the Development of Mucosal Inflammation. Mol Med 14, 645–659. https://doi.org/10.2119/2008-00035.Gribar

Groschwitz, K.R., Hogan, S.P., 2009. Intestinal barrier function: Molecular regulation and disease pathogenesis. Journal of Allergy and Clinical Immunology 124, 3–20. https://doi.org/10.1016/j.jaci.2009.05.038

Guo, Z., Cai, X., Guo, X., Xu, Y., Gong, J., Li, Y., Zhu, W., 2018. Let-7b ameliorates Crohn's disease-associated adherent-invasive E coli induced intestinal inflammation via modulating Toll-Like Receptor 4 expression in intestinal epithelial cells. Biochemical Pharmacology 156, 196–203. https://doi.org/10.1016/j.bcp.2018.08.029

Gupta, P., Sarkar, S., Das, B., Bhattacharjee, S., Tribedi, P., 2016. Biofilm, pathogenesis and prevention—a journey to break the wall: a review. Arch Microbiol 198, 1–15. https://doi.org/10.1007/s00203-015-1148-6

Gutierrez, M.G., Enninga, J., 2022. Intracellular niche switching as host subversion strategy of bacterial pathogens. Current Opinion in Cell Biology 76, 102081. https://doi.org/10.1016/j.ceb.2022.102081

Halfvarson, J., Bodin, L., Tysk, C., Lindberg, E., Järnerot, G., 2003. Inflammatory bowel disease in a Swedish twin cohort: a long-term follow-up of concordance and clinical characteristics. Gastroenterology 124, 1767–1773. https://doi.org/10.1016/S0016-5085(03)00385-8

Haller, D., Russo, M.P., Sartor, R.B., Jobin, C., 2002. IKKβ and Phosphatidylinositol 3-Kinase/Akt Participate in Non-pathogenic Gram-negative Enteric Bacteria-induced RelA Phosphorylation and NF-κB Activation in Both Primary and Intestinal Epithelial Cell Lines. Journal of Biological Chemistry 277, 38168–38178. https://doi.org/10.1074/jbc.M205737200

Hall-Stoodley, L., Stoodley, P., 2005. Biofilm formation and dispersal and the transmission of human pathogens. Trends in Microbiology 13, 7–10. https://doi.org/10.1016/j.tim.2004.11.004

Han, X., Mslati, M.A., Davies, E., Chen, Y., Allaire, J.M., Vallance, B.A., 2021. Creating a More Perfect Union: Modeling Intestinal Bacteria-Epithelial Interactions Using Organoids. Cell Mol Gastroenterol Hepatol 12, 769–782. https://doi.org/10.1016/j.jcmgh.2021.04.010

Hase, K., Kawano, K., Nochi, T., Pontes, G.S., Fukuda, S., Ebisawa, M., Kadokura, K., Tobe, T., Fujimura, Y., Kawano, S., Yabashi, A., Waguri, S., Nakato, G., Kimura, S., Murakami, T., Iimura, M., Hamura, K., Fukuoka, S.-I., Lowe, A.W., Itoh, K., Kiyono, H., Ohno, H., 2009. Uptake through glycoprotein 2 of FimH+ bacteria by M cells initiates mucosal immune response. Nature 462, 226–230. https://doi.org/10.1038/nature08529

Hensel, K.O., Boland, V., Postberg, J., Zilbauer, M., Heuschkel, R., Vogel, S., Gödde, D., Wirth, S., Jenke, A.C., 2015. Differential Expression of Mucosal Trefoil Factors and Mucins in Pediatric Inflammatory Bowel Diseases. Sci Rep 4, 7343. https://doi.org/10.1038/srep07343

Hernandez, R.E., Gallegos-Monterrosa, R., Coulthurst, S.J., 2020. Type VI secretion system effector proteins: Effective weapons for bacterial competitiveness. Cellular Microbiology 22. https://doi.org/10.1111/cmi.13241

Hibiya, S., Tsuchiya, K., Hayashi, R., Fukushima, K., Horita, N., Watanabe, S., Shirasaki, T., Nishimura, R., Kimura, N., Nishimura, T., Gotoh, N., Oshima, S., Okamoto, R., Nakamura, T., Watanabe, M., 2016. Long-term Inflammation Transforms Intestinal Epithelial Cells of Colonic Organoids. ECCOJC jjw186. https://doi.org/10.1093/ecco-jcc/jjw186

Hollander, D., Vadheim, C.M., Brettholz, E., Petersen, G.M., Delahunty, T., Rotter, J.I., 1986. Increased Intestinal Permeability in Patients with Crohn's Disease and Their Relatives: A Possible Etiologic Factor. Ann Intern Med 105, 883–885. https://doi.org/10.7326/0003-4819-105-6-883

Homer, C.R., Richmond, A.L., Rebert, N.A., Achkar, J., McDonald, C., 2010. ATG16L1 and NOD2 Interact in an Autophagy-Dependent Antibacterial Pathway Implicated in Crohn's Disease Pathogenesis. Gastroenterology 139, 1630-1641.e2. https://doi.org/10.1053/j.gastro.2010.07.006

Hufnagel, D.A., Depas, W.H., Chapman, M.R., 2015. The Biology of the *Escherichia coli* Extracellular Matrix. Microbiol Spectr 3, 3.3.23. https://doi.org/10.1128/microbiolspec.MB-0014-2014

Hugenholtz, F., de Vos, W.M., 2018. Mouse models for human intestinal microbiota research: a critical evaluation. Cell Mol Life Sci 75, 149–160. https://doi.org/10.1007/s00018-017-2693-8

Hugot, J.-P., Chamaillard, M., Zouali, H., Lesage, S., Cézard, J.-P., Belaiche, J., Almer, S., Tysk, C., O'Morain, C.A., Gassull, M., Binder, V., Finkel, Y., Cortot, A., Modigliani, R., Laurent-Puig, P., Gower-Rousseau, C., Macry, J., Colombel, J.-F., Sahbatou, M., Thomas, G., 2001. Association of NOD2 leucine-rich repeat variants with susceptibility to Crohn's disease. Nature 411, 599–603. https://doi.org/10.1038/35079107

Hugot, J.-P., Laurent-Puig, P., Gower-Rousseau, C., Olson, J.M., Lee, J.C., Beaugerie, L., Naom, I., Dupas, J.-L., Van Gossum, A., Groupe d'Etude Thérapeutique Des Af, Orholm, M., Bonaiti-Pellie, C., Weissenbach, J., Mathew, C.G., Lennard-Jones, J.E., Cortot, A., Colombel, J.-F., Thomas, G., 1996. Mapping of a susceptibility locus for Crohn's disease on chromosome 16. Nature 379, 821–823. https://doi.org/10.1038/379821a0

Ilantzis, C., Demarte, L., Screaton, R.A., Stanners, C.P., 2002. Deregulated Expression of the Human Tumor Marker CEA and CEA Family Member CEACAM6 Disrupts Tissue Architecture and Blocks Colonocyte Differentiation. Neoplasia 4, 151–163. https://doi.org/10.1038/sj.neo.7900201

Ilantzis, C., Jothy, S., Alpert, L.C., Draber, P., Stanners, C.P., 1997. Cell-surface levels of human carcinoembryonic antigen are inversely correlated with colonocyte differentiation in colon carcinogenesis. Lab Invest 76, 703–716.

In, J., Foulke-Abel, J., Zachos, N.C., Hansen, A.-M., Kaper, J.B., Bernstein, H.D., Halushka, M., Blutt, S., Estes, M.K., Donowitz, M., Kovbasnjuk, O., 2016. Enterohemorrhagic Escherichia coli Reduces Mucus and Intermicrovillar Bridges in Human Stem Cell-Derived Colonoids. Cellular and Molecular Gastroenterology and Hepatology 2, 48-62.e3. https://doi.org/10.1016/j.jcmgh.2015.10.001

Jafari, N.V., Kuehne, S.A., Minton, N.P., Allan, E., Bajaj-Elliott, M., 2016. Clostridium difficile-mediated effects on human intestinal epithelia: Modelling host-pathogen interactions in a vertical diffusion chamber. Anaerobe 37, 96–102. https://doi.org/10.1016/j.anaerobe.2015.12.007

Jalili-Firoozinezhad, S., Gazzaniga, F.S., Calamari, E.L., Camacho, D.M., Fadel, C.W., Bein, A., Swenor, B., Nestor, B., Cronce, M.J., Tovaglieri, A., Levy, O., Gregory, K.E., Breault, D.T., Cabral, J.M.S., Kasper, D.L., Novak, R., Ingber, D.E., 2019. A complex human gut microbiome cultured in an anaerobic intestine-on-a-chip. Nat Biomed Eng 3, 520–531. https://doi.org/10.1038/s41551-019-0397-0

Jarry, A., Crémet, L., Caroff, N., Bou-Hanna, C., Mussini, J.M., Reynaud, A., Servin, A.L., Mosnier, J.F., Liévin-Le Moal, V., Laboisse, C.L., 2015. Subversion of human intestinal mucosa innate immunity by a Crohn's disease-associated E. coli. Mucosal Immunol 8, 572–581. https://doi.org/10.1038/mi.2014.89

Jeshvaghani, Z.S., Argmann, C., Mokry, M., Van Es, J.H., De Vries, M.H., Collen, L.V., Kotlarz, D., Sveen, M., Comella, P., Snapper, S.B., Klein, C., Schadt, E., Clevers, H., Kuijk, E., Nieuwenhuis, E., 2025. A collection of patient-derived intestinal organoid lines reveals epithelial pheno-types associated with genetic drivers of pediatric inflammatory bowel disease. https://doi.org/10.1101/2025.06.11.659052

Jiang, F., Waterfield, N.R., Yang, J., Yang, G., Jin, Q., 2014. A Pseudomonas aeruginosa Type VI Secretion Phospholipase D Effector Targets Both Prokaryotic and Eukaryotic Cells. Cell Host & Microbe 15, 600–610. https://doi.org/10.1016/j.chom.2014.04.010

Journet, L., Cascales, E., 2016. The Type VI Secretion System in *Escherichia coli* and Related Species. EcoSal Plus 7, 10.1128/ecosalplus.ESP-0009–2015. https://doi.org/10.1128/ecosalplus.esp-0009-2015

Kakasis, A., Panitsa, G., 2019. Bacteriophage therapy as an alternative treatment for human infections. A comprehensive review. International Journal of Antimicrobial Agents 53, 16–21. https://doi.org/10.1016/j.ijantimicag.2018.09.004

Kang, G.G., Trevaskis, N.L., Murphy, A.J., Febbraio, M.A., 2023. Diet-induced gut dysbiosis and inflammation: Key drivers of obesity-driven NASH. iScience 26, 105905. https://doi.org/10.1016/j.isci.2022.105905

Kang, Y., Park, H., Choe, B.-H., Kang, B., 2022. The Role and Function of Mucins and Its Relationship to Inflammatory Bowel Disease. Front. Med. 9, 848344. https://doi.org/10.3389/fmed.2022.848344

Kaper, J.B., Nataro, J.P., Mobley, H.L.T., 2004. Pathogenic Escherichia coli. Nat Rev Microbiol 2, 123–140. https://doi.org/10.1038/nrmicro818

Kaplan, G.G., Ng, S.C., 2016. Globalisation of inflammatory bowel disease: perspectives from the evolution of inflammatory bowel disease in the UK and China. The Lancet Gastroenterology & Hepatology 1, 307–316. https://doi.org/10.1016/S2468-1253(16)30077-2

Karve, S.S., Pradhan, S., Ward, D.V., Weiss, A.A., 2017. Intestinal organoids model human responses to infection by commensal and Shiga toxin producing Escherichia coli. PLoS ONE 12, e0178966. https://doi.org/10.1371/journal.pone.0178966

Keita, Å.V., Alkaissi, L.Y., Holm, E.B., Heil, S.D.S., Chassaing, B., Darfeuille-Michaud, A., McKay, D.M., Söderholm, J.D., 2020. Enhanced E. coli LF82 Translocation through the Follicle-associated Epithelium in Crohn's Disease is Dependent on Long Polar Fimbriae and CEACAM6 expression, and Increases Paracellular Permeability. Journal of Crohn's and Colitis 14, 216–229. https://doi.org/10.1093/ecco-jcc/jjz144

Kellermayer, R., 2012. Epigenetics and the Developmental Origins of Inflammatory Bowel Diseases. Canadian Journal of Gastroenterology 26, 909–915. https://doi.org/10.1155/2012/526408

Kelly, D., Campbell, J.I., King, T.P., Grant, G., Jansson, E.A., Coutts, A.G.P., Pettersson, S., Conway, S., 2004. Commensal anaerobic gut bacteria attenuate inflammation by regulating nuclear-cytoplasmic shuttling of PPAR-γ and RelA. Nat Immunol 5, 104–112. https://doi.org/10.1038/ni1018

Kim, B.Y., Kang, J., Kim, K.S., 2005. Invasion processes of pathogenic Escherichia coli. Int J Med Microbiol 295, 463–470. https://doi.org/10.1016/j.ijmm.2005.07.004

Kim, H.J., Huh, D., Hamilton, G., Ingber, D.E., 2012. Human gut-on-a-chip inhabited by microbial flora that experiences intestinal peristalsis-like motions and flow. Lab Chip 12, 2165. https://doi.org/10.1039/c2lc40074j

Kobayashi, K.S., Chamaillard, M., Ogura, Y., Henegariu, O., Inohara, N., Nuñez, G., Flavell, R.A., 2005. Nod2-Dependent Regulation of Innate and Adaptive Immunity in the Intestinal Tract. Science 307, 731–734. https://doi.org/10.1126/science.1104911

Kobayashi, N., Takahashi, D., Takano, S., Kimura, S., Hase, K., 2019. The Roles of Peyer's Patches and Microfold Cells in the Gut Immune System: Relevance to Autoimmune Diseases. Front. Immunol. 10, 2345. https://doi.org/10.3389/fimmu.2019.02345

Korch, C.T., Capes-Davis, A., 2021. The Extensive and Expensive Impacts of HEp-2 [HeLa], Intestine 407 [HeLa], and Other False Cell Lines in Journal Publications. SLAS Discovery 26, 1268–1279. https://doi.org/10.1177/24725552211051963

Kostakioti, M., Hadjifrangiskou, M., Hultgren, S.J., 2013. Bacterial biofilms: development, dispersal, and therapeutic strategies in the dawn of the postantibiotic era. Cold Spring Harb Perspect Med 3, a010306. https://doi.org/10.1101/cshperspect.a010306

Kotlowski, R., Bernstein, C.N., Sepehri, S., Krause, D.O., 2007. High prevalence of Escherichia coli belonging to the B2+D phylogenetic group in inflammatory bowel disease. Gut 56, 669–675. https://doi.org/10.1136/gut.2006.099796

Kraiczy, J., Nayak, K.M., Howell, K.J., Ross, A., Forbester, J., Salvestrini, C., Mustata, R., Perkins, S., Andersson-Rolf, A., Leenen, E., Liebert, A., Vallier, L., Rosenstiel, P.C., Stegle, O., Dougan, G., Heuschkel, R., Koo, B.-K., Zilbauer, M., 2019. DNA methylation defines regional identity of human intestinal epithelial organoids and undergoes dynamic changes during development. Gut 68, 49–61. https://doi.org/10.1136/gutjnl-2017-314817

Kucharzik, T., 2005. Acute induction of human IL-8 production by intestinal epithelium triggers neutrophil infiltration without mucosal injury. Gut 54, 1565–1572. https://doi.org/10.1136/gut.2004.061168

Kuespert, K., Pils, S., Hauck, C.R., 2006. CEACAMs: their role in physiology and pathophysiology. Current Opinion in Cell Biology 18, 565–571. https://doi.org/10.1016/j.ceb.2006.08.008

Kumar, P., Kuhlmann, F.M., Chakraborty, S., Bourgeois, A.L., Foulke-Abel, J., Tumala, B., Vickers, T.J., Sack, D.A., DeNearing, B., Harro, C.D., Wright, W.S., Gildersleeve, J.C., Ciorba, M.A., Santhanam, S., Porter, C.K., Gutierrez, R.L., Prouty, M.G., Riddle, M.S., Polino, A., Sheikh, A., Donowitz, M., Fleckenstein, J.M., 2018. Enterotoxigenic Escherichia coli–blood group A interactions intensify diarrheal severity. Journal of Clinical Investigation 128, 3298–3311. https://doi.org/10.1172/JCI97659

Kurlinkus, B., Ger, M., Kaupinis, A., Jasiunas, E., Valius, M., Sileikis, A., 2021. CEACAM6's Role as a Chemoresistance and Prognostic Biomarker for Pancreatic Cancer: A Comparison of CEACAM6's Diagnostic and Prognostic Capabilities with Those of CA19-9 and CEA. Life 11, 542. https://doi.org/10.3390/life11060542

Langerholc, T., Maragkoudakis, P.A., Wollgast, J., Gradisnik, L., Cencic, A., 2011. Novel and established intestinal cell line models – An indispensable tool in food science and nutrition. Trends in Food Science & Technology 22, S11–S20. https://doi.org/10.1016/j.tifs.2011.03.010

Lapaquette, P., Bringer, M.-A., Darfeuille-Michaud, A., 2012. Defects in autophagy favour adherent-invasive Escherichia coli persistence within macrophages leading to increased pro-inflammatory response: Autophagy controls AIEC replication within macrophages. Cellular Microbiology 14, 791–807. https://doi.org/10.1111/j.1462-5822.2012.01768.x

Lapaquette, P., Glasser, A.-L., Huett, A., Xavier, R.J., Darfeuille-Michaud, A., 2010. Crohn's disease-associated adherent-invasive *E. coli* are selectively favoured by impaired autophagy to replicate intracellularly. Cellular Microbiology 12, 99–113. https://doi.org/10.1111/j.1462-5822.2009.01381.x

Larabi, A., Dalmasso, G., Delmas, J., Barnich, N., Nguyen, H.T.T., 2020. Exosomes transfer miRNAs from cell-to-cell to inhibit autophagy during infection with Crohn's disease-associated adherent-invasive *E. coli*. Gut Microbes 11, 1677–1694. https://doi.org/10.1080/19490976.2020.1771985

Lazzaro, M., Feldman, M.F., García Véscovi, E., 2017. A Transcriptional Regulatory Mechanism Finely Tunes the Firing of Type VI Secretion System in Response to Bacterial Enemies. mBio 8, e00559-17. https://doi.org/10.1128/mBio.00559-17

Lee, C., An, M., Joung, J.-G., Park, W.-Y., Chang, D.K., Kim, Y.-H., Hong, S.N., 2022. TNFα Induces LGR5+ Stem Cell Dysfunction In Patients With Crohn's Disease. Cellular and Molecular Gastroenterology and Hepatology 13, 789–808. https://doi.org/10.1016/j.jcmgh.2021.10.010

Lee, H.-J., Woo, Y., Hahn, T.-W., Jung, Y.M., Jung, Y.-J., 2020. Formation and Maturation of the Phagosome: A Key Mechanism in Innate Immunity against

Intracellular Bacterial Infection. Microorganisms 8, 1298. https://doi.org/10.3390/microorganisms8091298

Lee, S.H., 2015. Intestinal Permeability Regulation by Tight Junction: Implication on Inflammatory Bowel Diseases. Intest Res 13, 11. https://doi.org/10.5217/ir.2015.13.1.11

Leslie, J.L., Huang, S., Opp, J.S., Nagy, M.S., Kobayashi, M., Young, V.B., Spence, J.R., 2015. Persistence and Toxin Production by Clostridium difficile within Human Intestinal Organoids Result in Disruption of Epithelial Paracellular Barrier Function. Infect Immun 83, 138–145. https://doi.org/10.1128/IAI.02561-14

Leusch, H.G., Drzeniek, Z., Hefta, S.A., Markos-Pusztai, Z., Wagener, C., 1991a. The putative role of members of the CEA-gene family (CEA, NCA an BGP) as ligands for the bacterial colonization of different human epithelial tissues. Zentralbl Bakteriol 275, 118–122. https://doi.org/10.1016/s0934-8840(11)80775-9

Leusch, H.G., Drzeniek, Z., Markos-Pusztai, Z., Wagener, C., 1991b. Binding of Escherichia coli and Salmonella strains to members of the carcinoembryonic antigen family: differential binding inhibition by aromatic alpha-glycosides of mannose. Infect Immun 59, 2051–2057. https://doi.org/10.1128/iai.59.6.2051-2057.1991

Leusch, H.G., Hefta, S.A., Drzeniek, Z., Hummel, K., Markos-Pusztai, Z., Wagener, C., 1990. Escherichia coli of human origin binds to carcinoembryonic antigen (CEA) and non-specific crossreacting antigen (NCA). FEBS Lett 261, 405–409. https://doi.org/10.1016/0014-5793(90)80603-g

Levine, J.S., Burakoff, R., 2011. Extraintestinal manifestations of inflammatory bowel disease. Gastroenterol Hepatol (N Y) 7, 235–241.

Lewis, S.B., Prior, A., Ellis, S.J., Cook, V., Chan, S.S.M., Gelson, W., Schüller, S., 2016. Flagellin Induces β-Defensin 2 in Human Colonic Ex vivo Infection with Enterohemorrhagic Escherichia coli. Front Cell Infect Microbiol 6, 68. https://doi.org/10.3389/fcimb.2016.00068

Liang, G., Zhang, Y., 2013. Genetic and Epigenetic Variations in iPSCs: Potential Causes and Implications for Application. Cell Stem Cell 13, 149–159. https://doi.org/10.1016/j.stem.2013.07.001

Lien, Y.-W., Lai, E.-M., 2017. Type VI Secretion Effectors: Methodologies and Biology. Front. Cell. Infect. Microbiol. 7, 254. https://doi.org/10.3389/fcimb.2017.00254

Liévin-Le Moal, V., Servin, A.L., 2013. Pathogenesis of Human Enterovirulent Bacteria: Lessons from Cultured, Fully Differentiated Human Colon Cancer Cell Lines. Microbiol Mol Biol Rev 77, 380–439. https://doi.org/10.1128/MMBR.00064-12

Limoli, D.H., Jones, C.J., Wozniak, D.J., 2015. Bacterial Extracellular Polysaccharides in Biofilm Formation and Function. Microbiol Spectr 3, 3.3.29. https://doi.org/10.1128/microbiolspec.MB-0011-2014

Liu, B., Gulati, A.S., Cantillana, V., Henry, S.C., Schmidt, E.A., Daniell, X., Grossniklaus, E., Schoenborn, A.A., Sartor, R.B., Taylor, G.A., 2013. Irgm1-deficient mice exhibit Paneth cell abnormalities and increased susceptibility to acute intestinal inflammation. American Journal of Physiology-Gastrointestinal and Liver Physiology 305, G573–G584. https://doi.org/10.1152/ajpgi.00071.2013

Loh, G., Blaut, M., 2012. Role of commensal gut bacteria in inflammatory bowel diseases. Gut Microbes 3, 544–555. https://doi.org/10.4161/gmic.22156

Lonardi, E., Moonens, K., Buts, L., De Boer, A., Olsson, J., Weiss, M., Fabre, E., Guérardel, Y., Deelder, A., Oscarson, S., Wuhrer, M., Bouckaert, J., 2013. Structural Sampling of Glycan Interaction Profiles Reveals Mucosal Receptors for Fimbrial Adhesins of Enterotoxigenic Escherichia coli. Biology 2, 894–917. https://doi.org/10.3390/biology2030894

Low, D., Tran, H.T., Lee, I., Dreux, N., Kamba, A., Reinecker, H., Darfeuille–Michaud, A., Barnich, N., Mizoguchi, E., 2013. Chitin-Binding Domains of Escherichia Coli ChiA Mediate Interactions With Intestinal Epithelial Cells in Mice With Colitis. Gastroenterology 145, 602-612.e9. https://doi.org/10.1053/j.gastro.2013.05.017

Lu, Q., Yang, M., Liang, Y., Xu, J., Xu, H., Nie, Y., Wang, L., Yao, J., Li, D., 2022. Immunology of Inflammatory Bowel Disease: Molecular Mechanisms and Therapeutics. JIR Volume 15, 1825–1844. https://doi.org/10.2147/JIR.S353038

Ma, A.T., Mekalanos, J.J., 2010. In vivo actin cross-linking induced by Vibrio cholerae type VI secretion system is associated with intestinal inflammation. Proc Natl Acad Sci U S A 107, 4365–4370. https://doi.org/10.1073/pnas.0915156107

Ma, J., Pan, Z., Huang, J., Sun, M., Lu, C., Yao, H., 2017. The Hcp proteins fused with diverse extended-toxin domains represent a novel pattern of antibacterial effectors in type VI secretion systems. Virulence 8, 1189–1202. https://doi.org/10.1080/21505594.2017.1279374

Ma, L., Yu, J., Zhang, H., Zhao, B., Zhang, J., Yang, D., Luo, F., Wang, B., Jin, B., Liu, J., 2022. Effects of Immune Cells on Intestinal Stem Cells: Prospects for Therapeutic Targets. Stem Cell Rev and Rep 18, 2296–2314. https://doi.org/10.1007/s12015-022-10347-7

MacEachran, D.P., Ye, S., Bomberger, J.M., Hogan, D.A., Swiatecka-Urban, A., Stanton, B.A., O'Toole, G.A., 2007. The *Pseudomonas aeruginosa* Secreted Protein PA2934 Decreases Apical Membrane Expression of the Cystic Fibrosis Transmembrane Conductance Regulator. Infect Immun 75, 3902–3912. https://doi.org/10.1128/IAI.00338-07

Madara, J.L., Stafford, J., Dharmsathaphorn, K., Carlson, S., 1987. Structural Analysis of a Human Intestinal Epithelial Cell Line. Gastroenterology 92, 1133–1145. https://doi.org/10.1016/S0016-5085(87)91069-9

Magalhaes, J.G., Fritz, J.H., Le Bourhis, L., Sellge, G., Travassos, L.H., Selvanantham, T., Girardin, S.E., Gommerman, J.L., Philpott, D.J., 2008. Nod2-Dependent Th2 Polarization of Antigen-Specific Immunity. The Journal of Immunology 181, 7925–7935. https://doi.org/10.4049/jimmunol.181.11.7925

Magalhaes, J.G., Rubino, S.J., Travassos, L.H., Le Bourhis, L., Duan, W., Sellge, G., Geddes, K., Reardon, C., Lechmann, M., Carneiro, L.A., Selvanantham, T., Fritz, J.H., Taylor, B.C., Artis, D., Mak, T.W., Comeau, M.R., Croft, M., Girardin, S.E., Philpott, D.J., 2011. Nucleotide oligomerization domain-containing proteins instruct T cell helper type 2 immunity through stromal activation. Proc. Natl. Acad. Sci. U.S.A. 108, 14896–14901. https://doi.org/10.1073/pnas.1015063108

Mancini, N.L., Rajeev, S., Jayme, T.S., Wang, A., Keita, Å.V., Workentine, M.L., Hamed, S., Söderholm, J.D., Lopes, F., Shutt, T.E., Shearer, J., McKay, D.M., 2021. Crohn's Disease Pathobiont Adherent-Invasive E coli Disrupts Epithelial Mitochondrial Networks With Implications for Gut Permeability. Cellular and Molecular Gastroenterology and Hepatology 11, 551–571. https://doi.org/10.1016/j.jcmgh.2020.09.013

Marteyn, B., Scorza, F.B., Sansonetti, P.J., Tang, C., 2011. Breathing life into pathogens: the influence of oxygen on bacterial virulence and host responses in the gastrointestinal tract: Oxygen and intestinal pathogens. Cellular Microbiology 13, 171–176. https://doi.org/10.1111/j.1462-5822.2010.01549.x

Marteyn, B., West, N.P., Browning, D.F., Cole, J.A., Shaw, J.G., Palm, F., Mounier, J., Prévost, M.-C., Sansonetti, P., Tang, C.M., 2010. Modulation of Shigella virulence in response to available oxygen in vivo. Nature 465, 355–358. https://doi.org/10.1038/nature08970

Martin, H.M., Campbell, B.J., Hart, C.A., Mpofu, C., Nayar, M., Singh, R., Englyst, H., Williams, H.F., Rhodes, J.M., 2004. Enhanced Escherichia coli adherence and invasion in Crohn's disease and colon cancer. Gastroenterology 127, 80–93. https://doi.org/10.1053/j.gastro.2004.03.054

Martinez-Argudo, I., Sands, C., Jepson, M.A., 2007. Translocation of enteropathogenic Escherichia coli across an in vitro M cell model is regulated by its type III secretion system. Cell Microbiol 9, 1538–1546. https://doi.org/10.1111/j.1462-5822.2007.00891.x

Martinez-Medina, M., Denizot, J., Dreux, N., Robin, F., Billard, E., Bonnet, R., Darfeuille-Michaud, A., Barnich, N., 2014. Western diet induces dysbiosis with increased *E coli* in CEABAC10 mice , alters host barrier function favouring AIEC colonisation. Gut 63, 116–124. https://doi.org/10.1136/gutjnl-2012-304119

Martinez-Medina, M., Mora, A., Blanco, M., López, C., Alonso, M.P., Bonacorsi, S., Nicolas-Chanoine, M.-H., Darfeuille-Michaud, A., Garcia-Gil, J., Blanco, J., 2009a. Similarity and Divergence among Adherent-Invasive *Escherichia coli* and Extraintestinal Pathogenic *E. coli* Strains. J Clin Microbiol 47, 3968–3979. https://doi.org/10.1128/JCM.01484-09

Martinez-Medina, M., Naves, P., Blanco, J., Aldeguer, X., Blanco, J.E., Blanco, M., Ponte, C., Soriano, F., Darfeuille-Michaud, A., Garcia-Gil, L.J., 2009b. Biofilm formation as a novel phenotypic feature of adherent-invasive Escherichia coli(AIEC). BMC Microbiol 9, 202. https://doi.org/10.1186/1471-2180-9-202

Martinez-Medina, M., Strozzi, F., Castillo, B.R.D., Serrano-Morillas, N., Bustins, N.F., Martínez-Martínez, L., 2020. Antimicrobial Resistance Profiles of Adherent Invasive Escherichia coli Show Increased Resistance to β-Lactams. Antibiotics (Basel) 9, 251. https://doi.org/10.3390/antibiotics9050251

Massier, S., Miquel, S., Dreux, N., Agus, A., Ait-Bara, S., Denizot, J., Billard, E., Barnich, N., 2015. Mo1777 Involvement of Type VI Secretion Systems in Virulence of Adherent-Invasive Escherichia coli Isolated From Patients With Crohn's Disease. Gastroenterology 148, S-709. https://doi.org/10.1016/S0016-5085(15)32407-0

Mayhew, T.M., Myklebust, R., Whybrow, A., Jenkins, R., 1999. Epithelial integrity, cell death and cell loss in mammalian small intestine. Histol Histopathol 14, 257–267. https://doi.org/10.14670/HH-14.257

Mayorgas, A., Dotti, I., Martínez-Picola, M., Esteller, M., Bonet-Rossinyol, Q., Ricart, E., Salas, A., Martínez-Medina, M., 2021. A Novel Strategy to Study the Invasive Capability of Adherent-Invasive Escherichia coli by Using Human Primary Organoid-Derived Epithelial Monolayers. Front. Immunol. 12, 646906. https://doi.org/10.3389/fimmu.2021.646906

Mazzarella, G., Perna, A., Marano, A., Lucariello, A., Rotondi Aufiero, V., Sorrentino, A., Melina, R., Guerra, G., Taccone, F.S., Iaquinto, G., De Luca, A., 2017. Pathogenic Role of Associated Adherent-Invasive *Escherichia coli* in Crohn's Disease: ROLE OF ADHERENT-INVASIVE *E.COLI* IN CROHN DISEASE. J. Cell. Physiol. 232, 2860–2868. https://doi.org/10.1002/jcp.25717

McCormick, B.A., Hofman, P.M., Kim, J., Carnes, D.K., Miller, S.I., Madara, J.L., 1995. Surface attachment of Salmonella typhimurium to intestinal epithelia imprints the subepithelial matrix with gradients chemotactic for neutrophils. The Journal of cell biology 131, 1599–1608. https://doi.org/10.1083/jcb.131.6.1599

McGovern, D.P.B., Kugathasan, S., Cho, J.H., 2015. Genetics of Inflammatory Bowel Diseases. Gastroenterology 149, 1163-1176.e2. https://doi.org/10.1053/j.gastro.2015.08.001

McGrath, C.J., Laveckis, E., Bell, A., Crost, E., Juge, N., Schüller, S., 2022. Development of a novel human intestinal model to elucidate the effect of

anaerobic commensals on *Escherichia coli* infection. Disease Models & Mechanisms 15, dmm049365. https://doi.org/10.1242/dmm.049365

McGrath, C.J., Schüller, S., 2021. Determining Shiga Toxin-Producing Escherichia coli Interactions with Human Intestinal Epithelium in a Microaerobic Vertical Diffusion Chamber, in: Schüller, S., Bielaszewska, M. (Eds.), Shiga Toxin-Producing E. Coli, Methods in Molecular Biology. Springer US, New York, NY, pp. 273–283. https://doi.org/10.1007/978-1-0716-1339-9_12

McKay, D.M., Mancini, N.L., Shearer, J., Shutt, T., 2020. Perturbed mitochondrial dynamics, an emerging aspect of epithelial-microbe interactions. American Journal of Physiology-Gastrointestinal and Liver Physiology 318, G748–G762. https://doi.org/10.1152/ajpgi.00031.2020

McNees, A.L., Markesich, D., Zayyani, N.R., Graham, D.Y., 2015. Mycobacterium paratuberculosis as a cause of Crohn's disease. Expert Review of Gastroenterology & Hepatology 9, 1523–1534. https://doi.org/10.1586/17474124.2015.1093931

McPhee, J.B., Small, C.L., Reid-Yu, S.A., Brannon, J.R., Le Moual, H., Coombes, B.K., 2014. Host Defense Peptide Resistance Contributes to Colonization and Maximal Intestinal Pathology by Crohn's Disease-Associated Adherent-Invasive Escherichia coli. Infect Immun 82, 3383–3393. https://doi.org/10.1128/IAI.01888-14

Mehto, S., Jena, K.K., Nath, P., Chauhan, Swati, Kolapalli, S.P., Das, S.K., Sahoo, P.K., Jain, A., Taylor, G.A., Chauhan, Santosh, 2019. The Crohn's Disease Risk Factor IRGM Limits NLRP3 Inflammasome Activation by Impeding Its Assembly and by Mediating Its Selective Autophagy. Molecular Cell 73, 429-445.e7. https://doi.org/10.1016/j.molcel.2018.11.018

Michaudel, C., Sokol, H., 2020. The Gut Microbiota at the Service of Immunometabolism. Cell Metabolism 32, 514–523. https://doi.org/10.1016/j.cmet.2020.09.004

Michielan, A., D'Incà, R., 2015. Intestinal Permeability in Inflammatory Bowel Disease: Pathogenesis, Clinical Evaluation, and Therapy of Leaky Gut. Mediators of Inflammation 2015, 1–10. https://doi.org/10.1155/2015/628157

Middendorp, S., Schneeberger, K., Wiegerinck, C.L., Mokry, M., Akkerman, R.D.L., Wijngaarden, S., Clevers, H., Nieuwenhuis, E.E.S., 2014. Adult Stem Cells in the Small Intestine Are Intrinsically Programmed with Their Location-Specific Function. Stem Cells 32, 1083–1091. https://doi.org/10.1002/stem.1655

Migliore, F., Macchi, R., Landini, P., Paroni, M., 2018. Phagocytosis and Epithelial Cell Invasion by Crohn's Disease-Associated Adherent-Invasive Escherichia coli Are Inhibited by the Anti-inflammatory Drug 6-Mercaptopurine. Front. Microbiol. 9, 964. https://doi.org/10.3389/fmicb.2018.00964

Mills, D.C., Gundogdu, O., Elmi, A., Bajaj-Elliott, M., Taylor, P.W., Wren, B.W., Dorrell, N., 2012. Increase in Campylobacter jejuni Invasion of Intestinal Epithelial Cells under Low-Oxygen Coculture Conditions That Reflect the *In Vivo* Environment. Infect Immun 80, 1690–1698. https://doi.org/10.1128/IAI.06176-11

Mimouna, S., Gonçalvès, D., Barnich, N., Darfeuille-Michaud, A., Hofman, P., Vouret-Craviari, V., 2011. Crohn disease-associated Escherichia coli promote gastrointestinal inflammatory disorders by activation of HIF-dependent responses. Gut Microbes 2, 335–346. https://doi.org/10.4161/gmic.18771

Miquel, S., Peyretaillade, E., Claret, L., De Vallée, A., Dossat, C., Vacherie, B., Zineb, E.H., Segurens, B., Barbe, V., Sauvanet, P., Neut, C., Colombel, J.-F., Medigue, C., Mojica, F.J.M., Peyret, P., Bonnet, R., Darfeuille-Michaud, A., 2010. Complete Genome Sequence of Crohn's Disease-Associated Adherent-Invasive E. coli Strain LF82. PLoS ONE 5, e12714. https://doi.org/10.1371/journal.pone.0012714

Mizoguchi, E., 2006. Chitinase 3–Like-1 Exacerbates Intestinal Inflammation by Enhancing Bacterial Adhesion and Invasion in Colonic Epithelial Cells. Gastroenterology 130, 398–411. https://doi.org/10.1053/j.gastro.2005.12.007

Moayyedi, P., Surette, M.G., Kim, P.T., Libertucci, J., Wolfe, M., Onischi, C., Armstrong, D., Marshall, J.K., Kassam, Z., Reinisch, W., Lee, C.H., 2015. Fecal Microbiota Transplantation Induces Remission in Patients With Active Ulcerative Colitis in a Randomized Controlled Trial. Gastroenterology 149, 102-109.e6. https://doi.org/10.1053/j.gastro.2015.04.001

Moehle, C., Ackermann, N., Langmann, T., Aslanidis, C., Kel, A., Kel-Margoulis, O., Schmitz-Madry, A., Zahn, A., Stremmel, W., Schmitz, G., 2006. Aberrant intestinal expression and allelic variants of mucin genes associated with inflammatory bowel disease. J Mol Med 84, 1055–1066. https://doi.org/10.1007/s00109-006-0100-2

Moon, C., VanDussen, K.L., Miyoshi, H., Stappenbeck, T.S., 2014. Development of a primary mouse intestinal epithelial cell monolayer culture system to evaluate factors that modulate IgA transcytosis. Mucosal Immunol 7, 818–828. https://doi.org/10.1038/mi.2013.98

Mossman, K.L., Mian, M.F., Lauzon, N.M., Gyles, C.L., Lichty, B., Mackenzie, R., Gill, N., Ashkar, A.A., 2008. Cutting Edge: FimH Adhesin of Type 1 Fimbriae Is a Novel TLR4 Ligand. The Journal of Immunology 181, 6702–6706. https://doi.org/10.4049/jimmunol.181.10.6702

Nakamura, S., Minamino, T., 2019. Flagella-Driven Motility of Bacteria. Biomolecules 9, 279. https://doi.org/10.3390/biom9070279

Nash, J.H., Villegas, A., Kropinski, A.M., Aguilar-Valenzuela, R., Konczy, P., Mascarenhas, M., Ziebell, K., Torres, A.G., Karmali, M.A., Coombes, B.K., 2010. Genome sequence of adherent-invasive Escherichia coli and

comparative genomic analysis with other E. coli pathotypes. BMC Genomics 11, 667. https://doi.org/10.1186/1471-2164-11-667

Navabi, N., McGuckin, M.A., Lindén, S.K., 2013. Gastrointestinal Cell Lines Form Polarized Epithelia with an Adherent Mucus Layer when Cultured in Semi-Wet Interfaces with Mechanical Stimulation. PLoS ONE 8, e68761. https://doi.org/10.1371/journal.pone.0068761

Navarro-Garcia, F., Ruiz-Perez, F., Cataldi, Á., Larzábal, M., 2019. Type VI Secretion System in Pathogenic Escherichia coli: Structure, Role in Virulence, and Acquisition. Front. Microbiol. 10, 1965. https://doi.org/10.3389/fmicb.2019.01965

Naz, N., Mills, D.C., Wren, B.W., Dorrell, N., 2013. Enteric Bacterial Invasion Of Intestinal Epithelial Cells In Vitro Is Dramatically Enhanced Using a Vertical Diffusion Chamber Model. JoVE 50741. https://doi.org/10.3791/50741

Neurath, M.F., 2014. Cytokines in inflammatory bowel disease. Nat Rev Immunol 14, 329–342. https://doi.org/10.1038/nri3661

Nguyen, H.T.T., Dalmasso, G., Müller, S., Carrière, J., Seibold, F., Darfeuille–Michaud, A., 2014. Crohn's Disease–Associated Adherent Invasive Escherichia coli Modulate Levels of microRNAs in Intestinal Epithelial Cells to Reduce Autophagy. Gastroenterology 146, 508–519. https://doi.org/10.1053/j.gastro.2013.10.021

Nicholson, T.F., Watts, K.M., Hunstad, D.A., 2009. OmpA of Uropathogenic *Escherichia coli* Promotes Postinvasion Pathogenesis of Cystitis. Infect Immun 77, 5245–5251. https://doi.org/10.1128/IAI.00670-09

Nitzan, O., 2016. Role of antibiotics for treatment of inflammatory bowel disease. WJG 22, 1078. https://doi.org/10.3748/wjg.v22.i3.1078

Niv, Y., 2016. Mucin Genes Expression in the Intestine of Crohn's Disease Patients: a Systematic Review and Meta-analysis. JGLD 25, 351–357. https://doi.org/10.15403/jgld.2014.1121.253.niv

Noben, M., Verstockt, B., De Bruyn, M., Hendriks, N., Van Assche, G., Vermeire, S., Verfaillie, C., Ferrante, M., 2017. Epithelial organoid cultures from patients with ulcerative colitis and Crohn's disease: a truly long-term model to study the molecular basis for inflammatory bowel disease? Gut 66, 2193–2195. https://doi.org/10.1136/gutjnl-2016-313667

Ogura, Y., 2003. Expression of NOD2 in Paneth cells: a possible link to Crohn's ileitis. Gut 52, 1591–1597. https://doi.org/10.1136/gut.52.11.1591

Ogura, Y., Bonen, D.K., Inohara, N., Nicolae, D.L., Chen, F.F., Ramos, R., Britton, H., Moran, T., Karaliuskas, R., Duerr, R.H., Achkar, J.-P., Brant, S.R., Bayless, T.M., Kirschner, B.S., Hanauer, S.B., Nuñez, G., Cho, J.H., 2001. A frameshift mutation in NOD2 associated with susceptibility to Crohn's disease. Nature 411, 603–606. https://doi.org/10.1038/35079114

Ormsby, M.J., Johnson, S.A., Carpena, N., Meikle, L.M., Goldstone, R.J., McIntosh, A., Wessel, H.M., Hulme, H.E., McConnachie, C.C., Connolly, J.P.R., Roe, A.J., Hasson, C., Boyd, J., Fitzgerald, E., Gerasimidis, K., Morrison, D., Hold, G.L., Hansen, R., Walker, D., Smith, D.G.E., Wall, D.M., 2020. Propionic Acid Promotes the Virulent Phenotype of Crohn's Disease-Associated Adherent-Invasive Escherichia coli. Cell Reports 30, 2297-2305.e5. https://doi.org/10.1016/j.celrep.2020.01.078

Özkan, A., Merry, G., Chou, D.B., Posey, R.R., Stejskalova, A., Calderon, K., Sperry, M., Horvath, V., Ferri, L.E., Carlotti, E., McDonald, S.A.C., Winton, D.J., Riccardi, R., Bordeianou, L., Hall, S., Goyal, G., Ingber, D.E., 2024. Inflammatory Bowel Disease Drivers Revealed in Human Organ Chips. https://doi.org/10.1101/2024.12.05.24318563

Pandey, R., Zhou, M., Islam, S., Chen, B., Barker, N.K., Langlais, P., Srivastava, A., Luo, M., Cooke, L.S., Weterings, E., Mahadevan, D., 2019. Carcinoembryonic antigen cell adhesion molecule 6 (CEACAM6) in Pancreatic Ductal Adenocarcinoma (PDA): An integrative analysis of a novel therapeutic target. Sci Rep 9, 18347. https://doi.org/10.1038/s41598-019-54545-9

Pang, Z., Raudonis, R., Glick, B.R., Lin, T.-J., Cheng, Z., 2019. Antibiotic resistance in Pseudomonas aeruginosa: mechanisms and alternative therapeutic strategies. Biotechnology Advances 37, 177–192. https://doi.org/10.1016/j.biotechadv.2018.11.013

Pavlidis, P., Tsakmaki, A., Treveil, A., Li, K., Cozzetto, D., Yang, F., Niazi, U., Hayee, B.H., Saqi, M., Friedman, J., Korcsmaros, T., Bewick, G., Powell, N., 2022. Cytokine responsive networks in human colonic epithelial organoids unveil a molecular classification of inflammatory bowel disease. Cell Reports 40, 111439. https://doi.org/10.1016/j.celrep.2022.111439

Pei, J., Wu, Q., Kahl-McDonagh, M., Ficht, T.A., 2008. Cytotoxicity in Macrophages Infected with Rough *Brucella* Mutants Is Type IV Secretion System Dependent. Infect Immun 76, 30–37. https://doi.org/10.1128/IAI.00379-07

Pielage, J.F., Cichon, C., Greune, L., Hirashima, M., Kucharzik, T., Schmidt, M.A., 2007. Reversible differentiation of Caco-2 cells reveals galectin-9 as a surface marker molecule for human follicle-associated epithelia and M cell-like cells. The International Journal of Biochemistry & Cell Biology 39, 1886–1901. https://doi.org/10.1016/j.biocel.2007.05.009

Pinto, Moise, Robine-Leon, Sylvie, Appay, Marie-Dominique, Kedinger, Michele, Triadou, Nicole, Dussaulx, Elisabeth, Lacroix, Brigitte, Simon-Assmann, Patricia, Haffen, Katy, Fogh, Jorgen, 1983. Enterocyte-like differentiation and polarization of the human colon carcinoma cell line Caco-2 in culture. Biology of the Cell 323–330.

Prorok-Hamon, M., Friswell, M.K., Alswied, A., Roberts, C.L., Song, F., Flanagan, P.K., Knight, P., Codling, C., Marchesi, J.R., Winstanley, C., Hall, N., Rhodes,

J.M., Campbell, B.J., 2014. Colonic mucosa-associated diffusely adherent *afaC+ Escherichia coli* expressing *lpfA* and *pks* are increased in inflammatory bowel disease and colon cancer. Gut 63, 761–770. https://doi.org/10.1136/gutjnl-2013-304739

Prudent, V., Demarre, G., Vazeille, E., Wery, M., Quenech'Du, N., Ravet, A., Dauverd - Girault, J., van Dijk, E., Bringer, M.-A., Descrimes, M., Barnich, N., Rimsky, S., Morillon, A., Espéli, O., 2021. The Crohn's disease-related bacterial strain LF82 assembles biofilm-like communities to protect itself from phagolysosomal attack. Commun Biol 4, 627. https://doi.org/10.1038/s42003-021-02161-7

Quévrain, E., Maubert, M.A., Michon, C., Chain, F., Marquant, R., Tailhades, J., Miquel, S., Carlier, L., Bermúdez-Humarán, L.G., Pigneur, B., Lequin, O., Kharrat, P., Thomas, G., Rainteau, D., Aubry, C., Breyner, N., Afonso, C., Lavielle, S., Grill, J.-P., Chassaing, G., Chatel, J.M., Trugnan, G., Xavier, R., Langella, P., Sokol, H., Seksik, P., 2016. Identification of an anti-inflammatory protein from *Faecalibacterium prausnitzii* , a commensal bacterium deficient in Crohn's disease. Gut 65, 415–425. https://doi.org/10.1136/gutjnl-2014-307649

Rahman, S., Ghiboub, M., Donkers, J.M., van de Steeg, E., van Tol, E.A.F., Hakvoort, T.B.M., de Jonge, W.J., 2021. The Progress of Intestinal Epithelial Models from Cell Lines to Gut-On-Chip. Int J Mol Sci 22, 13472. https://doi.org/10.3390/ijms222413472

Ramos-Morales, F., 2012. Impact of *Salmonella enterica* Type III Secretion System Effectors on the Eukaryotic Host Cell. ISRN Cell Biology 2012, 1–36. https://doi.org/10.5402/2012/787934

Ranganathan, S., Doucet, M., Grassel, C.L., Delaine-Elias, B., Zachos, N.C., Barry, E.M., 2019. Evaluating Shigella flexneri Pathogenesis in the Human Enteroid Model. Infect Immun 87, e00740-18. https://doi.org/10.1128/IAI.00740-18

Raso, T., Crivellaro, S., Chirillo, M.G., Pais, P., Gaia, E., Savoia, D., 2011. Analysis of Escherichia coli Isolated from Patients Affected by Crohn's Disease. Curr Microbiol 63, 131–137. https://doi.org/10.1007/s00284-011-9947-8

Ray, A., Schwartz, N., De Souza Santos, M., Zhang, J., Orth, K., Salomon, D., 2017. Type VI secretion system MIX-effectors carry both antibacterial and anti-eukaryotic activities. EMBO Reports 18, 1978–1990. https://doi.org/10.15252/embr.201744226

Reisner, A., Krogfelt, K.A., Klein, B.M., Zechner, E.L., Molin, S., 2006. In Vitro Biofilm Formation of Commensal and Pathogenic *Escherichia coli* Strains: Impact of Environmental and Genetic Factors. J Bacteriol 188, 3572–3581. https://doi.org/10.1128/JB.188.10.3572-3581.2006

Rhodes, J.M., 2007. The role of Escherichia coli in inflammatory bowel disease. Gut 56, 610–612. https://doi.org/10.1136/gut.2006.111872

Roda, G., Chien Ng, S., Kotze, P.G., Argollo, M., Panaccione, R., Spinelli, A., Kaser, A., Peyrin-Biroulet, L., Danese, S., 2020. Crohn's disease. Nat Rev Dis Primers 6, 22. https://doi.org/10.1038/s41572-020-0156-2

Rolhion, N., Barnich, N., Bringer, M.-A., Glasser, A.-L., Ranc, J., Hébuterne, X., Hofman, P., Darfeuille-Michaud, A., 2010. Abnormally expressed ER stress response chaperone Gp96 in CD favours adherent-invasive Escherichia coli invasion. Gut 59, 1355. https://doi.org/10.1136/gut.2010.207456

Rolhion, N., Barnich, N., Claret, L., Darfeuille-Michaud, A., 2005. Strong Decrease in Invasive Ability and Outer Membrane Vesicle Release in Crohn's Disease-Associated Adherent-Invasive *Escherichia coli* Strain LF82 with the *yfgL* Gene Deleted. J Bacteriol 187, 2286–2296. https://doi.org/10.1128/JB.187.7.2286-2296.2005

Rolhion, N., Carvalho, F.A., Darfeuille-Michaud, A., 2007. OmpC and the σ^{E} regulatory pathway are involved in adhesion and invasion of the Crohn's disease-associated *Escherichia coli* strain LF82. Molecular Microbiology 63, 1684–1700. https://doi.org/10.1111/j.1365-2958.2007.05638.x

Rossen, N.G., Fuentes, S., Van Der Spek, M.J., Tijssen, J.G., Hartman, J.H.A., Duflou, A., Löwenberg, M., Van Den Brink, G.R., Mathus-Vliegen, E.M.H., De Vos, W.M., Zoetendal, E.G., D'Haens, G.R., Ponsioen, C.Y., 2015. Findings From a Randomized Controlled Trial of Fecal Transplantation for Patients With Ulcerative Colitis. Gastroenterology 149, 110-118.e4. https://doi.org/10.1053/j.gastro.2015.03.045

Roy, R.K., Hoppe, M.M., Srivastava, S., Samanta, A., Sharma, N., Tan, K.T., Yang, H., Voon, D.C., Pang, B., Teh, M., Murata-Kamiya, N., Hatakeyama, M., Chang, Y.-T., Yong, W.P., Ito, Y., Ho, K.Y., Tan, P., Soong, R., Koeffler, P.H., Yeoh, K.G., Jeyasekharan, A.D., 2016. CEACAM6 is upregulated by *Helicobacter pylori* CagA and is a biomarker for early gastric cancer. Oncotarget 7, 55290–55301. https://doi.org/10.18632/oncotarget.10528

Sambuy, Y., De Angelis, I., Ranaldi, G., Scarino, M.L., Stammati, A., Zucco, F., 2005. The Caco-2 cell line as a model of the intestinal barrier: influence of cell and culture-related factors on Caco-2 cell functional characteristics. Cell Biol Toxicol 21, 1–26. https://doi.org/10.1007/s10565-005-0085-6

Sana, T.G., Baumann, C., Merdes, A., Soscia, C., Rattei, T., Hachani, A., Jones, C., Bennett, K.L., Filloux, A., Superti-Furga, G., Voulhoux, R., Bleves, S., 2015. Internalization of Pseudomonas aeruginosa Strain PAO1 into Epithelial Cells Is Promoted by Interaction of a T6SS Effector with the Microtubule Network. mBio 6, e00712-15. https://doi.org/10.1128/mBio.00712-15

Sana, T.G., Flaugnatti, N., Lugo, K.A., Lam, L.H., Jacobson, A., Baylot, V., Durand, E., Journet, L., Cascales, E., Monack, D.M., 2016. Salmonella Typhimurium utilizes a T6SS-mediated antibacterial weapon to establish in the host gut. Proc Natl Acad Sci U S A 113, E5044-5051. https://doi.org/10.1073/pnas.1608858113

Sasaki, M., Sitaraman, S.V., Babbin, B.A., Gerner-Smidt, P., Ribot, E.M., Garrett, N., Alpern, J.A., Akyildiz, A., Theiss, A.L., Nusrat, A., Klapproth, J.-M.A., 2007. Invasive Escherichia coli are a feature of Crohn's disease. Lab Invest 87, 1042–1054. https://doi.org/10.1038/labinvest.3700661

Sato, T., Vries, R.G., Snippert, H.J., van de Wetering, M., Barker, N., Stange, D.E., van Es, J.H., Abo, A., Kujala, P., Peters, P.J., Clevers, H., 2009. Single Lgr5 stem cells build crypt-villus structures in vitro without a mesenchymal niche. Nature 459, 262–265. https://doi.org/10.1038/nature07935

Sauter, S.L., Rutherfurd, S.M., Wagener, C., Shively, J.E., Hefta, S.A., 1993. Identification of the specific oligosaccharide sites recognized by type 1 fimbriae from Escherichia coli on nonspecific cross-reacting antigen, a CD66 cluster granulocyte glycoprotein. J Biol Chem 268, 15510–15516.

Sauter, S.L., Rutherfurd, S.M., Wagener, C., Shively, J.E., Hefta, S.A., 1991. Binding of nonspecific cross-reacting antigen, a granulocyte membrane glycoprotein, to Escherichia coli expressing type 1 fimbriae. Infect Immun 59, 2485–2493. https://doi.org/10.1128/iai.59.7.2485-2493.1991

Sayed, I.M., Suarez, K., Lim, E., Singh, S., Pereira, M., Ibeawuchi, S., Katkar, G., Dunkel, Y., Mittal, Y., Chattopadhyay, R., Guma, M., Boland, B.S., Dulai, P.S., Sandborn, W.J., Ghosh, P., Das, S., 2020. Host engulfment pathway controls inflammation in inflammatory bowel disease. The FEBS Journal 287, 3967–3988. https://doi.org/10.1111/febs.15236

Sazonovs, A., Stevens, C.R., Venkataraman, G.R., Yuan, K., Avila, B., Abreu, M.T., Ahmad, T., Allez, M., Ananthakrishnan, A.N., Atzmon, G., Baras, A., Barrett, J.C., Barzilai, N., Beaugerie, L., Beecham, A., Bernstein, C.N., Bitton, A., Bokemeyer, B., Chan, A., Chung, D., Cleynen, I., Cosnes, J., Cutler, D.J., Daly, A., Damas, O.M., Datta, L.W., Dawany, N., Devoto, M., Dodge, S., Ellinghaus, E., Fachal, L., Farkkila, M., Faubion, W., Ferreira, M., Franchimont, D., Gabriel, S.B., Ge, T., Georges, M., Gettler, K., Giri, M., Glaser, B., Goerg, S., Goyette, P., Graham, D., Hämäläinen, E., Haritunians, T., Heap, G.A., Hiltunen, M., Hoeppner, M., Horowitz, J.E., Irving, P., Iyer, V., Jalas, C., Kelsen, J., Khalili, H., Kirschner, B.S., Kontula, K., Koskela, J.T., Kugathasan, S., Kupcinskas, J., Lamb, C.A., Laudes, M., Lévesque, C., Levine, A.P., Lewis, J.D., Liefferinckx, C., Loescher, B.-S., Louis, E., Mansfield, J., May, S., McCauley, J.L., Mengesha, E., Mni, M., Moayyedi, P., Moran, C.J., Newberry, R.D., O'Charoen, S., Okou, D.T., Oldenburg, B., Ostrer, H., Palotie, A., Paquette, J., Pekow, J., Peter, I., Pierik, M.J., Ponsioen, C.Y., Pontikos, N., Prescott, N., Pulver, A.E., Rahmouni, S., Rice, D.L., Saavalainen, P., Sands, B., Sartor, R.B., Schiff, E.R., Schreiber, S., Schumm, L.P., Segal, A.W., Seksik, P., Shawky, R., Sheikh, S.Z., Silverberg, M.S., Simmons, A., Skeiceviciene, J., Sokol, H., Solomonson, M., Somineni, H., Sun, D., Targan, S., Turner, D., Uhlig, H.H., Van Der Meulen, A.E., Vermeire, S., Verstockt, S., Voskuil, M.D., Winter, H.S., Young, J., Belgium IBD Consortium, Cedars-Sinai IBD, International IBD Genetics Consortium, NIDDK IBD Genetics Consortium, NIHR IBD BioResource, Regeneron Genetics Center, SHARE Consortium, SPARC IBD Network, UK IBD

Genetics Consortium, Duerr, R.H., Franke, A., Brant, S.R., Cho, J., Weersma, R.K., Parkes, M., Xavier, R.J., Rivas, M.A., Rioux, J.D., McGovern, D.P.B., Huang, H., Anderson, C.A., Daly, M.J., 2022. Large-scale sequencing identifies multiple genes and rare variants associated with Crohn's disease susceptibility. Nat Genet 54, 1275–1283. https://doi.org/10.1038/s41588-022-01156-2

Scaglione, F., Musazzi, U.M., Minghetti, P., 2021. Considerations on D-mannose Mechanism of Action and Consequent Classification of Marketed Healthcare Products. Front. Pharmacol. 12, 636377. https://doi.org/10.3389/fphar.2021.636377

Schneeberger, K., Roth, S., Nieuwenhuis, E.E.S., Middendorp, S., 2018. Intestinal epithelial cell polarity defects in disease: lessons from microvillus inclusion disease. Dis Model Mech 11, dmm031088. https://doi.org/10.1242/dmm.031088

Schüller, S., Phillips, A.D., 2010. Microaerobic conditions enhance type III secretion and adherence of enterohaemorrhagic Escherichia coli to polarized human intestinal epithelial cells: EHEC colonization under microaerobiosis. Environmental Microbiology 12, 2426–2435. https://doi.org/10.1111/j.1462-2920.2010.02216.x

Schwarz, S., Singh, P., Robertson, J.D., LeRoux, M., Skerrett, S.J., Goodlett, D.R., West, T.E., Mougous, J.D., 2014. VgrG-5 Is a Burkholderia Type VI Secretion System-Exported Protein Required for Multinucleated Giant Cell Formation and Virulence. Infect Immun 82, 1445–1452. https://doi.org/10.1128/IAI.01368-13

Scott, V.C.S., Haake, D.A., Churchill, B.M., Justice, S.S., Kim, J.-H., 2015. Intracellular Bacterial Communities: A Potential Etiology for Chronic Lower Urinary Tract Symptoms. Urology 86, 425–431. https://doi.org/10.1016/j.urology.2015.04.002

Scribano, D., Sarshar, M., Prezioso, C., Lucarelli, M., Angeloni, A., Zagaglia, C., Palamara, A.T., Ambrosi, C., 2020. d-Mannose Treatment neither Affects Uropathogenic Escherichia coli Properties nor Induces Stable FimH Modifications. Molecules 25, 316. https://doi.org/10.3390/molecules25020316

Segal, A.W., 2018. The role of neutrophils in the pathogenesis of Crohn's disease. Eur J Clin Investigation 48, e12983. https://doi.org/10.1111/eci.12983

Sepehri, S., Khafipour, E., Bernstein, C.N., Coombes, B.K., Pilar, A.V., Karmali, M., Ziebell, K., Krause, D.O., 2011. Characterization of Escherichia coli isolated from gut biopsies of newly diagnosed patients with inflammatory bowel disease: Inflammatory Bowel Diseases 17, 1451–1463. https://doi.org/10.1002/ibd.21509

Sevrin, G., Massier, S., Chassaing, B., Agus, A., Delmas, J., Denizot, J., Billard, E., Barnich, N., 2020. Adaptation of adherent-invasive *E. coli* to gut environment:

Impact on flagellum expression and bacterial colonization ability. Gut Microbes 11, 364–380. https://doi.org/10.1080/19490976.2017.1421886

Shah, P., Fritz, J.V., Glaab, E., Desai, M.S., Greenhalgh, K., Frachet, A., Niegowska, M., Estes, M., Jäger, C., Seguin-Devaux, C., Zenhausern, F., Wilmes, P., 2016. A microfluidics-based in vitro model of the gastrointestinal human–microbe interface. Nat Commun 7, 11535. https://doi.org/10.1038/ncomms11535

Sheikh, A., Fleckenstein, J.M., 2023. Interactions of pathogenic Escherichia coli with CEACAMs. Front. Immunol. 14, 1120331. https://doi.org/10.3389/fimmu.2023.1120331

Sheikh, A., Tumala, B., Vickers, T.J., Alvarado, D., Ciorba, M.A., Bhuiyan, T.R., Qadri, F., Singer, B.B., Fleckenstein, J.M., 2020. CEACAMs serve as toxin-stimulated receptors for enterotoxigenic *Escherichia coli*. Proc. Natl. Acad. Sci. U.S.A. 117, 29055–29062. https://doi.org/10.1073/pnas.2012480117

Sheikh, J., Hicks, S., Dall'Agnol, M., Phillips, A.D., Nataro, J.P., 2001. Roles for Fis and YafK in biofilm formation by enteroaggregative *Escherichia coli*. Molecular Microbiology 41, 983–997. https://doi.org/10.1046/j.1365-2958.2001.02512.x

Shih, D.Q., Barrett, R., Zhang, X., Yeager, N., Koon, H.W., Phaosawasdi, P., Song, Y., Ko, B., Wong, M.H., Michelsen, K.S., Martins, G., Pothoulakis, C., Targan, S.R., 2011. Constitutive TL1A (TNFSF15) Expression on Lymphoid or Myeloid Cells Leads to Mild Intestinal Inflammation and Fibrosis. PLoS ONE 6, e16090. https://doi.org/10.1371/journal.pone.0016090

Shree, P., Singh, C.K., Sodhi, K.K., Surya, J.N., Singh, D.K., 2023. Biofilms: Understanding the structure and contribution towards bacterial resistance in antibiotics. Medicine in Microecology 16, 100084. https://doi.org/10.1016/j.medmic.2023.100084

Sidiq, T., Yoshihama, S., Downs, I., Kobayashi, K.S., 2016. Nod2: A Critical Regulator of Ileal Microbiota and Crohn's Disease. Front. Immunol. 7. https://doi.org/10.3389/fimmu.2016.00367

Sivignon, A., Chervy, M., Chevarin, C., Ragot, E., Billard, E., Denizot, J., Barnich, N., 2022. An adherent-invasive *Escherichia coli* -colonized mouse model to evaluate microbiota-targeting strategies in Crohn's disease. Disease Models & Mechanisms 15, dmm049707. https://doi.org/10.1242/dmm.049707

Sivignon, A., De Vallée, A., Barnich, N., Denizot, J., Darcha, C., Pignède, G., Vandekerckove, P., Darfeuille-Michaud, A., 2015a. Saccharomyces cerevisiae CNCM I-3856 Prevents Colitis Induced by AIEC Bacteria in the Transgenic Mouse Model Mimicking Crohn's Disease: Inflammatory Bowel Diseases 21, 276–286. https://doi.org/10.1097/MIB.0000000000000280

Sivignon, A., Yan, X., Alvarez Dorta, D., Bonnet, R., Bouckaert, J., Fleury, E., Bernard, J., Gouin, S.G., Darfeuille-Michaud, A., Barnich, N., 2015b.

Development of Heptylmannoside-Based Glycoconjugate Antiadhesive Compounds against Adherent-Invasive Escherichia coli Bacteria Associated with Crohn's Disease. mBio 6, e01298-15. https://doi.org/10.1128/mBio.01298-15

Sokol, H., Pigneur, B., Watterlot, L., Lakhdari, O., Bermúdez-Humarán, L.G., Gratadoux, J.-J., Blugeon, S., Bridonneau, C., Furet, J.-P., Corthier, G., Grangette, C., Vasquez, N., Pochart, P., Trugnan, G., Thomas, G., Blottière, H.M., Doré, J., Marteau, P., Seksik, P., Langella, P., 2008. *Faecalibacterium prausnitzii* is an anti-inflammatory commensal bacterium identified by gut microbiota analysis of Crohn disease patients. Proc. Natl. Acad. Sci. U.S.A. 105, 16731–16736. https://doi.org/10.1073/pnas.0804812105

Sokol, H., Seksik, P., Furet, J.P., Firmesse, O., Nion-Larmurier, I., Beaugerie, L., Cosnes, J., Corthier, G., Marteau, P., Doré, J., 2009. Low counts of Faecalibacterium prausnitzii in colitis microbiota: Inflammatory Bowel Diseases 15, 1183–1189. https://doi.org/10.1002/ibd.20903

Staab, J.F., Lemme-Dumit, J.M., Latanich, R., Pasetti, M.F., Zachos, N.C., 2023. Co-culturing Human Intestinal Enteroid Monolayers with Innate Immune Cells, in: Ordóñez-Morán, P. (Ed.), Intestinal Differentiated Cells, Methods in Molecular Biology. Springer US, New York, NY, pp. 207–223. https://doi.org/10.1007/978-1-0716-3076-1_16

Strober, W., Fuss, I.J., 2011. Proinflammatory Cytokines in the Pathogenesis of Inflammatory Bowel Diseases. Gastroenterology 140, 1756-1767.e1. https://doi.org/10.1053/j.gastro.2011.02.016

Strober, W., Watanabe, T., 2011. NOD2, an intracellular innate immune sensor involved in host defense and Crohn's disease. Mucosal Immunol 4, 484–495. https://doi.org/10.1038/mi.2011.29

Suarez, G., Sierra, J.C., Erova, T.E., Sha, J., Horneman, A.J., Chopra, A.K., 2010. A type VI secretion system effector protein, VgrG1, from Aeromonas hydrophila that induces host cell toxicity by ADP ribosylation of actin. J Bacteriol 192, 155–168. https://doi.org/10.1128/JB.01260-09

Suárez, M., Rüssmann, H., 1998. Molecular mechanisms of Salmonella invasion: the type III secretion system of the pathogenicity island 1. Int Microbiol 1, 197–204.

Sumagin, R., Robin, A.Z., Nusrat, A., Parkos, C.A., 2014. Transmigrated neutrophils in the intestinal lumen engage ICAM-1 to regulate the epithelial barrier and neutrophil recruitment. Mucosal Immunology 7, 905–915. https://doi.org/10.1038/mi.2013.106

Sun, Q.-H., Wang, Y.-S., Liu, G., Zhou, H.-L., Jian, Y.-P., Liu, M.-D., Zhang, D., Ding, Q., Zhao, R.-X., Chen, J.-F., Li, Y.-N., Liang, J., Li, Y.-L., Quan, C.-S., Xu, Z.-X., 2020. Enhanced O-linked Glcnacylation in Crohn's disease promotes intestinal inflammation. EBioMedicine 53, 102693. https://doi.org/10.1016/j.ebiom.2020.102693

Suwandi, A., Galeev, A., Riedel, R., Sharma, S., Seeger, K., Sterzenbach, T., García Pastor, L., Boyle, E.C., Gal-Mor, O., Hensel, M., Casadesús, J., Baines, J.F., Grassl, G.A., 2019. Std fimbriae-fucose interaction increases Salmonella-induced intestinal inflammation and prolongs colonization. PLoS Pathog 15, e1007915. https://doi.org/10.1371/journal.ppat.1007915

Swidsinski, A., Khilkin, M., Kerjaschki, D., Schreiber, S., Ortner, M., Weber, J., Lochs, H., 1998. Association between intraepithelial Escherichia coli and colorectal cancer. Gastroenterology 115, 281–286. https://doi.org/10.1016/S0016-5085(98)70194-5

Swidsinski, A., Ladhoff, A., Pernthaler, A., Swidsinski, S., Loening–Baucke, V., Ortner, M., Weber, J., Hoffmann, U., Schreiber, S., Dietel, M., Lochs, H., 2002. Mucosal flora in inflammatory bowel disease. Gastroenterology 122, 44–54. https://doi.org/10.1053/gast.2002.30294

Thia, K.T., Sandborn, W.J., Harmsen, W.S., Zinsmeister, A.R., Loftus, E.V., 2010. Risk Factors Associated With Progression to Intestinal Complications of Crohn's Disease in a Population-Based Cohort. Gastroenterology 139, 1147–1155. https://doi.org/10.1053/j.gastro.2010.06.070

Tiralongo, J., Cooper, O., Litfin, T., Yang, Y., King, R., Zhan, J., Zhao, H., Bovin, N., Day, C.J., Zhou, Y., 2018. YesU from Bacillus subtilis preferentially binds fucosylated glycans. Sci Rep 8, 13139. https://doi.org/10.1038/s41598-018-31241-8

Toesca, I.J., French, C.T., Miller, J.F., 2014. The Type VI Secretion System Spike Protein VgrG5 Mediates Membrane Fusion during Intercellular Spread by Pseudomallei Group Burkholderia Species. Infect Immun 82, 1436–1444. https://doi.org/10.1128/IAI.01367-13

Torres, A.G., Kaper, J.B., 2003. Multiple Elements Controlling Adherence of Enterohemorrhagic *Escherichia coli* O157:H7 to HeLa Cells. Infect Immun 71, 4985–4995. https://doi.org/10.1128/IAI.71.9.4985-4995.2003

Torres, E.A., 2025. Crohn's disease [WWW Document]. American Gastroenterological Association. URL https://patient-staging.gastro.org/crohns-disease/ (accessed 1.13.25).

Torres, J., Mehandru, S., Colombel, J.-F., Peyrin-Biroulet, L., 2017. Crohn's disease. The Lancet 389, 1741–1755. https://doi.org/10.1016/S0140-6736(16)31711-1

Tran, S., Billoud, L., Lewis, S.B., Phillips, A.D., Schüller, S., 2014. Shiga toxin production and translocation during microaerobic human colonic infection with S higa toxin-producing *E . coli* O157:H7 and O104:H4. Cell Microbiol 16, 1255–1266. https://doi.org/10.1111/cmi.12281

Trunk, K., Peltier, J., Liu, Y.-C., Dill, B.D., Walker, L., Gow, N.A.R., Stark, M.J.R., Quinn, J., Strahl, H., Trost, M., Coulthurst, S.J., 2018. The type VI secretion

system deploys antifungal effectors against microbial competitors. Nat Microbiol 3, 920–931. https://doi.org/10.1038/s41564-018-0191-x

Tsilingiri, K., Barbosa, T., Penna, G., Caprioli, F., Sonzogni, A., Viale, G., Rescigno, M., 2012. Probiotic and postbiotic activity in health and disease: comparison on a novel polarised ex-vivo organ culture model. Gut 61, 1007–1015. https://doi.org/10.1136/gutjnl-2011-300971

Uhlig, H.H., Powrie, F., 2018. Translating Immunology into Therapeutic Concepts for Inflammatory Bowel Disease. Annu Rev Immunol 36, 755–781. https://doi.org/10.1146/annurev-immunol-042617-053055

Van Beelen, A.J., Zelinkova, Z., Taanman-Kueter, E.W., Muller, F.J., Hommes, D.W., Zaat, S.A.J., Kapsenberg, M.L., De Jong, E.C., 2007. Stimulation of the Intracellular Bacterial Sensor NOD2 Programs Dendritic Cells to Promote Interleukin-17 Production in Human Memory T Cells. Immunity 27, 660–669. https://doi.org/10.1016/j.immuni.2007.08.013

Van Den Abbeele, P., Marzorati, M., Derde, M., De Weirdt, R., Joan, V., Possemiers, S., Van De Wiele, T., 2016. Arabinoxylans, inulin and Lactobacillus reuteri 1063 repress the adherent-invasive Escherichia coli from mucus in a mucosa-comprising gut model. npj Biofilms Microbiomes 2, 16016. https://doi.org/10.1038/npjbiofilms.2016.16

Vazeille, E., Chassaing, B., Buisson, A., Dubois, A., De Vallée, A., Billard, E., Neut, C., Bommelaer, G., Colombel, J.-F., Barnich, N., Darfeuille-Michaud, A., Bringer, M.-A., 2016. GipA Factor Supports Colonization of Peyer's Patches by Crohn's Disease-associated Escherichia Coli: Inflammatory Bowel Diseases 22, 68–81. https://doi.org/10.1097/MIB.0000000000000609

Vejborg, R.M., Hancock, V., Petersen, A.M., Krogfelt, K.A., Klemm, P., 2011. Comparative genomics of Escherichia coli isolated from patients with inflammatory bowel disease. BMC Genomics 12, 316. https://doi.org/10.1186/1471-2164-12-316

Vogelstein, B., Kinzler, K.W., 2004. Cancer genes and the pathways they control. Nat Med 10, 789–799. https://doi.org/10.1038/nm1087

Von Martels, J.Z.H., Sadaghian Sadabad, M., Bourgonje, A.R., Blokzijl, T., Dijkstra, G., Faber, K.N., Harmsen, H.J.M., 2017. The role of gut microbiota in health and disease: In vitro modeling of host-microbe interactions at the aerobe-anaerobe interphase of the human gut. Anaerobe 44, 3–12. https://doi.org/10.1016/j.anaerobe.2017.01.001

Wang, Yuli, DiSalvo, M., Gunasekara, D.B., Dutton, J., Proctor, A., Lebhar, M.S., Williamson, I.A., Speer, J., Howard, R.L., Smiddy, N.M., Bultman, S.J., Sims, C.E., Magness, S.T., Allbritton, N.L., 2017. Self-renewing Monolayer of Primary Colonic or Rectal Epithelial Cells. Cellular and Molecular Gastroenterology and Hepatology 4, 165-182.e7. https://doi.org/10.1016/j.jcmgh.2017.02.011

Wang, Yaya, Mumm, J.B., Herbst, R., Kolbeck, R., Wang, Yue, 2017. IL-22 Increases Permeability of Intestinal Epithelial Tight Junctions by Enhancing Claudin-2 Expression. The Journal of Immunology 199, 3316–3325. https://doi.org/10.4049/jimmunol.1700152

Watanabe, T., Kitani, A., Murray, P.J., Strober, W., 2004. NOD2 is a negative regulator of Toll-like receptor 2–mediated T helper type 1 responses. Nat Immunol 5, 800–808. https://doi.org/10.1038/ni1092

Watari, A., Sakamoto, Y., Hisaie, K., Iwamoto, K., Fueta, M., Yagi, K., Kondoh, M., 2017. Rebeccamycin Attenuates TNF-α-Induced Intestinal Epithelial Barrier Dysfunction by Inhibiting Myosin Light Chain Kinase Production. Cell Physiol Biochem 41, 1924–1934. https://doi.org/10.1159/000472367

Wehkamp, J., Salzman, N.H., Porter, E., Nuding, S., Weichenthal, M., Petras, R.E., Shen, B., Schaeffeler, E., Schwab, M., Linzmeier, R., Feathers, R.W., Chu, H., Lima, H., Fellermann, K., Ganz, T., Stange, E.F., Bevins, C.L., 2005. Reduced Paneth cell α-defensins in ileal Crohn's disease. Proc. Natl. Acad. Sci. U.S.A. 102, 18129–18134. https://doi.org/10.1073/pnas.0505256102

Wehkamp, J., Stange, E.F., 2020. An Update Review on the Paneth Cell as Key to Ileal Crohn's Disease. Front. Immunol. 11, 646. https://doi.org/10.3389/fimmu.2020.00646

Weiser, J.N., Gotschlich, E.C., 1991. Outer membrane protein A (OmpA) contributes to serum resistance and pathogenicity of Escherichia coli K-1. Infect Immun 59, 2252–2258. https://doi.org/10.1128/iai.59.7.2252-2258.1991

Wilson, C., Lukowicz, R., Merchant, S., Valquier-Flynn, H., Caballero, J., Sandoval, J., Okuom, M., Huber, C., Brooks, T.D., Wilson, E., Clement, B., Wentworth, C.D., Holmes, A.E., 2017. Quantitative and Qualitative Assessment Methods for Biofilm Growth: A Mini-review. Res Rev J Eng Technol 6, http://www.rroij.com/open-access/quantitative-and-qualitative-assessment-methods-for-biofilm-growth-a-minireview-.pdf.

Wine, E., Ossa, J.C., Gray-Owen, S.D., Sherman, P.M., 2009. Adherent-invasive Escherichia coli, strain LF82 disrupts apical junctional complexes in polarized epithelia. BMC Microbiol 9, 180. https://doi.org/10.1186/1471-2180-9-180

Wirtz, S., Popp, V., Kindermann, M., Gerlach, K., Weigmann, B., Fichtner-Feigl, S., Neurath, M.F., 2017. Chemically induced mouse models of acute and chronic intestinal inflammation. Nat Protoc 12, 1295–1309. https://doi.org/10.1038/nprot.2017.044

Xie, C., Jones, K.L., Rayner, C.K., Wu, T., 2020. Enteroendocrine Hormone Secretion and Metabolic Control: Importance of the Region of the Gut Stimulation. Pharmaceutics 12, 790. https://doi.org/10.3390/pharmaceutics12090790

Xu, P., Becker, H., Elizalde, M., Masclee, A., Jonkers, D., 2018. Intestinal organoid culture model is a valuable system to study epithelial barrier function in IBD. Gut 67, 1905–1906. https://doi.org/10.1136/gutjnl-2017-315685

Xu, Z., Dong, X., Yang, K., Chevarin, C., Zhang, J., Lin, Y., Zuo, T., Chu, L.C., Sun, Y., Zhang, F., Chan, F.K., Sung, J.J., Yu, J., Buisson, A., Barnich, N., Colombel, J.-F., Wong, S.H., Miao, Y., Ng, S.C., 2021. Association of Adherent-invasive *Escherichia coli* with severe Gut Mucosal dysbiosis in Hong Kong Chinese population with Crohn's disease. Gut Microbes 13, 1994833. https://doi.org/10.1080/19490976.2021.1994833

Xue, J.-C., Hou, X.-T., Zhao, Y.-W., Yuan, S., 2025. Biological agents as attractive targets for inflammatory bowel disease therapeutics. Biochimica et Biophysica Acta (BBA) - Molecular Basis of Disease 1871, 167648. https://doi.org/10.1016/j.bbadis.2024.167648

Yan, L., Wang, Y., Wang, Z.-Z., Rong, Y.-T., Chen, L.-L., Li, Q., Liu, T., Chen, Y.-H., Li, Y.-D., Huang, Z.-H., Peng, J., 2016. Cell motility and spreading promoted by CEACAM6 through cyclin D1/CDK4 in human pancreatic carcinoma. Oncology Reports 35, 418–426. https://doi.org/10.3892/or.2015.4338

Yao, D., Dai, W., Dong, M., Dai, C., Wu, S., 2021. MUC2 and related bacterial factors: Therapeutic targets for ulcerative colitis. EBioMedicine 74, 103751. https://doi.org/10.1016/j.ebiom.2021.103751

Ye, X., Sun, M., 2017. AGR2 ameliorates tumor necrosis factor-α-induced epithelial barrier dysfunction via suppression of NF-κB p65-mediated MLCK/p-MLC pathway activation. International Journal of Molecular Medicine 39, 1206–1214. https://doi.org/10.3892/ijmm.2017.2928

Yu, H., Cook, T.J., Sinko, P.J., 1997. Evidence for diminished functional expression of intestinal transporters in Caco-2 cell monolayers at high passages. Pharm Res 14, 757–762. https://doi.org/10.1023/a:1012150405949

Yuan, Z., Ye, J., Liu, B., Zhang, L., 2024. Unraveling the role of autophagy regulation in Crohn's disease: from genetic mechanisms to potential therapeutics. Adv. Biotechnol. 2, 14. https://doi.org/10.1007/s44307-024-00021-z

Zachos, N.C., Kovbasnjuk, O., Foulke-Abel, J., In, J., Blutt, S.E., De Jonge, H.R., Estes, M.K., Donowitz, M., 2016. Human Enteroids/Colonoids and Intestinal Organoids Functionally Recapitulate Normal Intestinal Physiology and Pathophysiology. Journal of Biological Chemistry 291, 3759–3766. https://doi.org/10.1074/jbc.R114.635995

Zhang, J., Huang, Y.-J., Yoon, J.Y., Kemmitt, J., Wright, C., Schneider, K., Sphabmixay, P., Hernandez-Gordillo, V., Holcomb, S.J., Bhushan, B., Rohatgi, G., Benton, K., Carpenter, D., Kester, J.C., Eng, G., Breault, D.T., Yilmaz, O., Taketani, M., Voigt, C.A., Carrier, R.L., Trumper, D.L., Griffith, L.G., 2021. Primary Human Colonic Mucosal Barrier Crosstalk with Super Oxygen-Sensitive Faecalibacterium prausnitzii in Continuous Culture. Med 2, 74-98.e9. https://doi.org/10.1016/j.medj.2020.07.001

Zhao, A., Sun, J., Liu, Y., 2023. Understanding bacterial biofilms: From definition to treatment strategies. Front. Cell. Infect. Microbiol. 13, 1137947. https://doi.org/10.3389/fcimb.2023.1137947

Zhao, M., Gönczi, L., Lakatos, P.L., Burisch, J., 2021. The Burden of Inflammatory Bowel Disease in Europe in 2020. J Crohns Colitis 15, 1573–1587. https://doi.org/10.1093/ecco-jcc/jjab029

Zhao, X., Zeng, H., Lei, L., Tong, X., Yang, L., Yang, Y., Li, S., Zhou, Y., Luo, L., Huang, J., Xiao, R., Chen, J., Zeng, Q., 2021. Tight junctions and their regulation by non-coding RNAs. Int J Biol Sci 17, 712–727. https://doi.org/10.7150/ijbs.45885

Zheng, J., Meng, J., Zhao, S., Singh, R., Song, W., 2008. *Campylobacter* -Induced Interleukin-8 Secretion in Polarized Human Intestinal Epithelial Cells Requires *Campylobacter* -Secreted Cytolethal Distending Toxin- and Toll-Like Receptor-Mediated Activation of NF-κB. Infect Immun 76, 4498–4508. https://doi.org/10.1128/IAI.01317-07

Zong, W., Friedman, E.S., Allu, S.R., Firrman, J., Tu, V., Daniel, S.G., Bittinger, K., Liu, L., Vinogradov, S.A., Wu, G.D., 2024. Disruption of intestinal oxygen balance in acute colitis alters the gut microbiome. Gut Microbes 16, 2361493. https://doi.org/10.1080/19490976.2024.2361493